An Investigation into the Functionalization of Poly(styrene-*co*-maleic anhydride) with Calixarenes and Their Potential Applications

by

Seyed Babak Eghbali Dogaheh

Thesis presented in partial fulfilment of the requirements for the degree
Doctor of Philosophy in Science
at Stellenbosch University

Supervisor: Prof. G.E. Arnott
Co-supervisor: Prof. P.E. Mallon
Faculty of Science
Department of Chemistry and Polymer

December 2019

Stellenbosch University https://scholar.sun.ac.za

Declaration

By submitting this thesis electronically, I declare that the entirety of the work contained therein is my own, original work, that I am the sole author thereof (save to the extent explicitly otherwise stated), that reproduction and publication thereof by Stellenbosch University will not infringe any third party rights and that I have not previously in its entirety or in part submitted it for obtaining any qualification.

_____

Date: December 2019

Copyright © 2019 Stellenbosch University

All rights reserved

Stellenbosch University https://scholar.sun.ac.za

Abstract

This work describes the development of a new method for the synthesis of a calixarene grafted polymer. The method involves synthesizing a mono-alkylated calixarene that contains an amino-tether suitable for grafting onto polymers such as the polystyrene-maleic anhydride copolymer (PSMA). The amino-tether was synthesized through a Gabriel synthesis on the parent phthalimide-derivatized calix[4]arenes. Having successfully optimized the method, the next stage investigated the potential applications for this technology. Two divergent applications were investigated: 1) a colorimetric mercury sensor, and 2) supramolecular hydrogel formation.

The first application was based on the known sensing ability of functionalized calixarenes for the detection of different guests (cations, anions, neutral species, etc.). The most interesting one has been the colorimetric approach. Of interest in this work was the reported distal bis-allyl bis-arylazo calix[4]arene (also known as Chung's sensor), which is capable of detecting mercury cations with a rapid color change in the solution media (yellow to pink). Therefore, a polymer-supported version of the same calix[4]arene was targeted for synthesis to facilitate the formation of a sensing instrument for mercury. Despite all efforts (trying eight synthetic routes), the required functionalized calixarene could not be obtained. Several suggestions for future work have been offered to solve this challenge.

The second application aimed at in this project was to attach water-soluble calix[4]arenes to PSMA in order to make the polymer water soluble and to form a potential hydrogel. The most well-studied compound in this category has been the *p*-sulfonated calix[4]arene, which has been shown to form supramolecular complexes with bis-quaternary amines in aqueous solution. The possibility to achieve hydrogelation through a *p*-sulfonated calix[4]arene-grafted PSMA was therefore investigated. The primary amine-tethered *p*-sulfonated calix[4]arene was successfully synthesized and grafted onto PSMA. Unfortunately, the resulting grafts were unable to form a hydrogel in the presence of multiple quaternary amine-based compounds in spite of varying a large number of experiment parameters (i.e. stoichiometry, pH, temperature, concentration and so forth). One problem was that the grafts were not as water soluble as expected. Thus a second option was to replace PSMA with another polymer with higher water solubility upon grafting with the calix[4]arene. The polymer investigated was a polyvinylpyrrolidone maleic anhydride copolymer (PVP-MA). The grafting reaction was successfully carried out and much higher water solubility for the graft was achieved, but once

Stellenbosch University https://scholar.sun.ac.za

again a hydrogel could not be formed. It is believed that this failure most likely is due to the conformational issue of the calix[4]arene or the low degree of functionalization for the grafts. Several solutions to this these failures have been proposed.

Stellenbosch University https://scholar.sun.ac.za

Opsomming

Hierdie werk beskryf die ontwikkeling van 'n nuwe metode vir die sintese van 'n kalixarene-geënte polimeer. Die metode behels die sintetisering van 'n mono-gekalikeerde kalixarene wat 'n aminoteter bevat wat geskik is vir die inplanting op polimere soos die polistireen-maleïensanhidried kopolimeer (PSMA). Die aminoteter is gesintetiseer deur 'n Gabrielsintese op die ouer ftalimied-afgeleide kalix[4]arene. Met die suksesvolle optimalisering van die metode het die volgende stadium die moontlike toepassings vir hierdie tegnologie ondersoek. Twee uiteenlopende toepassings is ondersoek: 1) 'n kolorimetriese kwikssensor, en 2) supramolekulêre hidrogelvorming.

Die eerste aansoek was gebaseer op die bekende sensibilisering van funksionaliseerde kalixarenee vir die opsporing van verskillende gaste (katione, anione, neutrale spesies, ens.). Die interessantste is die kolorimetriese benadering. Belangrik in hierdie werk was die gerapporteerde distale bis-allyl bis-arylazo kalix[4]arene (ook bekend as Chung se sensor), wat in staat is om kwik katione op te spoor met 'n vinnige kleurverandering in die oplossing media (geel na pienk). Daarom is 'n polimeergesteunde weergawe van dieselfde kalix[4]arene gerig op sintese om die vorming van 'n senserende instrument vir kwik te fasiliteer. Ten spyte van alle pogings (probeer agt sintetiese roetes), kon die vereiste funksionaliseerde kalixarene nie verkry word nie. Verskeie voorstelle vir toekomstige werk is aangebied om hierdie uitdaging op te los.

Die tweede aansoek wat in hierdie projek gemik is, was om wateroplosbare kalix[4]arene aan PSMA te heg ten einde die polimeer wateroplosbaar te maak en 'n potensiële hidrogel te vorm. Die mees goed bestudeerde verbinding in hierdie kategorie is die *p*-gesulfoneerde kalix[4]arene, wat getoon is om supramolekulêre komplekse te vorm met bis-kwaternêre amiene in waterige oplossing. Die moontlikheid om hidrolgasie te verkry deur 'n *p*-gesulfoneerde kalix[4]arene-geënt PSMA is derhalwe ondersoek. Die primêre amien-vasgemaakte *p*-gesulfoneerde kalix[4]arene is suksesvol gesintetiseer en op PSMA ingeënt. Ongelukkig kon die resulterende grafte nie in staat wees om 'n hidrogel te vorm in die teenwoordigheid van verskeie kwaternêre aminebaseerde verbindings ten spyte van 'n groot aantal eksperimentparameters (dws stoïgiometrie, pH, temperatuur, konsentrasie en so meer). Een probleem was dat die grafte nie so wateroplosbaar was soos verwag nie. So 'n tweede opsie was om PSMA te vervang met 'n ander polimeer met hoër wateroplosbaarheid tydens die enting met die kalix[4]arene. Die polimeer wat ondersoek is, was 'n polivinielpirrolidoon-

Stellenbosch University https://scholar.sun.ac.za

maleïensanhidried kopolimeer (PVP-MA). Die entreaksie is suksesvol uitgevoer en 'n veel hoër wateroplosbaarheid vir die transplantaat is behaal, maar weer kon 'n hidrogel nie gevorm word nie. Daar word geglo dat hierdie mislukking waarskynlik die gevolg is van die konformasionele kwessie van die kalix[4]arene of die lae mate van funksionalisasie vir die grafte. Verskeie oplossings hiervoor is voorgestel.

Stellenbosch University https://scholar.sun.ac.za

Acknowledgements

First of all, I must thank my parents for all the support they have delivered to me not only for this project but throughout my entire life by their compassion and generosity which made me become the better person I am now. I must also thank my beloved brother Hamed Eghbali for his devotion, patience, and sacrifice during the time we spent together in South Africa. I express my greatest gratitude and respect to my dear supervisors Prof. Gareth Arnott and Prof. Peter Mallon who granted me this opportunity of doing chemistry research as a PhD student in Stellenbosch University as an honor and privilege that not everyone can possess. I thank them for not giving up on me even during the hard times in which I was hopeless about my project outcome and unable to resolve my challenges.

In the course of doing this project, I had the chance of meeting some of the best colleagues and friends one can ever make in life. I particularly am thankful to Luke Hudson and Alet van der Westhuyzen (my best friends ever) for their support, kindness, and positivity. I thank all members of Arnott's research group: Dr. Dominic Castell (my first mentor), Dr. Lonwabo Ngodwana, Dr. Sritama Bose, Christopher Jurisch, Asslly Mafaune, Kevin Visagie, Trégen Snayer, and Ashlyn Bhana.

I thank all members of GOMOC (the group of medicinal and organic chemistry) with whom I spent my best years of academic life especially Prof. Willem van Otterlo, Prof. Ivan Green, Dr. Leon Jacobs, Dr. Tanya Mabank, Dr. Anton Hamann, Johnathan Hay, and Chandre Sammy.

However, I did not spend most of my time in the polymer science department, I can never be ungrateful to the very knowledgeable and inspiring people by whom I was aided such as Dr. Helen Pfukwa, Dr. Rueben Pfukwa, Dr. Waled Hadasha, Dr. Divann Robertson, Megan Matthews, Gestél Kuyler and even Dr. Paul Reader (Kansai Plascon).

I especially thank Elsa Malherbe and Dr. Jaco Brand in the NMR spectroscopy unit of Central Analytical Facility, Dr. Wilhelmus Gerber for teaching me the NMR spectroscopic titration techniques and Dr. Katherine de Villiers for allowing me to use her lab instruments. I was pleased to spend my time in a department run by dedicated technical officers like Glen de Jongh and Mohamed Shafiek and hard-working staff members like Raymond, Debbie, Maxwell, and Mary (God rest her soul).

Overall, thanks for your never-ending support everyone and God bless you all.

Stellenbosch University https://scholar.sun.ac.za

Conferences

SACI-ACS, Binational Organic Chemistry Conference, November **2014**, The Stellenbosch Institute for Advanced Study (STIAS), Poster presentation.

Stellenbosch University https://scholar.sun.ac.za

Abbreviations

^{1}H-NMR	Proton nuclear magnetic resonance
^{13}C-NMR	Carbon nuclear magnetic resonance
AAS	Atomic absorption spectroscopy
AIBN	2,2′-Azobis(2-methylpropionitrile)
ATR-FTIR	Attenuated total reflectance Fourier transform infrared
BQA	Bis-quaternary amine
CE-ICP-MS	Capillary electrophoresis-inductively coupled plasma-mass spectrometry
CPG	Controlled pore glass
Đ	Dispersity
Da	Dalton
DCM	Dichloromethane
DIPEA	*N*-Ethyl-*N*-(propan-2-yl)propan-2-amine
DMAP	*N*,*N*-Dimethylpyridin-4-amine
DMF	*N*,*N*-Dimethylformamide
DMT	5'-Dimethoxytrityl-3'-deoxythymidine 2'-[(2-cyanoethyl)-(*N*,*N*-diisopropyl)]-phosphoramidite
DSC	Differential scanning calorimetry
ESI	Electrospray ionization
GPC	Gel permeation chromatography
HATU	1-[Bis(dimethylamino)methylene]-1H-1,2,3-triazolo[4,5-b]pyridinium 3-oxide hexafluorophosphate
HPLC	High-performance liquid chromatography
HPLC-ICP-MS	High-performance liquid chromatography-inductively coupled plasma-mass spectrometry
HRMS	High-resolution mass spectrometry

Stellenbosch University https://scholar.sun.ac.za

ICP-MS	Inductively coupled plasma-mass spectrometry
IDA	Isodecyl acrylate
IPN	Inter-penetrating network
LCST	Lower critical solution temperature
LLDPE	Linear low-density polyethylene
MEK	Methyl ethyl ketone
MM	Methyl methacrylate
M_n	Number average molar mass
Mp	Melting point
M_w	Weight average molar mass
MWCO	Molecular weight cut-off
PEG	Poly(ethylene glycol)
PES	Poly(ethersulfone)
PMDTA	*N*,*N*,*N*′,*N*″,*N*″-Pentamethyldiethylenetriamine
PMMA	Poly(methyl methacrylate)
POP	Poly(oxypropylene)
PSMA	Poly(styrene-*co*-maleic anhydride)
PVC	Poly(vinyl chloride)
PVP-MA	Poly[(*N*-vinylpyrrolidone)-*co*-(maleic anhydride)]
QCM	Quartz crystal microbalance
R_f	Retention factor
RI	Refractive index
ROMP	Ring-opening metathesis polymerization
RT	Room temperature
SAN	Styrene-acrylonitrile (monomer)
SEC	Size exclusion chromatography
SMA	Styrene-maleic anhydride (monomer)
TDI	2,4-Diisocyanato-1-methylbenzene
TFA	Trifluoroacetic acid
THF	Tetrahydrofuran

Stellenbosch University https://scholar.sun.ac.za

TLC	Thin layer chromatography
TMEDA	*N*,*N*,*N*′,*N*′-Tetramethylethane-1,2- diamine
TOF MS	Time of flight mass spectrometry
UV-Vis	Ultraviolet-visible

Stellenbosch University https://scholar.sun.ac.za

Table of contents

Stellenbosch University https://scholar.sun.ac.za

Stellenbosch University https://scholar.sun.ac.za

Stellenbosch University https://scholar.sun.ac.za

Stellenbosch University https://scholar.sun.ac.za

Stellenbosch University https://scholar.sun.ac.za

Stellenbosch University https://scholar.sun.ac.za

Chapter 1. General introduction (calixarene and PSMA basics)

1.1 Chapter overview

This chapter will introduce the essential components of this research, namely calix[4]arenes and poly(styrene-*co*-maleic anhydride) (PSMA). Thereafter, the synthetic methods and the applications of these compounds will be presented through examples from the literature. Finally, in line with the literature reports, possible approaches for grafting a number of desired functionalized calix[4]arenes onto PSMA, followed by potential applications for those grafts, will be discussed.

1.2 Calixarene introduction

Calix[4]arene is a well-known cyclic phenol-formaldehyde tetramer. This bowl-shaped compound was discovered by Adolf von Baeyer who managed to synthesize it through heating phenol with a formaldehyde solution. Unfortunately, due to the lack of sufficient advancement for the characterization of compounds in chemistry at the time, full structural analysis for the product was not possible.[1] Interestingly in the first decade of the 20th century, Leo Baekeland introduced a commercially successful resin named Bakelite using a similar process for phenol-formaldehyde condensation.[2] As a result of this great success, many researchers directed their attention to develop new methods for the synthesis of phenol-formaldehyde oligomers with interesting physical and chemical properties. Among them was Alois Zinke from the University of Graz, Austria, who carried out the base-facilitated synthesis of calix[4]arene employing a wide range of *para*-alkylated phenols with aqueous formaldehyde (during the 1940s to 1950s). The great advantage of Zinke's method was the elimination of the possibility of forming the crosslinked products due to the availability of one *para* and two *ortho* positions on phenol. Consequently, only one product for each reaction was acquired. These products had very high melting points and very poor solubility in organic solvents. Despite the lack of many modern techniques for structure determination, Zinke was able to suggest a cyclic structure for the *p*-alkylated calix[4]arenes (**Figure 1.1**).[3]

Comparing Zinke's proposed structure with the spectral data currently available for calix[4]arene proves that his prediction of the cyclic nature of calix[4]arene was correct.[4]

Stellenbosch University https://scholar.sun.ac.za

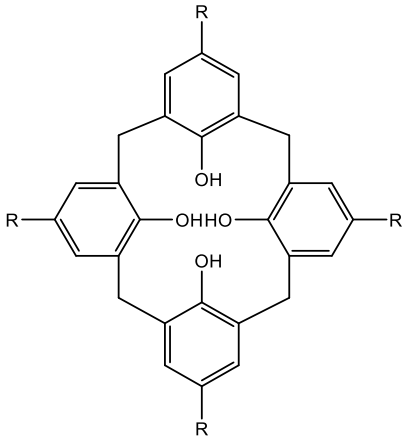

Figure 1.1 Zinke's proposed structure for calix[4]arene (R= Alkyl group)

Nonetheless, it was not Zinke who can be considered as the modernizer of calixarene science, but rather David Gutsche from Washington University in St Louis, USA. He was the first chemist who suggested that calixarenes could be used as potential enzyme mimics, which noticeably changed the focus of their study from commercial purposes to a more academic goal. Gutsche also proposed the term calixarene, which is a combination of *calix* (Greek for vase) and *arene* (aromatic ring) as an explicit term describes their steric structures.[4] The number of rings on calixarenes typically varies from 4 to 12, and therefore the synthetic procedure should be carefully controlled to afford a calixarene with the desired number of rings. In total, the reaction temperature, the base choice, the concentration and even the solvent play a very important role on the nature of the final product.[5] There have been many debates with respect to the precise mechanism through which the linear oligomer forms and then cyclization occurs, but overall it is almost certain that the first product of condensation is a hydroxymethyl phenol. This is capable of forming a Michael acceptor-like species which is attacked by another phenolic unit to produce the first linear oligomer, which can later expand by reacting with another phenolic unit (**Scheme 1.1**).[5] Sometimes small calixarenes can be synthesized as a consequence of large calixarenes fragmenting such as calix[4]arene which is believed to be achieved from calix[8]arene decomposition at higher temperatures.[5]

Regarding the three-dimensional appearance of calix[4]arene, the terms *upper rim* and *wide rim* are designated to the *exo* face (*para* position of phenol) while for its *endo* face, the terms *lower rim* and *narrow rim* are used (phenolic hydroxyls) (**Figure 1.2**).[5]

Stellenbosch University https://scholar.sun.ac.za

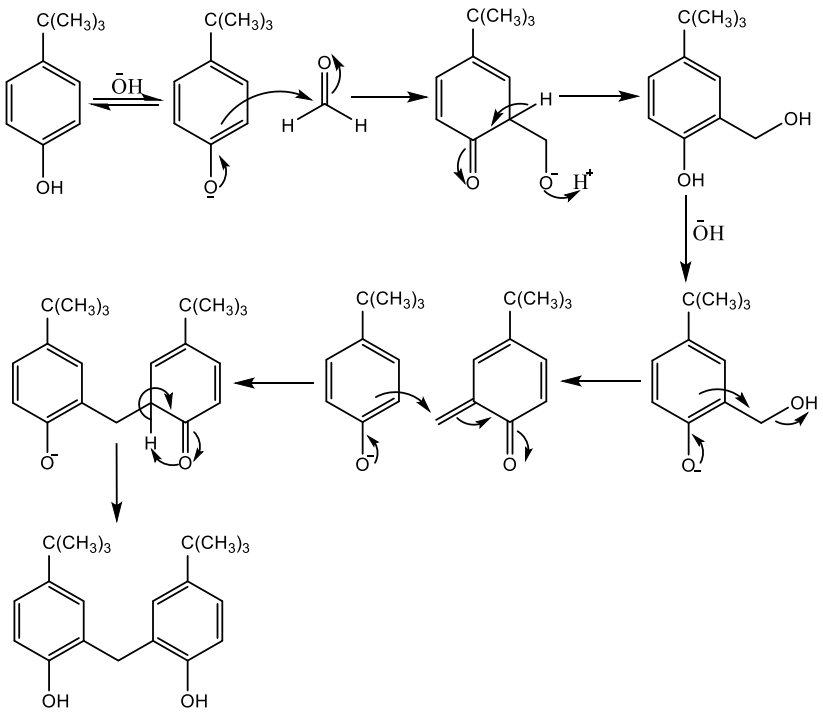

Scheme 1.1 Linear oligomer formation from p-t-butyl phenol

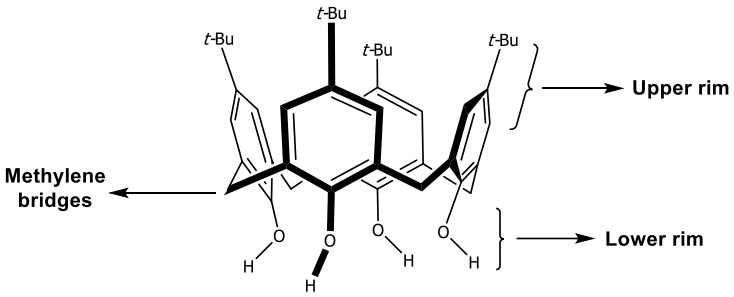

Figure 1.2 Three-dimensional depiction of p-t-butyl-calix[4]arene

One of the features of calixarenes is their diverse conformational nature. Cornforth *et al.* discovered four conformational isomers for calix[4]arene which were designated as cone, partial cone, 1,2-alternate and 1,3-alternate (**Figure 1.3**). In the solid state, calix[4]arene can only appear in the cone conformation which must be attributed to the strong hydrogen bonding between its lower rim hydroxyls which naturally leads to its exceptional thermal stability.[6] The other conformations are only found after synthetically modified calix[4]arenes are locked into these positions.

The development of NMR spectroscopy opened a new chapter in the evaluation of calix[4]arene conformations in solutions.[7] The astoundingly rapid inversion of calix[4]arene in solutions even at room temperature was initially shown by Kammerer who investigated the

Stellenbosch University https://scholar.sun.ac.za

behavior of the methylene bridges for *p*-alkylated calix[4]arene using ^{1}H-NMR spectroscopy.[8] It was perceived that above room temperature methylene bridges only showed one broad singlet (very rapid inversion), whereas below this temperature two separate doublets were observable (very slow inversion).[8] As expected, this inversion changes an axial methylene proton into an equatorial one and *vice versa* (**Scheme 1.2**).

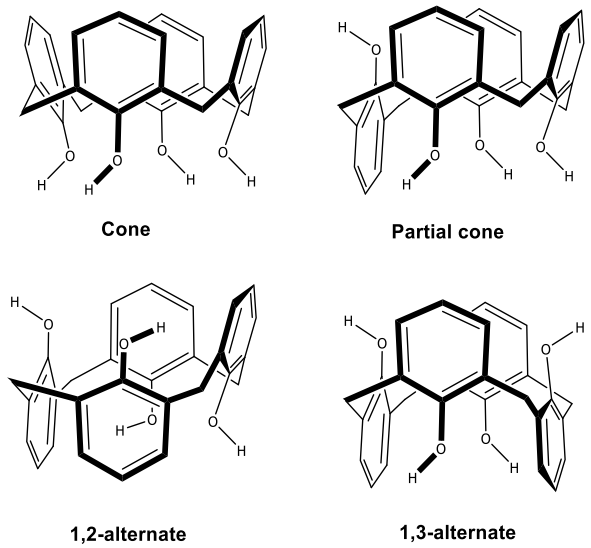

Figure 1.3 Different conformations for a calix[4]arene

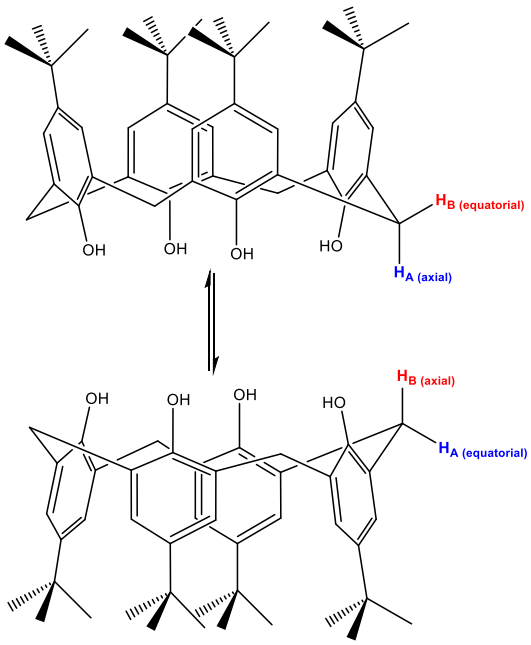

Scheme 1.2 An example of a calix[4]arene ring inversion

Different factors can affect the adoption of a specific conformation by a calixarene. Among them certainly, the effect of lower rim substituents matters the most. Reactions such as

Stellenbosch University https://scholar.sun.ac.za

etherification, esterification, etc. can lock a particular conformer via changing the steric hindrance around the lower rim. They also may disrupt the hydrogen bonding on the lower rim causing the appearance of new conformers. All in all, the cone conformer is the most common and the alternates (1,2 and 1,3) are the least common.[5] It is also essential to know that all the above-mentioned conformers are not absolute and that there are sub-conformers for each one of them. As a good example, the cone conformer can be observed as a true cone (in the solid state with C_4 symmetry) or as a pinched cone (in solutions with C_2 symmetry). It should be noted that ^{1}H-NMR spectroscopy is a potent technique to distinguish these two sub-conformers from each other (**Figure 1.4**).[5]

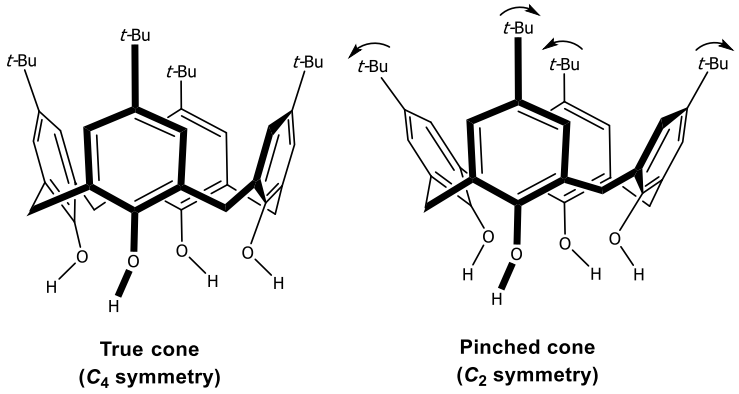

Figure 1.4 Different cone conformations for a calix[4]arene

1.3 Calixarene applications

Since its discovery in the late nineteenth century, calixarenes have been studied thoroughly and many useful applications, as compared to many other supramolecular structures, have been reported.[5] Its ability to be functionalized with ease on both its lower rim and upper rim has made it an ideal choice for research-related activities. One of the calixarene's features is complexation of other species (cationic, anionic or neutral) which enables it to be used in various applications.[a] Some examples include, as a chiral ligand together with several transition metals for asymmetric reaction catalysis[9] or as a stationary phase for chromatography,[10] as a polymerization initiator,[11] for enzyme-mimic studies,[12] for self-assembly,[13] for drug delivery and pharmaceutical purposes,[14] in biology[15] and biotechnology[16] and finally as an efficient sensing agent.[17] Calixarene binding and encapsulation potency will be investigated in the research performed in this dissertation with a focus on calixarene-grafted polymers. To do so,

[a] Comparatively, calixarene inclusion complexes are stronger than the ones of other supramolecular structures.[18,19]

Stellenbosch University https://scholar.sun.ac.za

first a brief literature review on calixarene-grafted materials will be presented and then our polymer choice, its applications and its role in this project will be introduced.

1.4 Materials incorporating calixarenes

There are multiple routes of synthesizing calixarene-grafted materials and these can be divided into two general approaches for the formation of a supported calixarene graft: 1- Attachment of the calixarene onto other materials (also known as ‘‘grafting onto approach’’) which can be classified into two separate categories: 1a- Attachment of the calixarene onto the surface of silica (**Figure 1.5A**);[20] 1b- Attachment of the calixarene onto a polymer (**Figure 1.5B**).[21] 2- Polymerization of the calixarene monomer possessing a polymerizable unit which in general leads to calixarene as part of the resulting polymer main chain (also known as ‘‘grafting through approach’’ in **Figure 1.5C**).[22] The approach 1b (using a synthesized polymer, which is styrene-maleic anhydride copolymer also known as PSMA) has been taken in this research and will be explained thoroughly in the dissertation.

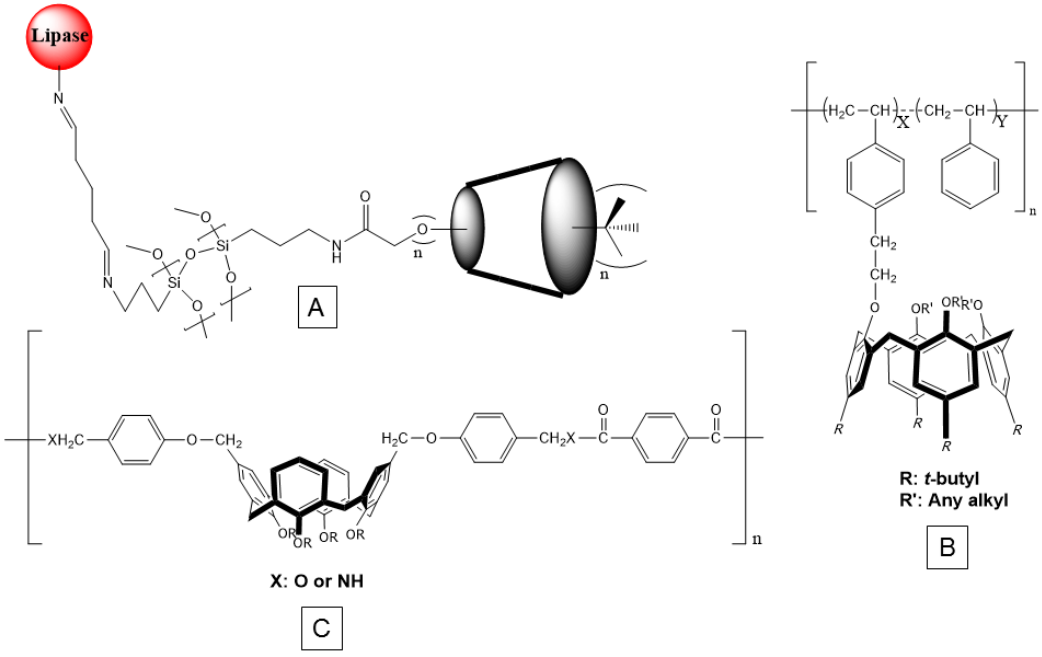

Figure 1.5 Different approaches for the formation of calixarene-grafted materials

1.4.1 Materials incorporating calixarenes – Calixarenes grafted onto silica

The first silica-bound calixarene ever reported was a triethoxy silane *p-n*-propylcalix[n]arene ethyl acetate (n=4,6) by McKervey and co-workers.[23] The first step was the reaction between a *p*-allylcalix[n]arene ethyl acetate and $(CH_3CH_2O)_3SiH$ (a hydrosilation addition) (**Scheme 1.3**). Then, this product was grafted onto activated silica gel (heating under reflux in toluene).

Stellenbosch University https://scholar.sun.ac.za

The resulting grafts were found to be useful as a chromatographic stationary phase for the selective encapsulation of Na^+ in the presence of other alkali cations (Li^+, K^+, and Cs^+). This behavior is due to calixarene's most important ability, which is to form strong complexes with different species as a result of possessing particular functional groups (here the lower-rim esters). Using diverse functional groups has resulted in producing calixarene polymers with different degrees of selectivity toward various guests. Later in this dissertation, more of these examples will be discussed.

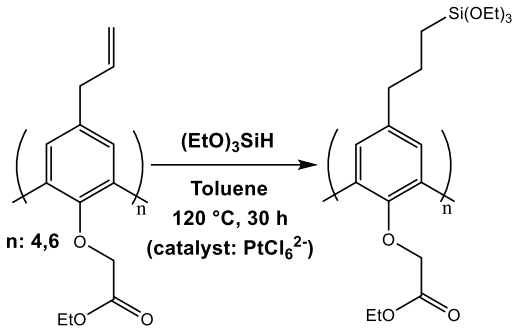

Scheme 1.3 Hydrosilation addition on a p-allylcalix[n]arene ethyl acetate based on the work of McKervey and co-workers[23]

Other than this hydrosilylation example, silica-bound calixarenes are typically prepared using a primary amine-tethered version of silica. In this case, the amine functional group of the silica source reacts with a highly reactive functional group of a functionalized calixarene (e.g. an acid chloride) to form a desired silica-bound calix[4]arene graft. As an example, in 2009 Erdemir and Yilmaz employed three silica-bound calixarenes for the immobilization of a particular type of lipase (*Candida rugosa*).[20] In this experiment, the fully esterified versions of calix[4]arene, calix[6]arene and calix[8]arene were reacted separately with the bis-amine-tethered silica (reflux in toluene/methanol, 120 h) forming an amide bond between the calixarene and the silica derivative through a nucleophilic acyl substitution mechanism. The resulting silica-bound calixarene was anchored to the enzyme through its free amine terminus with the help of glutaraldehyde as the coupling agent (imine bond formation in ethanol after 12 hours of shaking at pH=7). The temperature and pH were regulated for each case, resulting in relatively good stability and adaptability for the calixarene-grafted enzyme compared to the free enzyme (**Scheme 1.4**).

In the same regard, another example worth mentioning is the use of a mono acid chloride calix[4]arene for grafting onto a primary amine-tethered silica compound in a paper by Tabakci and Yilmaz.[24]

Stellenbosch University https://scholar.sun.ac.za

Calixarene-grafted silica has been used in applications for the removal of heavy metals due to their strong complexation ability. Tabakci and Yilmaz exploited this by using a silica-bound calix[4]arene for the removal of Cu(II) ion from aqueous media. Their mono acid-chloride calix[4]arene reacted with a primary amine-tethered silica gel (in toluene at room temperature for 5 hours) to yield the desired silica-bound calix[4]arene. This calix[4]arene bore nitrile functionalities which could show sorption properties for Cu(II) according to the previous reports by the same group.[25] This work reported that the best removal of Cu(II) could be achieved under mildly acidic conditions (pH=6) at 25 °C (**Scheme 1.5**).

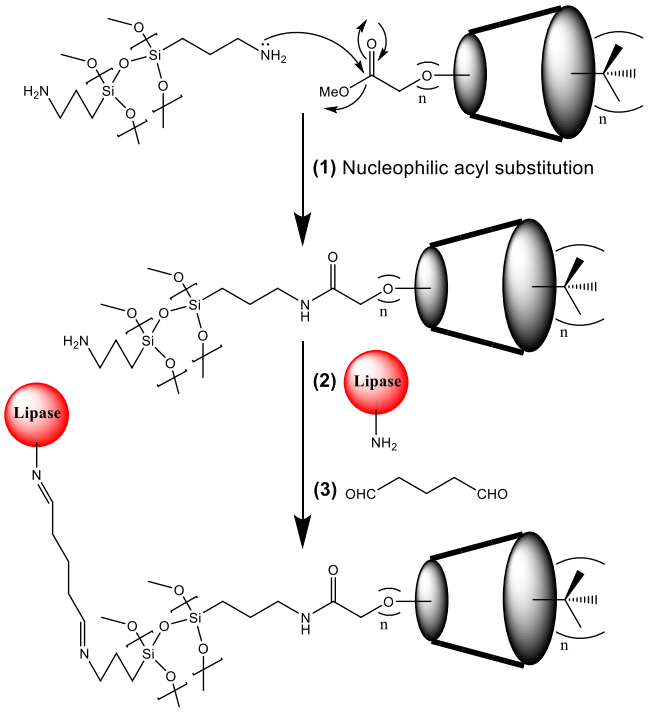

Scheme 1.4 Silica-bound calixarenes for lipase immobilization based on the work of Erdemir and Yilmaz[20]

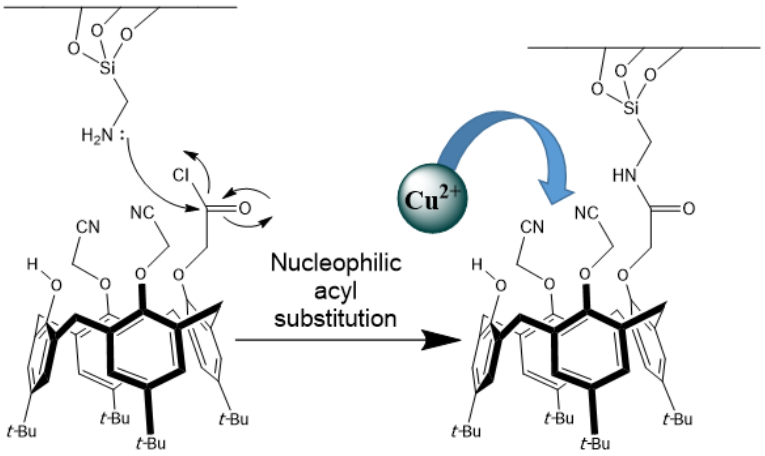

Scheme 1.5 Silica-bound calixarene for Cu(II) removal based on the work of Gezici et al.[25]

Stellenbosch University https://scholar.sun.ac.za

1.4.2 Materials incorporating calixarenes – Calixarenes grafted onto polymers

Calixarene-grafted polymers made using the grafting onto approach have also been a subject of interest for researchers. In this category, one of the earliest approaches for attachment of calixarenes was by using a very reactive acryloyl-based polymer. As was the case in the previous section, from the very beginning the calixarenes attached to the polymers have also been studied in terms of their potency to form strong complexes with other species. As an example, in 1995 Yilmaz and Deligöz published a paper on a calix[4]arene-tetraacetate attached by both an oligomer and more importantly an acryloyl-based polymer (polyacryloyl chloride). In both cases, $BF_3O(C_2H_5)_2$ was used as the Lewis acid to facilitate a Friedel-Crafts reaction putting an acyl group (in case of the polymer) and an alkyl group (in case of the oligomer) on the non-substituted *para* position of the calix[4]arene. The resulting grafts also showed selective complexation with Na^+ (NaSCN was used as the cation source) (**Scheme 1.6**).[26]

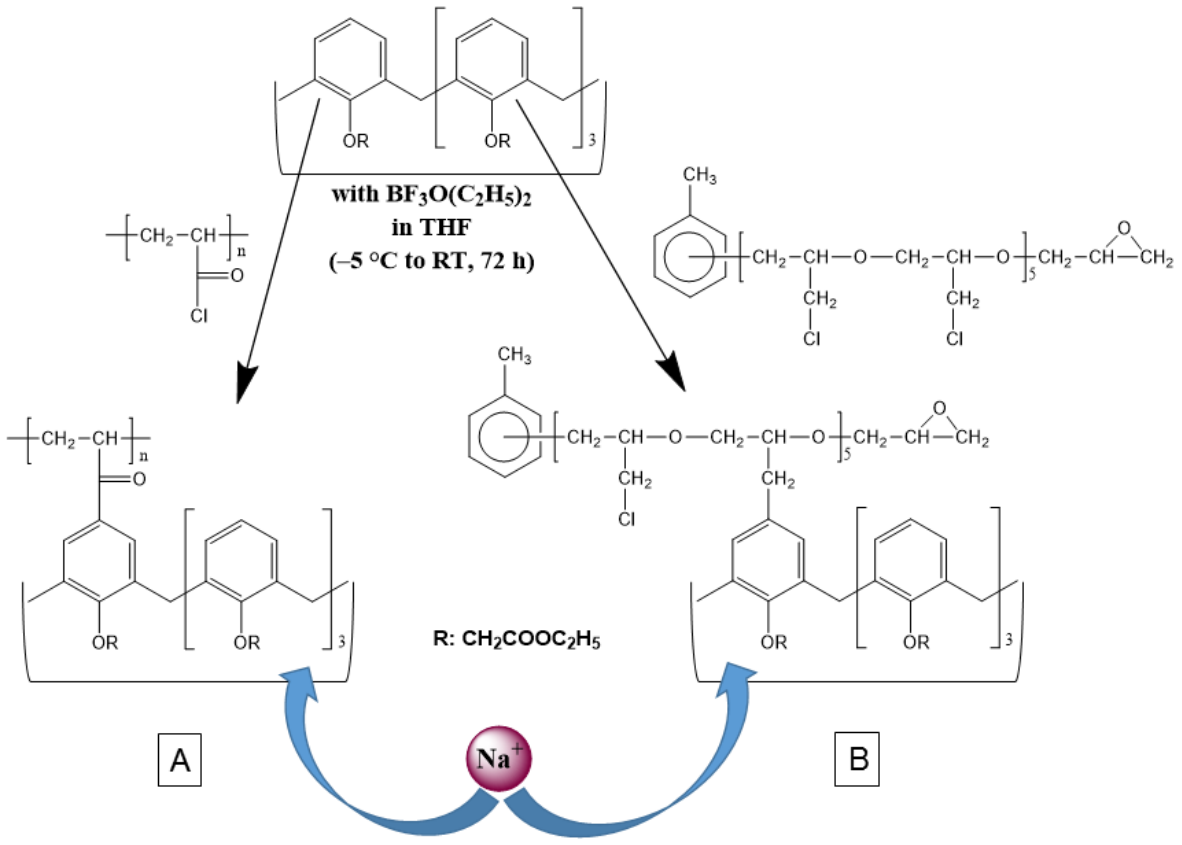

Scheme 1.6 Polymeric and oligomeric calix[4]arenes for Na^+ encapsulation based on the work of Yilmaz and Deligöz[26]

However, the most common polymer for attaching calixarenes has been polystyrene or its derivatives. As the first reported example, Yilmaz and Deligöz in 1996 attached a calix[4]arene

Stellenbosch University https://scholar.sun.ac.za

to a chloromethylated polystyrene polymer.[27] The ester-free product (after alkaline hydrolysis) exhibited selectivity toward Fe^{3+} cations in an aqueous solution containing multiple transition metal cations. It was also observed that the lower rim-supported calix[4]arene could act as a more competent carrier for cation extraction. This lower rim-supported calix[4]arene was produced through the reaction between the polymeric support and the calix[4]arene in an alkaline environment (using K_2CO_3 as the base in THF/acetone under reflux for 48 hours) that went through an S_N2 mechanism (**Scheme 1.7**). Employing $BF_3O(C_2H_5)_2$ as the Lewis acid (in THF at room temperature for 168 hours) on the other hand resulted in the formation of the upper rim-supported calix[4]arene which did not show the above-mentioned selectivity toward Fe^{3+}.

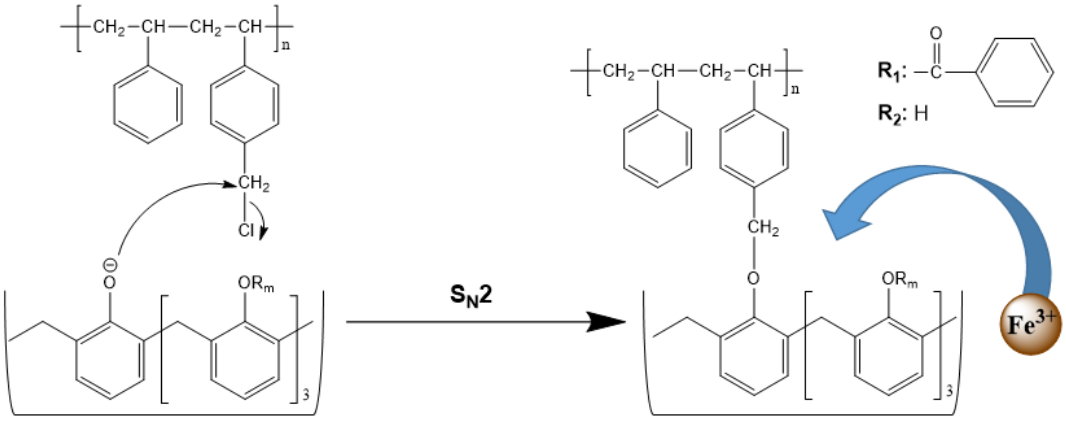

Scheme 1.7 Calix[4]arene-grafted polymer for Fe^{3+} extraction based on the work of Yilmaz and Deligöz[27]

In the same regard, Jain *et al.* published a paper on the use of a calix[4]arene-semicarbazone grafted onto a crosslinked chloromethylated polystyrene also known as Merrifield resin (a well-known resin in polymer science)[28] for the separation and preconcentration of four heavy metal cations: La(III), Ce(III), Th(IV) and U(VI).[29] Like the previous example, an S_N2 reaction (reflux in THF/DMF for 24 hours) furthered the calix[4]arene grafting onto the polymeric support. The mentioned resin demonstrated a proper separation of the cations, in addition to providing a high sorption degree for each of them at a specific pH (**Scheme 1.8**).

As another example in 2003, Yilmaz *et al.* published an article focusing on the synthesis of several *p-t*-butylated calix[4]arenes grafted on the lower rim with a bromoethylated polystyrene resin (again an S_N2 reaction for grafting in DMF with NaH as the base at 60-70 °C for 360 hours).[21] The chelating ability of these grafts was assessed through their response toward a series of alkali and transition metals. It was implied that the polymeric ionophores were not responding selectively to the cations, nonetheless, they all possessed better binding properties

Stellenbosch University https://scholar.sun.ac.za

compared to their corresponding calix[4]arene monomer. In addition, these ionophores were separately studied with regards to their dichromate encapsulation and surprisingly were found to be effective even at the neutral pH (pH=7). Overall, this report was important in terms of demonstrating that polymeric calix[4]arenes are capable of encapsulating both anions and cations (**Scheme 1.9**).

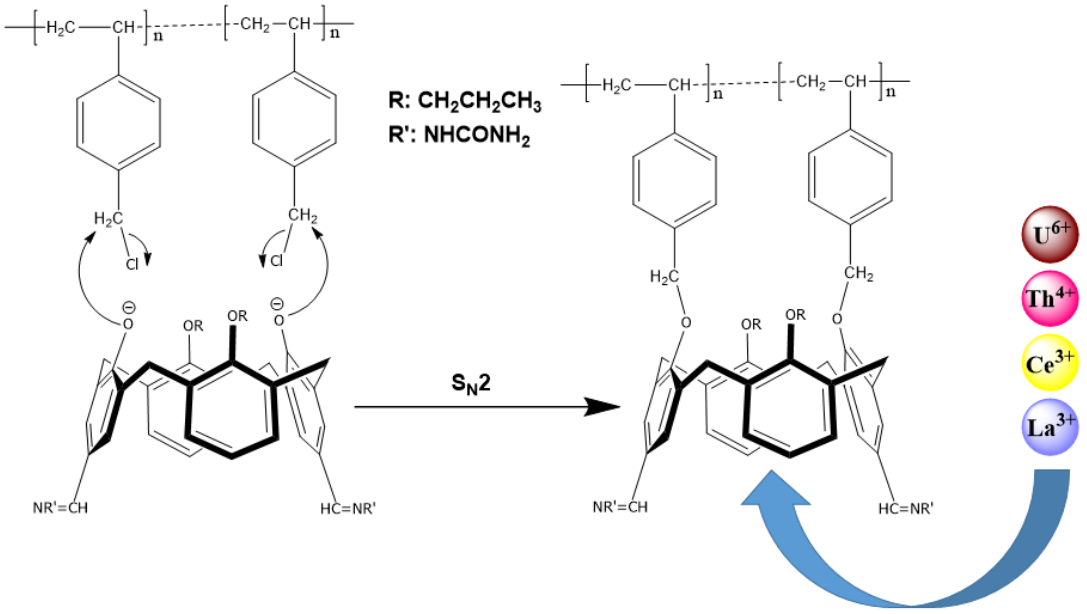

Scheme 1.8 Calix[4]arene-grafted polymer for heavy metal ion separation based on the work of Jain et al.[29]

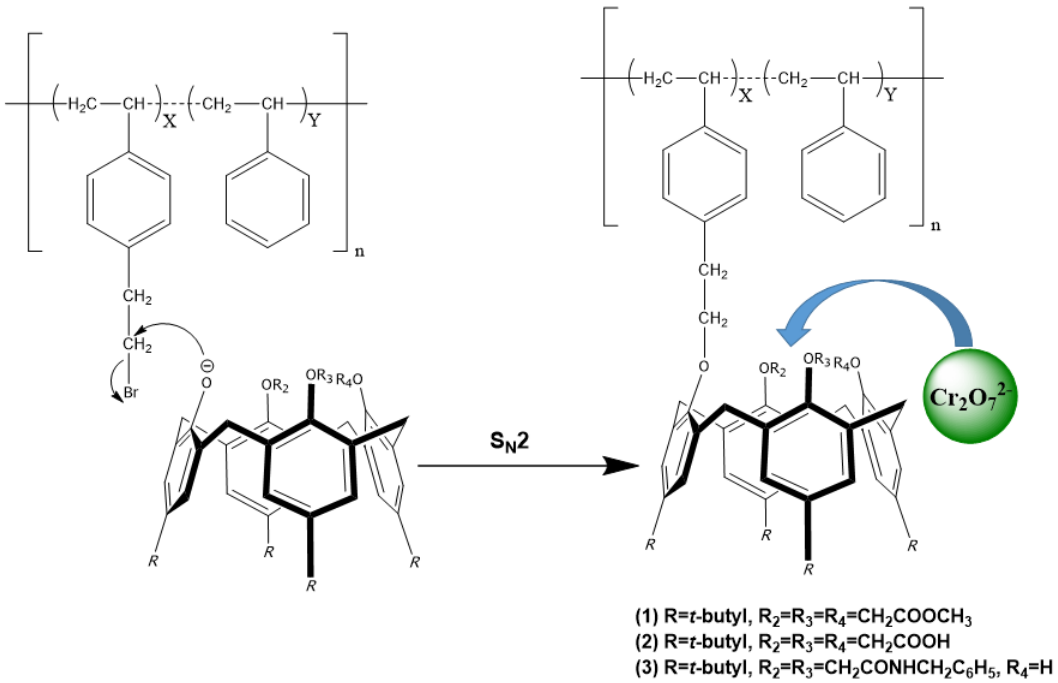

Scheme 1.9 Calix[4]arene-grafted polymers for both dichromate extraction and metal ion complexation based on the work of Yilmaz and co-workers[21]

Stellenbosch University https://scholar.sun.ac.za

After obtaining these promising results for dichromate encapsulation, the same group in 2006 also reported the synthesis of a couple of novel calix[4]arene-grafted Merrifield resins by means of a Mannich reaction.[30] These modified calix[4]arenes underwent an S_N2 reaction (using NaH and NaI in THF/DMF at 70 °C for 48 hours). These upper-rim modified grafts were employed for the extraction of dichromate anion under acidic pH ($Na_2Cr_2O_7$ was the dichromate origin). Liquid-liquid extraction and solid-liquid absorption techniques were used for both grafts. They demonstrated very good results regarding both extraction and absorption of dichromate anion (**Scheme 1.10**).

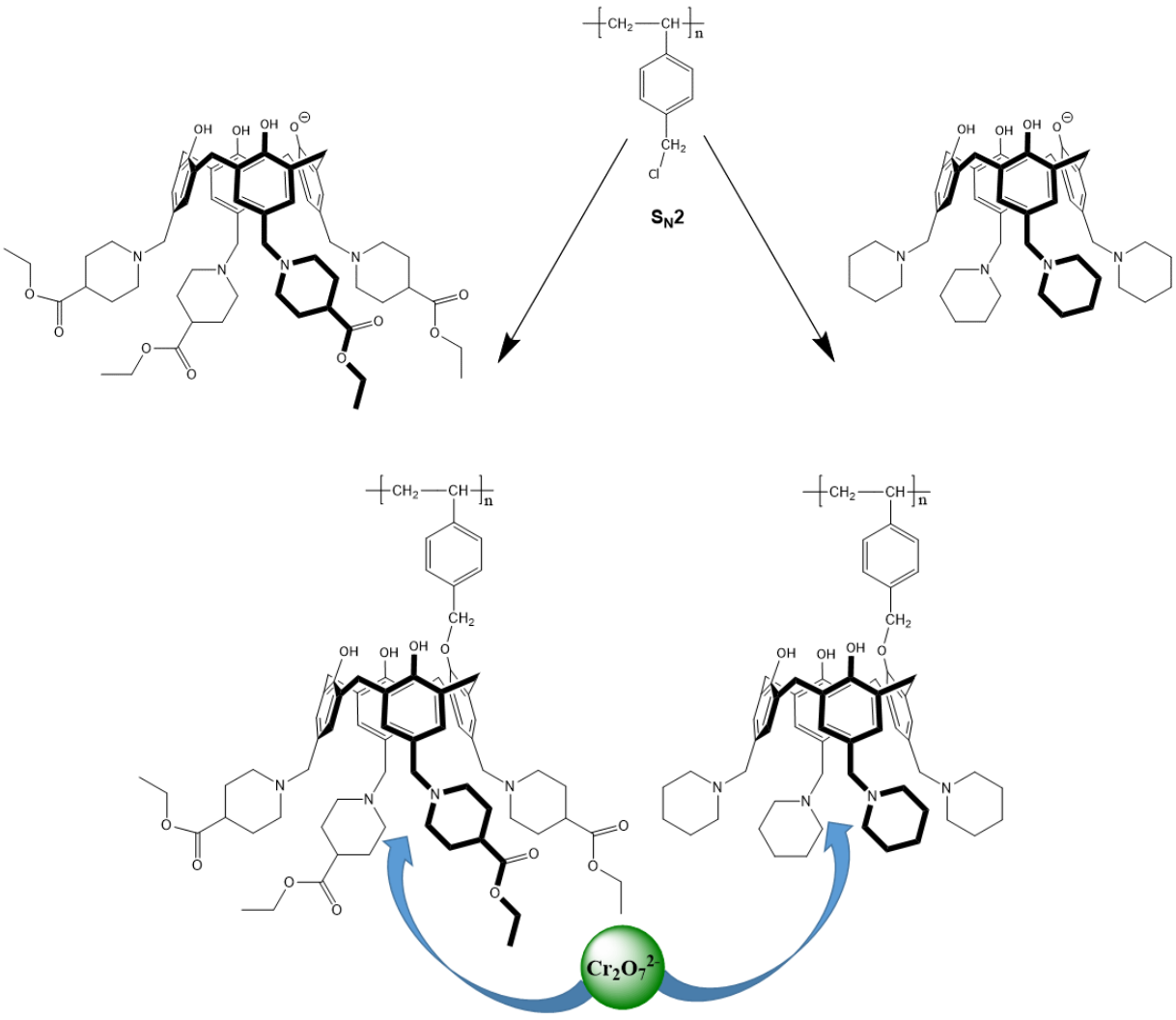

Scheme 1.10 Calix[4]arene-grafted polymers for dichromate extraction based on the work of Yilmaz and co-workers[30]

Ultimately, the same researchers in 2006 also developed another approach for the extraction and absorption of dichromate anion with Merrifield resin.[31] This time they produced three tetra-functionalized calix[4]arenes with a nucleophilic substitution method on the calix[4]arene

Stellenbosch University https://scholar.sun.ac.za

upper rim. The upper rim functionalities were respectively, a tertiary amine, an alkyl nitrile, and an alkylamine. These calix[4]arenes were grafted onto Merrifield resin (again an S_N2 approach with NaH and NaI in DMF at 60-70 °C for 52 hours). In addition, the selectivity of these grafts toward dichromate anion was examined in the presence of other anions. Overall, not only did the synthesized polymeric calix[4]arenes respond with highly selectively to dichromate anion (compared to other anions present in the environment), it was also shown that this form of the calix[4]arene could extract and absorb dichromate anion more efficiently than its corresponding monomer. Moreover, it was perceived that the liquid-liquid system was more successful in terms of dichromate removal from an aqueous media in comparison to the liquid-solid extraction (**Scheme 1.11**).

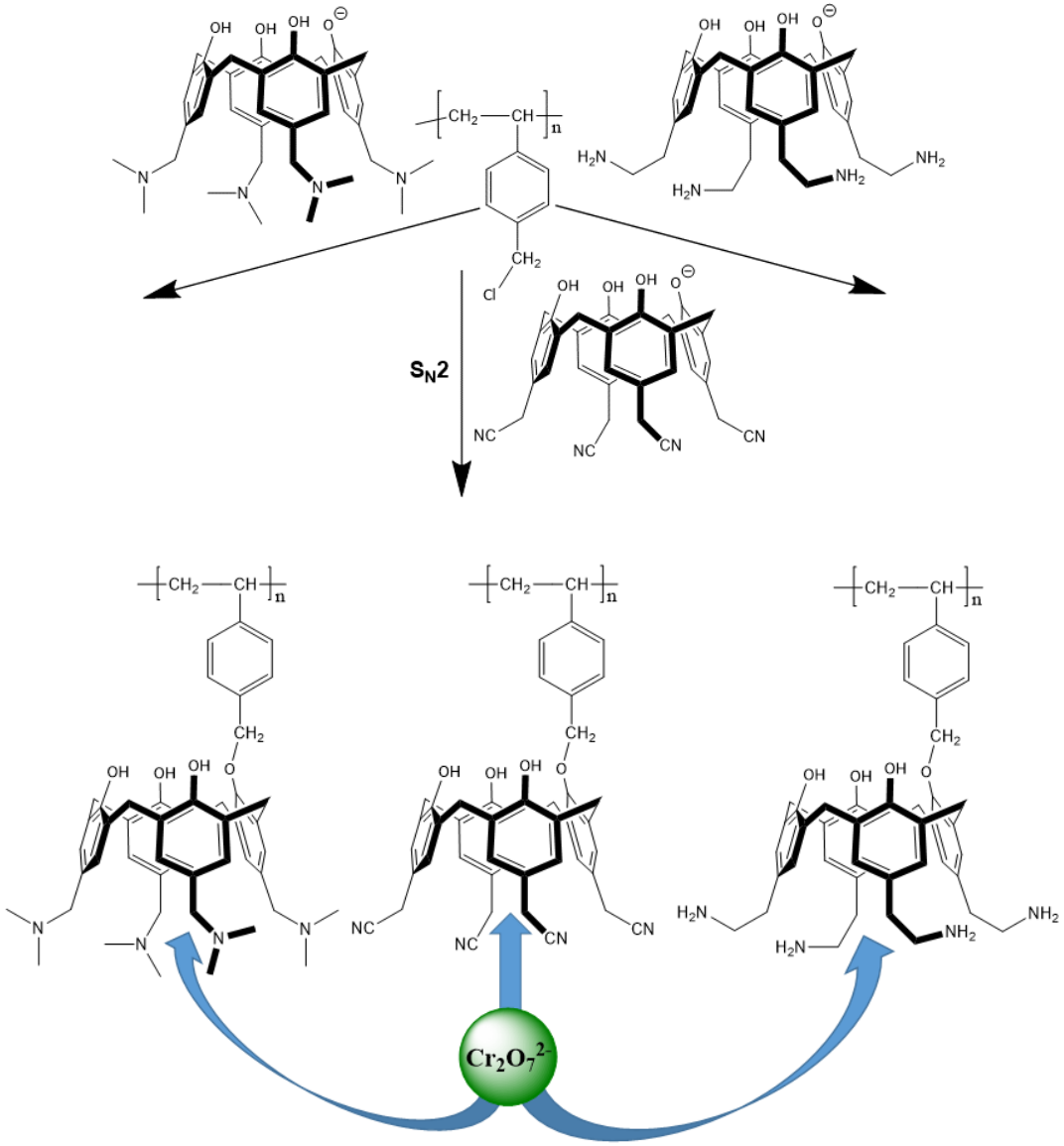

Scheme 1.11 Calix[4]arene-grafted polymers for dichromate extraction based on the work of Yilmaz and co-workers[31]

Stellenbosch University https://scholar.sun.ac.za

Poly(ethylene glycol) (PEG) has also been employed as the solid support for calixarenes. To give an example, for years the sensing and detection of NO_2 gas using the calixarene optical sensors used to be a challenge. NO_2 is a major air pollutant and an important threat to the natural environment through causing acid rains,[32] high cancer rate[33-35] and other biologically harmful effects.[36] In 2004, Kang and Rudkevich used a commercial PEG (a PEG monomethyl ether) and mesylated this with methanesulfonyl chloride (with Et_3N as the base in CH_2Cl_2 at 0-5 °C for 2 hours) to prepare the desired support.[37] This mesylated PEG support was used for the grafting of a 1,3-alternate calix[4]arene on its lower rim through a simple S_N2 reaction (with *t*-BuOK in THF at 50 °C for 20 minutes). With the help of this graft, colorimetric sensing of NO_2/N_2O_4 gases (in an equilibrium state) was achieved in both solution and solid state (**Scheme 1.12**). The group also suggested that the NO_2 group reacted with the calix[4]arene and formed a stable nitrosonium (NO^+)-calix[4]arene complex and speculated that its high association constant was due to the charge transfer interactions between the nitrosonium and the calix[4]arene π-rich cavity.

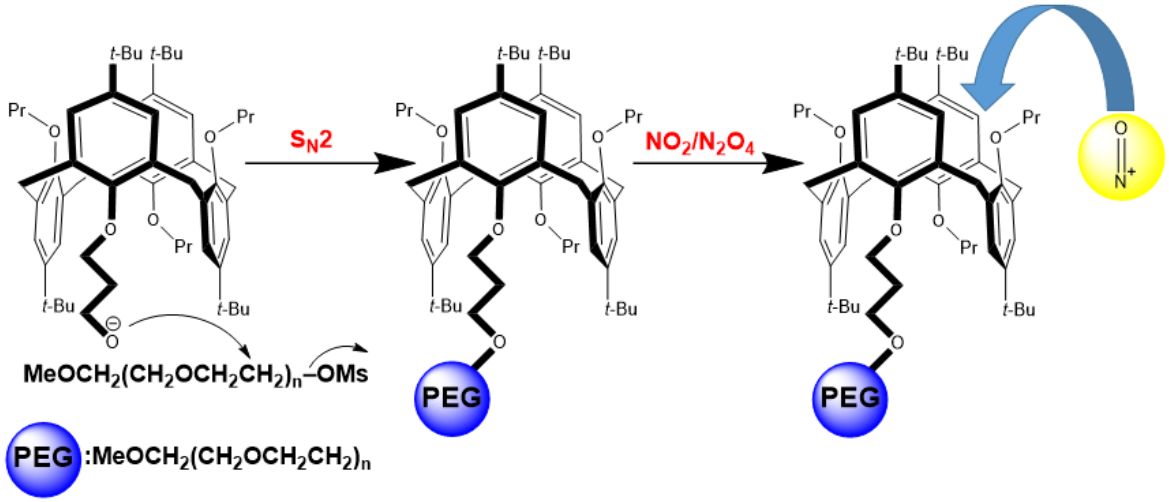

Scheme 1.12 Calix[4]arene-grafted poly(ethylene glycol) for conversion and storage of NO_2 based on the work of Kang and Rudkevich[37]

There have also been reports on using dextran (a naturally occurring polymer) as the polymeric support for calixarenes. For example, Engrand and Regnouf-de-Vains showed a multi-step approach for the synthesis of a bifunctional calix[4]arene which was later anchored onto a water-soluble dextran (Na_2CO_3 was the base choice to form the nucleophilic version of the dextran and grafting that onto the calix[4]arene through an S_NAr reaction with its cyanuric chloride moiety[b] in DMSO/DMF at 30-70 °C).[38] The graft formed a strong yellow-orange

[b] 2,4,6-Trichloro-1,3,5-triazine

Stellenbosch University https://scholar.sun.ac.za

complex with Cu^{+} in water and its chromophoric feature was confirmed with spectroscopic methods (including UV-Vis titration). However, the grafting was performed in low yield and required further optimization (**Scheme 1.13**).

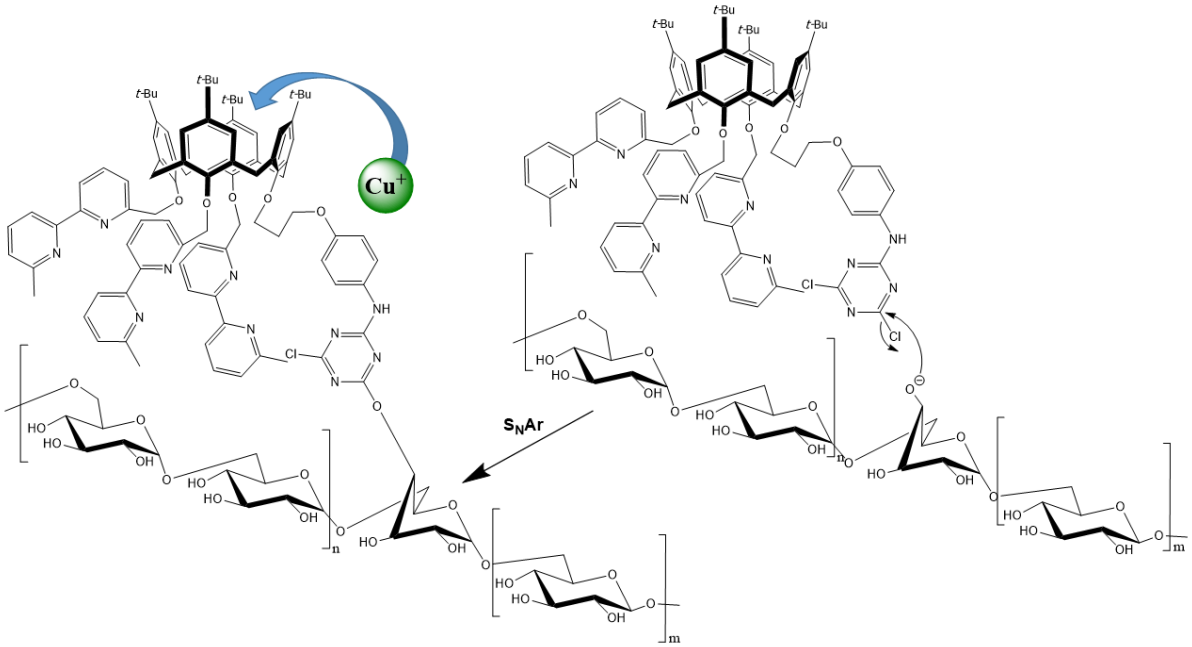

Scheme 1.13 Bifunctional calix[4]arene-grafted dextran for titration studies on Cu^{+} based on the work of Engrand and Regnouf-de-Vains[38]

There have also been reports of more uncommon polymeric supports used for grafting calixarenes. As an example, in 2010 Yilmaz and co-workers synthesized an upper rim bis-substituted calix[4]arene using *N*-methylglucamine functionalities and then grafted it onto poly[(phenyl glycidyl ether)-*co*-formaldehyde].[39] The grafting occurred as a result of a nucleophilic attack by the free lower-rim hydroxyls (facilitated by K_2CO_3 as the base) and opening of the epoxide moiety of the support in acetonitrile under reflux for 16 hours. This graft showed a high degree of selectivity not only toward dichromate anion, but also arsenate anion at very low pHs in the presence of several other anions (**Scheme 1.14**).

Another example that was introduced in 2010 was by Granata *et al*. on the synthesis of polymer-supported calix[4]arenes with potential for solid phase studies through condensation of thymine nucleotide units on their upper rim.[40] In that process, initially the calix[4]arene lower rim tether was separately anchored to two different supports (CPG[c] and TentaGel[d])

[c] Controlled pore glass[41,42]

[d] Grafted copolymer produced by polyethylene glycol and low-crosslinked polystyrene[43]

Stellenbosch University https://scholar.sun.ac.za

through a coupling reaction (facilitated by HATU,[e] DIPEA,[f] and DMAP[g] in DMF at room temperature for 24 hours) and ultimately the upper rim reaction with DMT groups[h], yielded the desired tetrasubstituted nucleotide–calixarene as a result of a solid phase synthesis (**Scheme 1.15**).

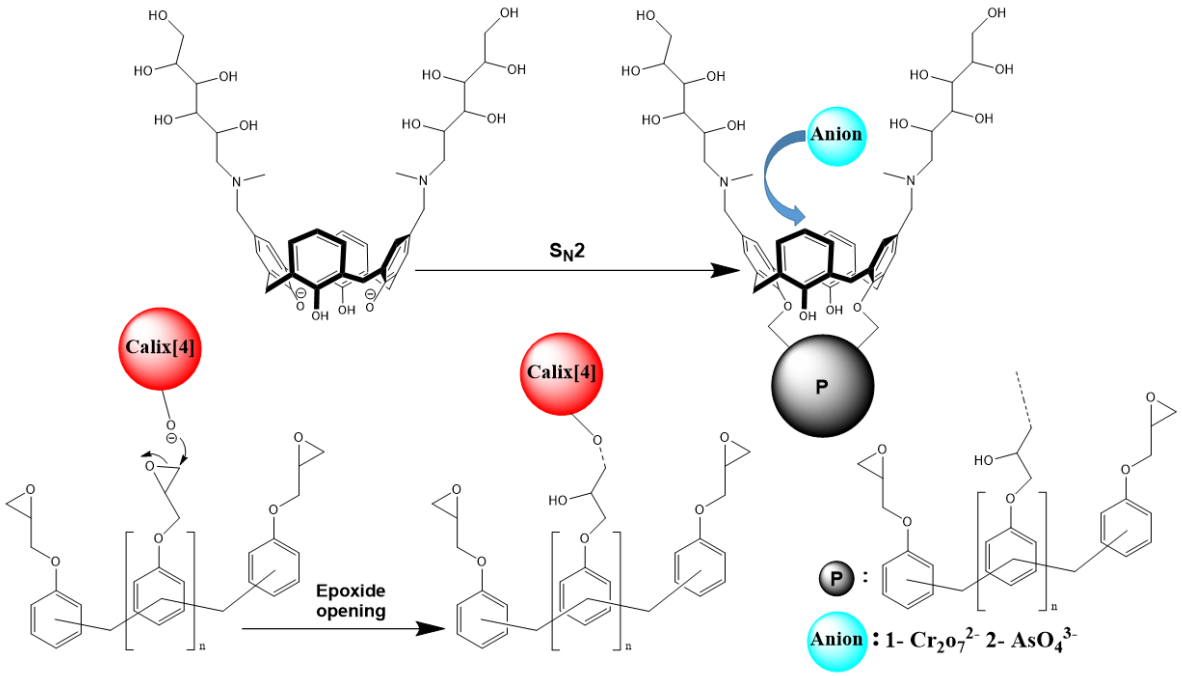

Scheme 1.14 Calix[4]arene-grafted polymer for dichromate and arsenate removal based on the work of Yilmaz and co-workers[39]

[e] 1-[Bis(dimethylamino)methylene]-1*H*-1,2,3-triazolo[4,5-*b*]pyridinium 3-oxide hexafluorophosphate

[f] *N*-Ethyl-*N*-(propan-2-yl)propan-2-amine

[g] *N*,*N*-Dimethylpyridin-4-amine

[h] 5'-Dimethoxytrityl-3'-deoxythymidine 2'-[(2-cyanoethyl)-(*N*,*N*-diisopropyl)]-phosphoramidite

Stellenbosch University https://scholar.sun.ac.za

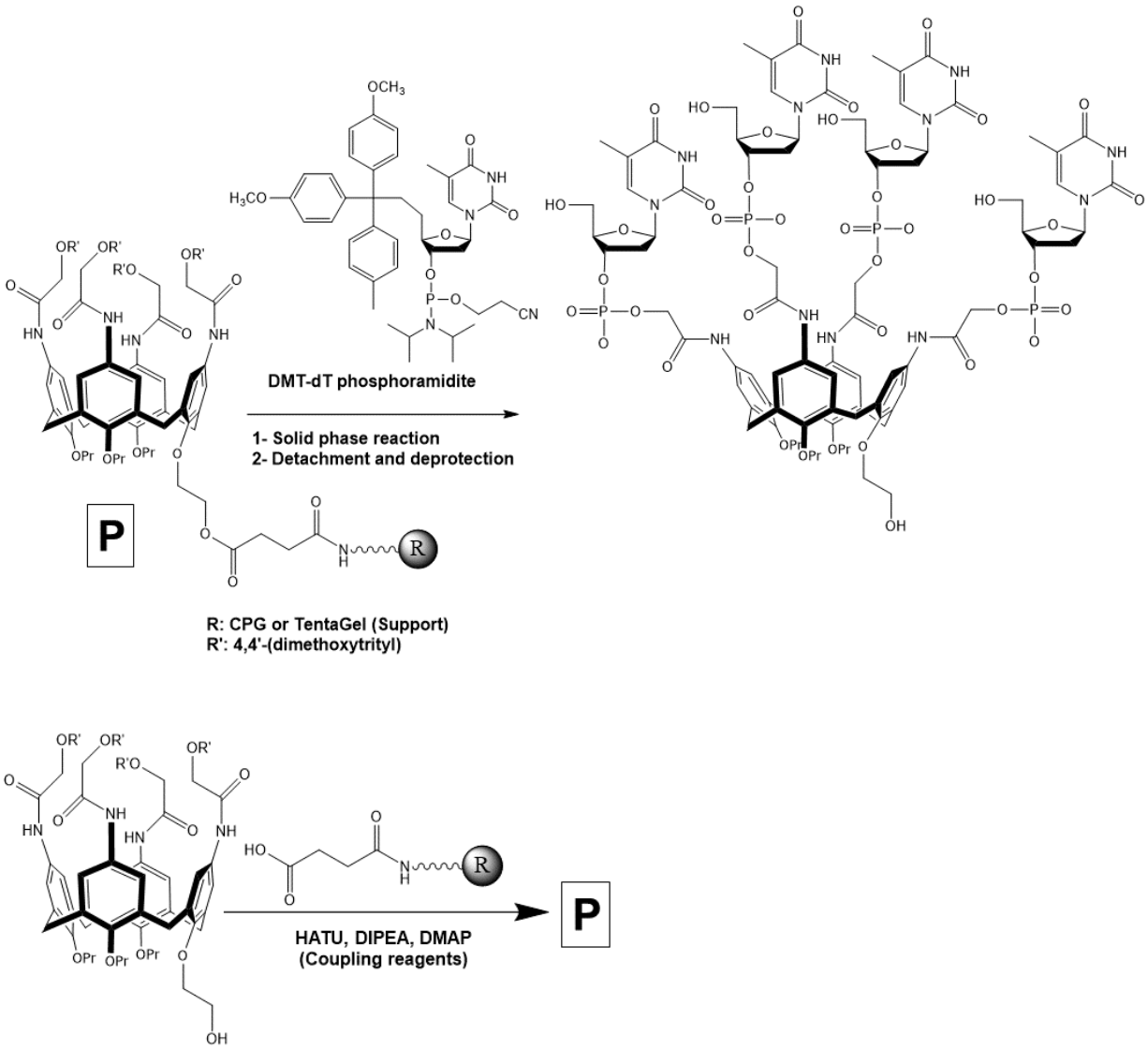

Scheme 1.15 Solid phase studies on calix[4]arene-grafted polymer based on the work of Granata et al.[40]

1.4.3 Materials incorporating calixarenes – Calixarenes grafted through polymers

There have been many reported examples for calixarenes grafted through polymers in the literature. The most common way of polymerizing a calix[4]arene is using an acryloyl-based calix[4]arene and either homo-polymerize it or add another vinyl-based monomer and copolymerize them together.

As an example, in 1991 Harris and McKervey reported the synthesis of a calix[4]arene methacrylate, which was later homo-polymerized with AIBN[i] (free radical conditions in toluene at 65 °C for 17 hours). Considering the fact that the polymerizable calixarenes can also form strong complexes with cations, this homopolymer of calix[4]arene was tested in terms of

[i] 2,2′-Azobis(2-methylpropionitrile)

Stellenbosch University https://scholar.sun.ac.za

its complexation ability with Na^+. The graft formed a strong complex with Na^+ upon adding sodium thiocyanate **(Scheme 1.16)**.[44]

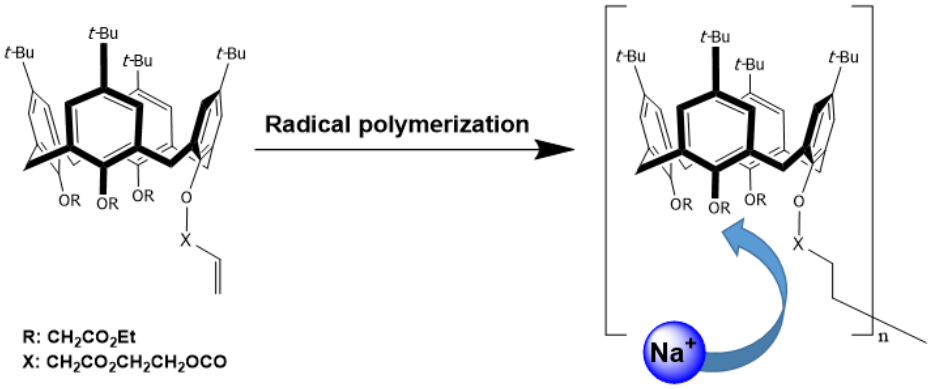

Scheme 1.16 Calix[4]arene-grafted polymer for Na^+ encapsulation based on the work of Harris and McKervey[44]

As another example, in 2000 Malinowska *et al*. showed the successful grafting of tetraethyl ester possessing a calix[4]arene (on the wider rim) and one polymerizable group (methacrylamide on the narrow rim) with an optimized polymeric matrix.[45] The matrix was based on an appropriate ratio between IDA (isodecyl acrylate) and MM (methyl methacrylate). The polymerization was performed using a redox system (ammonium persulfate as the initiator) in water at 70 °C until the full conversion of monomers was achieved. According to potentiometric studies, the synthesized copolymer acted as a proper ion-selective membrane for Na^+ whose results were comparable to the ones obtained from the PVC-made membranes with a free calix[4]arene as their ionophores (**Scheme 1.17**).

In 2004, Tabakci *et al.* produced a distal dibenzonitrile *p*-*t*-butylated calix[4]arene with an acrylamide substituent on its lower rim. The desired graft was acquired via copolymerization of the calix[4]arene with styrene under free radical conditions (AIBN at 65 °C). The product exhibited no selectively toward any metal cation, but it possessed some encapsulation capability for the dichromate anion. It was also shown that this graft was a more potent extractant than its calix[4]arene parent for the dichromate anion (**Scheme 1.18**).[46]

Stellenbosch University https://scholar.sun.ac.za

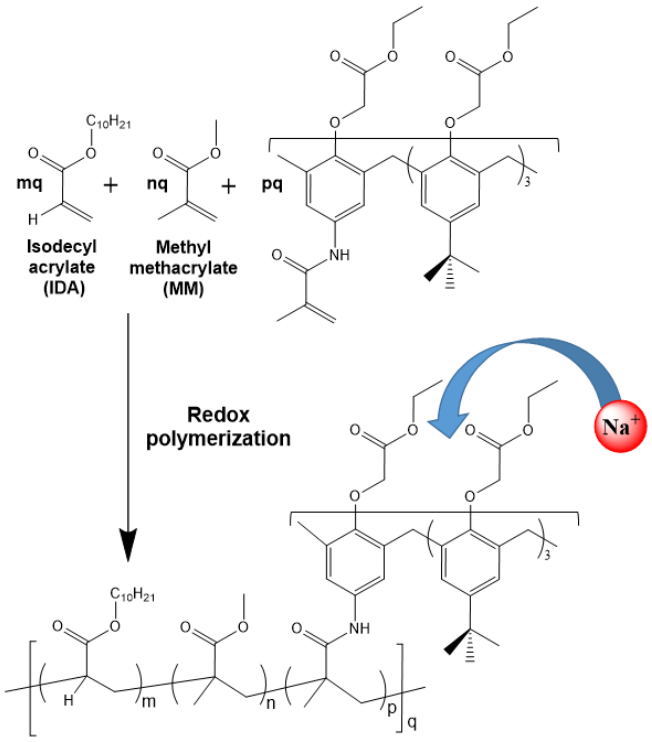

Scheme 1.17 Calix[4]arene-grafted polymer as an ion-selective membrane for Na^+ based on the work of Malinowska et al.[45]

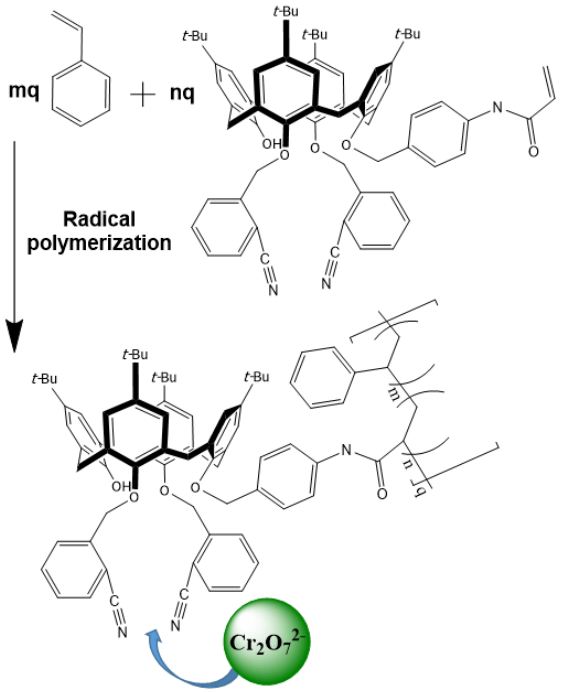

Scheme 1.18 Dibenzonitrile p-t-butylated calix[4]arene-grafted polymer for dichromate extraction based on the work of Tabakci et al.[46]

Stellenbosch University https://scholar.sun.ac.za

Synthesizing polymerizable calixarenes which can later be polymerized employing ROMP (ring opening metathesis polymerization) has also been a subject of interest. For example, Abd-El-Aziz *et al*. reported the successful synthesis of a diazotized calix[4]arene with a polymerizable group on its upper rim (norbornene).[47] It was known that the diazotized calixarenes have potent chromogenic centers that have shown potential in colorimetric studies.[48] Therefore, the polymerization of this functionalized calix[4]arene with the purpose of producing a graft which could provide these features on solid support was performed with Grubbs' second generation catalyst using ROMP approach (in DCM at room temperature for 45 minutes). The acquired azacalix[4]arene-grafted polymer showed a significant bathochromic shift under acidic conditions in THF; however, its thermal stability was substantially lower than that of the same polymer without an azo functionality (**Scheme 1.19**). Later in chapter 4 of this dissertation, a series of azacalix[4]arenes will be investigated thoroughly with regard to their potential colorimetric features.

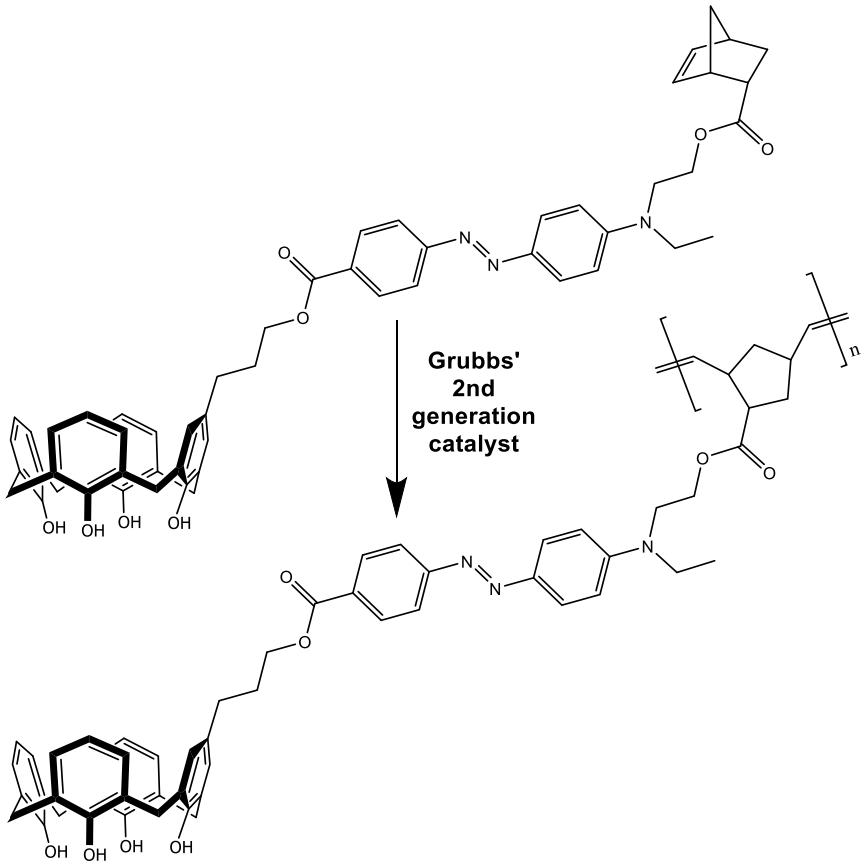

Scheme 1.19 Azacalix[4]arene-grafted polymer for colorimetric studies based on the work of Abd-El-Aziz et al.[47]

Polyether and polyester versions of calixarenes can also be made through condensation copolymerization of a functionalized calixarene together with another monomer. For example,

Stellenbosch University https://scholar.sun.ac.za

in 1997 Dondoni *et al*. synthesized a number of copolyethers and copolyesters grafts of calix[4]arene capable of extracting Ag^+.[49] This was achieved via copolymerization of several 1,3-dimethyl calix[4]arenes with bisphenol A.[j] In both cases, tetrabutylammonium hydrogen sulfate was used as the phase transfer catalyst. The picrate test was employed for studying the binding properties of these grafts toward the cation (following Pedersen's procedure).[50] No absorption could be achieved without the calix[4]arene presence (**Scheme 1.20**).

Polyurethane-based calixarenes are the last category of compounds worth mentioning in this section. Dondoni *et al*. reported the successful synthesis of a series of polyurethane-based calix[4]arenes (with both cone and 1,3-alternate conformations) through polycondensation reaction of several functionalized calix[4]arenes and 2,4-diisocyanato-1-methylbenzene (TDI) in the presence of $(C_{11}H_{23}CO_2)_2SnBu_2$ (the catalyst) in toluene (80 °C, 8 h). These polymerized calix[4]arenes were used for selective recognition and extraction of Ag^+ in addition to Rb^+ and Cs^+ ions (**Scheme 1.21**).[51]

Overall, due to the convenience of applying the ''grafting onto approach'' to our calix[4]arene scaffold (compared to the ''grafting through approach'' which could possibly undergo polymerization challenges), it was chosen as the first grafting choice of this project. In the next sections, our polymer choice for grafting and its features will be explained in detail.

[j] 4,4'-(Propane-2,2-diyl)diphenol

Stellenbosch University https://scholar.sun.ac.za

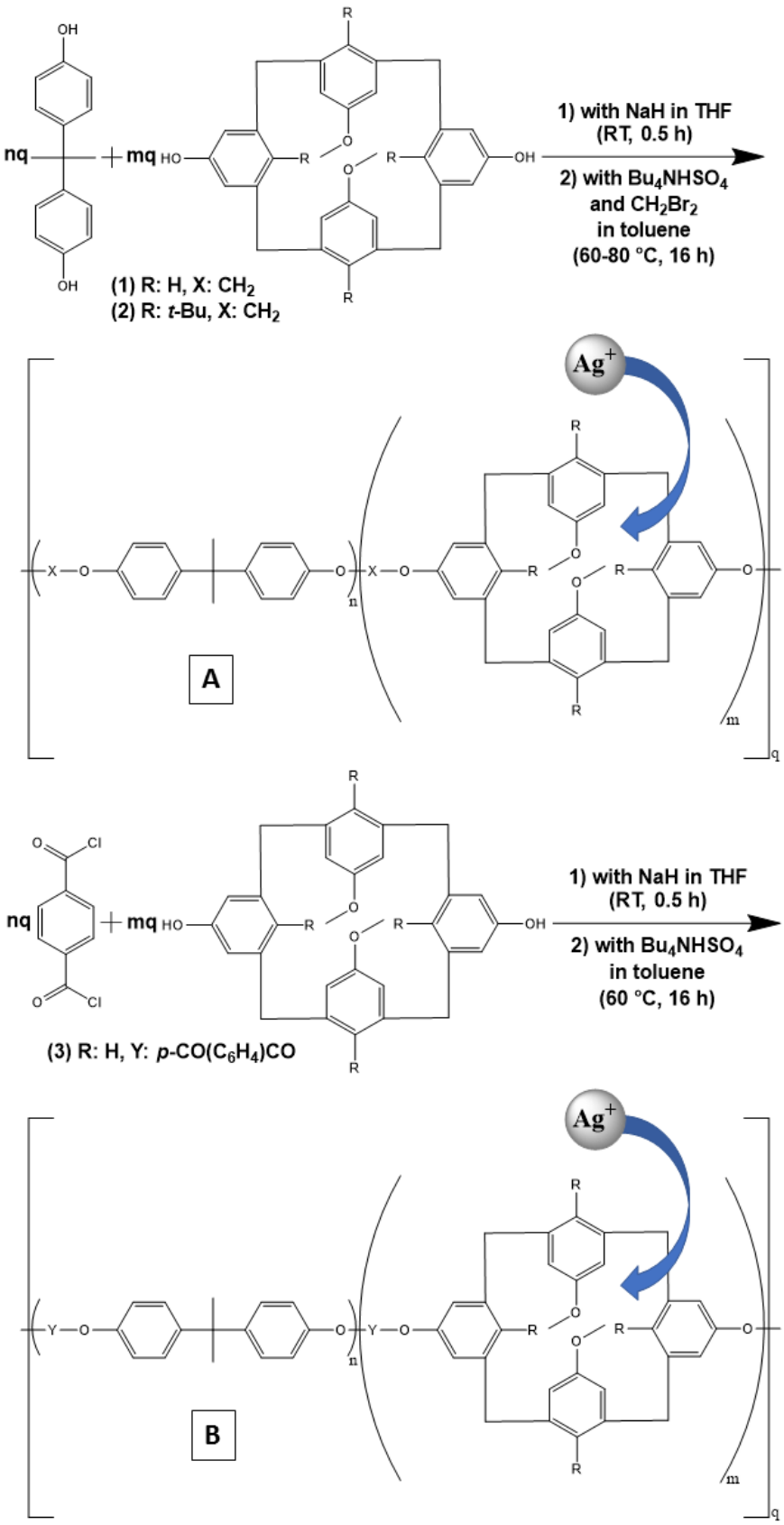

Scheme 1.20 Calix[4]arene-grafted polymer for Ag^+ complexation (A: Polyether, B: Polyester) based on the work of Dondoni et al.[49]

Stellenbosch University https://scholar.sun.ac.za

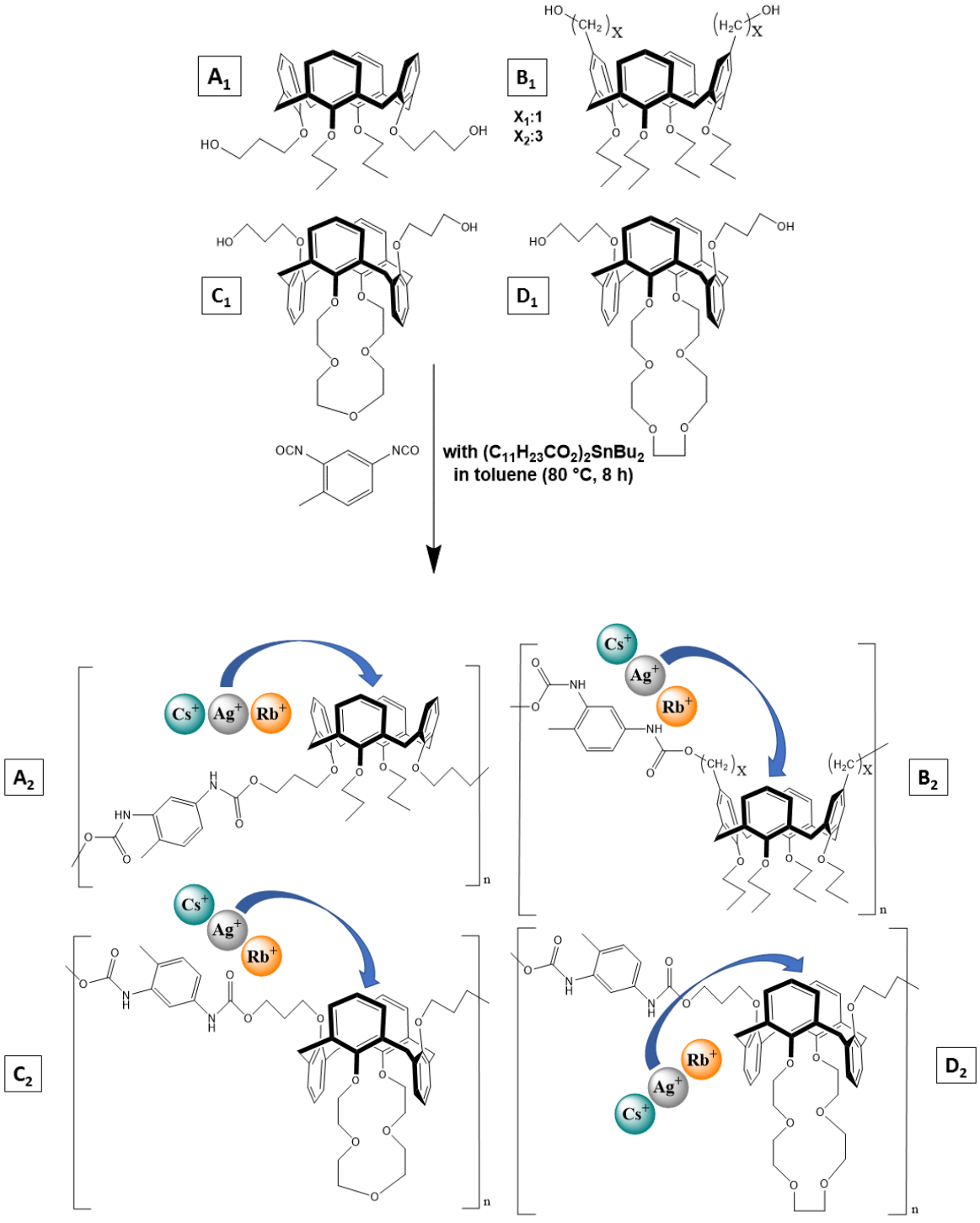

Scheme 1.21 Calix[4]arene-grafted polymers for selective recognition of Ag^+, Rb^+ and Cs^+ based on the work of Dondoni et al.[51]

1.5 PSMA introduction

Poly(styrene-*co*-maleic anhydride) (PSMA) is a well-known thermoplastic polymer that has been commercially available since the 1930s. It can be made as either a copolymer or as an alternating copolymer. Plenty of synthetic procedures have been presented for its synthesis

Stellenbosch University https://scholar.sun.ac.za

such as Ang and Harwood's method through which monomers (styrene and maleic anhydride) should be heated in dioxane with benzoyl peroxide (the radical initiator) to yield the desired polymer.[52] Depending on the approach, different PSMAs can be synthesized with different degrees of maleic anhydride which affects the chemical and physical properties of the polymer (**Figure 1.6**).[53]

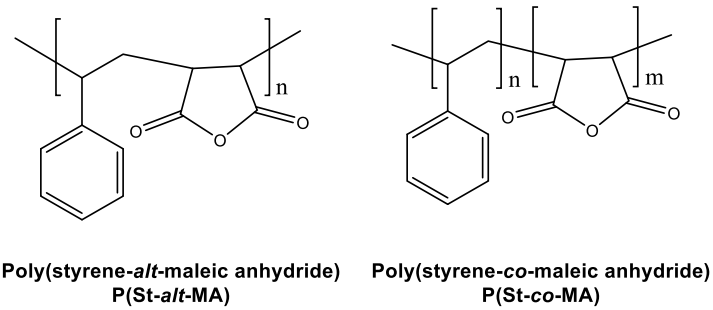

Figure 1.6 Different types of PSMA

Almost every kind of applicable change on PSMA which may result in different uses stems from the modification of its succinic anhydride moiety. This very reactive moiety can be easily modified with a wide range of nucleophilic reagents such as amines and alcohols.[54,55] This issue will be discussed in detail in chapter 3 of this dissertation.

SMA polymers (solely or as a blend with other polymers) possess features such as a high glass transition temperature, high heat resistance, dimensional stability, and rigidity.[56]

1.6 PSMA applications

As previously mentioned, due to their promising physical and chemical properties, PSMA derivatives have been used for many applications. PSMA's most important capability is grafting other chemical or biochemical species through reaction onto its succinic anhydride group. For chemical species attachment, the imidization of PSMA by aniline during an extrusion process,[54] or ethanolization of PSMA and its prospects for coating purposes,[57] or even a temperature and pH-dependent PSMA graft with POP (poly(oxypropylene)) pendant groups possessing lower critical solution temperature (LCST) in aqueous solutions in a particular temperature range,[58] are worth mentioning. Regarding biochemical species attachment, protein detection by grafted PSMA nanoparticles[59] or immobilization of enzymes[60] have also been reported (**Scheme 1.22**).

Stellenbosch University https://scholar.sun.ac.za

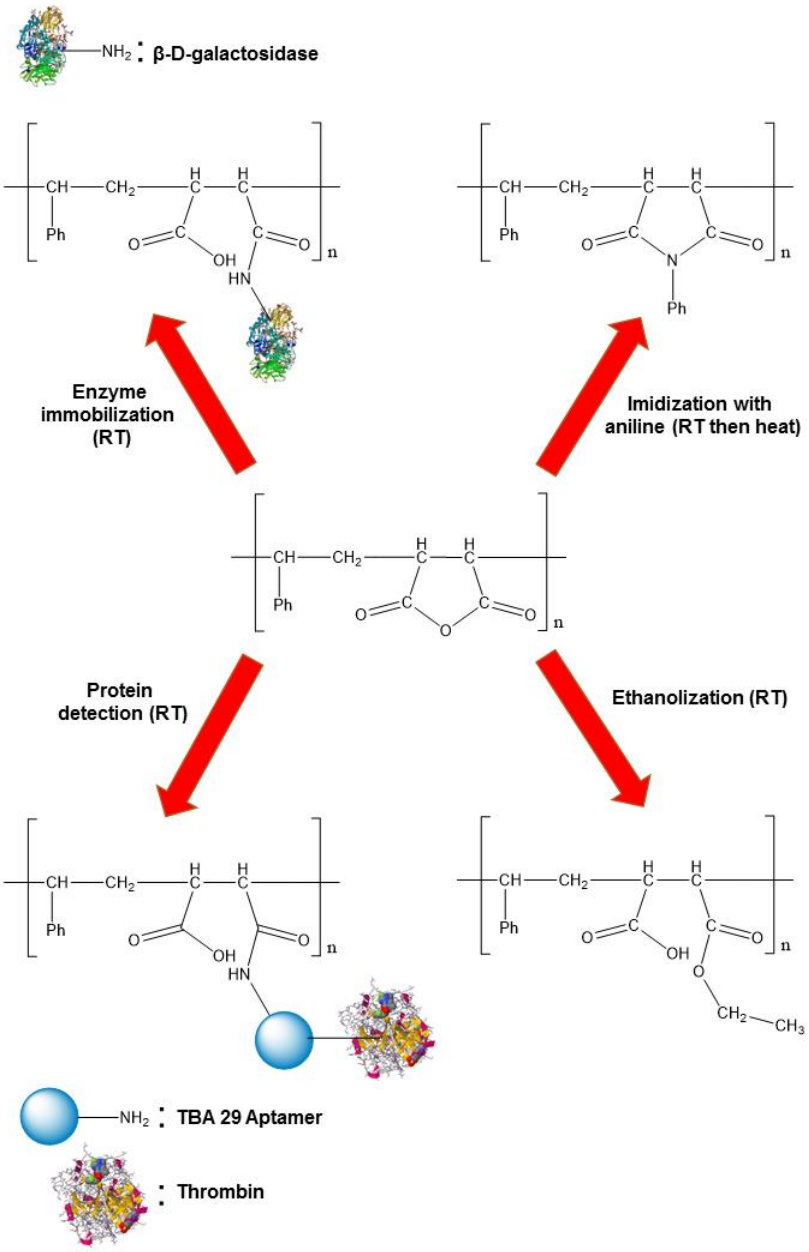

Scheme 1.22 Examples of PSMA applications

Thanks to their good miscibility, PSMA blends with other polymers have been found useful with respect to several applications. For example, an environmentally degradable blend was produced employing an esterified PSMA and LLDPE (linear low-density polyethylene) (**Figure 1.7A**),[55] or the use of a blend made up of SMA and SAN (styrene-acrylonitrile) copolymers for studying positron annihilation lifetime,[61] or even designing a high protein-absorption resistant membrane using a PSMA blend with PES (poly(ethersulfone)).[62] In addition, there have been papers published on other applications of PSMA, such as the development of microcapsules of PSMA for the encapsulation purposes,[62] regioselective

Stellenbosch University https://scholar.sun.ac.za

catalysis effect of imidized PSMA (**Figure 1.7B**)[63] and even as a template for growing silver nanoparticles.[64]

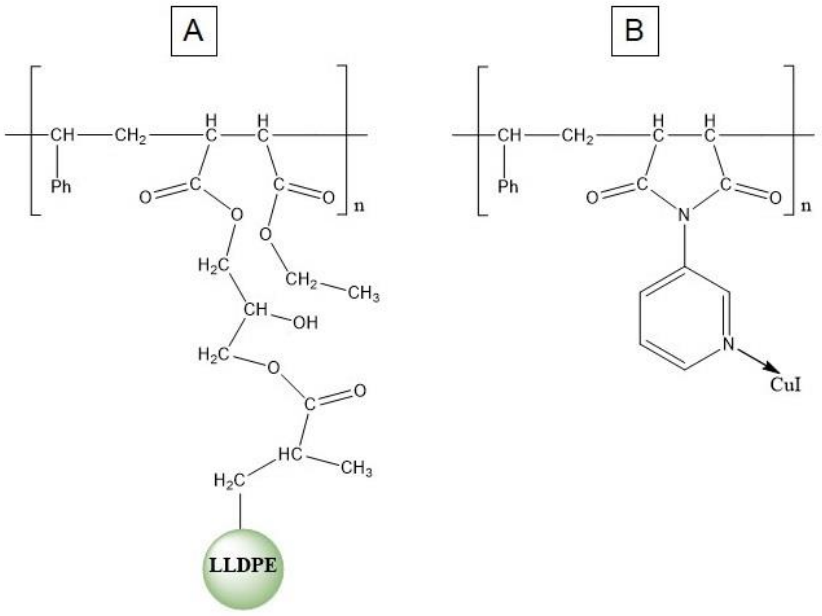

Figure 1.7 Examples of PSMA blends used in research

It must be noted that PSMA, like many other polymers, can be processed into nanofibers using a technique called electrospinning. In this technique a high voltage is applied to the polymer solution which induces a Taylor cone from which polymer nanofibers are formed.[65] The versatility of PSMA has therefore led to the idea of attaching a calixarene to it, in order to exploit the various functional possibilities that calixarenes possess.

1.7 Aims of the project

The main approach proposed in this dissertation was using a simple calix[4]arene functionalized with a primary amine tether in order to graft onto PSMA. Having synthesized a number of mono-substituted calix[4]arene-grafted PSMAs as our model compounds (in chapters 2 and 3), the simple calix[4]arene source could potentially be replaced with more sophisticated ones to be used for more elaborate purposes. In chapter 4, one of these purposes was the design and synthesis of a functionalized calix[4]arene capable of detecting mercury cation which is a major pollutant of biological systems[k].[66,67] From literature reports, it was known that a certain type of calix[4]arene (bis-allyl bis-arylazo calix[4]arene also known as

[k] The harmful effects of mercury emission on such systems including human cells will be discussed in detail in chapter 4 of this dissertation.

Stellenbosch University https://scholar.sun.ac.za

Chung's sensor) could act as a potent colorimetric sensor for mercury (exhibiting a strong color change from yellow to pink upon complexation with mercury in solution media).[68,69] Therefore, the production of a polymeric scaffold (based on the PSMA-originated grafts made in chapter 3) involving the mentioned calix[4]arene was planned. The purpose of this was to produce a stable, durable sensing instrument for mercury (due to the existence of PSMA support). However, the possibility of calix[4]arene sensing toward mercury being affected or even undermined after the attachment to PSMA support would have to be considered as well. To do so, first, the calix[4]arene compartment of the graft had to be synthesized. This compartment must contain the above-mentioned Chung's sensor plus a primary amine tether (resembling the amine-tethered models discussed in chapter 2) to be attached onto the PSMA support. Thus, a series of synthetic strategies for producing this desired amine-tethered calix[4]arene were pursued. Considering the complexation mechanism, caution was taken not to put the tether on the azo-possessing rings of the calix[4]arene due to the possible complexation disruption which might result in the dramatic decrease of our compound sensing capability (see **Figure 1.8** depicting the cartoon for this plan).

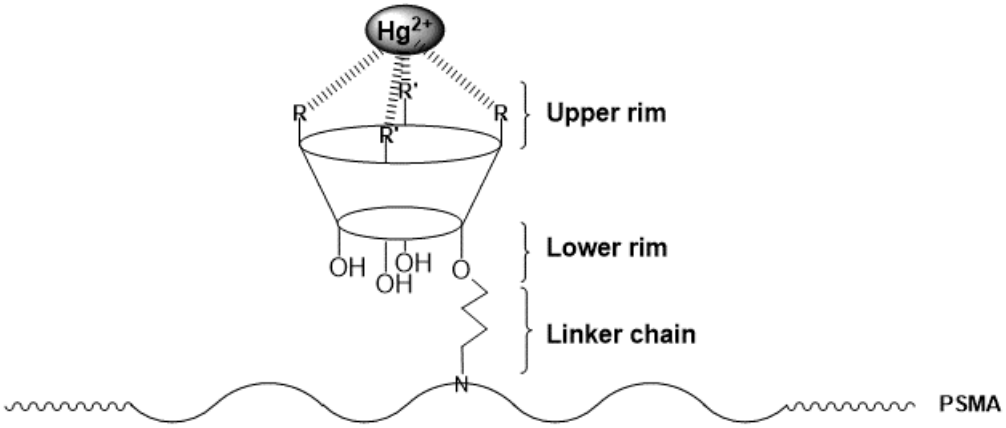

Figure 1.8 Modified Chung's sensor anchored to PSMA support (R: allyl, R': p-methoxyphenylazo)

Ultimately, in chapter 5 the synthesis of water-soluble *p*-sulfonated calix[4]arenes will be discussed. The purpose of making these compounds was as a result of the literature-reported example to produce hydrogels[l] in the presence of crosslinking agents[70] with numerous applications.[71-74] In order to do that, an amine-tethered *p*-sulfonated calix[4]arene (similar to

[l] Hydrogel is a three-dimensional crosslinked network of either a colloid or a polymer capable of swelling as a result of retaining an immense amount of water.[75] This phenomenon and its applications will be explained in detail in chapter 5 of this dissertation.

Stellenbosch University https://scholar.sun.ac.za

the mono-substituted model compound made in chapter 2) was synthesized and its grafting onto PSMA (with different maleic anhydride contents) was studied (using the previously mentioned methods from chapter 3). Next, these resulting water-soluble grafts were investigated with respect to their interactions with a series of viologen-based quaternary amines (potential crosslinking agents for *p*-sulfonated calix[4]arenes in accordance with literature[70]) to form hydrogels (see **Scheme 1.23** depicting the cartoon for this plan). Other polymeric supports (i.e. PVP-MA) would also be considered in case of PSMA-supported grafts failure to achieve the hydrogel formation.

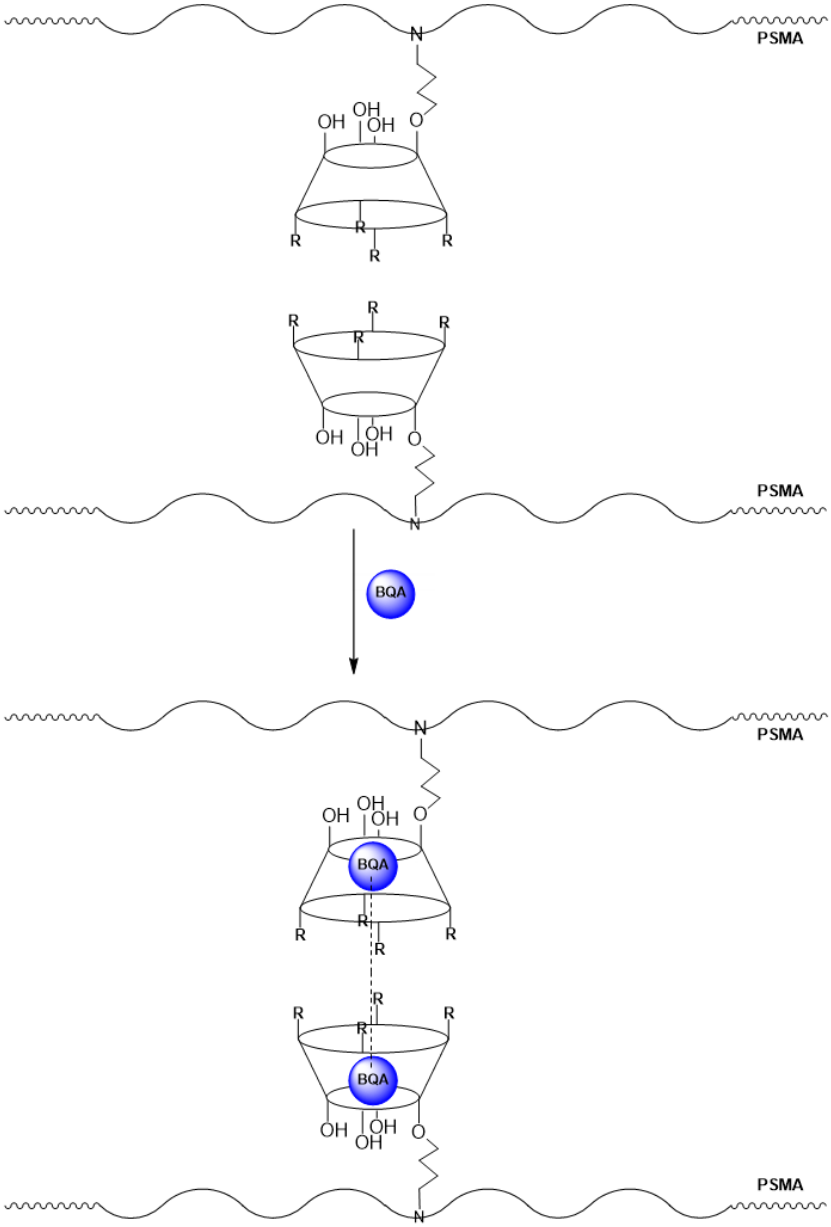

Scheme 1.23 Possible crosslinking between a p-sulfonated calix[4]arene-PSMA graft through encapsulated bis-quaternary amine units (R: tertiary butyl, BQA: bis-quaternary amine)

Stellenbosch University https://scholar.sun.ac.za

1-8 References

(1) von Baeyer, A. *Ber. Dtsch. Chem. Ges.* **1872**, *5*, 1094–1100.

(2) Baekeland, L. H. *Zndust. Eng. Chem.* **1913**, *5*, 506–511.

(3) Zinke, A.; Zigeuner, G.; Hossinger, K.; Hoffman, G. *Monatsh. Chem.* **1948**, *79*, 438–439.

(4) Gutsche, C. D. *Acc. Chem. Res.* **1983**, *16*, 161–170.

(5) Gutsche, C. D. *Calixarenes: An Introduction*, Royal Society of Chemistry, Cambridge, United Kingdom, **2008**, 2nd ed.

(6) Cornforth, J. W.; Hart, P. D.; Nicholls, G. A.; Rees, R. J. W.; Stock, J. A. *Br. J. Pharmacol.* **1955**, *10*, 73–86.

(7) Kammerer, H.; Happel, G.; Caesar, F. *Makromol. Chem.* **1972**, *162*, 179–197.

(8) Happel, G.; Mathiasch, B.; Kammerer, H. *Makromol. Chem.* **1975**, *176*, 3317–3334.

(9) Grootenhuis, P. D. J.; Kollman, P. A.; Groenen, L. C.; Reinhoudt, D. N.; van Hummel, G. J.; Ugozzoli, F.; Andreetti, G. D. *J. Am. Chem. Soc.* **1990**, *112*, 4165–4176.

(10) Verboom, W.; Durie, A.; Egberink, R. J. M.; Asfari, Z.; Reinhoudt, D. N. *J. Org. Chem.* **1992**, *57*, 1313–1316.

(11) Reece, D. A.; Pringle, J. M.; Ralph, S. F.; Wallace, G. G. *Solutions* **2005**, *38*, 1616–1622.

(12) Agrawal, Y. K.; Bhatt, H. *Bioinorg. Chem. Appl.* **2004**, *2*, 237–274.

(13) Chen, H.; Lee, M.; Choi, S.; Kim, J.; Choi, H. *Sensors* **2007**, *7*, 1091–1107.

(14) Consoli, G. M. L.; Granata, G.; Geraci, C. *Org. Biomol. Chem.* **2011**, *9*, 6491–6495.

(15) Baldini, L.; Casnati, A.; Sansone, F.; Ungaro, R. *Chem. Soc. Rev.* **2007**, *36*, 254–266.

(16) Shimojo, K.; Oshima, T.; Naganawa, H.; Goto, M. *Biomacromolecules* **2007**, *8*, 3061–3066.

(17) Sharma, K.; Cragg, P. J. *Chem. Sens.* **2011**, *1*, 1–18.

(18) Gutsche, C. D.; Bauer, L. J. *J. Am. Chem. Soc.* **1985**, *107*, 6063–6069.

Stellenbosch University https://scholar.sun.ac.za

(19) Nimse, S. B.; Kim, T. *Chem. Soc. Rev.* **2013**, *42*, 366–386.

(20) Erdemir, S.; Yilmaz, M. *J. Mol. Catal. B Enzym.* **2009**, *58*, 29–35.

(21) Memon, S.; Akceylan, E.; Sap, B.; Tabakci, M.; Roundhill, D. M.; Yilmaz, M. *J. Polym. Environ.* **2003**, *11*, 67–74.

(22) Blanda, M. T.; Adou, E. *Chem. Commun.* **1998**, 139–140.

(23) Glennon, J. D.; O'Connor, K.; Srijaranai, S.; Manley, K.; Harris, S. J.; McKervey, M. A. *Anal. Lett.* **1993**, *26*, 153–162.

(24) Tabakci, M.; Yilmaz, M. *J. Hazard. Mater.* **2008**, *151*, 331–338.

(25) Gezici, O.; Tabakci, M.; Kara, H.; Yilmaz, M. *J. Macromol. Sci., Part A: Pure Appl. Chem.* **2006**, *43*, 221–231.

(26) Yilmaz, M.; Deligöz, H. *J. Polym. Sci.; Polym. Chem.* **1995**, *33*, 2851–2853.

(27) Deligöz, H.; Yilmaz, M. *React. Funct. Polym.* **1996**, *31*, 81–88.

(28) Vaino, A. R.; Janda, K. D. *J. Comb. Chem*. **2000**, *2*, 579–596.

(29) Jain, V. K.; Handa, A.; Pandya, R.; Shrivastav, P.; Agrawal, Y. K. *React. Funct. Polym.* **2002**, *51*, 101–110.

(30) Akceylan, E.; Yilmaz, M.; Bartsch, R. A. *J. Macromol. Sci., Part A: Pure Appl. Chem.* **2006**, *43*, 477–486.

(31) Memon, S.; Tabakci, M.; Roundhill, D. M.; Yilmaz, M. *React. Funct. Polym.* **2006**, *66*, 1342–1349.

(32) Tisdale, M. J. *Science* **2000**, *289*, 2293–2294.

(33) Hoffmann, D.; Hoffmann, I.; El-Bayoumy, K. *Chem. Res. Toxicol.* **2001**, *14*, 767–790.

(34) Kirsch, M.; Korth, H. G.; Sustmann, R.; de Groot, H. *Biol. Chem.* **2002**, *383*, 389–399.

(35) Mirvish, S. S. *Cancer Lett.* **1995**, *93*, 17–48.

(36) Pfeiffer, S.; Mayer, B.; Hemmens, B. *Angew. Chem. Int. Ed.* **1998**, *38*, 1714–1731.

(37) Kang, Y.; Rudkevich, D. M. *Tetrahedron* **2004**, *60*, 11219–11225.

(38) Engrand, P.; Regnouf-de-Vains, J. B. *Tetrahedron Lett.* **2002**, *43*, 8863–8866.

Stellenbosch University https://scholar.sun.ac.za

(39) Sayin, S.; Ozcan, F.; Memon, S.; Yilmaz, M. *J. Incl. Phenom. Macrocycl. Chem.* **2010**, *67*, 385–391.

(40) Granata, G.; Consoli, G. M. L.; Sciuto, S.; Geraci, C. *Tetrahedron Lett.* **2010**, *51*, 6139–6142.

(41) Mazurin, O. V. *Phase Separation in Glass*, North-Holland, Amsterdam, Netherlands, **1984**, 1st ed.

(42) Vogel, W. *Glass Chemistry*, Springer Science & Business Media, Berlin, Germany **1994**, 2nd ed.

(43) Terrett, N. K. *Combinatorial Chemistry*, Oxford University Press, Oxford, United Kingdom, **1998**.

(44) Harris, S. J.; Barrett, G.; McKervey, M. A. *J. Chem. Soc. Chem. Commun.* **1991**, *17*, 1224–1225.

(45) Malinowska, E.; Gawart, L.; Parzuchowski, P. X.; Rokicki, G.; Brzózka, Z. *Anal. Chim. Acta* **2000**, *421*, 93–101.

(46) Tabakci, M.; Memon, S.; Sap, B.; Roundhill, D. M.; Yilmaz, M. *J. Macromol. Sci., Part A: Pure Appl. Chem.* **2004**, *41*, 811–825.

(47) Abd-El-Aziz, A. S.; Shipman, P. O.; Pilfold, J. L.; Shipley, P. R. *Macromol. Chem. Phys.* **2010**, *211*, 996–1002.

(48) Chang, K. C.; Su, I. H.; Lee, G. H.; Chung, W. S. *Tetrahedron Lett.* **2007**, *48*, 7274–7278.

(49) Dondoni, A.; Ghiglione, C.; Scoponi, M. *Chem. Commun.* **1997**, 673–674.

(50) Pedersen, C. J. *Fed. Proc., Fed. Am. Soc. Exp. Biol.* **1968**, *27*, 1305–1309.

(51) Dondoni, A.; Marra, A.; Rossi, M.; Scoponi, M. *Polymer* **2004**, *45*, 6195–6206.

(52) Ang, T. L.; Harwood, H. J. *Polymer Preprints Meeting*, American Chemical Society, Philadelphia, United States, **1964**, 1st ed.

(53) Wang, F. C. Y. *J. Chromatogr. A* **1997**, *765*, 279–285.

(54) Liu, H. Y.; Yao, Z.; Cao, K.; Li, B. G. *Chem. Eng. Sci.* **2010**, *65*, 1781–1789.

Stellenbosch University https://scholar.sun.ac.za

(55) Pal, J.; Ghosh, A. K.; Singh, H. *Eur. Polym. J.* **2008**, *44*, 1261–1274.

(56) Brydson, J. A. *Plastics Materials*, Butterworth-Heinemann, Oxford, United Kingdom, **1995**, 6th ed.

(57) Lai, X.; Sun, C.; Tian, H.; Zhao, W.; Gao, L. *Int. J. Pharm.* **2008**, *352*, 66–73.

(58) Lin, J. J.; Hsu, Y. C. *J. Colloid Interface Sci.* **2009**, *336*, 82–89.

(59) Lee, S. J.; Tatavarty, R.; Gu, M. B. *Biosens. Bioelectron.* **2012**, *38*, 302–307.

(60) Li, P.; Zhang, Y.; Zhang, S.; Wang, P.; Wang, M. *Adv. Chem. Eng. Pts 1-3*, **2012**, *396–398*, 1394–1397.

(61) Wästlund, C.; Maurer, F. H. J. *Polymer* **1998**, *39*, 2897–2902.

(62) Zhu, L. P.; Zhang, X. X.; Xu, L.; Du, C. H.; Zhu, B. K.; Xu, Y. Y. *Colloids Surf., B* **2007**, *57*, 189–197.

(63) Hossiennejad, T.; Daraie, M.; Heravi, M. M.; Tajoddin, N. N. *J. Inorg. Organomet.Polym.* **2017**, *27*, 861–870.

(64) Hsu, Y. C.; Chen, Y. M.; Lin, W. L.; Lan, Y. F.; Chan, Y. N.; Lin, J. J. *J. Colloid Interface Sci.* **2010**, *352*, 81–86.

(65) Tang, C.; Ye, S.; Liu, H. *Polymer* **2007**, *48*, 4482–4491.

(66) Järup, L. *Br. Med. Bull.* **2003**, *68*, 167–182.

(67) Gustin, M. S.; Taylor, G. E.; Leonard, T. L. *Environ. Health Perspect.* **1994**, *102*, 772–778.

(68) Kao, T-L.; Wang, C-C.; Pan, Y-T.; Shiao, Y-J.; Yen, J-Y.; Shu, C-M.; Lee, G-H.; Peng, S-M.; Chung, W-S. *J. Org. Chem.* **2005**, *70*, 2912–2920.

(69) Ho, I-T.; Lee, G-H.; Chung, W-S. *J. Org. Chem.*, **2007**, *72*, 2434–2442.

(70) Wang, K.; Chen, Y.; Liu, Y. *Chem. Commun.* **2015**, *51*, 1647–1649.

(71) Lee, K. Y.; Mooney, D. J. *Chem. Rev.* **2001**, *101*, 1869–1880.

(72) Langer, R.; Tirrell, D. A. *Nature* **2004**, *428*, 487–492.

(73) Lutolf, M. P. *Nat. Mater.* **2009**, *8*, 451–453.

Stellenbosch University https://scholar.sun.ac.za

(74) Harada, A.; Kobayashi, R.; Takashima, Y. Hashidzume, A.; Yamaguchi, H. *Nat. Chem.* **2011**, *3*, 34–37.

(75) Nic, M.; Jirat, J.; Kosata, B. *IUPAC Compendium of Chemical Terminology: The Gold Book, International Union of Pure and Applied Chemistry (IUPAC)*, **2014**, Version 2.3.3 (online: https://goldbook.iupac.org/).

Stellenbosch University https://scholar.sun.ac.za

Chapter 2. Synthesis of primary amine-tethered calix[4]arenes as polymer grafting models

2.1 Chapter overview

In this chapter, the alkylation of calix[4]arenes with an amine-precursor (various options) will be discussed. That will be followed by the discussion of reactions converting the amine-precursor into a primary amine which can be then used as a functional group to link a calix[4]arene to PSMA. The challenges around the purification of the amines in general and the solutions to address these will also be discussed.

2.2 Options with regards to making a primary amine-tethered calix[4]arene

From a literature point of view, many options can be employed for the synthesis of primary amines. Amongst them, perhaps the most famous ones are the reduction of a nitrile group,[1] a Staudinger reaction on an azide group,[2] reduction of a nitro group[3] and finally the Gabriel synthesis for the conversion of a phthalimide group into an amine.[4] In the case of the required alkyl-nitro compounds, the yields reported in literature for their synthesis can be very poor (<20%)[5] and reduction of the nitrile reagent with hydride reagents would likely be complicated by the calixarene phenolic groups (the hydride reagents may act as a base and react with the phenolic groups). Thus, in this study, the experiments were only attempted on the azide, and the phthalimide functional groups. Both of these approaches will be addressed in this chapter.

2.3 Synthesis of an alkyl azide reagent

In the first attempt to synthesize a primary amine-precursor, an azide reagent was prepared and used for monoalkylation of calix[4]arene. To begin with, butane-1,4-diyl bis(4-methylbenzenesulfonate) **1** was synthesized using butane-1,4-diol with *p*-toluenesulfonyl chloride (2.18 equiv.), triethylamine (2.99 equiv.) and DMAP (5 mol%) in anhydrous DCM (0 °C, then room temperature for 24 hours). A 66% yield was acquired for our desired bis-tosylated product **1** (a trace of the monotosylated product also formed) (**Scheme 2.1**) and the spectral data matched that from literature.[6]

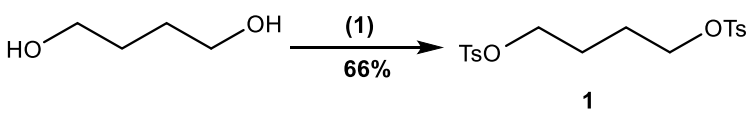

Scheme 2.1 Synthesis of the bistosylate reagent. Reagents and conditions: (1) p-toluenesulfonyl chloride (2.18 equiv.), triethylamine (2.99 equiv.), DCM, 0 °C then RT, 24 h

Stellenbosch University https://scholar.sun.ac.za

Next, bistosylate **1** and sodium azide (1.1 equiv.) were mixed and stirred in DMF (at room temperature for 72 hours) to afford novel alkyl azide reagent **2**. However, only 22% yield was obtained, with a significant amount of unreacted bistosylate remaining behind (**Scheme 2.2**).

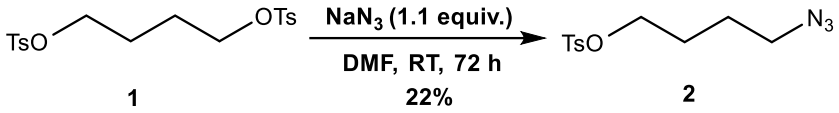

Scheme 2.2 Synthesis of the alkyl azide reagent

The ^{1}H-NMR spectrum for monoazide reagent **2** (**Figure 2.1**) showed an obvious dissymmetry in comparison to the starting material **1**. As a result of replacing a tosyl group with an azide, there were only four aromatic protons observed for the monotosylate compound **2**, while bistosylate compound **1** demonstrated eight aromatic protons in the same region (they both showed up as doublets). In addition, in the aliphatic region, the dissymmetry emerged for **2** as terminal methylenes revealed themselves as two different triplets (at 3.25 ppm for azide terminus and 4.05 ppm for tosylate terminus), while in the case of **1** there was only one multiplet for the equivalent tosylated terminals between 3.94-3.99 ppm. Finally, the integration ratios suggest that there was only one methyl for tosylate group on compound **2** at 2.45 ppm (while there were two equivalent methyls on compound **1**).

In addition, the FT-IR spectrum exhibited a strong stretch for the N=N=N group of product **2** at 2093 cm^{-1}.

Of interest, HRMS results revealed a molecular ion of 292.0725 Da (calculated for $[M+Na]^{+}$: 292.0732 Da). Also, there was a molecular ion of 242.0848 Da representing the compound molecular ion with loss of an N_2 which is common for azides (calculated for $[M+H–N_2]^{+}$: 242.0851 Da).

Although the yield of the reaction was low, it was decided to test the mono-alkylation strategy without further optimization at this point. The plan was to put the alkyl azide **2** on *p-t*-butyl-calix[4]arene **3** and then convert it into the desired alkylamine (**10$_b$**) via a Staudinger reaction. The mono-alkylation approach was chosen based on the successful method for monoalkylation of *p-t*-butyl-calix[4]arene **3** reported by our colleague Christopher Jurisch for his honours project (deprotonation of *p-t*-butyl-calix[4]arene **3** by NaH at 80 °C for 24 hours, followed by alkylation at the same temperature for another 24 hours).[7]

Stellenbosch University https://scholar.sun.ac.za

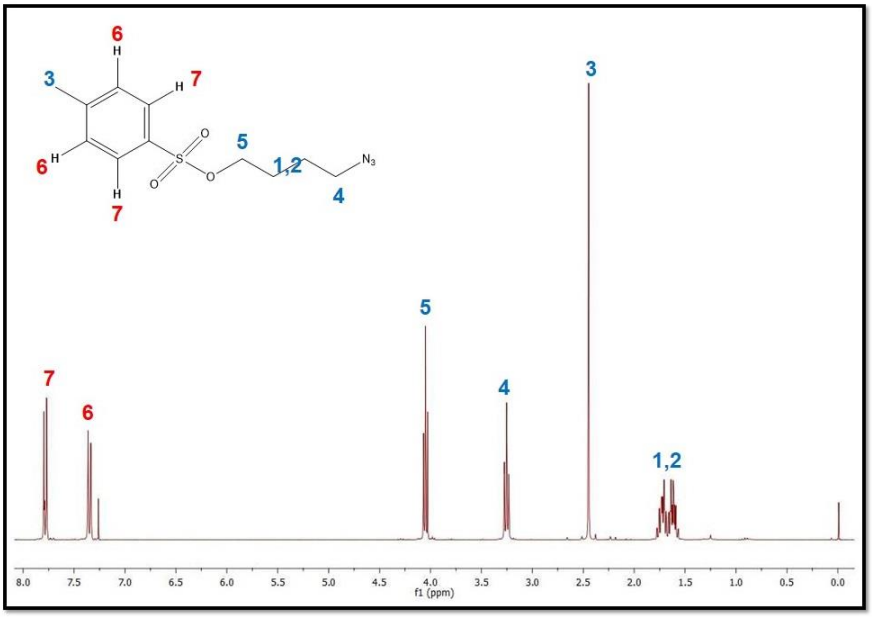

*Figure 2.1 ^{1}H-NMR spectrum (in $CDCl_3$) for the alkyl azide reagent (**2**)*

After the failure of the first attempt because of the azide reagent decomposition at 80 °C, the reaction temperature was decreased down to 50 °C (minimizing the possibility of the azide reagent decomposition), but the alkylation time increased to 72 hours (the lower the temperature, the slower the reaction). Regrettably, the result was an inseparable mixture of mono- and di-substituted *p*-*t*-butyl-calix[4]arene (only 40% collective yield). To check the solvent effect on the reaction and possibly get a better result, DMF was replaced by THF and the reaction was performed under the same conditions.[m] Unfortunately, poor results were once again obtained (an inseparable mixture of the mono- and di-substituted products, with even an even lower collective yield). Overall, due to the poor results for all of these attempts (See the summary in **Scheme 2.3** and **Table 2.1**), this method was discontinued and the making of the primary amine-tethered calix[4]arenes was pursued through an alkylphthalimide approach.

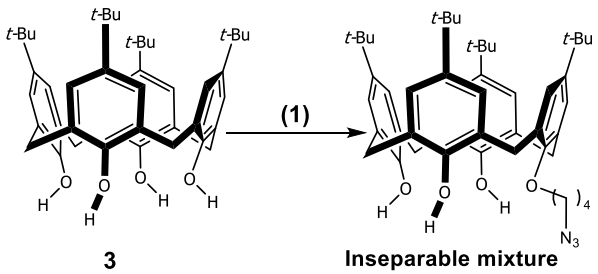

Scheme 2.3 Failed approach for synthesizing the amine-precursor through azide functionality

[m] THF is a very good aprotic solvent for calix[4]arene studies and can be used as an appropriate replacement for DMF).[8]

Stellenbosch University https://scholar.sun.ac.za

Table 2.1 Failed attempts to synthesize a monoalkylated p-t-butyl-calix[4]arene. 1.0 equiv. base (NaH) and 1.5 equiv. alkyl azide reagent used (Reaction concentration: 0.06 M).

Entry	Deprotonation time	Alkylation time	Solvent	Temp. (°C)	Yield (%)
1	24 h	24 h	DMF	80	0
2	24 h	72 h	DMF	50	Inseparable mixture (40% collective yield for mono and diazide)
3	24 h	72 h	THF	50	Inseparable mixture (30% collective yield for mono and diazide)

2.4 Synthesis of an alkylphthalimide reagent

The main alkylating reagents used successfully in this project were *N*-(*n*-bromoalkyl)-phthalimides (alkyl: ethyl, butyl, hexyl). These were found to be moderately stable with a straightforward synthesis, and unlike many other amine precursors, they were easily removed from the product after the reaction. They could be synthesized according to literature in high yield using potassium phthalimide and a bis-terminated dibromoalkane, either with heating under reflux (in case of 1,2-dibromoethane) to produce **4$_e$** or via heating at 100 °C in DMF (for 1,4-dibromobutane or 1,6-dibromohexane) to yield **4$_b$** and **4$_h$** (**Scheme 2.4**). The spectral data for all three compounds synthesized matched the values from literature.[9]

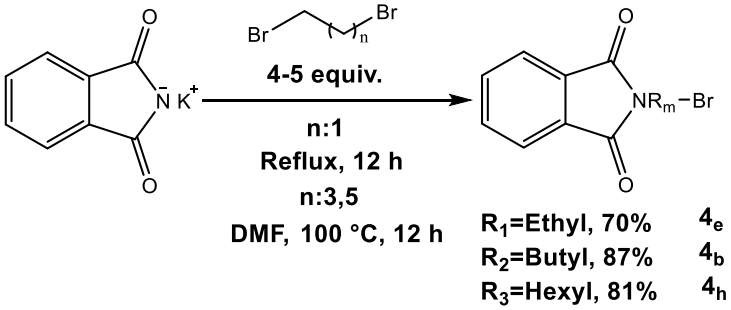

Scheme 2.4 Synthesis of the alkylphthalimide reagent

In the case of the butyl spacer, the iodide version was also synthesized as a potentially better alkylating agent. To do so, *N*-(4-bromobutyl)-phthalimide **4$_b$** was stirred with NaI (10.0 equiv.) in acetone at room temperature for 24 hours to afford *N*-(4-iodobutyl)-phthalimide **4$_{b\text{-}i}$** in 91% yield (**Scheme 2.5**) with complete correlation of its spectral data with the literature values.[10]

Stellenbosch University https://scholar.sun.ac.za

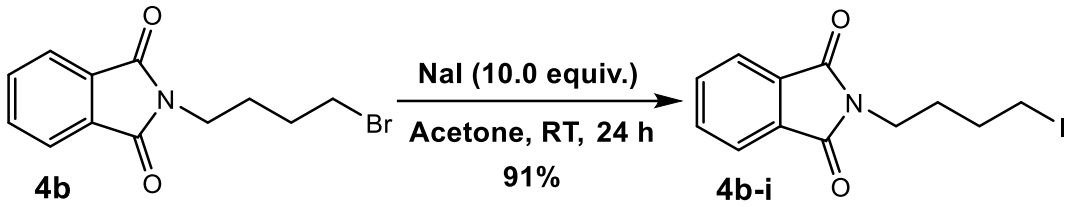

*Scheme 2.5 Synthesis of N-(4-iodobutyl)-phthalimide (**4b-i**)*

2.5 Monoalkylation of calix[4]arenes

The purpose of this reaction was to synthesize a mono primary amine-tethered calix[4]arene which could be used for the attachment onto a polymer. Here the monoalkylation will be discussed for both *p-t*-butyl-calix[4]arene **3** and calix[4]arene **7** individually, and the differences between the two will be pointed out.

2.5.1 Synthesis of monoalkylated *p-t*-butyl-calix[4]arene

Despite the failure of Christopher Jurisch's approach for monoalkylation[7] using the azide reagent (**2**), in practice, this approach exhibited very promising results in the case of using the phthalimide reagent as the alkyl halide. Various parameters affecting the reaction results were studied. Building on Christopher Jurisch's results, it was understood that the longer the deprotonation time, the greater the yield for the reaction. Second, with respect to the base choice and solvent, K_2CO_3 with acetonitrile (under reflux) and NaH with DMF (at 80 °C) were used and compared in action. It was found that K_2CO_3 solely (or in conjunction with NaI as part of a Finkelstein strategy[11]) in acetonitrile would drive the reaction toward the formation of a dialkylated *p-t*-butyl-calix[4]arene as the major product and a monoalkylated *p-t*-butyl-calix[4]arene as the minor product. In contrast with that, when NaH was used in dry DMF, it resulted in a good yield for a reaction with 24 hours for deprotonation and another 24 hours for alkylation (49% and 75% for butylphthalimide $\mathbf{5_b}$ and hexylphthalimide $\mathbf{5_h}$ respectively; **Scheme 2.6**). Moreover, regarding the latter approach, there was an attempt to increase the yield by replacing the alkyl bromide $\mathbf{4_b}$ with the alkyl iodide $\mathbf{4_{b\text{-}i}}$, but only a slight increase was observed (52% for butylphthalimide $\mathbf{5_b}$ compared to 49% obtained for the same spacer by alkyl bromide).

Stellenbosch University https://scholar.sun.ac.za

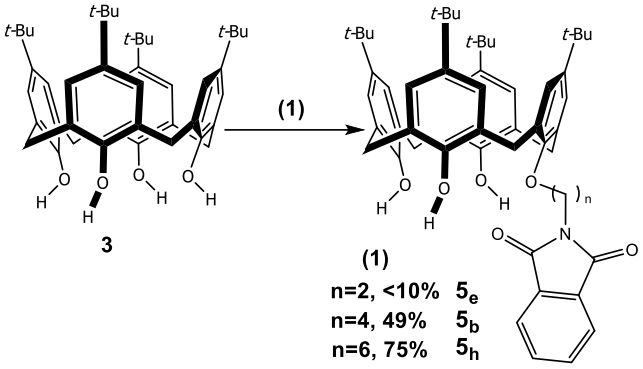

Scheme 2.6 Monoalkylation of p-t-butyl-calix[4]arene using N-(n-bromoalkyl)-phthalimide. Reagents and conditions: (1) NaH (1.0 equiv.), DMF, 80 °C, 24 h then N-(n-bromoalkyl)-phthalimide (1.5 equiv.), 80 °C, 24 h

However, the monoalkylation of *p*-*t*-butyl-calix[4]arene **3** failed to work well for the ethylphthalimide reactant possibly due to its susceptibility toward strong bases. What was observed was the formation of an elimination product, *N*-vinylphthalimide **6**, whose spectral data was available in literature and compared to that (**Figure 2.2**).[12] This was almost certainly the cause of the significant decrease in the reaction yield (<10% for ethylphthalimide $\mathbf{5_e}$).

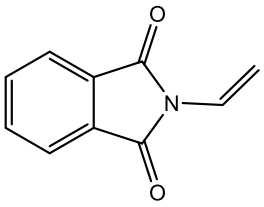

6

*Figure 2.2 N-vinylphthalimide **6***

Earlier work by Groenen *et al*. was found in literature which seemed to be very useful for the monoalkylation of calix[4]arene using a minimum amount of K_2CO_3 (0.6 equiv.) with acetonitrile (reflux), alongside an excess of the alkyl halide (3.3 equiv.).[13] In this case, the result was a monoalkylated product (major) and also a dialkylated product (minor) with a better yield (30% for ethylphthalimide $\mathbf{5_e}$) compared to that obtained with the NaH method (**Scheme 2.7**). However, this approach did not work as well for forming butylphthalimide $\mathbf{5_b}$ or hexylphthalimide $\mathbf{5_h}$, with yields respectively remaining the same 49%, or decreasing (from 75% to 62%).

Stellenbosch University https://scholar.sun.ac.za

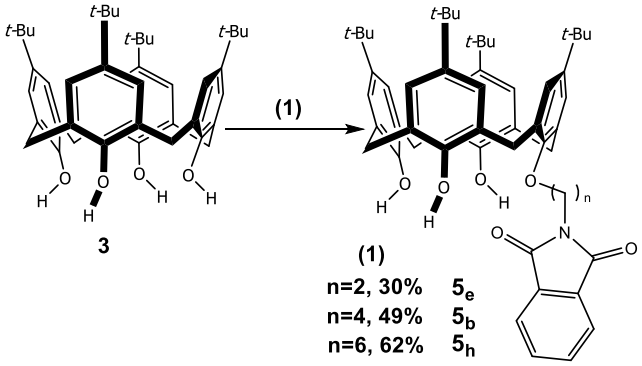

Scheme 2.7 Monoalkylation of p-t-butyl-calix[4]arene using N-(n-bromalkyl)-phthalimide. Reagents and conditions: (1) K_2CO_3 (0.6 equiv.), N-(n-bromalkyl)-phthalimide (3.3 equiv.), CH_3CN, reflux, 24 h

The ^{1}H-NMR spectrum (see **Figure 2.3** for butylphthalimide **5$_b$**) revealed the dissymmetry caused by the monoalkylation which caused the appearance of two broad singlets for the lower-rim phenolic protons with different integrations at 9.01 and 9.77 ppm (ethylphthalimide **5$_e$**), 9.51 and 10.08 ppm (butylphthalimide **5$_b$**), 9.60 and 10.19 ppm (hexylphthalimide **5$_h$)** (2 to 1 integration ratio). The dissymmetry was also backed by inequivalent aromatic protons between 6.90 and 7.10 ppm for all three compounds (compared to equivalent aromatic protons for **3**), in addition to three different tertiary butyl signals between 1.10 and 1.30 ppm. There were also two aromatic multiplets for the phthalimide group with equal integrations between 7.69-7.72 and 7.95-7.98 ppm (ethylphthalimide **5$_e$**), 7.68-7.70 and 7.85-7.88 ppm (butylphthalimide **5$_b$**), 7.62-7.65 and 7.81-7.83 ppm (hexylphthalimide **5$_h$**) (1 to 1 integration ratio).

Several conclusions could also be made on comparing the three ^{1}H-NMR spectra:

- The shorter the tether, the more upfield the phenolic protons. Compound **5$_e$** has the shortest tether and its phenolic protons may possibly undergo the anisotropic effect of the tether phthalimide more and occur more upfield compared to **5$_b$** and **5$_h$**.
- The shorter the tether, the more downfield the phthalimide protons. Compound **5$_e$**'s phthalimide protons are affected by the lower-rim strong hydrogen bonding more than the other two compounds due to possessing the shortest tether of all. The way this phenomenon possibly functions is as follows – hydrogen-bonding occurs between the carbonyl moiety of phthalimide and the phenolic protons, causing an electronic pull that deshields the phthalimide protons.

In the FT-IR spectrum, the best indication for the presence of a phthalimide group was the strong stretch at 1706 cm^{-1} (ethylphthalimide **5$_e$**), 1712 cm^{-1} (butylphthalimide **5$_b$**), 1707 cm^{-1} (hexylphthalimide **5$_h$**) for the imide carbonyl.

Stellenbosch University https://scholar.sun.ac.za

In addition, HRMS data revealed the existence of species with molecular ions of 844.4559 Da for **5e** (calculated for $[M+Na]^+$: 844.4553 Da), 867.5308 Da for **5b** (calculated for $[M+NH_4]^+$: 867.5312 Da) and 895.5637 Da for **5h** (calculated for $[M+NH_4]^+$: 895.5625 Da).

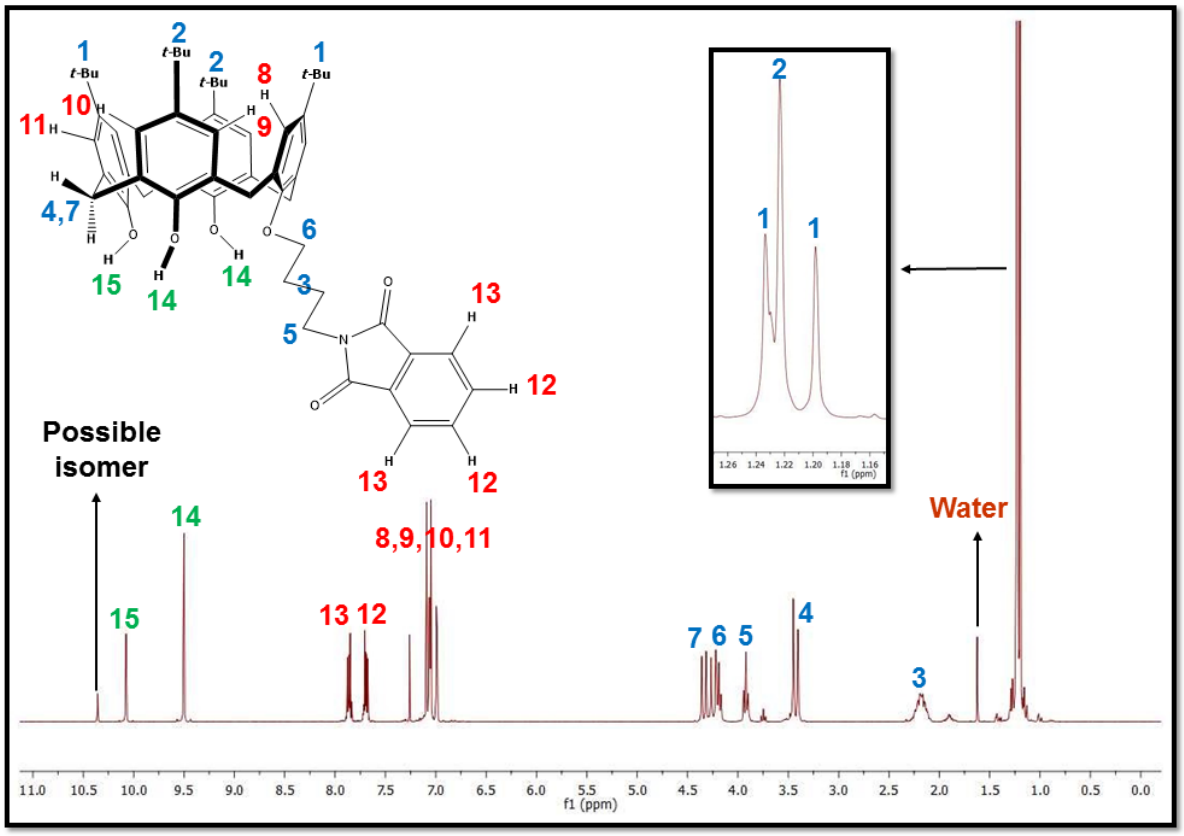

*Figure 2.3 An example of the ^{1}H-NMR spectrum (in $CDCl_3$) for a monoalkylated p-t-butyl-calix[4]arene (**5b**)*

2.5.2 Synthesis of monoalkylated de-butylated calix[4]arenes

The monoalkylation was again attempted, but this time on the de-butylated calix[4]arene **7**. The same conditions (reaction in DMF with NaH over a long deprotonation period at 80 °C) were employed, but the result was a mixture (inseparable by column chromatography) of monoalkylated calix[4]arene and 2-(pyrrolidine-1-carbonyl)benzoic acid **8** (**Figure 2.4**) in case of the butylphthalimide spacer. The side product (**8**) was isolated via trituration of the crude material with methanol (**8** was soluble in methanol while the calix[4]arene product **9b** remained insoluble and collected via filtration affording only 15% yield for the monoalkylated compound). It is believed that compound **8** (whose spectral data was also available in literature and was compared to that)[14] resulted from a ring-opening reaction of phthalimide, followed by an intramolecular ring-closing reaction (in case of the ethylphthalimide spacer the side product was *N*-vinylphthalimide **6** as a result of an elimination reaction while the desired product **9e** never formed).

Stellenbosch University https://scholar.sun.ac.za

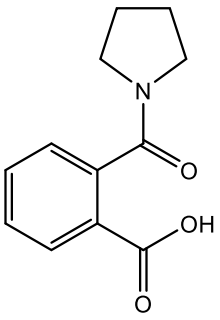

8

*Figure 2.4 2-(pyrrolidine-1-carbonyl)benzoic acid **8***

Comparing the monoalkylation results for calix[4]arene **7** with the ones for *p*-*t*-butyl-calix[4]arene **3** (both in the presence of NaH), suggested the decomposition of the alkyl halide before reaction with calix[4]arene **7**. Therefore, it suggested that the calix[4]arene anion is a stronger base than the *p*-*t*-butyl-calix[4]arene anion. Next, the method used by Shu *et al.*,[15] involving a more polar solvent (acetonitrile) and NaOMe as a base was attempted. In this case, the product formed, although the yields (36% and 48% for butylphthalimide $\mathbf{9_b}$ and hexylphthalimide $\mathbf{9_h}$ spacers) were not as good as the paper suggested (70 to 80%). The partial success was probably due to the more polar solvent reducing the basicity of the nucleophile. However, this method also did not produce the desired product for the ethylphthalimide spacer ($\mathbf{9_e}$). Thus, the K_2CO_3 method applied to *p*-*t*-butyl-calix[4]arene **3** and *N*-(2-bromoethyl)phthalimide $\mathbf{4_e}$ in the previous section was attempted. Satisfyingly, the approach not only produced the monoalkylated calix[4]arene with ethylphthalimide spacer (48% yield), but also improved the yield for the others (59% and 54% for butylphthalimide $\mathbf{9_b}$ and hexylphthalimide $\mathbf{9_h}$ spacers) (see **Scheme 2.8**).

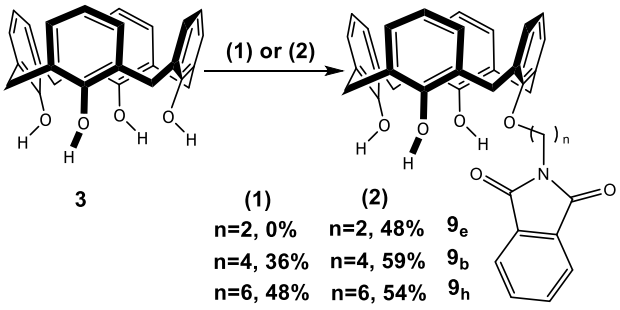

Scheme 2.8 Monoalkylation of calix[4]arene using N-(n-bromoalkyl)-phthalimide. Reagents and conditions: (1) NaOMe (1.2 equiv.), CH_3CN, reflux, 24 h then N-(n-bromoalkyl)-phthalimide (2.5 equiv.), reflux, 24 h; (2) K_2CO_3 (0.6 equiv.), N-(n-bromalkyl)-phthalimide (3.3 equiv.), CH_3CN, reflux, 24 h

Stellenbosch University https://scholar.sun.ac.za

As was seen previously, the ^{1}H-NMR spectrum (see **Figure 2.5** for butylphthalimide **9$_b$**) revealed the dissymmetry as a result of monoalkylation. Two phenolic protons (lower-rim) with different integration ratio (2 to 1) appeared at 8.79 and 9.24 ppm (ethylphthalimide **9$_e$**), 9.30 and 9.58 ppm (butylphthalimide **9$_b$**), 9.40 and 9.71 ppm (hexylphthalimide **9$_h$)** respectively. There were two triplets and one multiplet in the aromatic region for the upper-rim aromatic protons and two phthalimide multiplets (integration ratio: 1 to 1) between 7.66-7.69 and 7.96-7.98 ppm (ethylphthalimide **9$_e$**), 7.64-7.67 and 7.84-7.87 ppm (butylphthalimide **9$_b$**), 7.58-7.61 and 7.78-7.81 ppm (hexylphthalimide **9$_h$**).

Similar to the previous section:

- The compound with the shortest tether (ethylphthalimide **9$_e$**) has the most upfield phenolic protons, probably due to the anisotropic effect of the phthalimide group.
- Moreover, the same compound (ethylphthalimide **9$_e$**) most likely due to having the strongest hydrogen bonding between its phenolic protons and the phthalimide group (comparing to butylphthalimide **9$_b$** and hexylphthalimide **9$_h$**), had the most downfield phthalimide protons on its ^{1}H-NMR spectrum.

With regards to the FT-IR spectrum, the characteristic stretch for the imide carbonyl revealed itself at 1715 cm^{-1} (ethylphthalimide **9$_e$**), 1702 cm^{-1} (butylphthalimide **9$_b$**), 1705 cm^{-1} (hexylphthalimide **9$_h$**) indicating the existence of the phthalimide group.

In addition, HRMS (ESI^{-}) data showed the presence of molecular ions 596.2088 Da for ethylphthalimide **9$_e$** (calculated for $[M–H]^{+}$: 596.2073 Da), 624.2399 Da for butylphthalimide **9$_b$** (calculated for $[M–H]^{+}$: 624.2386 Da), 652.2722 Da for hexylphthalimide **9$_h$** (calculated for $[M–H]^{+}$: 652.2699 Da). Also, compound **9$_b$** showed a molecular ion of 423.1592 Da (calculated for [plain calix[4]arene–H]$^{+}$: 423.1596 Da).

Stellenbosch University https://scholar.sun.ac.za

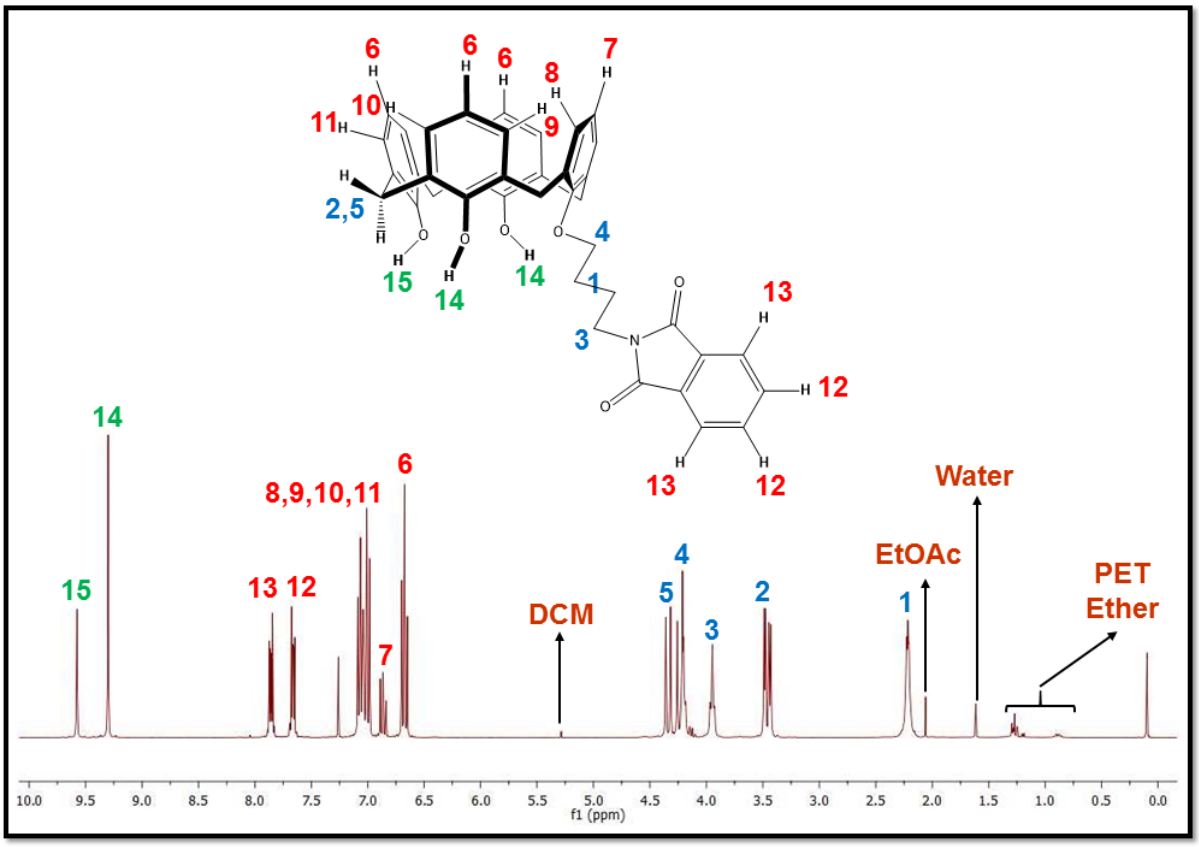

*Figure 2.5 An example of the ^{1}H-NMR spectrum (in $CDCl_3$) for a monoalkylated of calix[4]arene (**9b**)*

2.6 Different methods regarding the deprotection of phthalimide (Gabriel synthesis)

Three different methods to hydrolyze the phthalimide group to reveal the amine were examined.[16] The first one, in fact, one of the oldest approaches for phthalimide deprotection, included using methylamine hydrochloride in a basic environment.[17] Unfortunately, this approach failed to achieve its goal and only the starting material was recovered (**Scheme 2.9**).

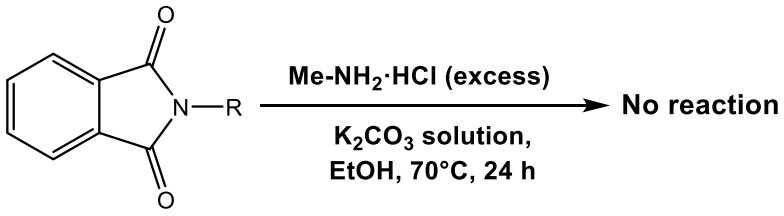

Scheme 2.9 Failed attempt for Gabriel synthesis using methylamine salt (R: calix[4]arene with its tether)

The second approach was based on a literature report by Ganem and co-workers, in which an alkylphthalimide ring was reductively opened with $NaBH_4$ in 2-propanol/H_2O and the resulting aromatic amide then hydrolyzed by glacial acetic acid into the primary amine (**Scheme 2.10**).[18]

Stellenbosch University https://scholar.sun.ac.za

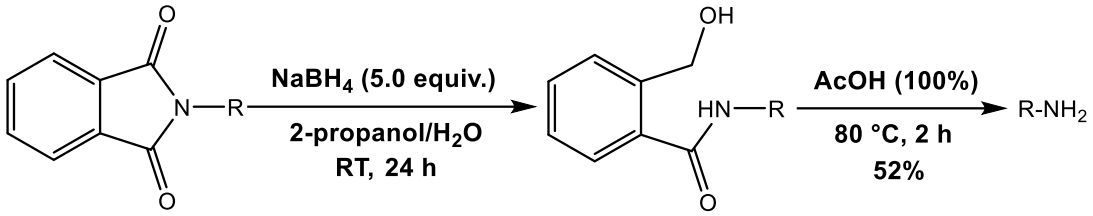

*Scheme 2.10 An example of Gabriel synthesis with $NaBH_4$/hydrolysis approach (R: **5b**)*

This approach was employed for our monoalkylated *p*-*t*-butyl-calix[4]arene **5b** and a moderate yield was acquired for that (52% for the butylphthalimide spacer).

The third approach was using hydrazine monohydrate, which is a potent nucleophile capable of opening the phthalimide ring on both its carbonyl groups due to its "bidentate" structure. The great advantage of this method is the formation of the ammonium salt of phthalhydrazide which theoretically can either transform into the hydrogen chloride salt of the amine (acidic work-up) or the neutral amine (basic work-up) (**Scheme 2.11**). The remaining hydrazide salt is reportedly insoluble in organic solvents and can be removed easily via filtration while the amine (or its salt) stays in the filtrate (This approach is also known as the Ing-Manske reaction).[19]

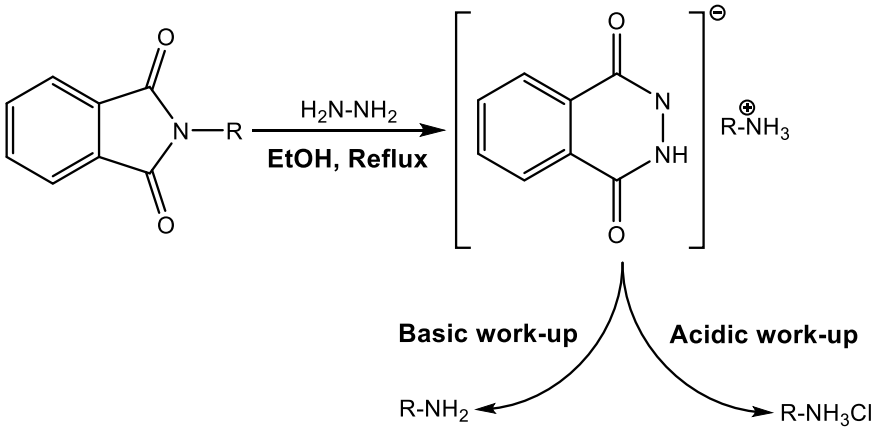

Scheme 2.11 Gabriel synthesis through hydrazinolysis (R: calix[4]arene with its tether)

In order to improve the solubility of calix[4]arene, THF was used as the co-solvent. Two very important findings were discovered after performing many experiments:

- The minimum amount of hydrazine monohydrate necessary for full deprotection of phthalimide was 10 equivalents per phthalimide group on the substrate. For example, a mono-alkylated calix[4]arene possessing 1 phthalimide group required at least 10 equivalents of hydrazine monohydrate for full conversion from the alkylphthalimide into alkylamine.

Stellenbosch University https://scholar.sun.ac.za

- The average time for the complete formation of the product was 5 hours. In addition, it was found that the longer the reaction time, the lower the yield (See **Table 2.2** for attempted Gabriel reactions summary).

*Table 2.2 Comparative results for Gabriel reaction on the monobutylated p-t-butyl-calix[4]arene **(5b)** using different approaches*

Entry	Deprotecting agent (equiv.)	Extra reagent (equiv.)	Conc. (M)	Time	Solvent	Temp. (°C)	Yield (%)
1	$NaBH_4$ (5.0)	Glacial acetic acid (16.2)	0.1	26 h	2-propanol/H_2O	25→80	52
2	$MeNH_2$·HCl (10.0)	K_2CO_3 solution (0.01 M) (until pH=10)	0.1	24 h	EtOH	70	No reaction
3	N_2H_4·H_2O (10.0)	-	0.05	72 h	EtOH/THF	Reflux	<10
4	N_2H_4·H_2O (10.0)	-	0.05	24 h	EtOH/THF	Reflux	45
5	N_2H_4·H_2O (10.0)	-	0.05	5 h	EtOH/THF	Reflux	81

2.7 Purification challenge for the synthesized aminocalix[4]arene and the solution

The first challenge in these reactions was the loss of a significant ammount of product after the reaction, when it was filtered and the insoluble salt was removed. A very poor yield was obtained, apparently due to the complexation of the newly formed amine with phthalhydrazide salt. In order to solve the problem, the crude reaction mixture was acidified (1<pH<2), filtered, then re-basified (9<pH<10) and finally the product (free amine) was re-extracted and dried *in vacuo*. This procedure significantly increased the yield for the hydrazinolysis.

2.8 Hydrazinolysis of alkylated *p-t*-butyl-calix[4]arenes

This section provides the reader with the interpretation of the spectral data for multiple examples of the hydrazinolysis reactions. It must be noted that the de-protection was only attempted on the alkylated *p-t*-butyl-calix[4]arenes (due to the simplicity of producing these compounds, the hydrazinolysis reactions were only done on them and not on the alkylated plain calix[4]arenes which had purification issues like the difficulty of removing many side-products, while not drastically increasing the yields compared to the alkylated *p-t*-butyl-calix[4]arenes) (**Scheme 2.12** shows examples of hydrazinolysis).

Stellenbosch University https://scholar.sun.ac.za

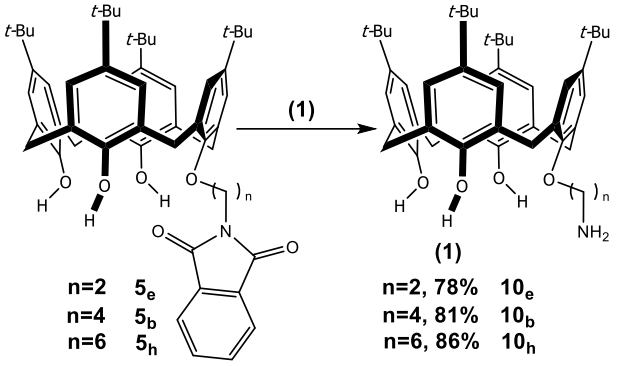

*Scheme 2.12 Hydrazinolysis of a series of monoalkylated p-t-butyl-calix[4]arene (**5e, 5b, 5h**). Reagents and conditions: (1) $N_2H_4{\cdot}H_2O$ (10.0 equiv.), EtOH/THF, reflux, 5 h*

In the ^{1}H-NMR spectra for monoalkylamino *p-t*-butyl-calix[4]arenes (compounds **10e**, **10b**, **10h**), the first noteworthy point was the disappearance of the phthalimide signals (between 7.50 and 8.00 ppm). The inequivalent aromatic protons also suggested dissymmetry (monofunctionalized *p-t*-butyl-calix[4]arene). On the other hand, these compounds behaved differently in terms of the whereabouts of the amine functionality and phenolic protons of the lower-rim. Ethylamine **10e**, which potentially possessed the strongest hydrogen bonding (shortest tether), did not reveal either of its NH_2 or OH groups in the ^{1}H-NMR spectrum, while for butylamine **10b** (**Figure 2.6** shows its ^{1}H-NMR spectrum) and hexylamine **10h**, these signals merged with each other to form a broad singlet. For butylamine **10b**, the signal was observable at 6.80 ppm, while for hexylamine **10h**, it is seen at 8.17 ppm. In truth, the one with the longest tether (**10h**) was supposed to have the weakest hydrogen bonding and naturally possess the most upfield phenolic protons (and obviously the slowest proton exchange between NH_2 and OH), but the experimental data suggest the other way around. In other words, the ^{1}H-NMR spectral data may propose that due to some unusual steric effects the hexylamine **10h** formed a hydrogen bond stronger than that of butylamine **10b**, resulting in the shifting of the phenolic protons more downfield than initially expected. However, given too many contradictory parameters here, the chemical shift values are still too complex to be interpreted without any further supporting evidence.

In the FT-IR spectrum, there were two characteristic signals indicating the existence of the primary amine group. The first was a medium bend related to N-H group observable at 1599 cm^{-1} (ethylamine **10e**), 1573 cm^{-1} (butylamine **10b**) and 1600 cm^{-1} (hexylamine **10h**). The second one was a medium stretch for C-N which could be observed at 1300 cm^{-1} (ethylamine **10e**), 1296 cm^{-1} (butylamine **10b**) and 1298 cm^{-1} (hexylamine **10h**).

Stellenbosch University https://scholar.sun.ac.za

According to HRMS results, there were molecular ions 692.4688 Da for ethylamine **10_e** (calculated for $[M+H]^+$: 692.4679 Da), 720.4979 Da for butylamine **10_b** (calculated for $[M+H]^+$: 720.4992 Da) and 748.5308 Da for hexylamine **10_h** (calculated for $[M+H]^+$: 748.5305 Da).

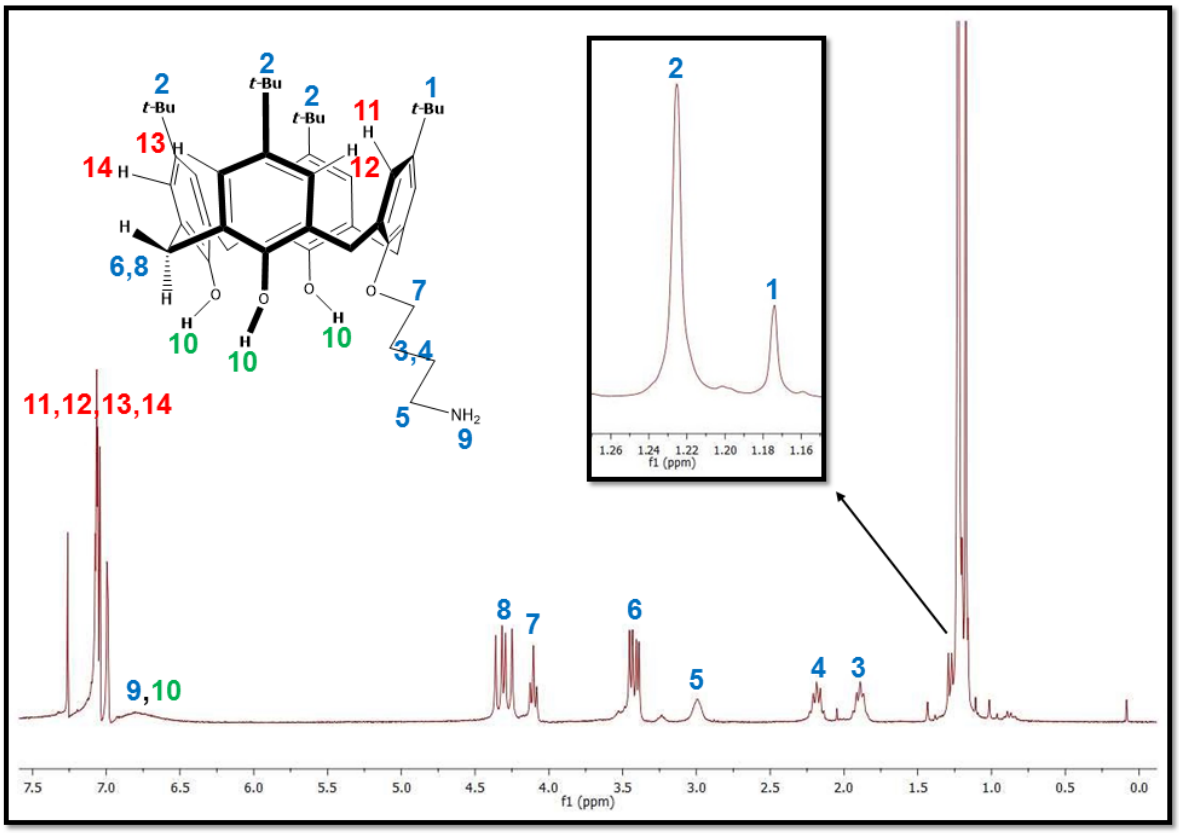

*Figure 2.6 An example of the ^{1}H-NMR spectrum (in $CDCl_3$) for a monoalkylamino p-t-butyl-calix[4]arene (**10_e**)*

2.9 Concluding remarks

Overall in this chapter, initially different conditions (including various bases, solvents, and temperatures) were applied in order to synthesize mono-alkylated calix[4]arenes (as precursors for amine) with different chain lengths were investigated. The synthesis of mono-alkylated calix[4]renes was carried out in high yield and then the synthesized alkylated calix[4]arenes were subjected to several deprotection methods. Amongst all of these methods, only one of them was found efficient enough for producing primary amine-tethered calix[4]arene in appropriate yields (hydrazinolysis). However, the purification issues for the newly synthesized amines turned into a challenge and a solution was considered with respect to that. To resolve this, acidification of the crude amine with 4 M HCl, filtration, re-basification with 2 M NaOH and finally re-extraction (into DCM) were utilized to achieve the pure free amine. These

Stellenbosch University https://scholar.sun.ac.za

successfully synthesized aminocalix[4]arenes will be studied in chapter 3 for their capabilities to be grafted onto PSMA.

2.10 Experimental section

2.10.1 Chemicals

All chemicals (solvents and reagents) involved with this project were sourced from either Sigma-Aldrich or Merck. Toluene and THF were distilled under nitrogen using sodium wires. In the case of THF, benzophenone was used as the color-changing indicator (color change from brown to blue upon moisture removal). DCM, acetonitrile and DMF were distilled from calcium hydride (the first two under nitrogen and the third one under vacuum). Ethanol was distilled under nitrogen with magnesium turnings plus iodine. All distilled solvents were stored in sealed containers with 4 Å molecular sieves. The remaining solvents were purified with the common methods available in literature.[20,21]

2.10.2 Inert conditions

All reactions were carried out under a positive pressure of argon using a typical Schlenk system equipped with a mercury bubbler for pressure regulation.

2.10.3 Chromatographic techniques

All column chromatography was performed with Merck silica gel (mesh size: 230-400, particle size: 0.04 to 0.063 mm). The elution operation was done with one or a mixture of the following solvents: Ethyl acetate, DCM, petroleum ether, methanol and lastly ethanol. Aluminum backed Merck silica gel 60 F_{254} plates were employed for thin layer chromatography (TLC) and the results were visualized with a UV lamp. In some cases, in order to better visualize the products, the plates were dipped in either CAM stain solution (cerium ammonium molybdate) and heated afterward or kept in iodine stain (a mixture of silica gel and molecular iodine) for a short period.

2.10.4 Characterization techniques

2.10.4.1 ATR-FTIR (attenuated total reflectance Fourier transform infrared) spectroscopy

A Nicolet FTIR spectrometer (model is10) from Thermo-Scientific equipped with a diamond internal reflection crystal was used for IR experiments. All spectra were obtained from the solid samples producing results between 4000 cm^{-1} and 650 cm^{-1}, while the spectral resolution was

Stellenbosch University https://scholar.sun.ac.za

4 cm^{-1} and the sum of the individual scans were 128 cm^{-1}. Acquiring data and processing them were done by Omnic software (version 7.0).

2.10.4.2 NMR (nuclear magnetic resonance) spectroscopy

A Varian VNMRS 300 MHz instrument (75 MHz for ^{13}C-NMR) was employed to obtain all NMR spectra. Considering the solubility status of our products, the deuterated chloroform ($CDCl_3$) was chosen for dissolving the products for analysis. The deuterated solvent included tetramethylsilane (TMS) as the internal standard (δ=0 ppm) from which all chemical shift values were measured in ppm downfield at room temperature.[n]

2.10.4.3 HRMS (high-resolution mass spectrometry)

High-resolution mass spectrometry operations were carried out by Waters API Q-TOF Ultima spectrometer in Stellenbosch Central Analytical Facility.

2.10.4.4 Melting point

Gallenkamp Melting Point Apparatus was employed to determine all melting points.

2.10.5 Synthetic procedures

In this section, the synthetic procedures for producing the compounds discussed in chapter 2 will be presented. Also, the characterization data for each compound will be provided.

2.10.5.1 Synthesis of project starting materials

Here the synthesis of calix[4]arenes, phthalimide reagents, the azide reagent, and some other compounds will be explained and the spectral data will be provided accordingly.

2.10.5.1.1 Synthesis of calix[4]arenes

5,11,17,23-Tetra-*t*-butyl-25,26,27,28-tetrahydroxy-calix[4]arene – 3

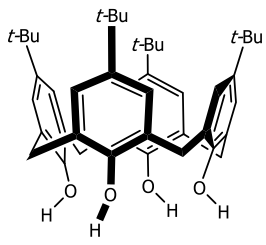

para t-Butyl phenol (104 g, 692 mmol), formaldehyde solution (37%) (64.5 mL, 795 mmol) and NaOH pellets (500 mg, 13.0 mmol) in H_2O (2.5 mL) were placed in a 2 L three-neck round-bottom flask. It was then equipped with a mechanical stirrer and while stirring it was put under a steady nitrogen flow and heated at 120 °C for almost 45 minutes until

[n] In the last chapter of this dissertation, the high temperature experiments were run using a 400 MHz Varian Unity Inova (100 MHz for ^{13}C-NMR).

Stellenbosch University https://scholar.sun.ac.za

the formation of a green-yellow viscous mass. At this point the stirring was stopped, the reaction was cooled down to room temperature and diphenyl ether (850 mL) was added. Thereafter toluene (50 mL) was added, stirring restarted and the temperature was raised to 120 °C in order to remove the remnants of water (azeotropic effect of toluene). Having finished that stage, the nitrogen outlet was fitted with a reflux condenser (with compressed air flow) and the reaction was brought to reflux for 4 hours. After that, the heating was stopped, but not the stirring and when the reaction became cold enough, ethyl acetate (600 mL) was added (another one hour of stirring). The reaction vessel contents were filtered and the solid was rinsed with small portions of ethyl acetate. The resulting solid was then triturated first with glacial acetic acid (100 mL) and then with diethyl ether (100 mL) to afford a white fine powder (65.6 g, 58%). The spectral data were correlated with that from literature.[22] ^{1}H-NMR (300 MHz, $CDCl_3$) δ ppm 1.22 (s, 36H, $C(CH_3)_3$), 3.44-3.58 (m, 4H, $ArCH_2Ar$), 4.18-4.36 (m, 4H, $ArCH_2Ar$), 7.06 (s, 8H, ArH), 10.35 (s, 4H, ArOH).

25,26,27,28-Tetrahydroxy-calix[4]arene – 7

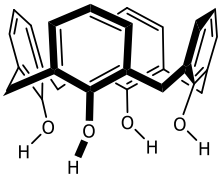

5,11,17,23-Tetra-*t*-butyl-25,26,27,28-tetrahydroxy-calix[4]arene **3** (9.60 g, 15.0 mmol) was suspended in dry toluene (90 mL) under an argon atmosphere in a two-neck 500 mL round-bottom flask. To that was added $AlCl_3$ (15.6 g, 120 mmol) and phenol (11.4 g, 120 mmol) and the reaction was stirred at room temperature for 4 hours. After that, 0.2 N HCl (150 mL) was added and stirring continued for another 5 minutes. Then the reaction was transferred into a separation funnel and extracted three times with DCM (3×150 mL). The organic layer was dried over anhydrous $MgSO_4$ and the solvent was removed under the reduced pressure. The crude finally was triturated with methanol (150 mL) to reveal a white solid (5.50 g, 86%). The spectral data were correlated with that from literature.[23] ^{1}H-NMR (300 MHz, $CDCl_3$) δ ppm 3.58 (br. s, 4H, $ArCH_2Ar$), 4.29 (br. s, 4H, $ArCH_2Ar$), 6.76 (t, *J*=7.6 Hz, 4H, ArH), 7.08 (d, *J*=7.6 Hz, 8H, ArH), 10.23 (s, 4H, ArOH).

2.10.5.1.2 Synthesis of phthalimide reagents

2.10.5.1.2.1 General procedure for the synthesis of phthalimide reagents

Potassium phthalimide was either heated under reflux in 1,*n*-dibromoalkane or mixed with it in DMF and heated at 100 °C for 12 hours. For the 1st approach, the reaction was quenched with water (50 mL) and the product was extracted with DCM (3×50 mL). The DCM layer was dried over anhydrous $MgSO_4$ and concentrated *in vacuo*. For the 2nd approach, the reaction was

Stellenbosch University https://scholar.sun.ac.za

quenched with water (50 mL), extracted with ethyl acetate (3×50 mL), washed with water (6×50 mL) and dried like the 1st approach. The crude was purified with a column chromatography (2% EtOAc/petroleum ether) to yield the final product as a colorless solid. They are described below:

_N_-(2-bromoethyl)-phthalimide – 4_e

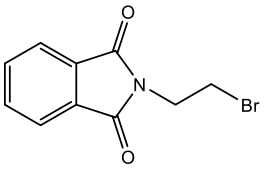

It was made following the general procedure (approach 1) with potassium phthalimide (3.00 g, 16.1 mmol) and 1,2-dibromoethane (12.1 g, 64.4 mmol). (2.87 g, 70%); The spectral data were correlated with that from literature.[9] ^{1}H-NMR (300 MHz, $CDCl_3$) δ ppm 3.60 (t, *J*=6.9 Hz, 2H, C-CH_2Br), 4.09 (t, *J*=6.9 Hz, 2H, NCH_2-C), 7.73-7.76 (m, 2H, ArH), 7.86-7.89 (m, 2H, ArH).

_N_-(4-bromobutyl)-phthalimide – 4_b

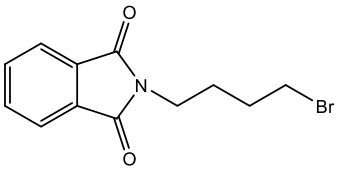

It was made following the general procedure (approach 2) with potassium phthalimide (930 mg, 5.00 mmol) and 1,4-dibromobutane (5.40 g, 25.0 mmol) in DMF (10 mL). (1.23 g, 87%); The spectral data were correlated with that from literature.[9] ^{1}H-NMR (300 MHz, $CDCl_3$) δ ppm 1.80-1.96 (m, 4H, CH_2-CH_2), 3.45 (t, *J*=6.9 Hz, 2H, C-CH_2Br), 3.73 (t, *J*=6.9 Hz, 2H, NCH_2-C), 7.70-7.73 (m, 2H, ArH), 7.83-7.86 (m, 2H, ArH).

_N_-(6-bromohexyl)-phthalimide – 4_h

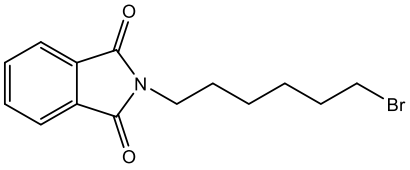

It was made following the general procedure (approach 2) with potassium phthalimide (1.86 g, 10.0 mmol) and 1,6-dibromohexane (12.2 g, 50.0 mmol) in DMF (10 mL). (2.50 g, 81%); The spectral data were correlated with that from literature.[9] ^{1}H-NMR (300 MHz, $CDCl_3$) δ ppm 1.30-1.53 (m, 4H, CH_2), 1.64-1.89 (m, 4H, CH_2), 3.40 (t, *J*=6.9 Hz, 2H, C-CH_2Br), 3.69 (t, *J*=6.9 Hz, 2H, NCH_2-C), 7.69-7.71 (m, 2H, ArH), 7.82-7.84 (m, 2H, ArH).

Stellenbosch University https://scholar.sun.ac.za

2.10.5.1.3 Spectral data for other reagents

Butane-1,4-diyl bis(4-methylbenzenesulfonate) – 1

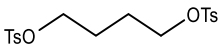

To a stirring solution of *p*-toluenesulfonyl chloride (3.17 g, 16.6 mmol) and triethylamine (3.00 mL, 22.7 mmol) and DMAP (5 mol%) in anhydrous DCM (6 mL) at 0 °C, was added a solution of 1,4-butanediol (620 mg, 7.60 mmol) in DCM (5 mL). The reaction was slowly warmed up to room temperature and the stirring continued for 24 hours. Thereafter the reaction was diluted with DCM (50 mL) and got cooled down to 0 °C and quenched with 0.2 M HCl (50 mL). The reaction was transferred into a separation funnel, its DCM layer was separated and the remaining product was extracted from the aqueous layer with DCM (5×50 mL). The combined organic phase was dried over anhydrous $MgSO_4$ and DCM evaporated *in vacuo*. The oily crude was purified via a column chromatography (10% EtOAc/petroleum ether) to afford the desired bistosylate as a yellow solid (2.00 g, 66%); The spectral data were correlated with that from literature.[6] ^{1}H-NMR (300 MHz, $CDCl_3$) δ ppm 1.65-1.69 (m, 4H, CH_2-CH_2), 2.43 (s, 6H, CH_3), 3.97 (br. t, *J* =5.8 Hz, 4H, OCH_2-C), 7.32 (d, *J*=8.4 Hz, 4H, ArH), 7.73 (d, *J* =8.4 Hz, 4H, ArH).

Azidomethyl 4-methylbenzenesulfonate – 2

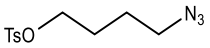

Butane-1,4-diyl bis(4-methylbenzenesulfonate) **1** (200 mg, 0.500 mmol) and NaN_3 (40.0 mg, 0.550 mmol) were placed in a 10-mL round-bottom flask containing DMF (5 mL). The mixture was stirred at room temperature for 72 hours. The reaction was quenched with water and extracted into a separation funnel with EtOAc (3×50 mL) and washed with water again (6×50 mL). The organic layer was dried over anhydrous $MgSO_4$ and removed under the reduced pressure. The crude was purified with a column chromatography (10% EtOAc/petroleum ether) to produce a yellow oil (30.0 mg, 22%). R_f=0.46 (25% EtOAc/Petroleum ether); ^{1}H-NMR (300 MHz, $CDCl_3$) δ ppm 1.56-1.78 (m, 4H, CH_2-CH_2), 2.45 (s, 3H, CH_3), 3.25 (t, *J*=6.6 Hz, 2H, CH_2N), 4.05 (t, *J*=6.0 Hz, 2H, OCH_2), 7.34 (d, *J*=8.2 Hz, 2H, ArH), 7.75 (d, *J*=8.2 Hz, 2H, ArH). ^{13}C-NMR (75 MHz, $CDCl_3$) δ ppm 21.5 (CH_3), 25.0 (C-CH_2-C), 26.0 (C-CH_2-C), 50.6 (CH_2N_3), 69.7 (OCH_2), 127.9 (2 × $C_{Ar}H$), 129.9 (2 × $C_{Ar}H$), 133.0 (C-C_{Ar}), 144.9 ($C_{Ar}SO_3$).

Stellenbosch University https://scholar.sun.ac.za

FT-IR (ATR) cm^{-1}: 2951 (m, Aliphatic C-H stretch), 2093 (s, N=N=N stretch), 1354 (s, Aliphatic C-H bend), 1173 (s, C-O stretch).

HRMS-TOF MS ESI$^+$: *m/z* $[M+Na]^+$ calculated for $C_{11}H_{15}N_3O_3SNa$ 292.0732 Da; found: 292.0725 Da. Also: 242.0848 Da (calculated for $[M+H-N_2]^+$: 242.0851 Da).

***N*-(4-iodobutyl)-phthalimide – $4_{b\text{-}i}$**

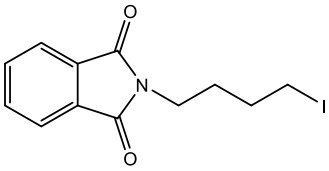

N-(4-bromobutyl)-phthalimide **4_b** (310 mg, 1.10 mmol) and NaI (1.64 g, 11.0 mmol) were stirred in acetone (12 mL) for 24 hours at room temperature. After that, the solvent was removed under the reduced pressure and water (50 mL) was added to the remaining crude. The crude was transferred to a separation funnel and the product was extracted with DCM (3×50 mL). The organic phase was collected and evaporated *in vacuo*. The final crude was purified with a column chromatography (10% EtOAc/Petroleum ether) resulting in a white solid (300 mg, 91%); The spectral data were correlated with that from literature.[10] ^{1}H-NMR (300 MHz, $CDCl_3$) δ ppm 1.7-1.89 (m, 4H, CH_2-CH_2), 3.19 (t, *J*=6.6 Hz, 2H, C-CH_2I), 3.68 (t, *J*=6.6 Hz, 2H, NCH_2-C), 7.67-7.70 (m, 2H, ArH), 7.79-7.82 (m, 2H, ArH).

2.10.5.2 Synthesis of alkylated calix[4]arenes

This part is dedicated to the methods for producing alkylated calix[4]arenes.

2.10.5.2.1 General procedure for the synthesis of mono-alkylated calix[4]arenes

With *p*-*t*-butyl-calix[4]arene:

(A) NaH approach: A mixture of 5,11,17,23-tetra-*t*-butyl-25,26,27,28-tetrahydroxy-calix[4]arene **3** and NaH (60% in oil) (1.0 equiv.) in dry DMF in a round-bottom flask was stirred at 80 °C for 24 hours under argon. *N*-(*n*-bromoalkyl)-phthalimide (1.5 equiv.) was added and the stirring continued under the same conditions for another 24 hours. The reaction was cooled down and quenched with 50 mL of NH_4Cl (saturated solution). Ethyl acetate (3×50 mL) was added and then everything was transferred into a separation funnel. The organic phase was separated and washed with water (6×50 mL) and brine (50 mL) and dried over anhydrous $MgSO_4$. The EtOAc layer was removed under the reduced pressure and the crude left was purified via a column chromatography (10% EtOAc/petroleum ether). Finally, the columned material was

Stellenbosch University https://scholar.sun.ac.za

triturated with methanol to afford the desired monoalkylated *p*-*t*-butyl-calix[4]arene as a white foam.

(B) K_2CO_3 approach: In this case, a mixture of 5,11,17,23-tetra-*t*-butyl-25,26,27,28-tetrahydroxy-calix[4]arene **3**, alkyl halide (3.3 equiv.) and K_2CO_3 (0.6 equiv.) in acetonitrile in a round-bottom flask equipped with a condenser was heated under reflux for 24 hours under argon. The reaction was quenched with 1 M HCl (50 mL), extracted with DCM (5×50 mL) and the resulting crude was columned with (10% EtOAc/petroleum ether). The columned material was triturated with methanol producing a white foam.

5,11,17,23-Tetra-*t*-butyl-25-mono-phthalimideethoxy-26,27,28-trihydroxy-calix[4]arene – 5_e

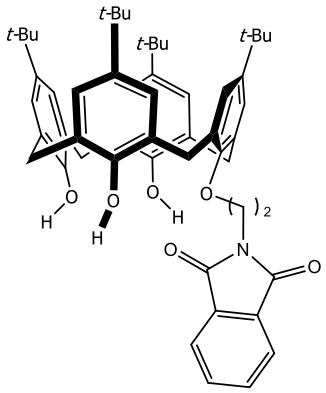

Synthesized following the general procedure (approach B) with 5,11,17,23-tetra-*t*-butyl-25,26,27,28-tetrahydroxy-calix[4]arene **3** (1.00 g, 1.55 mmol), anhydrous K_2CO_3 (140 mg, 0.920 mmol) and *N*-(2-bromoethyl)-phthalimide **4_e** (1.28 g, 5.08 mmol) in acetonitrile (48 mL). (390 mg, 30%); Mp 194 °C; R_f=0.38 (25% EtOAc/Petroleum ether); ^{1}H-NMR (300 MHz, $CDCl_3$) δ ppm 1.18 (s, 9H, $C(CH_3)_3$), 1.22 (s, 18H, $C(CH_3)_3$), 1.23 (s, 9H, $C(CH_3)_3$), 3.36 (d, 2H, *J*=8.1 Hz, $ArCH_2Ar$), 3.41 (d, *J*=8.1 Hz, 2H, $ArCH_2Ar$), 4.13 (d, *J*=13.3 Hz, 2H, $ArCH_2Ar$), 4.24 (d, *J*=13.3 Hz, 2H, $ArCH_2Ar$), 4.41 (s, 4H, OCH_2-CH_2N), 6.95 (d, *J*=2.4 Hz, 2H, ArH), 7.02 (s, 2H, ArH), 7.03 (d, *J*=2.4 Hz, 2H, ArH), 7.07 (s, 2H, ArH), 7.69-7.72 (m, 2H, phthalimide ArH), 7.95-7.98 (m, 2H, phthalimide ArH), 9.01 (s, 2H, ArOH), 9.77 (s, 1H, ArOH). ^{13}C-NMR (75 MHz, $CDCl_3$) δ ppm 31.3, 31.6, 31.7, 32.0, 33.0, 34.0, 34.1, 34.3, 38.0 (C-CH_2N), 73.3 (OCH_2-C), 123.5 (Ar), 125.6 (Ar), 125.7 (Ar), 125.8 (Ar), 126.7 (Ar), 127.3 (Ar), 127.7 (Ar), 128.3 (Ar), 132.6 (Ar), 133.3 (Ar), 134.0 (Ar), 142.8 (Ar), 143.5 (Ar), 147.7 (Ar), 148.5 (Ar), 148.6 (Ar), 148.8 (Ar), 168.8 (2 × C=O).

FT-IR (ATR) cm^{-1}: 3305 (b, O-H stretch), 2953 (b, Aliphatic C-H stretch), 1706 (s, C=O stretch), 1485 (m, Aliphatic C-H bend), 1194 (m, C-O stretch), 870 (m, C–H oop bend), 716 (s, C–H oop bend).

HRMS-TOF MS ESI$^+$: *m/z* $[M+Na]^+$ calculated for $C_{54}H_{63}NO_6Na$ 844.4553 Da; found: 844.4559 Da.

Stellenbosch University https://scholar.sun.ac.za

5,11,17,23-Tetra-*t*-butyl-25-mono-phthalimidebutoxy-26,27,28-trihydroxy-calix[4]arene – 5_b

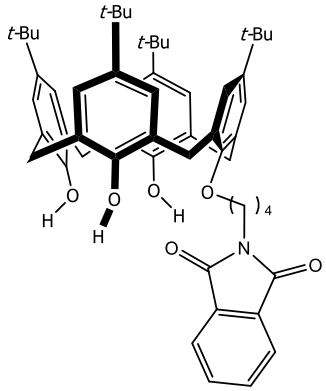

Synthesized following the general procedure (approach A) with 5,11,17,23-tetra-*t*-butyl-25,26,27,28-tetrahydroxy-calix[4]arene **3** (1.00 g, 1.55 mmol), NaH (60% in oil) (62.0 mg, 1.55 mmol) and *N*-(4-bromobutyl)-phthalimide $\mathbf{4_b}$ (650 mg, 2.32 mmol) in DMF (26 mL) producing 640 mg (49%) of the product. Alternatively, in case of using *N*-(4-iodobutyl)-phthalimide $\mathbf{4_{b\text{-}i}}$, 52% product was acquired. The K_2CO_3 method (approach B) with **3** (1.00 g, 1.55 mmol), K_2CO_3 (140 mg, 0.920 mmol) and *N*-(4-bromobutyl)phthalimide $\mathbf{4_b}$ (1.43 g, 5.08 mmol) in acetonitrile (48 mL) yielded 640 mg (49%) of the product; Mp 215 °C; R_f=0.69 (25% EtOAc/Petroleum ether); ^{1}H-NMR (300 MHz, $CDCl_3$) δ ppm 1.21 (s, 9H, $C(CH_3)_3$), 1.23 (s, 18H, $C(CH_3)_3$), 1.24 (s, 9H, $C(CH_3)_3$), 2.10-2.28 (m, 4H, C-CH_2-C), 3.38-3.48 (m, 4H, ArCH_2Ar), 3.93 (t, *J*=6.6 Hz, 2H, C-CH_2N), 4.19 (t, *J*=6.3 Hz, 2H, OCH_2-C), 4.24 (d, *J*=13.3 Hz, 2H, ArCH_2Ar), 4.34 (d, *J*=13.3 Hz, 2H, ArCH_2Ar), 6.99 (d, *J*=2.5 Hz, 2H, ArH), 7.05 (s, 2H, ArH), 7.06 (d, *J*=2.5 Hz, 2H, ArH), 7.09 (s, 2H, ArH), 7.68-7.70 (m, 2H, phthalimide ArH), 7.85-7.88 (m, 2H, phthalimide ArH), 9.51 (s, 2H, ArOH), 10.08 (s, 1H, ArOH) (Water signal was not removed even after heating the product under vacuum at 100 °C).[o] ^{13}C-NMR (75 MHz, $CDCl_3$) δ ppm 25.4, 27.2, 31.3, 31.5, 31.6, 32.3, 32.7, 33.1, 34.0, 34.1, 34.3, 37.6 (C-CH_2N), 76.3 (OCH_2-C), 123.4 (Ar), 125.7 (Ar), 125.8 (Ar), 126.0 (Ar), 126.5 (Ar), 127.7 (Ar), 127.8 (Ar), 128.2 (Ar), 128.4 (Ar), 132.2 (Ar), 133.6 (Ar), 134.0 (Ar), 143.1 (Ar), 143.6 (Ar), 144.5 (Ar), 146.8 (Ar), 147.8 (Ar), 148.2 (Ar), 148.6 (Ar), 149.3 (Ar), 168.6 (2 × C=O).

FT-IR (ATR) cm^{-1}: 3274 (b, O-H stretch), 2952 (b, Aliphatic C-H stretch), 1712 (s, C=O stretch), 1483 (m, Aliphatic C-H bend), 1200 (m, C-O stretch), 872 (m, C–H oop bend), 719 (m, C–H oop bend).

HRMS-TOF MS ESI$^+$: *m/z* $[M+NH_4]^+$ calculated for $C_{56}H_{71}N_2O_6$ 867.5312 Da; found: 867.5308 Da.

[o] There is also a singlet corresponding to another possible isomer of this compound at 10.36 ppm.

Stellenbosch University https://scholar.sun.ac.za

5,11,17,23-Tetra-*t*-butyl-25-mono-phthalimidehexoxy-26,27,28-trihydroxy-calix[4]arene – 5_h

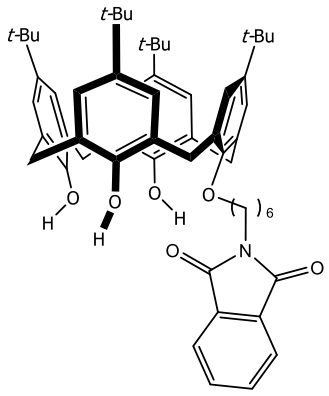

Synthesized following the general procedure (approach A) with 5,11,17,23-tetra-*t*-butyl-25,26,27,28-tetrahydroxy-calix[4]arene **3** (1.00 g, 1.55 mmol), NaH (60% in oil) (62.0 mg, 1.55 mmol) and *N*-(6-bromohexyl)-phthalimide **4_h** (710 mg, 2.28 mmol) in DMF (26 mL) producing 1.00 g (75%) of the product. The K_2CO_3 method (approach B) with **3** (1.00 g, 1.55 mmol), K_2CO_3 (140 mg, 0.920 mmol) and *N*-(6-bromohexyl)phthalimide **4_h** (1.58 g, 5.08 mmol) in acetonitrile (48 mL) yielded 840 mg (62%) of the product; Mp 234 °C DEC;[p] R_f=0.61 (25% EtOAc/Petroleum ether); ^{1}H-NMR (300 MHz, $CDCl_3$) δ ppm 1.23 (s, 9H, $C(CH_3)_3$), 1.26 (s, 18H, $C(CH_3)_3$), 1.27 (s, 9H, $C(CH_3)_3$), 1.56-1.66 (m, 2H, C-CH_2-C), 1.73-1.80 (m, 2H, C-CH_2-C), 1.83-1.92 (m, 2H, C-CH_2-C), 2.15-2.25 (m, 2H, C-CH_2-C), 3.44 (d, *J*=5.1 Hz, 2H, ArCH_2Ar), 3.47 (d, *J*=5.1 Hz, 2H, ArCH_2Ar), 3.81 (t, *J*=6.9 Hz, 2H, C-CH_2N), 4.16 (t, *J*=6.9 Hz, 2H, OCH_2-C), 4.29 (d, *J*=13.3 Hz, 2H, ArCH_2Ar), 4.36 (d, *J*=13.3 Hz, 2H, ArCH_2Ar), 7.02 (d, *J*=2.6 Hz, 2H, ArH), 7.07 (s, 2H, ArH), 7.09 (d, *J*=2.6 Hz, 2H, ArH), 7.12 (s, 2H, ArH), 7.62-7.65 (m, 2H, phthalimide ArH), 7.81-7.83 (m, 2H, phthalimide ArH), 9.60 (s, 2H, ArOH), 10.19 (s, 1H, ArOH).[q] ^{13}C-NMR (75 MHz, $CDCl_3$) δ ppm 25.7, 26.8, 28.8, 29.8, 31.4, 31.5, 31.6, 31.7, 32.4, 32.7, 33.1, 34.0, 34.1, 34.3, 38.0 (C-CH_2N), 77.0 (OCH_2-C), 123.2 (Ar), 125.8 (Ar), 126.0 (Ar), 126.5 (Ar), 127.8 (Ar), 128.2 (Ar), 128.4 (Ar), 132.2 (Ar), 133.6 (Ar), 133.8 (Ar), 143.1 (Ar), 143.6 (Ar), 144.5 (Ar), 146.8 (Ar), 147.9 (Ar), 148.1 (Ar), 148.6 (Ar), 149.4 (Ar), 168.6 (2 × C=O).

FT-IR (ATR) cm^{-1}: 3167 (b, O-H stretch), 2954 (b, Aliphatic C-H stretch), 1707 (s, C=O stretch), 1482 (m, Aliphatic C-H bend), 1202 (m, C-O stretch), 870 (m, C–H oop bend), 718 (m, C–H oop bend).

HRMS-TOF MS ESI$^+$: *m/z* $[M+NH_4]^+$ calculated for $C_{58}H_{75}N_2O_6$ 895.5625 Da; found: 895.5637 Da.

[p] Decomposition

[q] There is also a singlet corresponding to another possible isomer of this compound at 10.39 ppm.

Stellenbosch University https://scholar.sun.ac.za

With de-butylated calix[4]arene:

(A) NaOMe approach: A mixture of 25,26,27,28-Tetrahydroxyl-calix[4]arene **7** and NaOMe (1.2 equiv.) in dry acetonitrile in a round-bottom flask equipped with a condenser was heated under reflux for 24 under argon. Afterward, the desired *N*-(*n*-bromoalkyl)-phthalimide (2.5 equiv.) was added and the stirring continued under the same conditions for another 24 hours. The reaction got cooled down and quenched with 1 M HCl (50 mL) and transferred into a separation funnel. The acetonitrile layer was separated and the aqueous layer was re-extracted with DCM (5×50 mL). The combined organic layer was dried over anhydrous $MgSO_4$ and the solvent was removed under the reduced pressure. The resulting crude was purified via a column chromatography (10% EtOAc/petroleum ether) to afford the desired monoalkylated calix[4]arene.

(B) K_2CO_3 approach: A mixture of 25,26,27,28-Tetrahydroxyl-calix[4]arene **7**, anhydrous K_2CO_3 (0.6 equiv.) and *N*-(*n*-bromoalkyl)-phthalimide (3.3 equiv.) in dry acetonitrile in a round-bottom flask equipped with a condenser was heated under reflux for 24 hours under argon. Then the reaction was cooled down and quenched with 1 M HCl (50 mL) and the product was extracted with DCM (5×50 mL) into a separation funnel. The DCM layer was dried over anhydrous $MgSO_4$ and the solvent was removed under the reduced pressure. The crude was purified with a column chromatography (10% EtOAc/petroleum ether) to afford a white foam-like solid.

25-Mono-phthalimideethoxy-26,27,28-trihydroxy-calix[4]arene – 9_e

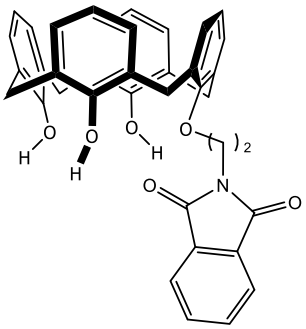

Synthesized following the general procedure (approach B) with 25,26,27,28-tetrahydroxy-calix[4]arene **7** (1.00 g, 2.36 mmol), anhydrous K_2CO_3 (190 mg, 1.40 mmol) and *N*-(2-bromoethyl)-phthalimide $\mathbf{4_e}$ (2.00 g, 7.94 mmol) in acetonitrile (72 mL) (680 mg, 48%); Mp 231°C DEC; R_f=0.61 (40% EtOAc/Petroleum ether); ^{1}H-NMR (300 MHz, $CDCl_3$) δ ppm 3.37 (d, *J*=8.9 Hz, 2H, $ArCH_2Ar$), 3.42 (d, *J*=8.9 Hz, 2H, $ArCH_2Ar$), 4.11 (d, *J*=13.3 Hz, 2H, $ArCH_2Ar$), 4.19 (d, *J*=13.3 Hz, 2H, $ArCH_2Ar$), 4.34-4.46 (m, 4H, OCH_2-CH_2N), 6.63 (t, *J*=7.9 Hz, 3H, ArH), 6.83 (t, *J*=7.9 Hz, 1H, ArH), 6.93 (d, *J*=7.9 Hz, 2H, ArH), 6.95-6.99 (m, 4H, ArH), 7.01 (d, *J*=7.9 Hz, 2H, ArH), 7.66-7.69 (m, 2H, phthalimide ArH), 7.96-7.98 (m, 2H, phthalimide ArH), 8.79 (s, 2H, ArOH), 9.24 (s, 1H, ArOH) (*n*-hexane, water and ethyl acetate signals were not

Stellenbosch University https://scholar.sun.ac.za

removed even after heating the product under vacuum at 100 °C).[r] ^{13}C-NMR (75 MHz, $CDCl_3$) δ ppm 31.17 (2 × $ArCH_2Ar$), 31.84 (2 × $ArCH_2Ar$), 37.93 (C-CH_2N), 73.45 (OCH_2-C), 120.5 (Ar), 122.0 (Ar), 123.5 (Ar), 126.5 (Ar), 127.8 (Ar), 128.1 (Ar), 128.3 (Ar), 128.7 (Ar), 128.8 (Ar), 128.9 (Ar), 129.6 (Ar), 132.5 (Ar), 133.8 (Ar), 134.1 (Ar), 148.9 (2 × $C_{Ar}O$), 150.6 ($C_{Ar}O$), 151.3 ($C_{Ar}OC$), 169.0 (2 × C=O).

FT-IR (ATR) cm^{-1}: 3296 (b, O-H stretch), 2932 (b, Aliphatic C-H stretch), 1715 (s, C=O stretch), 1466 (m, Aliphatic C-H bend), 1193 (m, C-O stretch), 916 (m, C–H oop bend), 720 (s, C–H oop bend).

HRMS-TOF MS ESI$^-$: *m/z* $[M–H]^+$ calculated for $C_{38}H_{30}NO_6$ 596.2073 Da; found: 596.2088 Da.

25-Mono-phthalimidebutoxy-26,27,28-trihydroxy-calix[4]arene – 9_b

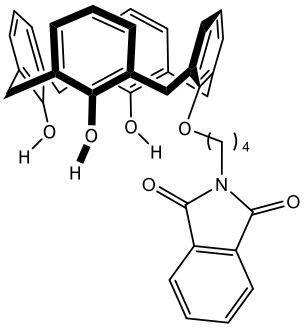

Synthesized following the general procedure (approach A) with 25,26,27,28-tetrahydroxy-calix[4]arene **7** (1.00 g, 2.36 mmol), NaOMe (160 mg, 2.84 mmol) and *N*-(4-bromobutyl)-phthalimide **4_b** (1.69 g, 5.92 mmol) in acetonitrile (70 mL) (530 mg, 36%). Alternatively in case of using K_2CO_3 (approach B), **7** (1.00 g, 2.36 mmol), K_2CO_3 (190 mg, 1.40 mmol) and *N*-(4-bromobutyl)phthalimide **4_b** (2.20 g, 7.79 mmol) in acetonitrile (72 mL) yielded 880 mg (59%) of the product. Mp 209 °C; R_f=0.54 (40% EtOAc/Petroleum ether); ^{1}H-NMR (300 MHz, $CDCl_3$) δ ppm 2.15-2.27 (m, 4H, C-CH_2-C), 3.43 (d, *J*=4.1 Hz, 2H, $ArCH_2Ar$), 3.48 (d, *J*=4.1 Hz, 2H, $ArCH_2Ar$), 3.95 (t, *J*=6.6 Hz, 2H, C-CH_2N), 4.20 (t, *J*=5.8 Hz,, 2H, OCH_2-C), 4.23 (d, *J*=13.4 Hz, 2H, $ArCH_2Ar$), 4.34 (d, *J*=13.4 Hz, 2H, $ArCH_2Ar$), 6.67 (t, *J*=7.4 Hz, 3H, ArH), 6.86 (t, *J*=7.4, 1H, ArH), 6.99 (d, *J*=7.4 Hz, 2H, ArH), 7.04-7.06 (m, 4H, ArH), 7.08 (d, *J*=7.4 Hz, 2H, ArH), 7.64-7.67 (m, 2H, phthalimide ArH), 7.84-7.87 (m, 2H, phthalimide ArH), 9.30 (s, 2H, ArOH), 9.58 (s, 1H, ArOH) (*n*-hexane, water, ethyl acetate and dichloromethane signals were not removed even after heating the product under vacuum at 100 °C).[s] ^{13}C-NMR (75 MHz, $CDCl_3$) δ ppm 25.4 (C-CH_2-C), 27.4 (C-CH_2-C), 31.5 (2 × $ArCH_2Ar$), 31.9 (2 × $ArCH_2Ar$), 37.7 (C-CH_2N), 76.5 (OCH_2-C), 120.9 (Ar), 122.0 (Ar), 123.4 (Ar), 126.3 (Ar),

[r] There are also two singlets corresponding to another possible isomer of this compound at 1.13 and 1.14 ppm.

[s] There is also a singlet corresponding to another possible isomer of this compound at 5.29 ppm.

Stellenbosch University https://scholar.sun.ac.za

128.4 (Ar), 128.5 (Ar), 128.8 (Ar), 128.9 (Ar), 129.5 (Ar), 132.2 (Ar), 134.0 (Ar), 134.2 (Ar), 149.2 ($C_{Ar}O$), 151.0 ($C_{Ar}O$), 151.4 ($C_{Ar}OC$), 168.6 (2 × C=O).

FT-IR (ATR) cm^{-1}: 3452 (m, O-H stretch), 2920 (m, Aliphatic C-H stretch), 1702 (s, C=O stretch), 1466 (m, Aliphatic C-H bend), 1036 (m, C-O stretch), 756 (m, C–H oop bend), 714 (m, C–H oop bend).

HRMS-TOF MS ESI$^-$: *m/z* $[M–H]^+$ calculated for $C_{40}H_{34}NO_6$ 624.2386 Da; found: 624.2399 Da.

Also: [plain calix[4]arene–H]$^+$ calculated for $C_{28}H_{23}O_4$ 423.1596 Da; found: 423.1592 Da.

25-Mono-phthalimidehexoxy-26,27,28-trihydroxy-calix[4]arene – 9_h

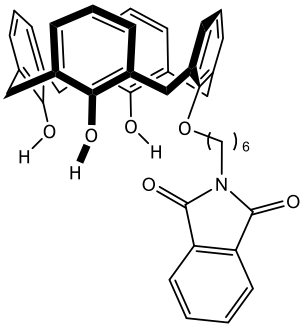

Synthesized following the general procedure (approach A) with 25,26,27,28-tetrahydroxy-calix[4]arene **7** (250 mg, 0.590 mmol), NaOMe (40.0 mg, 0.710 mmol) and *N*-(6-bromohexyl)-phthalimide **4_h** (460 mg, 1.48 mmol) in acetonitrile (18 mL) (180 mg, 48%). Alternatively, in case of using K_2CO_3 (approach B), **7** (1.00 g, 2.36 mmol), K_2CO_3 (190 mg, 1.40 mmol) and *N*-(6-bromohexyl)phthalimide **4_h** (2.41 g, 7.79 mmol) in acetonitrile (72 mL) yielded 830 mg (54%) of the product. Mp 212 °C; R_f=0.54 (40% EtOAc/Petroleum ether); ^{1}H-NMR (300 MHz, $CDCl_3$) δ ppm 1.57-1.69 (m, 2H, C-CH_2-C), 1.75-1.83 (m, 2H, C-CH_2-C), 1.86-1.93 (m, 2H, C-CH_2-C), 2.16-2.25 (m, 2H, C-CH_2-C), 3.44 (d, *J*=2.5 Hz, 2H, ArCH_2Ar), 3.48 (d, *J*=2.5 Hz, 2H, ArCH_2Ar), 3.82 (t, *J*=7.2 Hz, 2H, C-CH_2N), 4.17 (t, *J*=6.9 Hz, 2H, OCH_2-C), 4.28 (d, *J*=13.3 Hz, 2H, ArCH_2Ar), 4.36 (d, *J*=13.3 Hz, 2H, ArCH_2Ar), 6.69 (t, *J*=7.5 Hz, 3H, ArH), 6.87 (t, *J*=7.5 Hz, 1H, ArH), 7.01 (d, *J*=7.5 Hz, 2H, ArH), 7.03-7.07 (m, 4H, ArH), 7.09 (d, *J*=7.5 Hz, 2H, ArH), 7.58-7.61 (m, 2H, phthalimide ArH), 7.78-7.81 (m, 2H, phthalimide ArH), 9.40 (s, 2H, ArOH), 9.71 (s, 1H, ArOH) (Ethyl acetate signal was not removed even after heating the product under vacuum at 100 °C). ^{13}C-NMR (300 MHz, $CDCl_3$) δ ppm 25.7 (C-CH_2-C), 26.8 (C-CH_2-C), 28.8 (C-CH_2-C), 29.8 (C-CH_2-C), 31.5 (2 × ArCH_2Ar), 32.0 (2 × ArCH_2Ar), 38.0 (C-CH_2N), 77.2 (OCH_2-C), 121.0 (Ar), 122.0 (Ar), 123.2 (Ar), 126.2 (Ar), 128.5 (Ar), 128.8 (Ar), 128.9 (Ar), 129.4 (Ar), 132.2 (Ar), 133.8 (Ar), 134.3 (Ar), 149.3 ($C_{Ar}O$), 150.9 (2 × $C_{Ar}O$), 151.5 ($C_{Ar}OC$), 168.6 (2 × C=O).

Stellenbosch University https://scholar.sun.ac.za

FT-IR (ATR) cm^{-1}: 3322 (b, O-H stretch), 2938 (m, Aliphatic C-H stretch), 1705 (s, C=O stretch), 1465 (m, Aliphatic C-H bend), 1395 (m, Aliphatic C-H bend), 1263 (m, C-O stretch), 754 (m, C–H oop bend), 718 (m, C–H oop bend).

HRMS-TOF MS ESI$^-$: *m/z* $[M–H]^+$ calculated for $C_{42}H_{38}NO_6$ 652.2699 Da; found: 652.2722 Da.

2.10.5.3 Synthesis of aminocalix[4]arenes

As mentioned earlier, Gabrial synthesis was done efficiently by hydrazine monohydrate.

2.10.5.3.1 General procedure for the synthesis of aminocalix[4]arenes

The alkylated *p*-*t*-butyl-calix[4]arene was dissolved in a solution of EtOH/THF (volume ratio: 1:1). To this solution, was added hydrazine monohydrate (10.0 equiv. per every phthalimide group) and the solution was heated under reflux for 5 hours under argon. After several minutes, a white solid started crashing out of the solution (phthalhydrazide salt) which marks the beginning of the phthalimide deprotection. After that, the reaction was cooled down and acidified with 4 M HCl until 1<pH<2 and the liquor was filtered through a sintered funnel while the filter was washed with EtOH and EtOAc. The bottom liquor was this time basified with 2 M NaOH until 9<pH<10 and the product was re-extracted with DCM (5×50 mL) using a separation funnel. The organic phase was removed under the reduced pressure and the crude was pure enough to be used for the subsequent reactions.

5,11,17,23-Tetra-*t*-butyl-25-mono-(2-aminoethoxy)-26,27,28-trihydroxy-calix[4]arene – 10_e

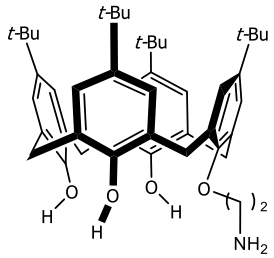

Following the general procedure, 5,11,17,23-tetra-*t*-butyl-25-mono-phthalimideethoxy-26,27,28-trihydroxy-calix[4]arene **5_e** (340 mg, 0.570 mmol) and hydrazine monohydrate (0.290 mL, 5.70 mmol) were placed in EtOH/THF (5.7 mL/5.7 mL). A white foam-like solid (310 mg, 78%) was collected. Mp 201 °C DEC; R_f=0.59 (7% MeOH/DCM); ^{1}H-NMR (300 MHz, $CDCl_3$) δ ppm 1.27 (s, 9H, $C(CH_3)_3$), 1.29 (s, 18H, $C(CH_3)_3$), 1.31 (s, 9H, $C(CH_3)_3$), 3.44-3.58 (m, 6H, $ArCH_2Ar$ and $C\text{-}CH_2N$), 4.27 (t, *J*=4.6 Hz, 2H, OCH_2-C), 4.34 (d, *J*=13.4 Hz, 2H, $ArCH_2Ar$), 4.43 (d, *J*=13.4 Hz, 2H, $ArCH_2Ar$), 7.06 (d, *J*=2.3 Hz, 2H, ArH), 7.13 (s, 2H, ArH), 7.14 (d, *J*=2.3 Hz, 2H, ArH), 7.17 (s, 2H, ArH) (Ethyl acetate signal was not removed even after heating the product under vacuum at 100 °C). ^{13}C-NMR (75 MHz, $CDCl_3$) δ ppm 31.1, 31.4, 32.1, 33.0, 33.8, 33.9, 34.1, 42.0 ($C\text{-}CH_2N$),

Stellenbosch University https://scholar.sun.ac.za

76.5, 78.4, 125.7 (Ar), 126.4 (Ar), 127.4 (Ar), 127.9 (Ar), 128.2 (Ar), 133.4 (Ar), 143.2 (Ar), 143.5 (Ar), 147.6 (Ar), 148.2 (Ar), 148.3 (Ar), 148.7 (Ar).

FT-IR (ATR) cm^{-1}: 3221 (b, O-H stretch), 2952 (s, Aliphatic C-H stretch), 1678 (m, Aromatic C-H bend), 1599 (m, N-H bend), 1482 (s, Aliphatic C-H bend), 1361 (m, Aliphatic C-H bend), 1300 (m, C-N stretch), 1201 (s, C-O stretch), 870 (m, C–H oop bend), 782 (m, C–H oop bend).

HRMS-TOF MS ESI$^+$: *m/z* $[M+H]^+$ calculated for $C_{46}H_{62}NO_4$ 692.4679 Da; found: 692.4688 Da.

5,11,17,23-Tetra-*t*-butyl-25-mono-(4-aminobutoxy)-26,27,28-trihydroxy-calix[4]arene – 10_b

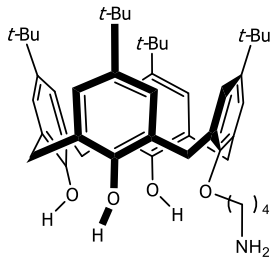

Following the general procedure, 5,11,17,23-tetra-*t*-butyl-25-mono-phthalimidebutoxy-26,27,28-trihydroxy-calix[4]arene **5_b** (770 mg, 0.850 mmol) and hydrazine monohydrate (0.440 mL, 8.50 mmol) were placed in EtOH/THF (8.5 mL/8.5 mL). A white foam-like solid (500 mg, 81%) was collected.

Mp 238 °C DEC; R_f=0.50 (7% MeOH/DCM); ^{1}H-NMR (300 MHz, $CDCl_3$) δ ppm 1.17 (s, 9H, $C(CH_3)_3$), 1.22 (s, 27H, $C(CH_3)_3$), 1.84-1.94 (m, 2H, C-CH_2-C), 2.14-2.23 (m, 2H, C-CH_2-C), 2.99 (br. s, 2H, C-CH_2N), 3.39 (d, *J*=5.9 Hz, 2H, ArCH_2Ar), 3.44 (d, *J*=5.9 Hz, 2H, ArCH_2Ar), 4.11 (t, *J*=6.8 Hz, 2H, OCH_2-C), 4.27 (d, *J*=13.2 Hz, 2H, ArCH_2Ar), 4.34 (d, *J*=13.2 Hz, 2H, ArCH_2Ar), 6.80 (br. s, 5H, ArOH and C-NH_2), 6.99 (d, *J*=2.1 Hz, 2H, ArH), 7.04 (s, 2H, ArH), 7.06 (d, *J*=2.1 Hz, 4H, ArH), 7.07 (s, 2H, ArH). ^{13}C-NMR (75 MHz, $CDCl_3$) δ ppm 20.1, 27.2, 29.8, 31.3, 31.5, 31.6, 31.7, 32.3, 32.8, 33.3, 34.0, 34.1, 34.2, 34.3, 40.9, 77.4 (OCH_2-C), 125.8 (Ar), 125.9 (Ar), 126.1 (Ar), 126.5 (Ar), 127.8 (Ar), 127.9 (Ar), 128.4 (Ar), 128.6 (Ar), 133.4 (Ar), 143.2 (Ar), 143.4 (Ar), 144.5 (Ar), 146.8 (Ar), 148.1 (Ar), 148.4 (Ar), 148.7 (Ar), 149.5 (Ar).

FT-IR (ATR) cm^{-1}: 2915 (s, Aliphatic C-H stretch), 2848 (s, Aliphatic C-H stretch), 1573 (m, N-H bend), 1405 (s, Aliphatic C-H bend), 1296 (m, C-N stretch), 1201 (m, C-O stretch), 922 (m, C–H oop bend), 791 (m, C–H oop bend).

HRMS-TOF MS ESI$^+$: *m/z* $[M+H]^+$ calculated for $C_{48}H_{66}NO_4$ 720.4992 Da; found: 720.4979 Da.

Stellenbosch University https://scholar.sun.ac.za

5,11,17,23-Tetra-*t*-butyl-25-mono-(6-aminohexoxy)-26,27,28-trihydroxy-calix[4]arene – 10_h

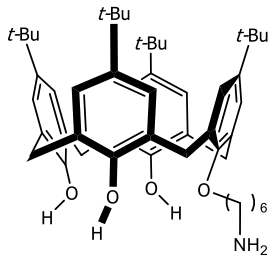

Following the general procedure, 5,11,17,23-tetra-*t*-butyl-25-mono-phthalimidehexoxy-26,27,28-trihydroxy-calix[4]arene **5_h** (820 mg, 0.930 mmol) and hydrazine monohydrate (0.460 mL, 9.30 mmol) were placed in EtOH/THF (9.3 mL/9.3 mL). A white foam-like solid (700 mg, 86%) was collected. Mp 232 °C DEC; R_f= 0.37 (7% MeOH/DCM); ^{1}H-NMR (300 MHz, $CDCl_3$) δ ppm 1.23 (s, 9H, $C(CH_3)_3$), 1.25 (s, 18H, $C(CH_3)_3$), 1.26 (s, 9H, $C(CH_3)_3$), 1.55-1.65 (m, 2H, C-CH_2-C), 1.68-1.78 (m, 2H, C-CH_2-C), 1.81-1.92 (m, 2H, C-CH_2-C), 2.13-2.23 (m, 2H, C-CH_2-C), 3.04 (br. s, 2H, C-CH_2N), 3.43 (d, *J*=4.5 Hz, 2H, ArCH_2Ar), 3.47 (d, *J*=4.5 Hz, 2H, ArCH_2Ar), 4.15 (t, *J*=6.6 Hz, 2H, OCH_2-C), 4.31 (d, *J*=13.5 Hz, 2H, ArCH_2Ar), 4.37 (d, *J*=13.5 Hz, 2H, ArCH_2Ar), 7.02 (d, *J*=2.3 Hz, 2H, ArH), 7.09 (s, 4H, ArH), 7.12 (d, *J*=2.3 Hz, 2H, ArH), 8.17 (br. s, 5H, ArOH and C-NH_2). ^{13}C-NMR (75 MHz, $CDCl_3$) δ ppm 25.3 (C-CH_2-C), 26.3 (C-CH_2-C), 28.6, 29.6, 31.2, 31.4, 32.1, 33.0, 33.8, 33.9, 34.1, 40.1 (C-CH_2N), 76.5 (OCH_2-C), 125.6 (Ar), 126.3 (Ar), 127.6 (Ar), 128.1 (Ar), 128.2 (Ar), 133.4 (Ar), 143.0 (Ar), 143.5 (Ar), 147.7 (Ar), 148.0 (Ar), 148.3 (Ar), 149.2 (Ar).

FT-IR (ATR) cm^{-1}: 3159 (b, O-H stretch), 2953 (s, Aliphatic C-H stretch), 1600 (m, N-H bend), 1482 (s, Aliphatic C-H bend), 1362 (m, Aliphatic C-H bend), 1298 (m, C-N stretch), 1201 (s, C-O stretch), 872 (m, C–H oop bend), 738 (m, C–H oop bend).

HRMS-TOF MS ESI$^+$: *m/z* $[M+H]^+$ calculated for $C_{50}H_{70}NO_4$ 748.5305 Da; found: 748.5308 Da.

2.11 References

(1) Nishimura, S. *Handbook of Heterogeneous Catalytic Hydrogenation for Organic Synthesis*, Wiley, Hoboken, New Jersey, United States, **2001**, 1st ed.

(2) Li, J. J.; Corey, E. J. *Name Reactions of Functional Group Transformations*, John Wiley & Sons, Hoboken, New Jersey, United States, **2007**.

(3) Ono, N. *The Nitro Group in Organic Synthesis*, John Wiley & Sons, Hoboken, New Jersey, United States, **2003**.

(4) Katritzky, A. R.; Ley, S. V.; Meth-Cohn, O.; Rees, C. W. *Comprehensive Organic*

Stellenbosch University https://scholar.sun.ac.za

Functional Group Transformations: Synthesis: Carbon with one heteroatom attached by a single bond, Elsevier, Amsterdam, Netherlands, **1995**.

(5) Dolphini, J. E.; Swain, E. J. *J. Org. Chem.* **1968**, *33*, 2079–2082.

(6) Van Wieringen, J. P.; Shalgunov, V.; Janssen, H. M.; Fransen, P. M.; Janssen, A. G. M.; Michel, M. C.; Booij, J.; Elsinga, P. H. *J. Med. Chem.* **2014**, *57*, 391–410.

(7) Jurisch, C. D. *A calix[4]arene polymer hybrid: attachment methodology*, Honours project, Department of Chemistry and Polymer, Stellenbosch University, **2016**.

(8) Gutsche, C. D. *Calixarenes: An Introduction*, Royal Society of Chemistry, Cambridge, United Kingdom, **2008**, 2nd ed.

(9) Kong, X.; He, Z.; Zhang, Y.; Mu, L.; Liang, C.; Chen, B.; Jing, X.; Cammidge, A. N. *Org. Lett.* **2011**, 13, 764–767.

(10) Thiruvengadam, T. K.; Gould, S. J.; Aberhart, D. J.; Lin, H. J. *J. Am. Chem. Soc.* **1983**, *105*, 5470–5476.

(11) Li, J. J. *Name Reactions: A Collection of Detailed Reaction Mechanisms*, Springer Science & Business Media, Berlin, Germany, **2013**, 2nd ed.

(12) Cox, M.; Prager, R. H.; Svensson, C. E. *Aust. J. Chem.* **2003**, *56*, 887–896.

(13) Groenen, L. C.; Ruël, B. H. M.; Casnati, A.; Verboom, W.; Pochini, A.; Ungaro, R.; Reinhoudt, D. N. *Tetrahedron* **1991**, *47*, 8379–8384.

(14) Sato, I.; Morihira, K.; Inami, H.; Kubota, H.; Morokata, T.; Suzuki, K.; Iura, Y.; Nitta, A.; Imaoka, T.; Takahashi, T.; Takeuchi, M.; Ohta, M.; Tsukamoto, S-I. *Bioorg. Med. Chem.* **2008**, *16*, 8607–8618.

(15) Shu, C.; Chung, W.; Wu, S.; Ho, Z.; Lin, L. *J. Org. Chem.* **1999**, *64*, 2673–2679.

(16) Gibson, M. S.; Bradshaw, R. W. *Angew. Chem. Int. Ed.* **1968**, *7*, 919–930.

(17) Kormendy, L. K. *Acta chim. Acad. SCI. Hung.* **1958**, *17*, 255–264.

(18) Osby, J. O.; Martin, M. G.; Ganem, B. *Tetrahedron Lett.* **1984**, *25*, 2093–2096.

(19) Ing, H.R.; Manske, R. H. F. *J. Chem. Soc.* **1926**, *129*, 2348–2351.

(20) Burfield, D. R.; Smithers, R. H.; Sui, A.; Tan, C. *J. Org. Chem.* **1981**, *46*, 629–631.

Stellenbosch University https://scholar.sun.ac.za

(21) Williams, D. B. G.; Lawton, M. *J. Org. Chem.* **2010**, *75*, 8351–8354.

(22) Gutsche, C. D.; Dhawan, B.; Kwang, H. *J. Am. Chem. Soc.* **1981**, *103*, 3782–3792.

(23) Gutsche, C. D.; Levine, J. A. *J. Am. Chem. Soc.* **1982**, *517*, 2652–2653.

Stellenbosch University https://scholar.sun.ac.za

Chapter 3. Synthesis of calix[4]arene-grafted PSMAs

3.1 Chapter overview

In this chapter, the synthesis and characterization methods for the calix[4]arene-grafted PSMAs using the calix[4]arene-tethered amines (synthesized in chapter 2) will be discussed. In the synthetic sections, the main focus will be on the effect of solvent choice (DMF or glacial acetic acid) and the reaction temperature (room temperature, reflux or 150 °C) on the nature of the final products. In the characterization sections, the main area of concern will be the proof of the formation of the characteristic functional groups like the maleamic acid or maleimide (through FT-IR and NMR spectroscopies) and also proof for the attachment of calix[4]arene onto PSMA to form the grafted polymer (using UV-Vis spectroscopy, SEC and DSC). In addition, the degree of functionalization for PSMA for different spacers (ethyl, butyl, and hexyl) of the graft polymers, together with their solubility in different solvents, will be determined. This study will enable us to suggest an appropriate calix[4]arene-tethered scaffold for our further studies in the following chapters. For further clarification, several examples will also be provided in detail.

3.2 Formation of maleimide functionality on the PSMA backbone using aminocalix[4]arene as the pendant group

It is known that the ring-opening reaction for PSMA can be done with ease, even at room temperature in solvents like DMF,[1] acetone[2] or methyl ethyl ketone,[3] and so forth. On the contrary, the ring-closing reaction requires much harsher conditions which include high reaction temperature (T>100 °C), acidic catalyst, for example, depending on the pendant group (here calix[4]arene) (**Scheme 3.1**).[4-9]

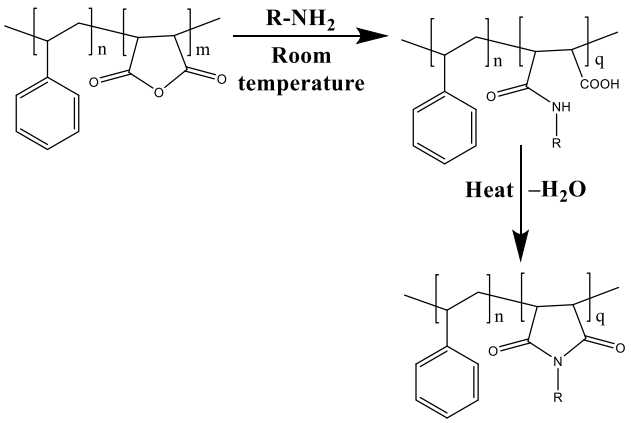

Scheme 3.1 General depiction of maleic anhydride modification first into maleamic acid and finally into maleimide (R: calix[4]arene alongside its tether, q: number of reacted maleic anhydride units)

Stellenbosch University https://scholar.sun.ac.za

It is, therefore, essential to discover a method through which the maleimide forms after the initial ring-opening stage on the maleic anhydride functionality. In order to do so, some studies were done regarding the different conditions for both ring-opening and ring-closing reactions on PSMA with primary amines through investigation of the literature. First of all, due to the good solubility of both aminocalix[4]arene and PSMA in DMF, this solvent was chosen for the ring-opening reaction at room temperature (**GP.A**). Secondly, with regards to the ring-closing reaction, different options were considered. One of them was based on using glacial acetic acid (as both solvent and catalyst for closing the ring) for the aminocalix[4]arenes which were soluble in acetic acid (**GP.B**). For the acetic acid-insoluble amines, a 2-step process (the ring-opening in DMF at room temperature, followed by the ring-closing via heating of the acquired product from the first step under reflux in acetic acid) was performed (**GP.C**). The other attempted choices were either directly heating the aminocalix[4]arene and PSMA in DMF at 150 °C (**GP.D**) or another 2-step reaction (the ring-opening in DMF at room temperature, followed by heating the same reaction vessel in DMF at 150 °C with the purpose of ring-closure) (**GP.E**). In the experimental section of this chapter, the difference between these methods and the acquired products out of them will be discussed, alongside an example for the primary amine-tethered calix[4]arene as the pendant group for PSMA.

3.3 Characterization methods for the graft polymer

3.3.1 Spectroscopic methods (FT-IR, ^{1}H-NMR, UV-Vis spectroscopies)

3.3.1.1 ATR-FTIR (attenuated total reflectance Fourier transform infrared) spectroscopy

All FT-IR spectra were obtained following the protocols explained in chapter 2. In addition, the degree of functionalization for PSMA by calix[4]arene was determined as follows: A bending frequency is observable at ~700 cm^{-1} which represents the out of plane mode for C-H (styrene groups).[6] This signal can be considered as an internal standard since styrene groups do not take part in the modification of the maleic anhydride group. The above-mentioned internal standard can be used for comparing the data for the starting material and the grafted product (the styrene signal possesses the same intensity before and after every reaction). By comparing the intensity of the maleic anhydride carbonyl (~1780 cm^{-1}) in the pristine PSMA and the same signal for the graft, proves how successfully the reaction has occurred. The decrease in the intensity of that signal, which is due to the formation of a new carbonyl (whether it belongs to maleamic acid as a broad signal which rarely shows up after 1700 cm^{-1} or maleimide as a sharp strong stretch between 1695-1735 cm^{-1}), demonstrates the extent that the

Stellenbosch University https://scholar.sun.ac.za

PSMA has reacted to form the pendant group (the primary-amine tethered calix[4]arene). It is also important to know that due to the peak-broadening effect caused by carboxylic acid functionality, all vibrational modes between 1700 cm^{-1} to 1900 cm^{-1} will be affected. Under these circumstances, it is impossible to determine the real intensity of the maleic anhydride carbonyl (~1780 cm^{-1}) after the reaction and so too the degree of functionalization for the ring-opened grafts. The solution to that is to perform a post-functionalization ring-closure reaction to get rid of the carboxylic acid functionality and also its effect on the other signals.

3.3.1.2 NMR (nuclear magnetic resonance) spectroscopy

The ^{1}H-NMR spectra were acquired by the protocols mentioned in chapter 2. Considering the solubility of the grafts, deuterated chloroform ($CDCl_3$) and deuterated dimethyl sulfoxide (DMSO-d_6) were chosen as solvents for analysis of the products. The deuterated solvents included tetramethylsilane (TMS) as the internal standard (δ=0 ppm) from which all chemical shift values were measured in ppm downfield (see **Figure 3.1** as an example).

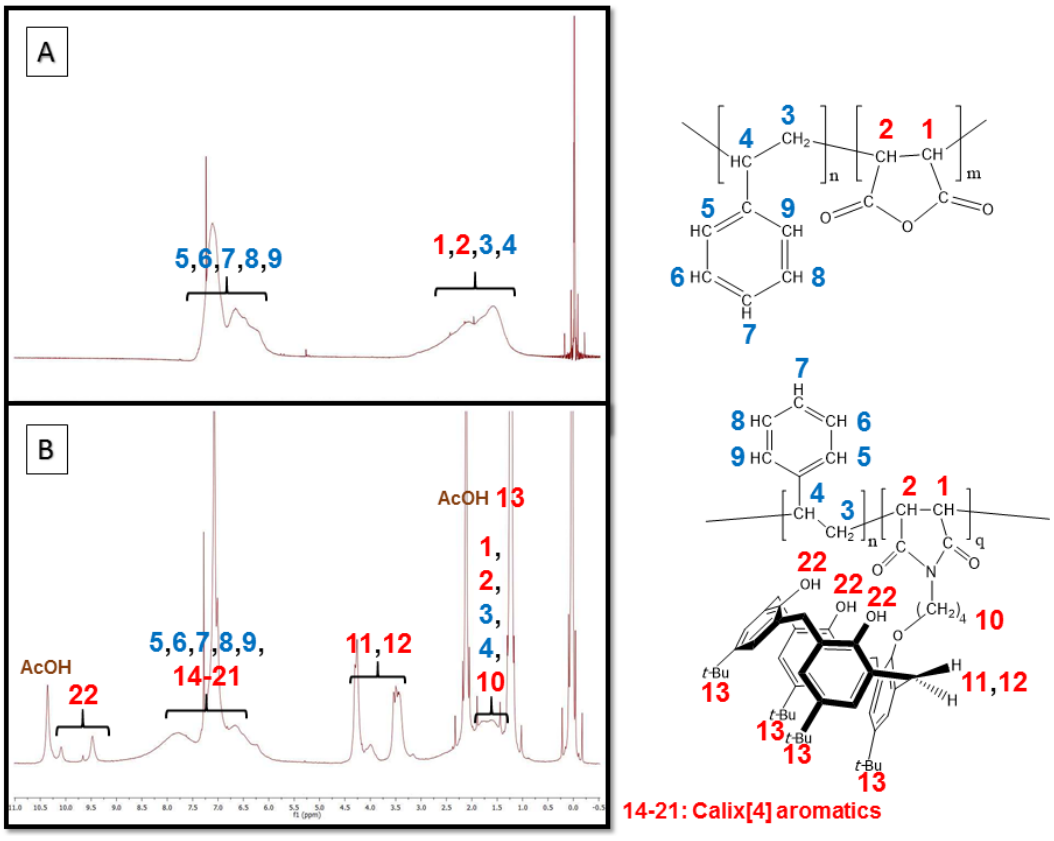

*Figure 3.1 An example of NMR spectrum (in $CDCl_3$) before and after functionalization of PSMA 30% **11**. A: NMR spectrum for pristine PSMA 30% **11**, B: NMR spectrum for PSMA graft with an aminocalix[4]arene (**10$_b$**)[t]*

[t] q: Number of reacted maleic anhydride units.

Stellenbosch University https://scholar.sun.ac.za

The appearance of the calix[4]arene characteristic signals in the NMR spectrum (most importantly the methylene bridges) is indicative of the successful grafting of the PSMA by the calix[4]arene. Generally, two methylene bridges are observed as two broad peaks between 3.00 and 4.50 ppm. In addition, one or two phenolic signals for the calix[4]arene moiety of the graft are observable between 8.00 to 10.00 ppm.

3.3.1.3 UV-Vis (ultraviolet-visible) spectroscopy

All UV-Vis spectra were recorded using a Specord 210 Plus instrument from Analytic Jena AG and were recorded between 190 nm and 900 nm. The data was collected using WinAspect Plus software. In order to perform the experiment, it is necessary to make a 0.1 mg/mL solution of the graft in THF.

For the most part, a new absorption band between 280 nm to 290 nm can be seen for the graft which is an indication of the successful reaction between PSMA and the calix[4]arene.

3.3.2 Thermal studies (DSC)

Differential scanning calorimetry (DSC) thermograms were recorded using a Q100 TA in nitrogen gas (with a flow of 50 $mL.min^{-1}$) at a heating rate of 20 $^{\circ}C.min^{-1}$. The samples were first heated in the temperature range 0-180 °C for the first heating cycle, followed by a cooling cycle. Finally, the thermograms were recorded in the range 0-250 $^{\circ}C$ as the second heating cycle for the investigation of the thermal behavior of grafts.

Since PSMA and its derivatives are amorphous polymers,[10-12] there is no crystalline melt peak observed. DSC was used to determine if the calix[4]arene had an influence on T_g values for graft polymers. In this series of experiments, for the most part, an increase on the value of T_g was observed, which can be allocated to the presence of a bulky pendant group on the polymer backbone.

3.3.3 Size exclusion chromatography (SEC) or gel permeation chromatography (GPC)

Size exclusion analysis was performed using an Agilent 1260 HPLC system comprised of:

- Agilent 1260 diode array UV detector.
- Agilent 1260 quaternary pump.
- Agilent 1260 differential refractometer (at 40 °C).
- Agilent 1260 auto sampler.
- Agilent 1260 thermostated column compartment (also at 40 °C).

Stellenbosch University https://scholar.sun.ac.za

Column set-up was done employing PSS 10µm GRAM columns consisting of one guard column and three analytical columns (2x3000 Å and 1x100 Å). The eluent system was based on DMF (HPLC grade with 0.05M LiBr) at a flow rate of 0.8 mL/min, while the sample concentration was set at 2.0 mg/mL. The calibration was carried out using narrow PMMA calibration standards possessing a molecular weight range of 800-2 200 000 g/mol. All molar mass data was reported as being relative to these linear PMMA standards.[u]

According to the results received from UV-Vis spectra, it was known that a range of 280 nm to 290 nm had to be used as the wavelength for the SEC experiment. In all cases, there were some differences in the appearance of our SEC graphs compared to the same graph for the pristine PSMA which is indicative of PSMA modification. More importantly, the grafts relatively possessed much stronger UV signals which proves the existence of a strong chromophore due to the calix[4]arene graft.

3.4 Experimental section

In this section, the modification of PSMA with the primary amine-tethered calix[4]arenes will be discussed, using an example in conjunction with the full spectral analysis of the produced grafts.

3.4.1 General procedure for the modification of PSMA with an aminocalix[4]arene

PSMA (30% maleic anhydride) **11** was supplied as pellets from Polyscope Xiran (Grade: SZ26180),[v] while all aminocalix[4]arenes were synthesized and purified according to the approaches explained in chapter 2 of this dissertation.

3.4.1.1 General procedure for the attachment in DMF (room temperature) (GP.A)

Alkyl amine-tethered calix[4]arene and PSMA (30% maleic anhydride) **11** (weight ratio: 2 to 1) were placed in a sealed vial containing DMF and stirred at room temperature for 24 h. Water

[u] In the last chapter of this dissertation, this technique will also be used to determine M_n (number average molar mass), M_w (weight average molar mass) and Đ (dispersity) of the synthesized poly(styrene-*alt*-maleic anhydride).

[v] Its molar mass data are as follows: M_n = 132 310 g.mol^{-1}, M_w = 199 160 g.mol^{-1}, Đ = 1.50.

Stellenbosch University https://scholar.sun.ac.za

was added to the reaction and the resulting solid was filtered through a Büchner funnel. The remaining solid was triturated with acetonitrile.[w] The final graft was dried under vacuum.

3.4.1.2 General procedure for the attachment in glacial acetic acid (reflux) (GP.B)

Alkyl amine-tethered calix[4]arene and PSMA (30% maleic anhydride) **11** (weight ratio: 4 to 1) were placed in a sealed vial containing glacial acetic acid and heated under reflux for 24 h. The reaction was cooled down and water was added. The solid floating in the solution was filtered through a Büchner funnel, triturated with acetonitrile and dried under vacuum.

3.4.1.3 General procedure for the attachment in DMF-glacial acetic acid (2-step reaction) (GP.C)

The calix[4]arene-grafted PSMA synthesized in section 3.4.1.1 (**GP.A**) was placed in a sealed vial with glacial acetic acid and heated under reflux for 24 h. After removing from the heat source, the contents of the vial were transferred into a small round-bottom flask and the solvent was removed under reduced pressure with the help of toluene as the azeotrope. This crude was filtered using a Büchner funnel and the resulting solid was dried under vacuum.

3.4.1.4 General procedure for the attachment in DMF (150 °C) (GP.D)

Alkyl amine-tethered calix[4]arene and PSMA (30% maleic anhydride) **11** (weight ratio: 2 to 1) were placed in a sealed vial containing DMF and heated at 150 °C for 24 h. The vial was removed from the heat and water was added to the reaction and the resulting solid was filtered using a Büchner funnel. The remaining solid was triturated with acetonitrile. The final graft was dried under vacuum.

3.4.1.5 General procedure for the attachment in DMF (2-step reaction) (GP.E)

Alkyl amine-tethered calix[4]arene and PSMA (30% maleic anhydride) **11** (weight ratio: 2 to 1) were placed in a sealed vial containing DMF and stirred at room temperature for 24 h and then heated at 150 °C for another 24 h. The vial was removed from the heat and water was added to the reaction and the resulting solid was collected using a Büchner funnel. The remaining solid was triturated with acetonitrile. The final graft was dried under vacuum.

[w] Trituration with acetonitrile was done in order to remove the unreacted calix[4]arene from the graft since practically it was found to be the best solvent for the unreacted calix[4]arene. However, it also dissolved some of our graft resulting in considerable loss of product.

Stellenbosch University https://scholar.sun.ac.za

3.4.2 *p*-*t*-Butylated calix[4]arene-grafted PSMAs

These grafts were synthesized from primary amine-tethered calix[4]arenes. Solvent choice was a very challenging aspect of this study. From the literature point of view, DMF is one of the best solvents for PSMA reactions,[1,6,8,9,13] but in terms of maleimide formation, glacial acetic acid is an extremely good choice (particularly due to its catalytic effect on the ring closing).[4,5] Unfortunately, due to the insolubility of most of our amines in glacial acetic acid, only a few of them were capable of maleimide formation on PSMA in acetic acid in just one step. For this reason, after the attachment onto PSMA in DMF at room temperature, for the rest of these amines, a post-functionalization reaction was carried out with heating separately in DMF and acetic acid. An example is given below for which all the above-mentioned approaches were used to make a calix[4]arene-grafted PSMA (**Figure 3.2**).

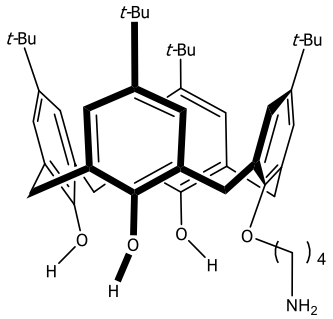

*Figure 3.2 An example of a primary amine-tethered calix[4]arene (**10$_b$**) used for the synthesis of t-butylated calix[4]arene-grafted PSMAs*

3.4.2.1 *p*-*t*-Butylated calix[4]arene-grafted PSMA synthesis from *p*-*t*-butyl-calix[4]arene-monobutylamine (10$_b$)

3.4.2.1.1 Reaction in DMF (room temperature) approach

Following **GP.A**, **10$_b$** (220 mg, 0.300 mmol) and PSMA (30% maleic anhydride) **11** (110 mg) were mixed in DMF (6 mL). The resulting product was a white amorphous powder **A$_{30}$-10$_b$**[x] (120 mg).

[x] As a rule, in this thesis, the left-hand side letter refers to the general procedure type (usually **A** or **C**) while its subscript determines the percentage maleic anhydride content of the polymer (30 or 50). The right-hand side letter specifies the amine with which the graft is synthesized. For example, here, **A** stands for general procedure A, **30** for PSMA 30%, and **10$_b$** for *p*-*t*-butyl-calix[4]arene-monobutylamine (**10$_b$**).

Stellenbosch University https://scholar.sun.ac.za

3.4.2.1.2 Reaction in glacial acetic acid (reflux) approach

Following **GP.B**, **10_b** (320 mg, 0.450 mmol) and PSMA (30% maleic anhydride) **11** (80.0 mg) were mixed in glacial acetic acid (5.5 mL). The product was obtained as a pale brown rubber-like solid **B_{30}-10_b** (100 mg).

3.4.2.1.3 2-step reaction in DMF (room temperature) then in glacial acetic acid (reflux) approach

Following **GP.C**, **A_{30}-10_b** (50.0 mg) was placed in glacial acetic acid (5 mL). The product was obtained as a brown powder **C_{30}-10_b** (50.0 mg).

3.4.2.1.4 Reaction in DMF (150 °C) approach

Following **GP.D**, **10_b** (230 mg, 0.320 mmol) and PSMA (30% maleic anhydride) **11** (115 mg) were mixed in DMF (6 mL). The product was obtained as a brown powder **D_{30}-10_b** (120 mg).

3.4.2.1.5 2-step reaction in DMF (room temperature to 150 °C) approach

Following **GP.E**, **10_b** (180 mg, 0.250 mmol) and PSMA (30% maleic anhydride) **11** (90.0 mg) were mixed in DMF (5 mL). The product was obtained as a dark brown powder **E_{30}-10_b** (100 mg).

3.4.3 Characterization of a series of *p-t*-butylated calix[4]arene-grafted PSMAs

The analytical techniques explained in section 3.3 were used for the characterization of all synthesized grafts. For the above-mentioned calix[4]arene, below the characterization methods will be provided in a detailed manner.

3.4.3.1 ATR-FTIR spectroscopy

All the grafts infrared data were compared to the ones of the pristine PSMA (**11** in **Figure 3.3a**), the graft made in DMF (room temperature) **A_{30}-10_b** showed the weakening of the symmetric anhydride stretch at 1780 cm^{-1} (maleic anhydride), the increase of a very weak smooth signal at 1730 cm^{-1} (maleamic acid) indicating the ring-opening (**Figure 3.3b**). There was also a new carbonyl stretch at 1675 cm^{-1} for the reaction solvent (DMF). For the graft made in glacial acetic acid (reflux) **B_{30}-10_b**, the symmetric anhydride stretch at 1778 cm^{-1} (maleic anhydride) was significantly decreased (compared to the pristine PSMA IR) and a new carbonyl signal at 1701 cm^{-1} (maleimide) appeared which indicates the ring-closing (**Figure 3.3c**). The graft synthesized in 2 steps (at room temperature in DMF and then under reflux

Stellenbosch University https://scholar.sun.ac.za

conditions in glacial acetic acid) **C_{30}-10_b**, also exhibited suppression of the symmetric anhydride stretch at 1776 cm^{-1} (maleic anhydride) and an emerging carbonyl signal at 1707 cm^{-1} (maleimide) suggesting the ring-closing (**Figure 3.3d**). The graft made in DMF (150 °C) **D_{30}-10_b** also showed the disappearance of the carbonyl group at 1773 cm^{-1} (maleic anhydride) as a sign of the ring-opening, while the reaction solvent (DMF) peak was seen at 1677 cm^{-1}. In spite of that, there was no new signal proving the existence of a maleimide group (**Figure 3.3e**). Likewise, for the other graft synthesized in 2 steps (at room temperature in DMF and then at 150 °C in the same solvent) **E_{30}-10_b** carbonyl group at 1780 cm^{-1} (maleic anhydride) did not vanish but its intensity decreased, while the solvent (DMF) residual peak was observable at 1677 cm^{-1} (**Figure 3.3f**). Overall this set of data also demonstrated that the maleic anhydride group only opened and was not re-closed in the last two samples.

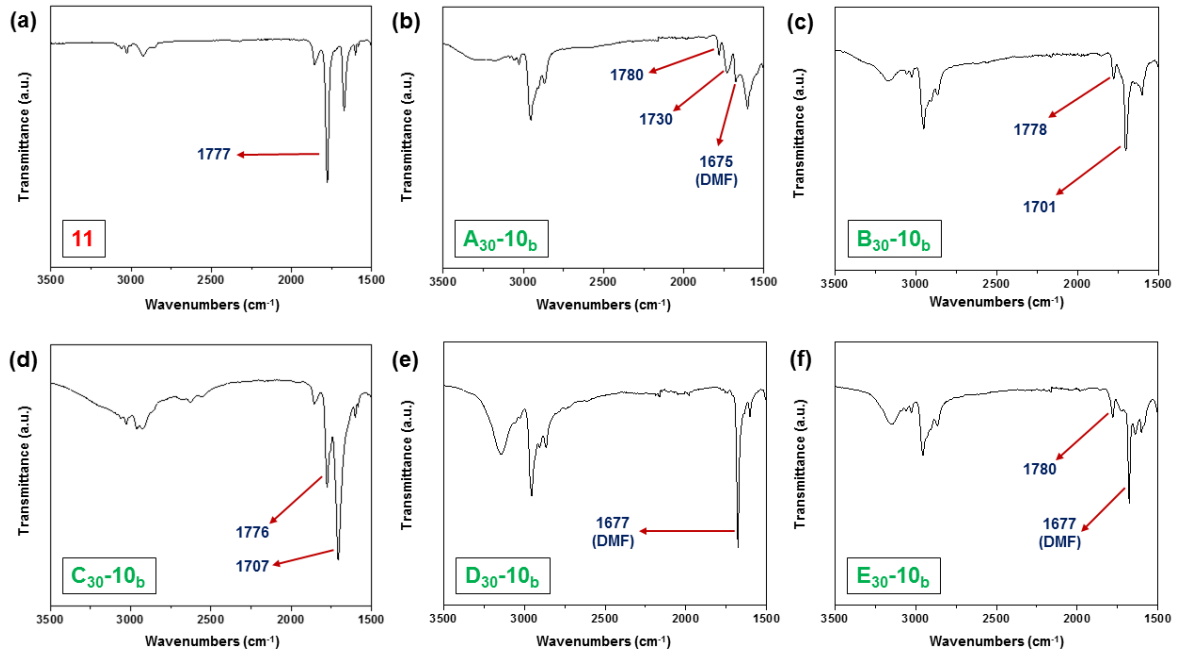

Figure 3.3 ATR-FTIR results under different reaction conditions for p-t-butylated calix[4]arene-grafted PSMAs produced (Transmittance values were normalized to styrene bend at 700 cm^{-1}, a.u: arbitrary unit)

3.4.3.2 Degree of functionalization

Using the general method explained above (FT-IR approach), the degree of functionalization was calculated for the grafts displayed in **Table 3.1**.

Stellenbosch University https://scholar.sun.ac.za

Table 3.1 Degree of functionalization for several p-t-butylated calix[4]arene-grafted PSMAs based on FT-IR spectroscopy speculation

Entry	Compound name	Degree of functionalization (%)
1	**A_{30}-10_b**	NA[y]
2	**B_{30}-10_b**	78
3	**C_{30}-10_b**	32
4	**D_{30}-10_b**	NA
5	**E_{30}-10_b**	NA

To corroborate the values obtained by this approach, as an example, the ^{1}H-NMR spectrum of the graft **B_{30}-10_b** was looked at again. **Figure 3.1B** showed the methylene bridges of the pendant group (calix[4]arene) respectively at 3.50 and 4.25 ppm, each possessing 4 protons. The aromatic region (6.00-8.50 ppm) showed 23 aromatic protons for the styrene units and the calix[4]arene groups together. Having 8 methylene bridge protons means having 8 aromatic protons for the calix[4]arene. Thus, this number was subtracted from 23 to give the number of aromatic protons of styrene which was 15. Each styrene unit possesses 5 aromatic protons, therefore, dividing 15 by 5 gave us the relative number of styrene units in the polymeric chain which was 3. Relatively, PSMA 30% has 7 styrene units and 3 maleic anhydride units. Thus, when it had 3 styrene units, logically the total number of maleic anhydride units (reacted and unreacted units together) had to be 1.28. Since our hypothesis was based on having only 1 calix[4]arene unit, so dividing that number by 1.28 finally gave us the degree of PSMA modification by our aminocalix[4]arene **10_b** (78%). Repeating the same value, this time by the ^{1}H-NMR spectroscopy, corroborated the accuracy of the FT-IR spectroscopy speculation.[z]

3.4.3.3 NMR spectroscopy

The ^{1}H-NMR spectral results were as follows:

3.4.3.3.1 Reaction in DMF (room temperature) approach – A_{30}-10_b ^{1}H-NMR spectrum

^{1}H-NMR (300 MHz, $CDCl_3$) δ ppm 1.25 (calix[4]arene tertiary butyl groups), 1.50-2.50 (aliphatic protons for calix[4]arene and PSMA), 2.88 (DMF), 2.96 (DMF), 3.50 (calix[4]arene methylene bridge), 4.25 (calix[4]arene methylene bridge), 6.00-7.50 (aromatic protons for

[y] Not assigned, due to the fact that the degree of functionalization can only be determined for the ring-closed grafts.

[z] As was the case for FT-IR spectroscopy, this approach could not be applied to the ring-opened grafts. Since those grafts underwent massive peak-broadening (due to possessing carboxylic acid groups), it was not possible to read the integration of the peaks accurately. In addition, to the ring-closed grafts, which lacked solubility in NMR spectroscopy solvents, this approach was not applicable either and FT-IR spectroscopy was the only tool to determine their degree of functionalization.

Stellenbosch University https://scholar.sun.ac.za

styrene and calix[4]arene), 8.02 (DMF), 9.70 (calix[4]arene phenolic proton), 10.20 (calix[4]arene phenolic proton).

3.4.3.3.2 Reaction in glacial acetic acid (reflux) approach – B_{30}-10_b ^{1}H-NMR spectrum

^{1}H-NMR (300 MHz, $CDCl_3$) δ ppm 1.25 (calix[4]arene tertiary butyl groups), 1.40-2.00 (aliphatic protons for calix[4]arene and PSMA), 2.20 (acetic acid), 3.50 (calix[4]arene methylene bridge), 4.25 (calix[4]arene methylene bridge), 6.00-8.50 (aromatic protons for styrene and calix[4]arene), 9.50 (calix[4]arene phenolic proton), 10.10 (calix[4]arene phenolic proton), 10.40 (acetic acid).

3.4.3.3.3 2-step reaction in DMF (room temperature) then in glacial acetic acid (reflux) approach – C_{30}-10_b ^{1}H-NMR spectrum

^{1}H-NMR (300 MHz, DMSO-d_6) δ ppm 1.19 (calix[4]arene tertiary butyl groups), 1.66-2.13 (aliphatic protons for calix[4]arene and PSMA), 4.05 (calix[4]arene methylene bridge), 4.27 (calix[4]arene methylene bridge), 6.73-7.62 (aromatic protons for styrene and calix[4]arene), 8.02 (DMF).

3.4.3.3.4 Reaction in DMF (150 °C) approach – D_{30}-10_b ^{1}H-NMR spectrum

^{1}H-NMR (300 MHz, $CDCl_3$) δ ppm 1.25 (calix[4]arene tertiary butyl groups), 1.50-2.50 (aliphatic protons for calix[4]arene and PSMA), 2.88 (DMF), 2.96 (DMF), 3.50 (calix[4]arene methylene bridge), 4.25 (calix[4]arene methylene bridge), 6.00-7.50 (aromatic protons for styrene and calix[4]arene), 8.02 (DMF).

3.4.3.3.5 2-step reaction in DMF (room temperature to 150 °C) approach – E_{30}-10_b ^{1}H-NMR spectrum

^{1}H-NMR (300 MHz, $CDCl_3$) δ ppm 1.25 (calix[4]arene tertiary butyl groups), 1.50-2.50 (aliphatic protons for calix[4]arene and PSMA), 2.88 (DMF), 2.96 (DMF), 3.50 (calix[4]arene methylene bridge), 4.25 (calix[4]arene methylene bridge), 6.00-7.50 (aromatic protons for styrene and calix[4]arene), 8.02 (DMF), 10.40 (carboxylic acid proton).

3.4.3.4 UV-Vis spectroscopy

As stated earlier, the newly-made graft should show a new broad absorption band between 280 nm to 290 nm in the UV spectrum. This observation was attributed to the attachment of calix[4]arene (as a strong chromophore) onto PSMA (a weaker chromophore) (see **Figure 3.4**).

Stellenbosch University https://scholar.sun.ac.za

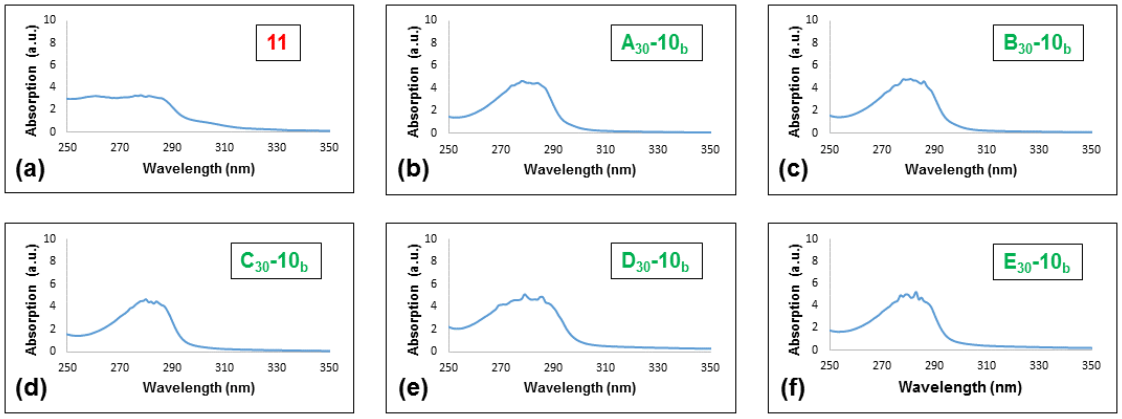

Figure 3.4 UV-Vis results for several p-t-butylated calix[4]arene-grafted PSMAs

The calix[4]arene attachment resulted in an increase in the absorption for the modified graft compared (**Figures 3.4b, 3.4c, 3.4d, 3.4e, 3.4f**) to the pristine PSMA (**Figure 3.4a**). More interestingly, this absorption wavelength could be used as a wavelength for the detection of the grafts by way of a SEC (GPC) UV-Vis detector. More or less, all of the studied grafts showed the same band on their UV-Vis spectra.

3.4.3.5 SEC (GPC)

As explained above, the appearance of UV-visible signals between 280 nm to 290 nm added proof of the attachment of our desired calix[4]arene to PSMA. As mentioned in the introduction part, SEC experiments were carried out using a dual detecting system of RI (refractive index) detector and UV-Vis detector (280nm) (see **Figure 3.5**).

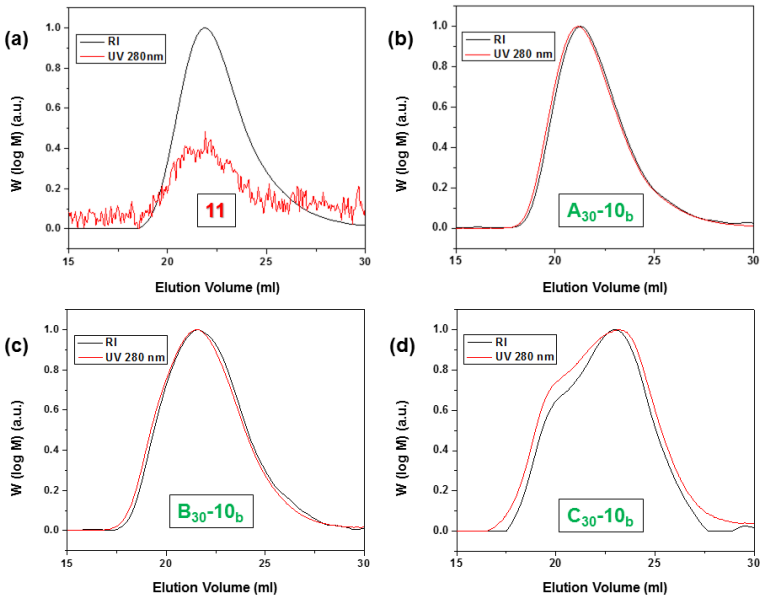

Figure 3.5 SEC results for several p-t-butylated calix[4]arene-grafted PSMAs

Stellenbosch University https://scholar.sun.ac.za

Comparing the results for the pristine PSMA **11** and the grafts showed that RI detector signal almost remained the same (**Figures 3.5a**, **3.5b**, **3.5c**, **3.5d**), but there was a significant increase for the intensity of the UV detector signal corresponding to the RI detector signal (280 nm to 290 nm) (**Figures 3.5b, 3.5c, 3.5d**). In addition, in the case of **C_{30}-10_b**, a bimodal distribution with a shoulder on the longer elution volume was observed (**Figure 3.5d**). This observation revealed the existence of not one, but two polymer species – one with shorter elution volume (larger relative molar mass) and one with longer elution volume (smaller relative molar mass). This phenomenon might suggest an incomplete closure of the anhydride units upon heating the ring-opened graft in glacial acetic acid under reflux; however, the reason for this possibly incomplete conversion was unknown. Obviously, since the different forms of the grafts possessed different elution volumes, they exhibited different relative molar masses while ejecting the column.[aa] Moreover, it must be noted that due to the lack of solubility for both grafts synthesized in DMF under heating, they were not analyzed by SEC.[bb]

3.4.3.6 DSC

DSC analysis was done on all the graft copolymers. The grafts made in DMF (room temperature) **A_{30}-10_b**, in glacial acetic acid (reflux) **B_{30}-10_b** and in 2 steps (room temperature then reflux) in DMF/glacial acetic acid **C_{30}-10_b** all showed an increase in the T_g which means that the addition of calix[4]arene and its interactions with PSMA backbone groups restricts the overall movement of the chains. The change in heat capacity (ΔC_P) on the contrary decreased compared to the one for pristine PSMA during the transition. The grafts made in DMF (150 °C **D_{30}-10_b** and room temperature then 150 °C **E_{30}-10_b**) on the other hand, displayed no easily identifiable glass transition. This may be the result of a very weak T_g making it very difficult to detect. Lack of an observable T_g, in this case, cannot be due to the crosslinking issue,[14]

[aa] Logically, having more COOH groups (the anhydride open form) contributes to stronger polymer-column interactions resulting in longer elution volume and smaller relative molar mass.

[bb] This insolubility could be due to the nature of the crude materials. The crude materials in this case (grafts **D_{30}-10_b** and **E_{30}-10_b**), could be partially ring-closed grafts which did not possess the solubility behavior of either of ring-opened (**A_{30}-10_b**) or ring-closed (**B_{30}-10_b** and **C_{30}-10_b**) grafts. However, since the FT-IR spectra did not show any sign of ring-closure for these grafts, it could imply that relatively the ratio of the opened rings to the closed rings was drastically in favor of the opened rings. As a result, the signals corresponding to the closed rings in the carbonyl region of FT-IR spectroscopy were cloaked (by the massively broad baseline of the opened rings) and not observed.

Stellenbosch University https://scholar.sun.ac.za

because the mono-functionalized aminocalix[4]arene is simply not capable of causing crosslinking[cc] (see **Table 3.2** for DSC data and the appendix section for the thermograms).

Table 3.2 DSC results for several p-t-butylated calix[4]arene-grafted PSMAs

Entry	Compound name	T_g (°C)	Height ($W.g^{-1}$)	$\Delta C_{P\ (J.g^{-1}.°C^{-1})}$
1	**11**	159.82	0.07628	0.2289
2	**A_{30}-10_b**	186.20	0.04234	0.1273
3	**B_{30}-10_b**	178.55	0.05891	0.1773
4	**C_{30}-10_b**	167.48	0.02727	0.08125
5	**D_{30}-10_b**	-	-	-
6	**E_{30}-10_b**	-	-	-

3.4.3.7 Final analysis

In accordance with the experimental data received, it can be said that: with respect to graft made in DMF (room temperature) **A_{30}-10_b**, the desired product in the form of a ring-opened compound (maleamic acid) was made. Regarding the graft made in glacial acetic acid (reflux) **B_{30}-10_b**, the desired product in the form of a ring-closed compound (maleimide) was successfully synthesized. The graft produced as a result a 2-step reaction (in DMF first at room temperature and then in glacial acetic acid under reflux conditions) **C_{30}-10_b**, also exhibited the existence of a ring-closed compound (maleimide), despite its lower degree of modification compared to the previous approach. Nonetheless, the same graft also showed the presence of a low-molar mass compound (most likely an indication of the incomplete closure of the ring-opened polymer). On the other hand, the graft made in DMF (150 °C) **D_{30}-10_b** was not favorable and it only showed the existence of maleamic acid functionality (the ring-opened product). The graft made in 2 steps (in DMF first at room temperature and then at 150 °C) **E_{30}-10_b** was not a ring-closed product either, but remained as the ring-opened product. With regards to the solubility status of the grafts, both grafts synthesized in DMF with heating (**D_{30}-10_b** and **E_{30}-10_b**) showed poor solubility.

3.5 Concluding remarks

Overall, after all the experiments performed regarding the modification of PSMA, it is now known that the functionalization of PSMA with primary amine-tethered calix[4]arene could be done conveniently at room temperature (with no need for any catalyst, etc.) in DMF with an appropriate degree of functionalization. The product, in this case, possessed a maleamic acid functionality. Conversely, the functionalization, followed by the ring-closure for PSMA in case of using an aminocalix[4]arene almost always requires very harsh conditions. Four attempted

[cc] It can only be the case for multifunctional amines. The concept of crosslinking will be discussed in detail in the last chapter of this thesis.

Stellenbosch University https://scholar.sun.ac.za

conditions were used, respectively: The reaction in DMF at 150 °C, the 2-step reaction in DMF (first at room temperature and then at 150 °C), the reaction in glacial acetic acid (reflux) and finally the 2-step reaction first in DMF (the attachment) followed by heating under reflux in glacial acetic acid (ring closure). The first two options were proven to be efficient in terms of attachment, but inefficient in terms of ring-closing, while the other two showed promising results in terms of both matters of attachment and ring-closing (the 2-step reaction in DMF/glacial acetic acid; however, apparently contributed to the formation of a low molar mass intermediate as well). Nevertheless, unfortunately, the one-pot reaction in acetic acid was only a viable option for the butylamine-tethered calix[4]arene **10$_b$**, due to the poor solubility of other aminocalix[4]arenes in glacial acetic acid. Knowing that, the ring-closed grafts for the rest of our aminocalix[4]arenes were prepared using the 2-step reaction in DMF/glacial acetic acid. Also considering the degree of functionalization for all grafts made in this chapter, it was understood that in total the grafts with butyl spacers possessed the best modification rate (**Table 3.3**).[dd]

Table 3.3 The effect of tether length on the degree of modification (based on FT-IR spectroscopy speculation) for p-t-butylated calix[4]arene-grafted PSMAs

Entry	Compound name	Spacer type	Degree of functionalization (%)
1	**C$_{30}$-10$_e$**	Ethyl	21
2	**B$_{30}$-10$_b$**	Butyl	78
3	**C$_{30}$-10$_b$**	Butyl	32
4	**C$_{30}$-10$_h$**	Hexyl	20

Overall, for future studies in this dissertation (especially the ones focused on the applications of calix[4]arene in the aqueous media), it is highly recommended to use a functionalized calix[4]arene-tethered amine with a butyl spacer.

3.6 References

(1) Jeong, J. H.; Byoun, Y. S.; Lee, Y. S. *React. Funct. Polym.* **2002**, *50*, 257–263.

(2) Soer, W. J.; Ming, W.; Klumperman, B.; Koning, C.; van Benthem, R. *Polymer* **2006**, *47*, 7621–7627.

(3) Vermeesch, I.; Groeninckx, G. *J. Appl. Polym. Sci.* **1994**, *53*, 1365–1373.

[dd] *t*-Butyl-calix[4]arene-monoalkylamine with ethyl (**10$_e$**) and hexyl (**10$_h$**) spacers had very poor solubility in glacial acetic acid and therefore the PSMA grafting onto them was only performed using the 2-step reaction in DMF/glacial acetic acid (**GP.C**).

Stellenbosch University https://scholar.sun.ac.za

(4) Haubler, L.; Wienhold, U.; Albrecht, V.; Zschoche, S. *Thermochim Acta.* **1996**, *277*, 17–27.

(5) Gietzelt, T. *J. Mater. Sci.* **2001**, *36*, 2073–2079.

(6) Cronje, L.; Klumperman, B. *Eur. Polym. J.* **2013**, *49*, 3814–3824.

(7) Wang, K.; Huang, W.; Xia, P.; Gao, C.; Yan, D. *React. Funct. Polym.* **2002**, *52*, 143–148.

(8) Gule, N. P.; Bshena, O.; De Kwaadsteniet, M.; Cloete, T. E.; Klumperman, B. *Biomacromolecules* **2012**, *13*, 3138–3150.

(9) Lee, W.; Hwong, G. Y. *J. Appl. Polym. Sci.* **1996**, *59*, 599–608.

(10) Fischer, J. *Handbook of Molded Part Shrinkage and Warpage*, William Andrew (Elsevier), Norwich, New York, United States, **2012**, 2nd ed.

(11) Campbell, F. C. *Fatigue and Fracture: Understanding the Basics*, ASM International, Materials Park, Ohio, United States, **2012**, 2nd ed.

(12) Campbell, F. C. *Lightweight Materials: Understanding the Basics*, ASM International, Materials Park, Ohio, United States, **2012**.

(13) Fang, W.; Cai, Y.; Chen, X.; Su, R.; Chen, T.; Xia, N.; Li, L.; Yang, Q.; Han, J.; Han, S. *Bioorganic Med. Chem. Lett.* **2009**, *19*, 1903–1907.

(14) Chompff, A. *Polymer Networks: Structure and Mechanical Properties*, Springer Science & Business Media, Berlin, Germany, **2013**.

Stellenbosch University https://scholar.sun.ac.za

Chapter 4. A strategy toward synthesizing a calix[4]arene colorimetric sensor with PSMA for mercury detection

4.1 Chapter overview

In this chapter, the design and synthesis of a potential colorimetric sensor capable of detecting mercury were pursued. For this purpose, a modified azacalix[4]arene, known for its ability to detect mercury cations, was targeted to be synthesized and then grafted onto PSMA. However, in practice, the main strategy and the alternative approaches to making the targeted calixarene for attachment onto PSMA failed. Nevertheless, before discussing the synthetic strategies of this chapter, a brief introduction focusing on mercury, its importantly biological effects, and its sensing techniques will be presented.

4.2 Mercury: Occurrence, emission sources, and biological effects

Due to the industrialization phenomenon, the concentration of hazardous heavy metals has significantly increased in the environment, risking our health and also other living organisms vital for our preservation.[1,2] Amongst them is mercury as a d-block element (group 12, period 6) of the periodic table which is highly useful for production of measuring instruments (e.g. thermometers, manometers, etc.), electrical switches, batteries, fluorescent light sources, detonators, antiseptics, and even dental fillings.[3,4,5]

Naturally, mercury is found in two oxidation states which are mercury (I) and mercury (II). Mercury (I) or mercurous mercury is the least naturally abundant form of mercury and probably the most important example of that is mercury(I) chloride (Hg_2Cl_2) also known as calomel which is widely in use in electrochemical studies (as calomel electrode).[6,7] Mercury (II) or mercuric mercury is the most naturally abundant form of mercury whose most famous mineral is mercury(II) sulfide (HgS) best-known as cinnabar (or cinnabarite). Cinnabar is the amplest mineral source of mercury on the planet earth useable for refining mercury (the element), and also production of mercury-based pigments.[8,9] Mercury (II) can also be seen in organic forms such as methylmercury(II) cation (CH_3Hg^+ as the main source of organic mercury and a biological toxicant),[10] merbromin[ee11] and thiomersal[ff] (both well-established antiseptics).[12]

[ee] IUPAC name: Dibromohydroxymercurifluorescein

[ff] IUPAC name: Ethyl(2-mercaptobenzoato-(2-)-O,S) mercurate(1-) sodium

Stellenbosch University https://scholar.sun.ac.za

Approximately, half of mercury release into the environment is due to natural sources like lava (generated by volcanic eruption) while the other half stems from human-involved activities. In accordance with the environmental studies, the estimated percentages of human-related sources of mercury emission are as follows:

- Stationary combustion particularly in coal power plants: 65%
- Gold mining: 11%
- Non-ferrous metal smelting: 6.8%
- Cement industry: 6.4%
- Waste disposal: 3%
- Sodium hydroxide manufacturing: 3%
- Steel industry: 1.4%
- Mercury battery production: 1.1%
- Other sources: 2% [13,14,15]

Mercury poisoning can occur upon exposure to elemental, inorganic, and even organic form of mercury (liquid or vapor). The exposure mostly comes from fish eating,[gg] dental amalgam, and also occupational environment.[16] In serious cases, the exposure may result in well-known diseases such as Minamata disease,[17] Hunter-Russell syndrome,[18] and Acrodynia (also known as pink disease).[19] In a few cases, the biological mechanism of mercury toxification is clearly known. For example, by irreversible inhibition of selenoenzymes (e.g. thioredoxin reductase), mercury disrupts the restoration process for vitamins C and E and many other antioxidants responsible for brain cells protection from oxidative damages. Should this disruption continue, the result will be irreparable brain damage and even death.[20] In the case of pregnant women with significant amount of dietary selenium intake, mercury is similarly capable of harming fetuses resulting in congenital disorders.[21] Methylmercury exposure causes an auto-immune response toward myelin[hh] which contributes to myelin degradation and dysfunction of central nervous system.[22]

Different sources of mercury can cause different degrees of toxicity. Liquid elemental mercury (also known as quicksilver), due to its very poor absorption through skin contact and ingestion, does not pose the kind of health threat that its vaporized form does.[23] The latter form after

[gg] Due to biomagnification (the increase of a toxicant concentration in the tissues of a tolerant organism), many fish species manage to concentrate large amounts of mercury in their bodies.[24]

[hh] The lipoprotein substance which acts as the nerve cell axon insulator.[25]

Stellenbosch University https://scholar.sun.ac.za

absorption through the respiratory tract and entering the circulatory system can cause symptoms such as impaired cognitive skills, sensational problems, muscular disorders, memory loss, and insomnia.[26]

By comparison, among inorganic mercury sources, mercuric salts are far more toxic than mercurous ones which is due to their higher solubility in aqueous media. These compounds can inflict severe damage on kidneys, liver, and the gastrointestinal tract; however, unless chronic exposure happens, they cannot cause any serious brain damage.[27] In this category, mercuric cyanide ($Hg(CN)_2$) is considered the most dangerous source of mercury whose toxicity is mostly due to its cyanide anion and not the mercury cation.[28]

As stated earlier, methylmercury is the main source of organomercury and due to its high water-solubility can become involved in the food web affecting many species and more importantly fish.[29] Compared to the elemental and inorganic forms of mercury, the latent period for methylmercury is often much longer (up to five months) and the initial symptom is usually paresthesia (skin numbness) which in serious cases can be followed by acute conditions ending in death. In this regard, dimethylmercury ($(CH_3)_2Hg$) is known as the most lethal organic source of mercury.[23] There are, however, less serious consequences upon exposure to methylmercury. For example, gestation for humans is also sensitive to methylmercury exposure. As a result of this gestational methylmercury exposure, dopamine (a major neurotransmitter) release by prefrontal cortex will be influenced leading to long-time behavioral effects.[30]

Overall, the biological threats caused by mercury emission into the environment (particularly the contamination of aqueous media), highlight the importance of effective sensing devices for that. In the next section, multiple approaches for mercury sensing with focus on the colorimetric approach including that of our project will be explained.

4.3 Mercury sensing, Chung sensor, and our preliminary assessment of the method

Commonly, mercury sensing is done by the analytical techniques such as inductively coupled plasma-mass spectrometry (ICP-MS),[31,32] high performance liquid chromatography-inductively coupled plasma-mass spectrometry (HPLC-ICP-MS),[33,34] capillary electrophoresis-inductively coupled plasma-mass spectrometry (CE-ICP-MS),[35] and also atomic absorption spectroscopy (AAS).[36,37] Despite their high efficiency, these methods still suffer from disadvantages like costly instrumentation, sophisticated operation, and long-time analysis which have stimulated the researchers to develop alternative solutions in order to avoid

Stellenbosch University https://scholar.sun.ac.za

facing these challenges. These solutions include colorimetric techniques,[38,39] fluorescent techniques,[40,41] electrochemical techniques,[42,43] and finally quartz crystal microbalance (QCM) techniques.[44,45]

Amongst these techniques, the most inexpensive and simplest method is the colorimetric one. Naturally, a specific color change for the detection of a cation is ideal for its identification, owing to its visibility to the naked eye, and more importantly the lack of any need for sophisticated instrumentation. Thus, the discovery of a colorimetric sensor can be very advantageous for heavy metals and particularly mercury in many ways. In the calixarene field, the first paper addressing the potential for colorimetric detection of cations was published by Shinkai and co-workers in 1991 and involved calix[4]arenes possessing azophenol units.[46] Since then there have been other literature examples describing the use of calixarenes with azophenol functionalities consolidating its role as a potent chromogenic center for cation sensing.[47-49] This chapter is based on a work by Chung and co-workers who showed the successful recognition of Hg^{2+} cations using a series of upper rim substituted calix[4]arenes with both arylazo and allyl functionalities.[50,51] Chung and his co-workers revealed that among all the calix[4]arenes they worked with, the ones possessed *p*-methoxyphenylazo groups yielded the strongest bathochromic shift upon complexation with mercury perchlorate (compounds **14_x**, **14_y**, and **15** in **Figure 4.1**).

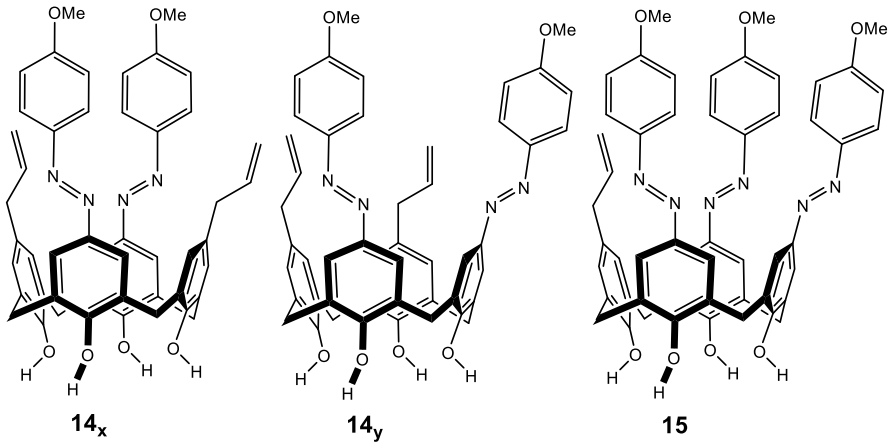

*Figure 4.1 Distal bis(p-methoxyphenylazo)calix[4]arene (**14_x**), Proximal bis(p-methoxyphenylazo)calix[4]arene (**14_y**), tris(p-methoxyphenylazo)calix[4]arene (**15**) (based on the work of Chung and co-workers)[51]*

In Chung's research, UV-Vis studies were performed using a solution of azacalix[4]arene in a methanol-chloroform (v/v=1/399) cosolvent system which was complexed with a large excess of the mercuric salt. The researchers believed that the color change (pale yellow to strong pink)

Stellenbosch University https://scholar.sun.ac.za

occurs because of an azophenol to quinone-hydrazone tautomerism (see **Scheme 4.1** and **Scheme 4.2**).

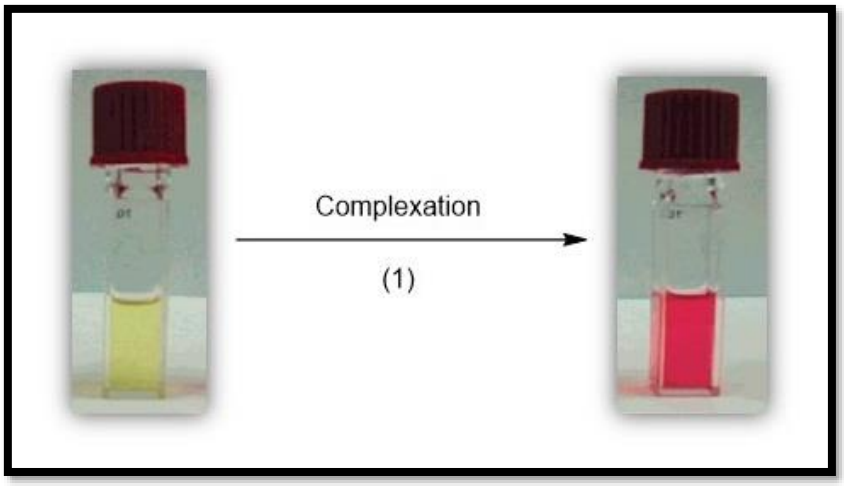

Scheme 4.1 Color change for the solution of azacalix[4]arene as a result of mercury cation addition (taken from reference[50]) – (1): 10 μM solution of the azo dye in $CHCl_3$/MeOH (v/v= 1/399) plus 5 equivalents of Hg^{2+} salt

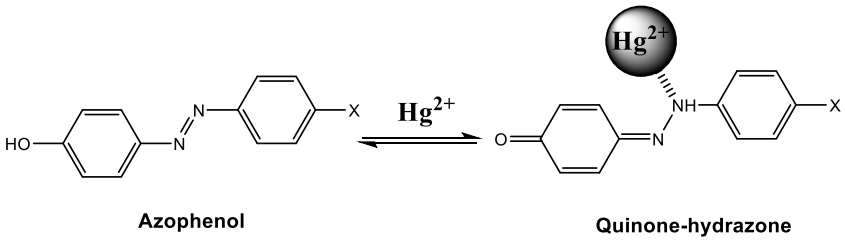

Scheme 4.2 Azophenol to quinone-hydrazone tautomerism (X: Calix[4]arene)

In a later article, the same researchers reported a comparative study on different responses of 14 cations to bis(*p*-methoxyphenylazo)calix[4]arenes **14_x**, **14_y** (distal and proximal) and also tris(*p*-methoxyphenylazo)calix[4]arene **15**. The results demonstrated that *p*-methoxyphenylazo groups in the distal orientation had greater binding to Hg^{2+} (greater K_a value), compared to the proximal one. The addition of a third *p*-methoxyphenylazo functionality also disturbed the binding of other azo substituents to Hg^{2+} (lesser K_a value) and also had the calix[4]arene respond unselectively to mercury and other cations. All these results came from complex association constants determined by ^{1}H-NMR spectroscopic titrations for the above-mentioned calix[4]arenes (**Figure 4.1**).[50,51]

4.4 Main strategy toward the synthesis of the modified Chung sensor

In accordance with the aforementioned results from literature, the best sensor for Hg^{2+} detection should contain a distal diallyl-bis(*p*-methoxyphenylazo)calix[4]arene, so our calix[4]arene moiety of the scaffold should be a modified version of that. The modified azacalix[4]arene also

Stellenbosch University https://scholar.sun.ac.za

requires an amine tether so that it can be attached onto PSMA (see the target molecule on **Figure 4.2**).

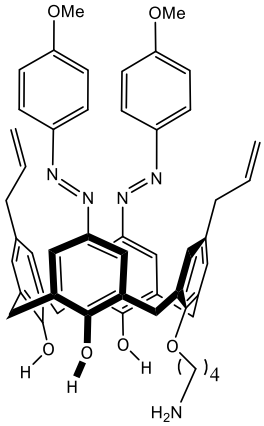

Figure 4.2 Target molecule for chapter 5

Considering the proposed chelation mechanism (depicted on **Scheme 4.2**), it was potentially also important that this tether should not reside on the phenolic ring with the azobenzene functionality, but on the one with allyl functionality, otherwise, the above-mentioned tautomerism could not occur after introducing mercury.

The first step was to confirm the literature report on Chung's synthetic procedure to make the sensor. As reported in literature, the synthesis of diallyl-bis(*p*-methoxyphenylazo)calix[4]arene $\mathbf{14_x}$ was carried out with the procedures by Shu *et al*. in a very straight-forward manner (**Scheme 4.3**).[52] Starting from calix[4]arene **7**, a distal diallyloxycalix[4]arene **12** was synthesized with anhydrous K_2CO_3 and allyl bromide in refluxing acetonitrile. After purification by recrystallization, with complete correlation of its spectral data with that from literature was possible (62%).[52] Then distal diallyloxycalix[4]arene **12** underwent a thermal Claisen rearrangement ([3+3] sigmatropic rearrangement) with heating under reflux in *N*,*N*-diethylaniline resulting in a distal diallylcalix[4]arene **13** whose spectral results again matched the values reported in literature (84%).[52] It must be noted that replacing the current solvent with diphenyl ether was also attempted in order to increase the reaction yield, but the starting material decomposed under the reflux conditions.

Stellenbosch University https://scholar.sun.ac.za

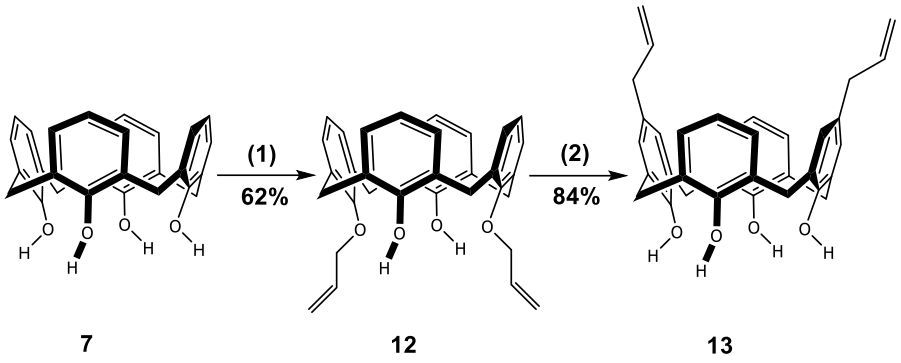

*Scheme 4.3 Formation of distal diallylcalix[4]arene (**13**). Reagents and conditions: (1) K_2CO_3 (1.0 equiv.), allyl bromide (2.22 equiv.), CH_3CN, reflux, 4 h; (2) N,N- diethylaniline, reflux, 4 h (based on the work of Shu et al.)*[52]

Finally, the diallylcalix[4]arene **13** was dissolved in cold pyridine and diazotized with a pre-made diazonium salt from *p*-anisidine, $NaNO_2$ and 4 M HCl in cold acetone and recrystallized to afford a distal diallyl-bis(*p*-methoxyphenylazo)calix[4]arene $\mathbf{14_x}$ (82%). It was found to be important to maintain the temperature at 0 °C while making the diazonium salt, otherwise, the salt would not survive. The reaction proceeded quickly toward completion (one hour) and again the identical spectral results for that and the literature values proved the successful formation of the diallyl-bis(*p*-methoxyphenylazo)calix[4]arene $\mathbf{14_x}$ (**Scheme 4.4**).[52]

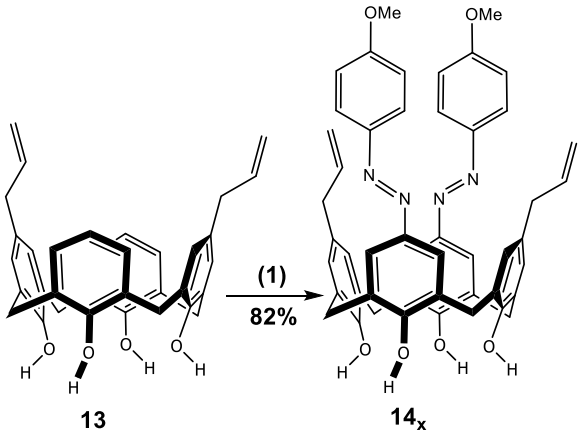

Scheme 4.4 Formation of Chung's sensor. Reagents and conditions: (1)(a) pyridine, 0 °C (b) p-anisidine (4.0 equiv.), $NaNO_2$ (6.15 equiv.), 4 M HCl (50.0 equiv.), acetone, 0 °C then RT, 1 h (based on the work of Shu et al.)[52]

Repeating the procedure provided by literature for complexation of $\mathbf{14_x}$ with mercury,[50,51] proved that this compound could be used as a mercury sensor (see **Scheme 4.5**).

Stellenbosch University https://scholar.sun.ac.za

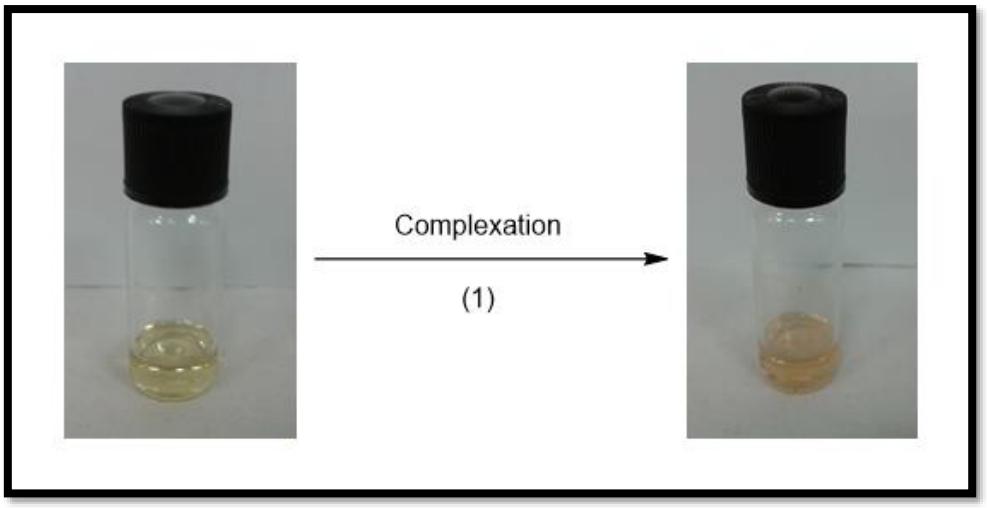

Scheme 4.5 Repeating Chung's result for the color change of the azacalix[4]arene solution as a result of mercury cation addition – (1): 10 μM solution of the azo dye in $CHCl_3$/MeOH (v/v= 1/399) plus 5 equivalents of Hg^{2+} salt[ii]

Having established this, the first strategy undertaken for synthesizing the modified Chung's sensor involved a monoalkylation of diallyl-bis(*p*-methoxyphenylazo)calix[4]arene with *N*-(4-bromobutyl)-phthalimide (our established primary amine precursor). As established in chapter 2, the best way for monoalkylation of calix[4]arene is either through an extended-time reaction with NaH as the base and DMF as the solvent at 80 °C or with a minimum amount of K_2CO_3 and a large excess of the alkyl halide in refluxing acetonitrile as the solvent. In the case of NaH, the reaction did not give any product and eventually, Chung's sensor $\mathbf{14_x}$ decomposed. In the same regard, even adding KI (to promote the Finkelstein reaction) was not helpful and the same failure resulted. The K_2CO_3 method also did not give us the desired product and even using too much of the base, together with an excess of NaI, did not help either and resulted in decomposition of Chung's sensor $\mathbf{14_x}$ under the reaction conditions. Overall, the desired monoalkylated Chung's sensor did not form, in spite of employing different bases and solvents, which necessitated a change of plan. The problem appeared to be that the azo groups were unstable in the reaction or applied some deactivation effect on the calix[4]arene, thus reducing its overall nucleophilicity so that it could not react with the alkyl halide (see **Scheme 4.6** and **Table 4.1**).

[ii] $HgCl_2$ was used since $Hg(ClO_4)_2$ was unavailable.

Stellenbosch University https://scholar.sun.ac.za

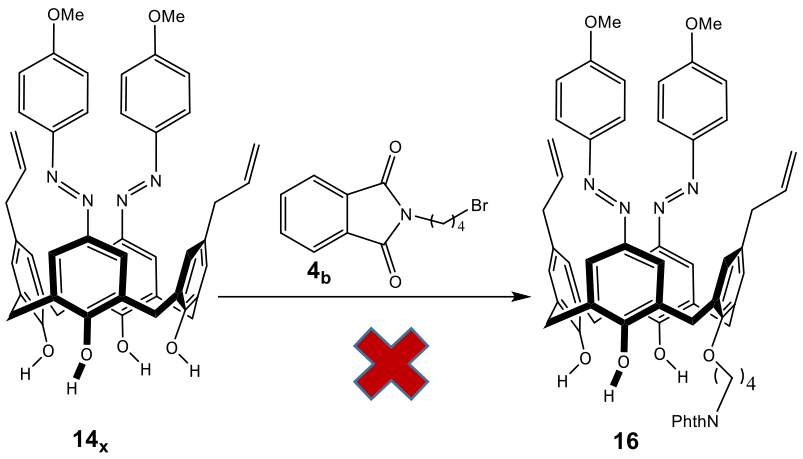

Scheme 4.6 Failed attempts to put the amine tether on Chung's sensor

Table 4.1 Reagents and conditions of the alkylation on Chung's sensor using phthalimide derivative

Entry	Base (equiv.)	4_b Alkylating agent (equiv.)	Additive (equiv.)	Solvent	Conc. (M)	Temp. (˚C)	Time	Result
1	NaH (1.0)	1.5	-	DMF	0.06	80	48 h	Decomposition of Chung's sensor
2	NaH (1.0)	1.5	KI (1.0)	DMF	0.06	80	48 h	Decomposition of Chung's sensor
3	K_2CO_3 (0.6)	3.3	-	CH_3CN	0.03	Reflux	24 h	Decomposition of Chung's sensor
4	K_2CO_3 (4.0)	3.3	-	CH_3CN	0.03	Reflux	24 h	Decomposition of Chung's sensor
5	K_2CO_3 (4.0)	3.3	NaI (4.0)	CH_3CN	0.03	Reflux	24 h	Decomposition of Chung's sensor

4.5 Alternative strategies

The first alternative plan was based on a literature report by Lin *et al*. for the synthesis of a calix[4]quinone from dialkoxycalix[4]arene with ClO_2 solution (a mild oxidizing agent to avoid over-oxidation) at room temperature in acetonitrile (**Scheme 4.7**)[jj].[53]

[jj] Thallium tris-trifluroacetate was another common choice for calix[4]arene oxidation; however, it was more expensive and in accordance with literature less effective.[54,55]

Stellenbosch University https://scholar.sun.ac.za

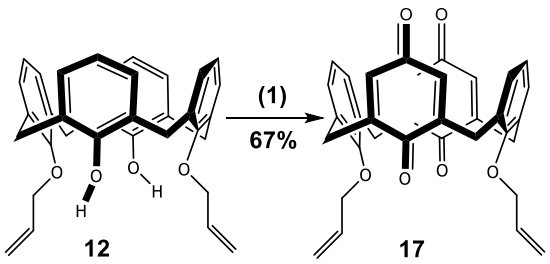

*Scheme 4.7 Oxidation approach for the distal diallyloxycalix[4]arene (**17**). Reagents and conditions: ClO_2 solution (7.4 equiv.), CH_3CN, RT, 4 h (based on the work of Lin et al.)*[53]

In a later paper by Chawla *et al.*,[56] a series of calix[4]quinones from Lin's very same paper[53] underwent a diazotization reaction with a number of substituted phenyl hydrazines and concentrated sulfuric acid in ethanol/chloroform at room temperature to afford substituted bisazocalix[4]arenes (the calix[4]quinone **17** was not involved in those experiments) (**Scheme 4.8**).

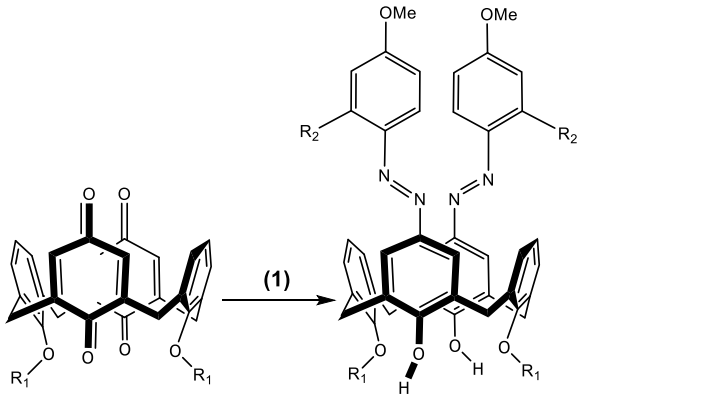

No.	R_1
1	$-COC_6H_5$
2	$-CH_2C_6H_5$

No.	R_1	R_2	Yield
3	$-COC_6H_5$	-H	78%
4	$-COC_6H_5$	$-NO_2$	84%
5	$-CH_2C_6H_5$	-H	78%
6	$-CH_2C_6H_5$	$-NO_2$	81%

Scheme 4.8 Chawla's diazotization approach for producing bisazocalix[4]arene from calix[4]quinone. Reagents and conditions: the substituted phenyl hydrazine, conc. H_2SO_4, $EtOH/CHCl_3$, RT, 4 h (based on the work of Chawla et al.)[56]

Therefore our proposed plan included the thermal Claisen rearrangement on the synthesized diallyloxycalix[4]diquinone **17**, monoalkylation of that product and ultimately the diazotization by means of a substituted phenyl hydrazine (**Scheme 4.9**).

Stellenbosch University https://scholar.sun.ac.za

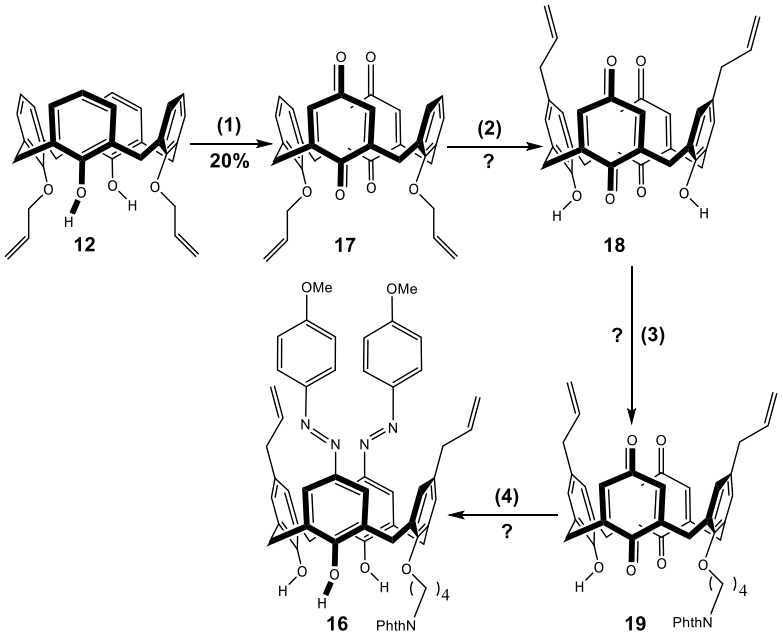

Scheme 4.9 First alternative plan to make the modified Chung's sensor. Reagents and conditions: (1) ClO_2 solution (7.4 equiv.), CH_3CN, RT, 4 h; (2) Claisen rearrangement (in diphenyl ether); (3) Monoalkylation with Finkelstein reaction (reflux in CH_3CN); (4) Diazotization (with substituted phenyl hydrazine in acidic media in $EtOH/CHCl_3$)

The first oxidation step was successfully performed in accordance with literature; however, in practice the yield was only 20% (compared to the reported 67% yield). After confirming our spectral data with literature values,[53] the Claisen rearrangement was attempted to obtain **18**, but failed since heating between 150 °C to 200 °C gave no reaction, whilst at higher temperatures our calix[4]diquinone **17** decomposed.

After this, we attempted to directly oxidize diallylcalix[4]arene **13** to avoid the decomposition problem caused by the thermal rearrangement. Unfortunately, treatment with ClO_2, resulted in over-oxidation in all cases and so this strategy was discarded (**Scheme 4.10**).

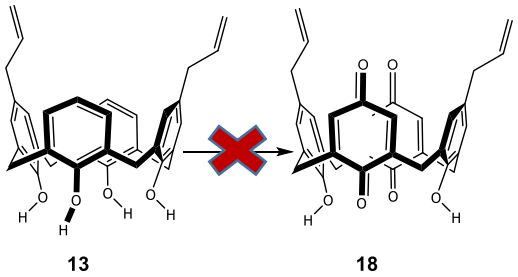

Scheme 4.10 Failed attempt to directly oxidize diallylcalix[4]arene

Next, it was decided to directly monoalkylate diallylcalix[4]arene **13** using the phthalimide derivative diazotization with the method employed earlier for the synthesis of Chung's sensor (**Scheme 4.11**). One obvious potential problem was the alkylation regioselectivity as it could

Stellenbosch University https://scholar.sun.ac.za

result in the formation of two different products; one could possess the butylphthalimide on the allyl-substituted ring, whereas the other one could have the same functionality on the allyl-free ring.

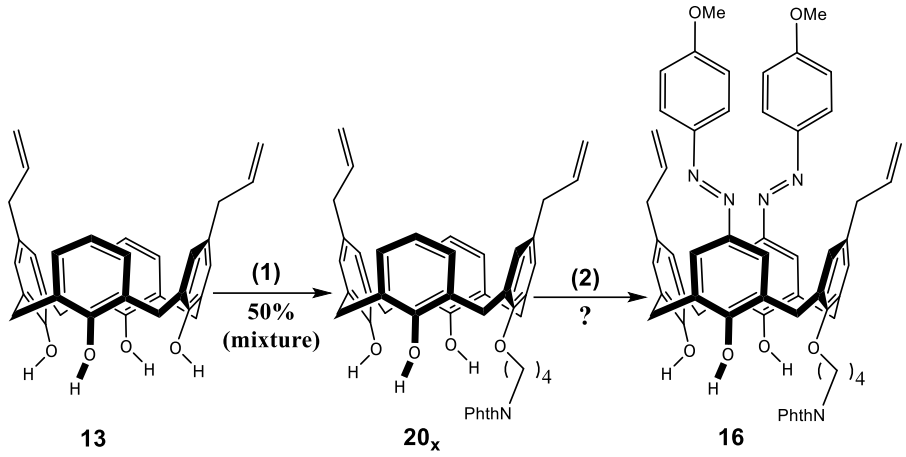

Scheme 4.11 Third alternative plan to make the modified Chung's sensor. Reagents and conditions: (1) (a) NaH (60% in oil) (1.0 equiv.), DMF, 80 °C, 24 h; (b) N-(4-bromobutyl)phthalimide (1.5 equiv.), DMF, 80 °C, 24 h; (2) Diazotization (with p-anisidine in acidic media)

Unfortunately, the ^{1}H-NMR spectrum for monoalkylation of **13** (**Figure 4.3**) suggested the formation of both predicted products (**20$_x$** and **20$_y$**, both on **Figure 4.3**) and owing to their identical R_f values, they could not be separated from each other (50% collective yield). The ^{1}H-NMR spectrum depicted two singlets at 9.20 and 9.39 ppm (with equal integrations) and another two singlets at 9.59 and 9.66 ppm (again with equal integrations but half the ratio for the previous couple) corresponding to the phenolic protons and thus representing a mixture of two regioisomers. The phthalimide aromatic signals also showed up between 7.68-7.71 and 7.85-7.88 ppm. Regrettably, aside from the phenolic region signals and the integration of all signals across the spectrum (which could only be meaningful in presence of two regioisomers), there was no further rationale to prove the doubling case. Overall, this set of data suggested the mole percentage of each of the products in the recovered crude was so close to one another which made the determination of the major and minor products via NMR spectroscopy impossible.

Although the likelihood of success was deemed low, it was decided to diazotize the mixture of monoalkylated isomers with the hope that the diazotized products would have a substantial difference in polarity, so that they could be separated from each other with ease. For this approach, calix[4]arene itself acted as the nucleophile, the amine source was *p*-anisidine, and $NaNO_2$ was used as the nitrosonium ion origin with 4 M HCl the acid in use. After the reaction, the TLC showed the formation of only one spot and the crude was passed through a column of

Stellenbosch University https://scholar.sun.ac.za

silica gel using EtOAc as the eluent. The product came off with 25% EtOAc/*n*-hexane; however, the ^{1}H-NMR spectrum for this product was not conclusive enough (complicated and unclear) (see the diazotization reaction conditions in **Table 4.2**).

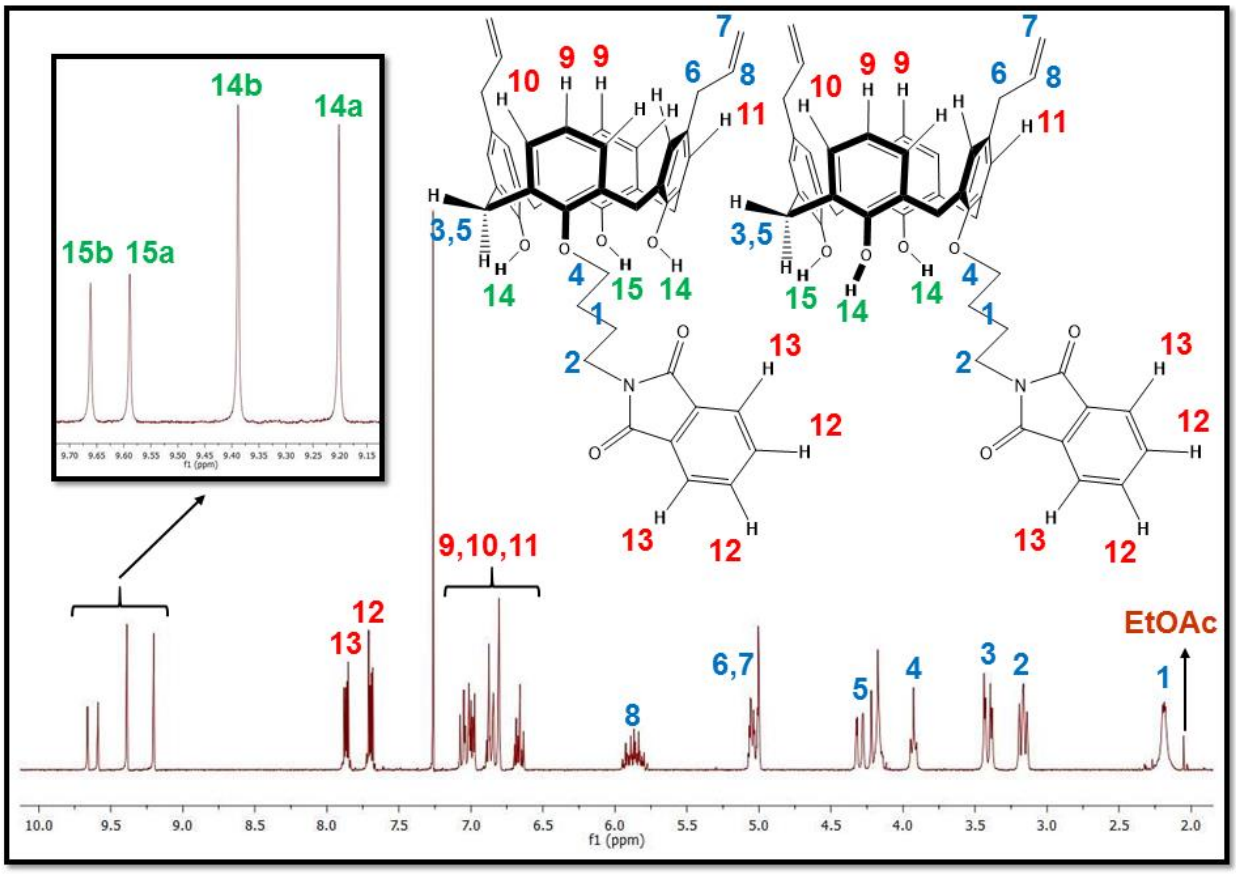

*Figure 4.3 ^{1}H-NMR spectrum (in $CDCl_3$) for **20**$_x$ (right-hand side structure) and **20**$_y$ (left-hand side structure)*

Table 4.2 Diazotization attempts on diallylcalix[4]arene-monobutylphthalimide mixture of isomers

Entry	*p*-anisidine (equiv.)	$NaNO_2$ (equiv.)	Acid (equiv.)	NaOAc (equiv.)	Solvent	Conc. (M)	Temp. (°C)	Time	Result
1	5.0	10.0	50.0	10.0	Acetone/MeOH/DMF (6.4:1:4.1)	0.03	0→25	24 h	One TLC spot for azo products
2	6.0	6.0	50.0	-	Acetone/Pyridine (1:1)	0.04	0→25	2 h	One TLC spot for azo products

Due to the vague and insufficient ^{1}H-NMR spectral results, the sample was submitted for a mass spectroscopy experiment (see the HRMS in **Figure 4.4**).

Stellenbosch University https://scholar.sun.ac.za

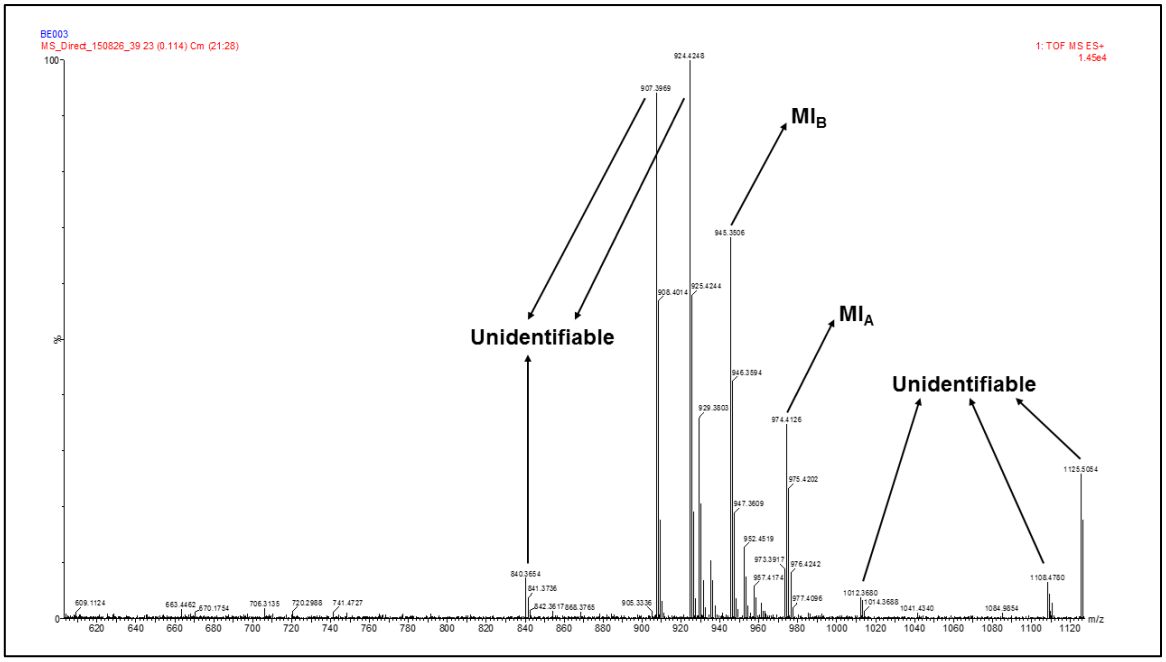

*Figure 4.4 HRMS results for the diazotization attempt on diallylcalix[4]arene-monobutylphthalimide mixture (**20**$_x$, **20**$_y$)*

According to the HRMS result, there were only two molecular ions attributable to meaningful structures: the molecular ion **MI$_A$** (974.4126 Da) could be attributed to a compound with the molar mass of our desired azacalix[4]arene **16** and its regioisomer (the ideal calculated value for $[M+H]^+$ should be 974.4129 Da), and also the molecular ion **MI$_B$** (945.3506 Da) which represented compound **16** (and its regioisomer) which had lost both its *p*-anisidine moiety methyl groups due to its etheric bond dissociation through the ionization process in the instrument (the ideal calculated value for $[M+H]^+$ should be 945.3738 Da). The suggested structures for these molecular ions can be seen in **Figure 4.5**.

As a consequence of the HRMS results, a mercury-sensing test was attempted by preparing a solution of our products mixture in $CHCl_3$/CH_3OH (399:1) and adding 5 equivalents of $HgCl_2$ which resulted in a color change from yellow to pale pink, i.e. a positive result. However, despite the indications for the existence of the desired product (HRMS and mercury test), the inconclusive NMR spectrum and the purification issues meant it was impossible to carry on with the plan as envisaged.

Stellenbosch University https://scholar.sun.ac.za

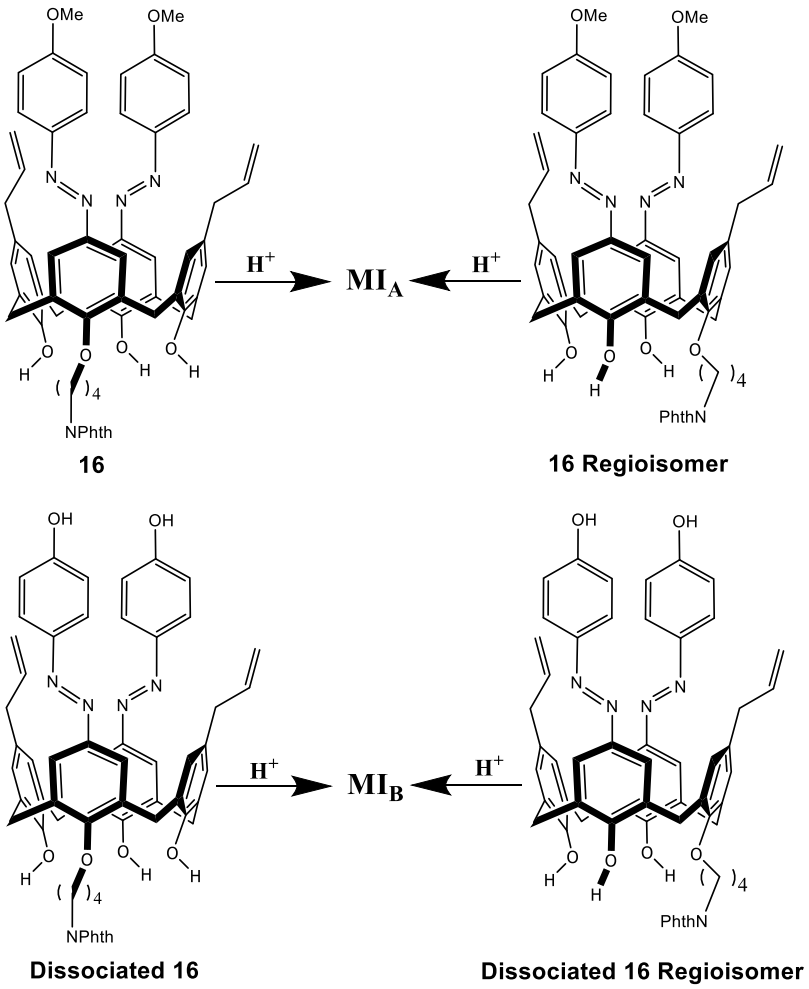

Figure 4.5 Suggested structures for MI_A and MI_B

Since regioselectivity appeared to be an issue, the next strategy considered protecting the phenolic protons by acylating diallyloxycalix[4]arene **12** followed by the Claisen rearrangement. The rest of the synthesis would then be very similar to the former approaches already discussed (**Scheme 4.12**).

The acetylation reaction was carried out in dry DCM with triethylamine (as the base) and catalytic DMAP on **12** (first at 0 °C and then room temperature) using an excess of acetic anhydride. Although the mass spectrum proved the existence of a diacetylated calix[4]arene, the ^{1}H-NMR spectrum revealed the formation of not the desired cone conformer, but the partial cone in 43% yield. The lack of any phenolic protons in the ^{1}H NMR spectrum was a sign of full protection at the lower rim. However, the existence of two different singlets at 1.52 and 1.89 ppm for acyl protons provides evidence for the dissymmetry of the structure (conformational change). This was also supported by the presence of 3 different doublets for the methylene bridges of the calix[4]arene (2 protons at 3.21, 2 protons at 3.57 and 4 protons

Stellenbosch University https://scholar.sun.ac.za

at 3.89 ppm) which confirmed the formation of a new conformer. Typically, only 2 chemically inequivalent protons should be observable (i.e. axial and equatorial) for a symmetrical cone conformation. Facing this unfavorable conformational issue, it was decided to implement a series of different acetylations on our starting material (acylating reagent: acetic anhydride) using different bases, solvents and so forth to possibly sort out this matter (see **Scheme 4.13** and **Table 4.3**).[kk]

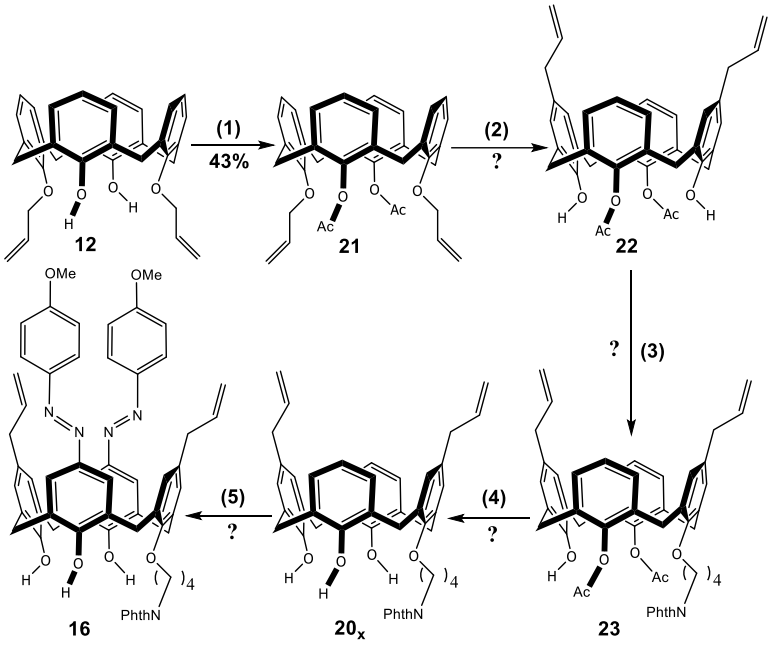

Scheme 4.12 Fourth alternative plan to make the modified Chung's sensor. Reagents and conditions: (1) Acetic anhydride (18.0 equiv.), triethylamine (18.0 equiv.), DMAP (5 mol%), DCM, 0 °C then RT, 15 h; (2) Claisen rearrangement (in diphenyl ether); (3) Monoalkylation with Finkelstein reaction (reflux in CH_3CN); (4) De-acetylation reaction (alkaline hydrolysis); (5) Diazotization (with p-anisidine in acidic media)

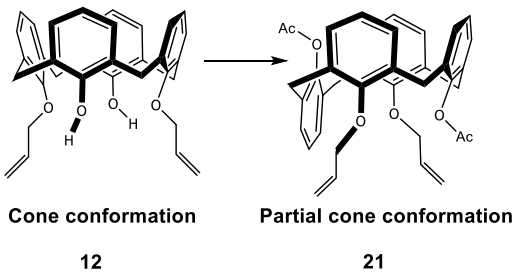

Scheme 4.13 Conformational change through acetylation

[kk] Conformational changes for calixarenes usually happen as a result of reactions or heating at very high temperatures.[57] Only if a calixarene holds a mobile conformation, it is able to transform from one conformer to another back and forth at room temperature.[58] The latter phenomenon will be later explained in chapter 5 of this dissertation.

Stellenbosch University https://scholar.sun.ac.za

*Table 4.3 Attempts to diacetylate diallyloxycalix[4]arene (**12**). 10.0 equiv. Ac_2O and base used. [a]pyridine used as a reagent and not as a solvent; [b]partial cone obtained*

Entry	Base	Catalyst	Solvent	Temp. (°C)	Time	Yield (%)
1	Na_2CO_3	-	DMF	0→25	24 h	-
2	Na_2CO_3	DMAP	DMF	0→25	24 h	-
3	Na_2CO_3	DMAP	DMF	100	7 h	-
4	Na_2CO_3	-	CH_3CN	Reflux	24 h	-
5	K_2CO_3	-	DMF	0→25	24 h	-
6	K_2CO_3	-	CH_3CN	Reflux	24 h	-
7	Pyridine[a]	DMAP	DMF	0→25	24 h	-
8	Pyridine[a]	DMAP	DMF	100	7 h	30[b]
9	Et_3N	DMAP	DCM	0→25	15 h	43[b]

Unfortunately, different conditions did not result in the desired cone conformation, so as a last resort the thermal rearrangement on our partial cone compound was tried with the hope of a conformational change of our starting material from partial cone to cone. Regrettably, the plan failed since it gave no reaction between 150 °C to 200 °C whilst our starting material (**21**) decomposed at higher temperatures (**Scheme 4.14**). It implies that acyl groups were not stable enough to resist such harsh thermal conditions and caused complications in product formation.

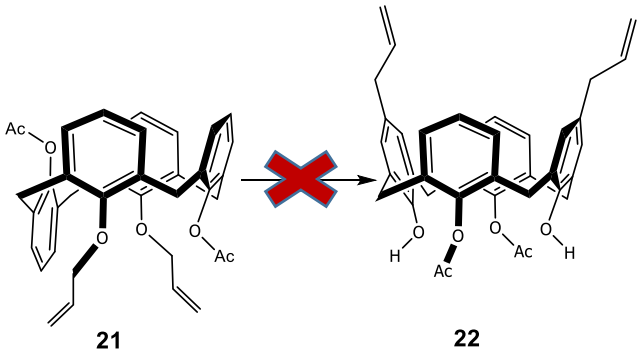

Scheme 4.14 Failed thermal rearrangement on partial cone diallyloxy-diacetyloxycalix[4]arene (5th alternative plan to make the modified Chung's sensor)

After the failure of the strategies that involved the reaction between a functionalized calix[4]arene (the nucleophile) and *p*-anisidine (the diazotization reagent), it was suggested that the functionalized calix[4]arene's role had to be re-defined. Thus, the roles were reversed and a diaminocalix[4]arene was targeted as the precursor to the formation of a diazonium salt which could be reacted with a nucleophilic source such as phenol or anisole (**Scheme 4.15**).

Stellenbosch University https://scholar.sun.ac.za

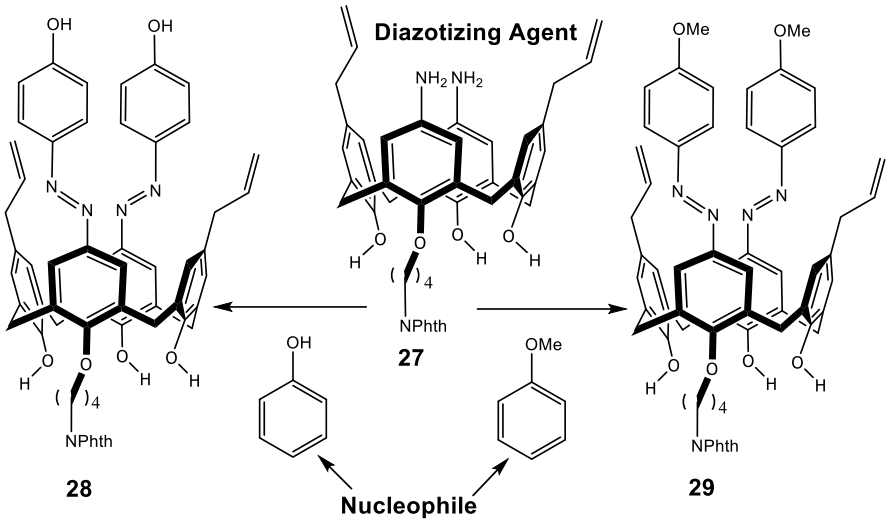

Scheme 4.15 Calix[4]arene's new role as the diazotization agent for the formation of the modified Chung's sensor

In order to obtain the diamino calixarene **27**, distal diallyloxycalix[4]arene **12** was nitrated by nitric acid (70%) in a mixture of glacial acetic acid and DCM. Different temperatures and reaction times were applied to optimize the reaction yield. In the end, it was realized that if the reaction time or the temperature (or both of them) increases, the yield would decrease dramatically. Finally, it was discovered that the best yield for producing **24** could be achieved at –10 °C for a 35-minute reaction (53% yield) (see **Scheme 4.16** and **Table 4.4**).

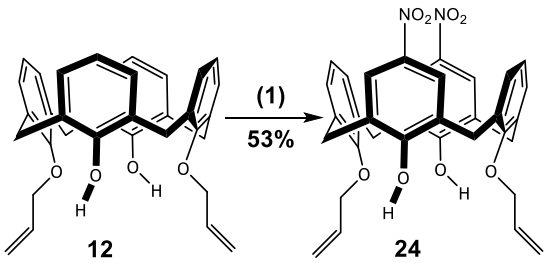

*Scheme 4.16 Synthesis of compound **24**. Reagents and conditions: (1) HNO_3 70% (18.0 equiv.), DCM/glacial AcOH, –10 °C, 35 min*

*Table 4.4 Optimization attempts for the nitration of **12**. 18.0 equiv. nitric acid 70% used in DCM/glacial acetic acid (3:4) (Reaction concentration: 0.09 M)*

Entry	Temp. (°C)	Time	Yield (%)
1	0	5 h	<10
2	0	2 h	18
3	0	1 h	25
4	–10	24 h	<10
5	–10	2 h	38
6	–10	35 min	53

Stellenbosch University https://scholar.sun.ac.za

The ^{1}H-NMR spectrum (**Figure 4.6**) primarily revealed the existence of product **24** by the presence of a singlet at 8.05 ppm (four aromatic protons de-shielded by *p*-substituted nitro groups). To corroborate this, two phenolic protons of the lower rim at 9.18 ppm could be seen as a singlet (downfield compared to the same ones in the starting material **12**), owing to their greater acidity induced by the *p*-nitro group).

The product also respectively showed an asymmetric N-O stretch at 1506 cm^{-1} and a symmetric N-O stretch at 1331 cm^{-1} in its IR spectrum. Finally, the HRMS result demonstrated the presence of a species with molecular ion of 612.2336 Da (the calculated molecular ion for $[M+NH_4]^+$: 612.2346 Da).

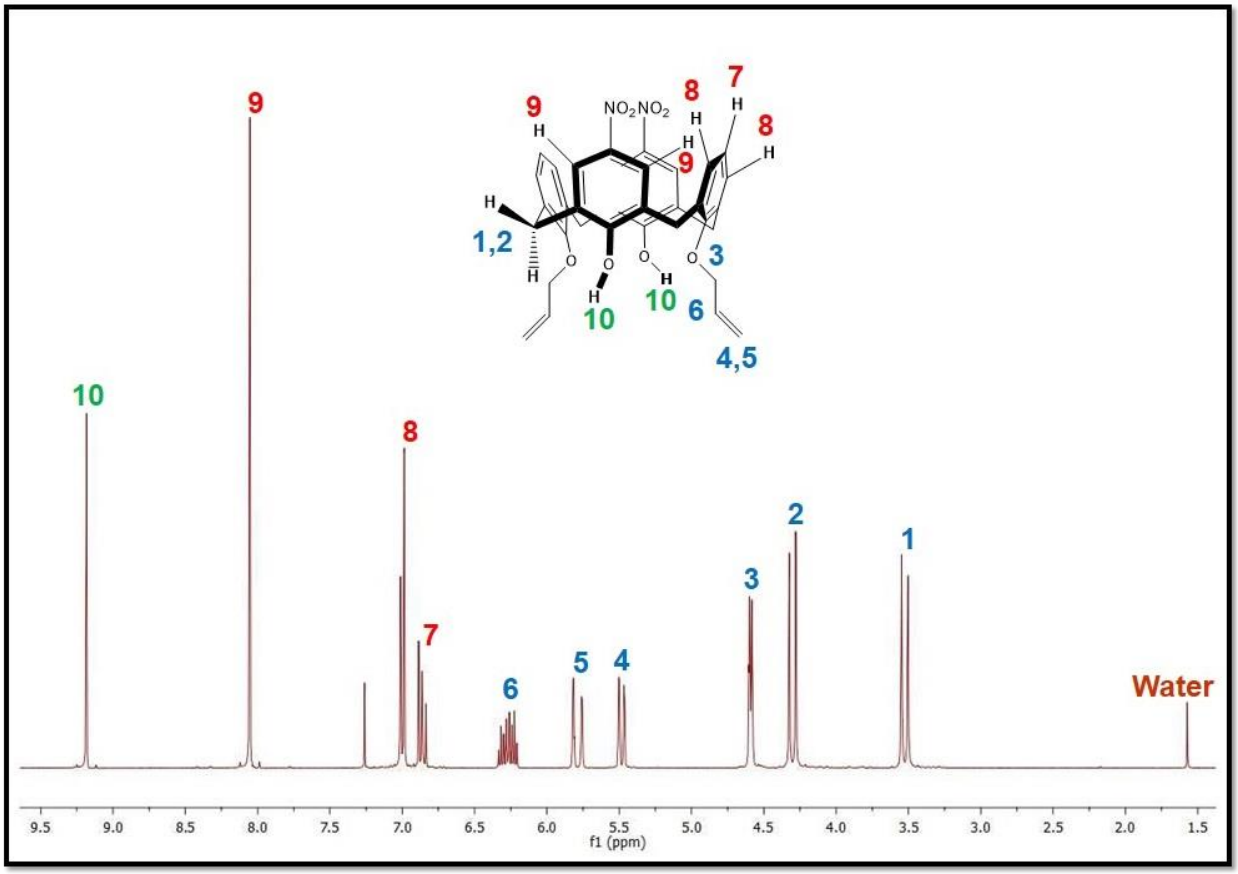

*Figure 4.6 ^{1}H-NMR spectrum (in $CDCl_3$) for **24***

Then compound **24** underwent a thermal Claisen rearrangement at 150 °C in diphenyl ether to form compound **25** (72% yield). Diphenyl ether was chosen because of its easy removal process after reaction (trituration with petroleum ether) and also owing to the decomposition of starting material in higher boiling point solvents (e.g. *N*,*N*-diethylaniline) under reflux conditions (**Scheme 4.17**).

Stellenbosch University https://scholar.sun.ac.za

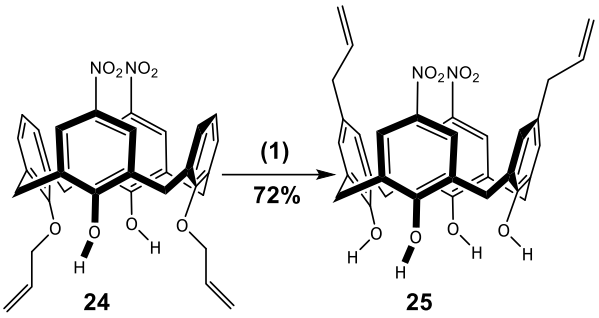

*Scheme 4.17 Synthesis of compound **25**. Reagents and conditions: (1) Diphenyl ether, 150 °C, 4h*

In the ^{1}H-NMR spectrum of **25** (**Figure 4.7**), four phenolic protons were observed as a broad singlet at 10.13 ppm which proved the successful [3+3] Claisen rearrangement, together with the existence of a strong hydrogen bonding between lower rim hydroxyls. Moreover, there were two singlets each representing four protons for *p*-substituted rings of calix[4]arenes at 6.98 ppm (allyl-substituted) and 8.0 ppm (nitro-substituted).

N-O stretches are visible at 1332 and 1513 cm^{-1} on IR spectrum while HRMS detected the molecular ion 612.2338 Da (the calculated molecular ion for $[M+NH_4]^+$: 612.2346 Da).

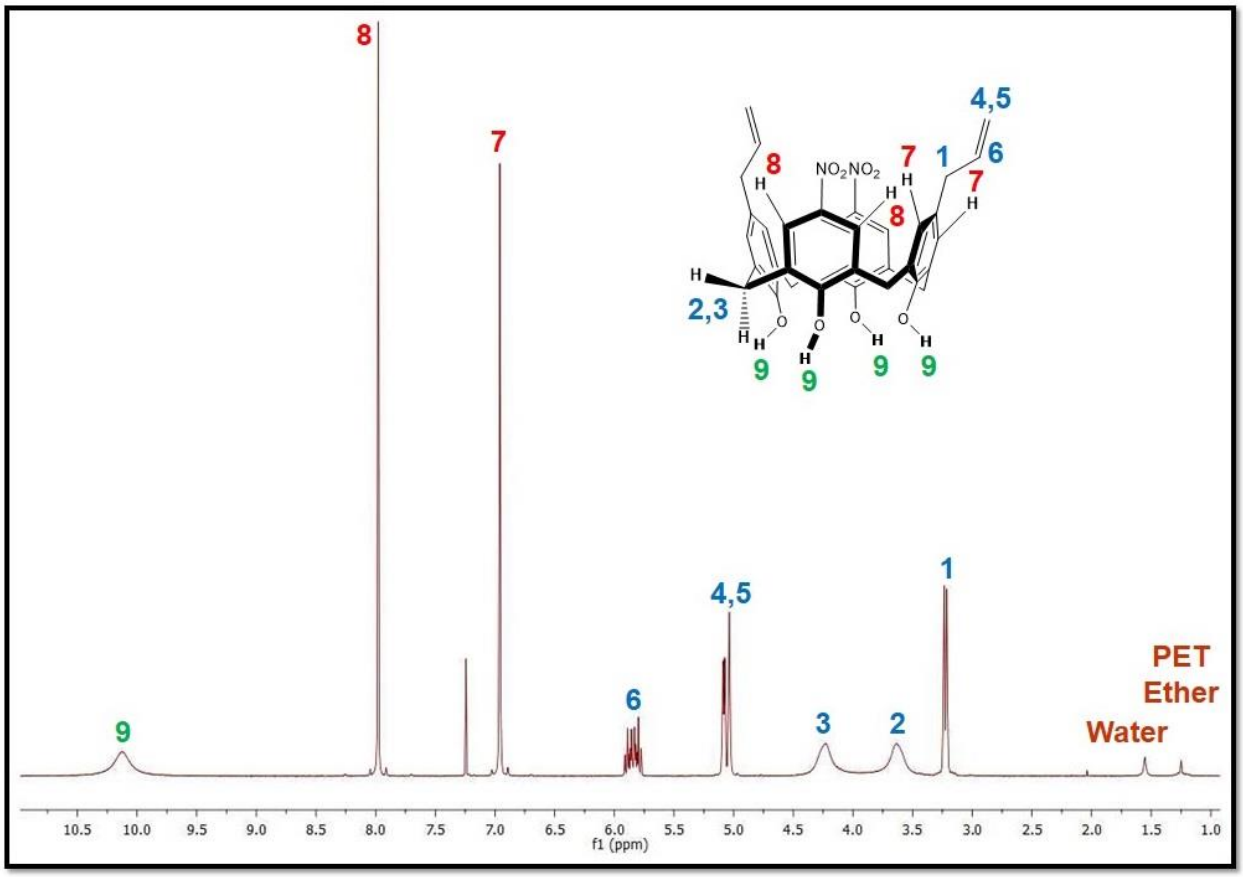

*Figure 4.7 ^{1}H-NMR spectrum (in $CDCl_3$) for **25***

Stellenbosch University https://scholar.sun.ac.za

The diallyl-dinitrocalix[4]arene **25** was then monoalkylated with *N*-(4-bromobutyl)-phthalimide in refluxing acetonitrile to produce **26**. It was found that using a minimum amount of K_2CO_3 did not give a good yield (<50%), therefore an excess of the base together with NaI were used (Finkelstein reaction) and this time a much better yield was achieved (71%) (see **Scheme 4.18**).[ll]

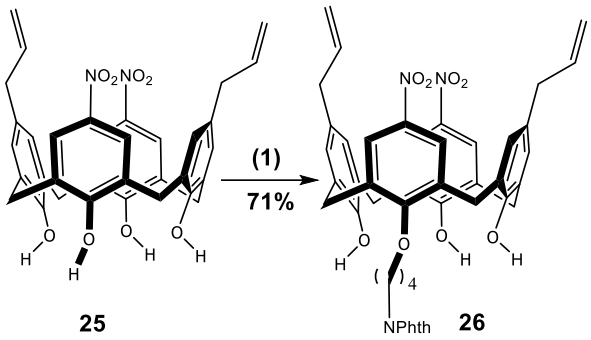

*Scheme 4.18 Synthesis of compound **26**. Reagents and conditions: (1) N-(4-bromobutyl)phthalimide (1.2 equiv.), K_2CO_3 (4.0 equiv.), NaI (1.0 equiv.), CH_3CN, reflux, 15 h*

The ^{1}H-NMR spectrum of **26** (**Figure 4.8**) revealed dissymmetry in the phenolic region which was caused by monoalkylation, and importantly that only one regioisomer had been formed. It was, however, important to know whether the butylphthalimide group was situated on the allyl-substituted phenolic ring, since in the future, after diazotization, only a non-modified phenolic ring can tautomerize to the quinone-hydrazone on complexation with mercury. In addition, two singlets were observed for the phenolic protons, one integrating for 2H at 8.66 ppm and 1H at 10.06 ppm. Since the nitro-substituted ring has a more acidic proton, one can hypothesize that the more downfield proton (1H) signal corresponded to this, and thus alkylation, unfortunately, occurred on this position. Chemically, it makes sense that it would undergo deprotonation first and thus the alkylation would occur here. In addition, phthalimide aromatic protons can be seen as two multiplets with 4 protons between 7.70-7.72 and 7.85-7.88 ppm. Because of dissymmetry in the system, the upper rim protons were not seen as two singlets anymore but as two doublets at 6.92 and 6.96 ppm (inequivalent aromatic protons of the allyl-substituted phenolic rings) and two singlets at 7.92 and 7.94 ppm (inequivalent aromatic protons of the nitro-substituted phenolic rings). With respect to the tether, the oxygen-linked methylene

[ll] In this case, NaH was not a favorable option. Due to the literature results by Gutsche *et al.* on both alkylation and acylation of distal dinitrocalix[4]arene, using NaH as the base would facilitate the formation of a tetra-substituted product. To avert that, K_2CO_3 was employed which as Gutsche suggested could only produce a mono-substituted product. The same report also claimed that only the nitro-substituted phenolic moiety would be alkylated and the other phenolic moiety would not partake in the reaction.[59]

Stellenbosch University https://scholar.sun.ac.za

shows up at 4.26 ppm, which is more downfield, compared to the nitrogen-linked methylene appearing at 3.93 ppm (oxygen is obviously more electronegative). Overall the argument that the nitro-substituted phenol was alkylated was not definitive, but likely and this may seriously impact the complexation ability of our final modified Chung's sensor (as only one of the azophenol groups can tautomerize in the presence of mercury).[mm]

The IR spectrum of **26** revealed the presence of a carbonyl stretch at 1708 cm^{-1} related to the imide group of the phthalimide. In addition, HRMS detection of a species with molecular ion 813.3144 Da matched the calculated molecular ion of 813.3136 Da assigned to $[M+NH_4]^+$ for compound **26**.

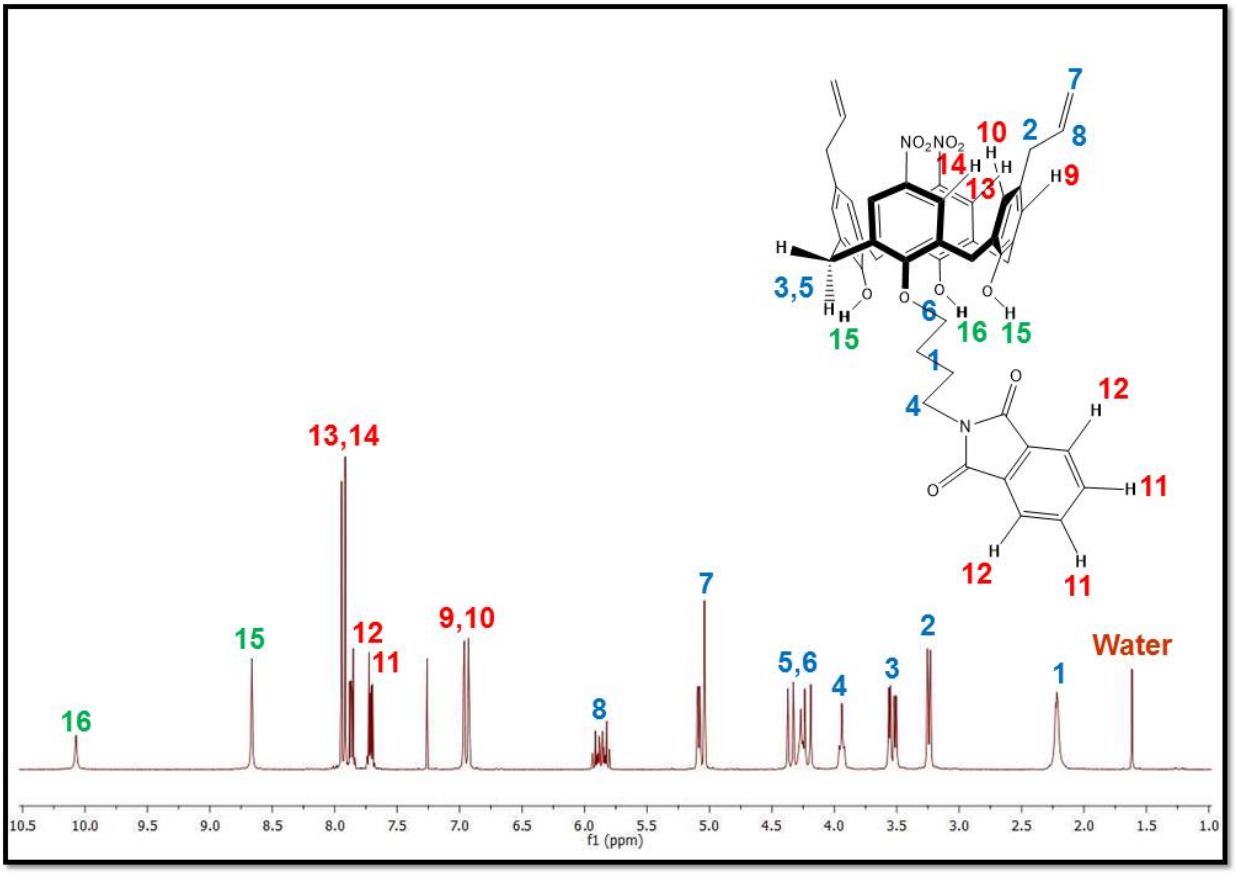

*Figure 4.8 ^{1}H-NMR spectrum (in $CDCl_3$) for **26***

In the next step, the two nitro functional groups on compound **26** were reduced with powdered iron with the help of an acidic medium (1 M HCl solution). In this case, the starting material

[mm] A 2D ^{1}H-NMR spectroscopic method (e.g. NOESY) could be the solution to fully ascertain the regioselectivity status of our product (**26**); however, due to the previously-mentioned report by Gutsche *et al.*,[59] the high cost of the experiment, and the fact that this approach ended in failure, it was deemed unnecessary and not attempted.

Stellenbosch University https://scholar.sun.ac.za

was heated under reflux in EtOH/THF to yield compound **27** (62% product recovery) (see **Scheme 4.19**).

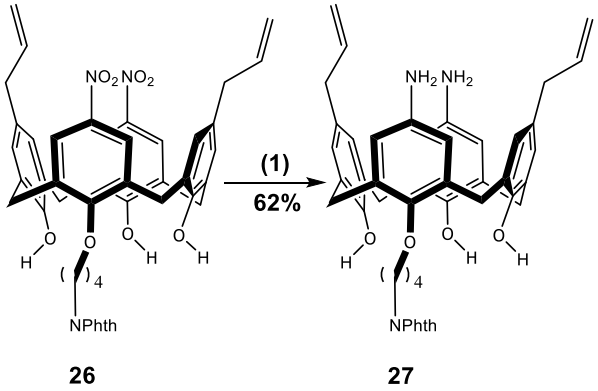

*Scheme 4.19 Synthesis of compound **27**. Reagents and conditions: (1) Iron powder (20.0 equiv.), 1 M HCl (20.0 equiv.) in EtOH/THF, reflux, 15 h*

The ^{1}H-NMR spectrum (**Figure 4.9**) indicated a very broad signal (observed as a split singlet) encompassing all 3 phenolic protons of the lower rim between 9.09-9.35 ppm. These protons showed up more upfield in comparison to the one for **26**, due to the far weaker electron-withdrawing nature of -NH_2 than -NO_2. Possibly due to the strong hydrogen bonding between the upper rim -NH_2 groups, they most likely have hidden somewhere between 3.00 and 4.50 ppm on the baseline and therefore were not observed. Aside from that, there was a singlet at 7.92 ppm which could not be assigned to any specific proton of the desired product casting doubts on the purity of the product.

Nevertheless, HRMS revealed the existence of the molecular ion 736.3392 Da (the calculated molecular ion for $[M+H]^{+}$: 736.3387 Da) and also the molecular ion 368.6735 Da (the double-charged ion) and to support the claim of the synthesis of **27**, the IR spectrum also showed a characteristic bend for N-H at 1603 cm^{-1}.

Overall, despite some uncertainty around the product purity (which could not get sorted by and re-running the product through a column chromatography and even attempted recrystallization), the desired product **27** was successfully synthesized after four steps.

Stellenbosch University https://scholar.sun.ac.za

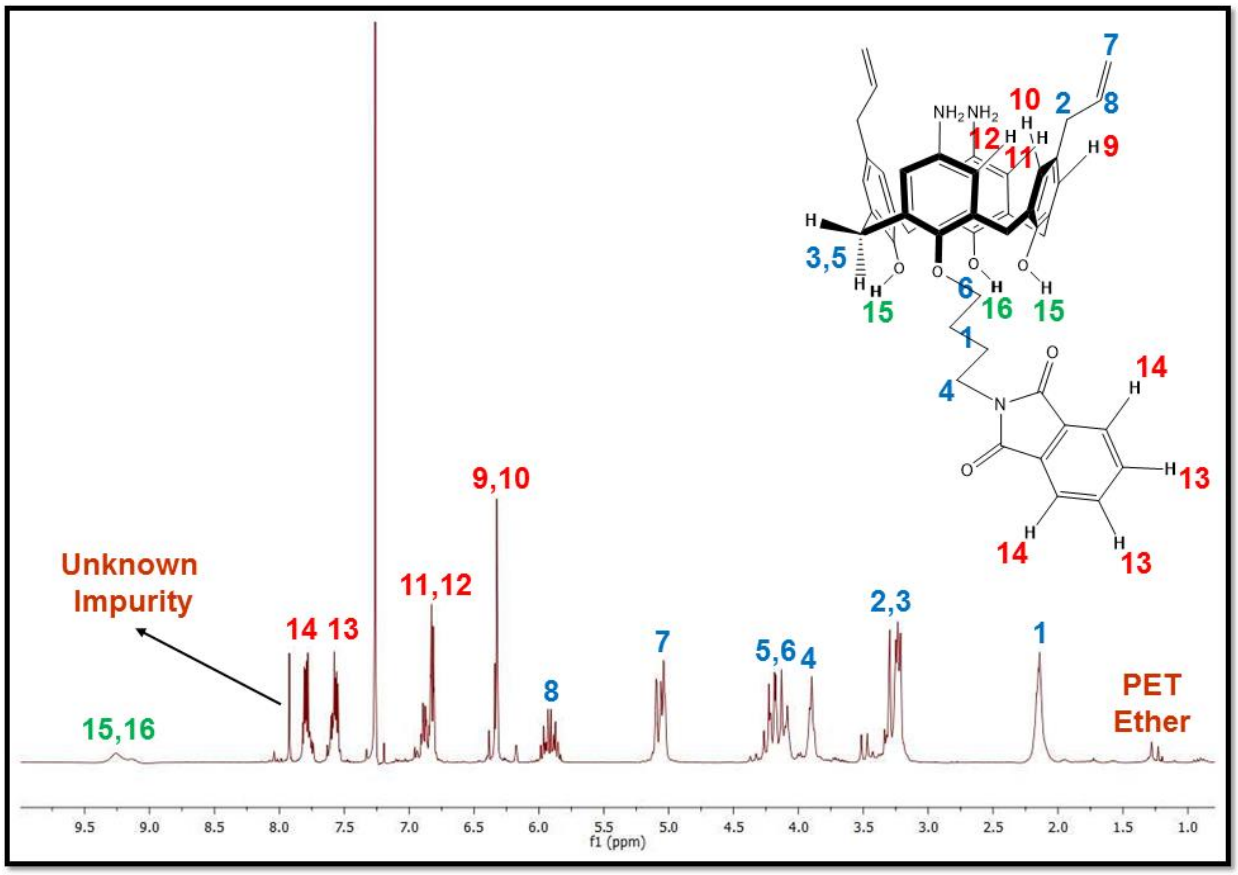

*Figure 4.9 ^{1}H-NMR spectrum (in $CDCl_3$) for **27***

Although admittedly impure, the monoalkylated diaminocalix[4]arene **27** was submitted to diazotization conditions and then treated with a nucleophilic source (phenol or anisole). The diazotization step required the formation of the nitrosonium ion (generated from 5 to 10 equivalents of $NaNO_2$ and an acid). In some cases, for the second reaction, NaOAc was used to increase the basicity of the reaction to pH=9 in order to facilitate the nucleophilic attack (through the formation of the phenolate anion, since phenol itself is not a potent nucleophile).[60,61] Despite that, the diazotization did not occur and the same diaminocalix[4]arene starting material **27** was recovered in all cases after the reaction work-up (see **Scheme 4.20** and **Table 4.5**).

Stellenbosch University https://scholar.sun.ac.za

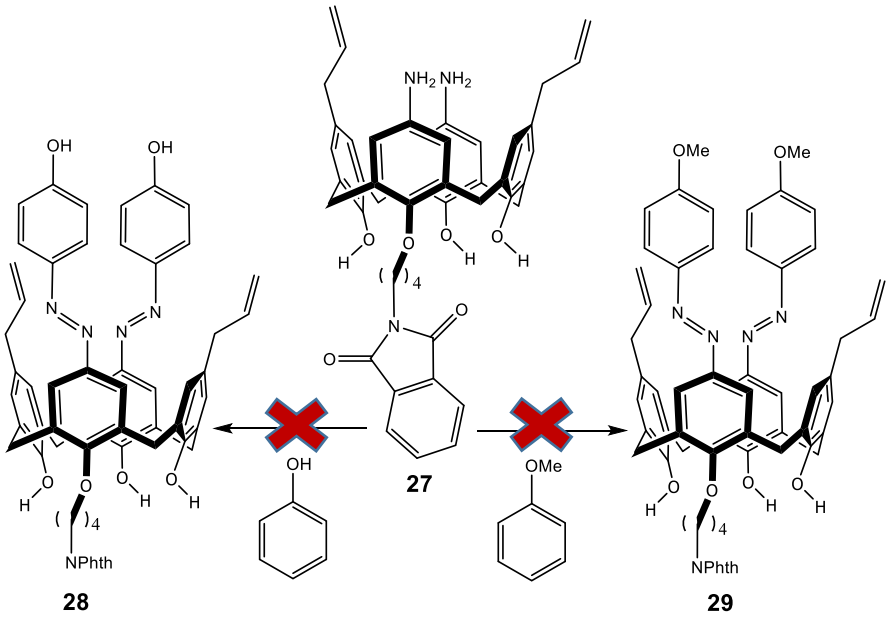

Scheme 4.20 Failure of the sixth alternative plan to make the modified Chung's sensor

*Table 4.5 Reagents and conditions of diazotization of monoalkylated diallyl-diaminocalix[4]arene (**27**) (0 °C then RT, 24 hours)*

Entry	Nucleophile (equiv.)	Acid (equiv.)	Extra reagent (equiv.)	Solvent	Conc. (M)	Result
1	Anisole (8.0)	4 M HCl (123.0)	-	Acetone	0.03	No Reaction
2	Anisole (10.0)	4 M HCl (14.3)	-	Acetone	0.29	No Reaction
3	Anisole (10.0)	0.8 M HCl (8.0)	-	THF/Pyridine (4.5:1)	0.01	No Reaction
4	Phenol (10.0)	0.8 M HCl (8.0)	-	THF/Pyridine (4.5:1)	0.01	No Reaction
5	Phenol (10.0)	12 M HCl (60 drops)	-	THF/Pyridine (3.5:1)	0.01	No Reaction
6	Anisole (10.0)	12 M HCl (60 drops)	-	THF/Pyridine (3.5:1)	0.01	No Reaction
7	Phenol (10.0)	12 M HCl (21 drops)	-	THF/MeOH (1.86:1)	0.03	No Reaction
8	Phenol (10.0)	AcOH (100%) (0.9 mL) H_2SO_4 (Conc.) (0.3 mL)	-	THF/MeOH (1:1)	0.04	No Reaction
9	Phenol (10.0)	AcOH (100%) (0.45 mL) H_2SO_4 (Conc.) (0.3 mL)	-	THF/MeOH (1.23:1)	0.04	No Reaction
10	Phenol (10.0)	12 M HCl (21 drops)	-	THF/MeOH (4.7:1)	0.02	No Reaction
11	Phenol (10.0)	12 M HCl (27 drops)	-	THF/MeOH (1.67:1)	0.02	No Reaction
12	Phenol (10.0)	12 M HCl (27 drops)	NaOAc (100.0)	THF/MeOH (1.44:1)	0.01	No Reaction
13	Phenol (10.0)	12 M HCl (18 drops)	NaOAc (100.0)	THF/MeOH/DMF (1:1.25:1.25)	0.01	No Reaction
14	Phenol (10.0)	4 M HCl (4.0)	-	THF/Pyridine (2:1)	0.02	No Reaction

Stellenbosch University https://scholar.sun.ac.za

Searching for a solution within literature, it was suggested that the *para* OH group of an aniline derivative had to be protected in order to let the diazotization happen, otherwise, the strong electron-donating effect of the OH group could prevent the reaction between the NH_2 group and the nitrosonium ion to form the diazonium salt.[62] To do so, full protection of the lower rim was carried out from the step before the reduction of the nitro groups by means of acylation of **26** with acetic anhydride and triethylamine in anhydrous DCM at 0 °C, then room temperature to form **30** (68% yield) (see **Scheme 4.21**).

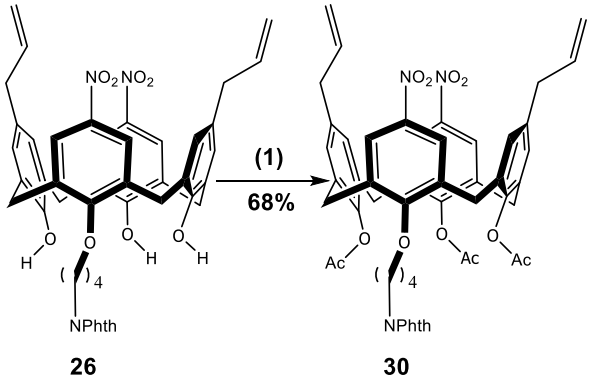

*Scheme 4.21 Synthesis of compound **30**. Reagents and conditions: (1) Acetic anhydride (18.0 equiv.), triethylamine (18.0 equiv.), DMAP (5 mol%), DCM, 0 °C then RT, 15 h*

According to ^{1}H-NMR spectrum (**Figure 4.10**), there was no sign of phenolic protons as a proof for the full protection of the lower rim, alongside the emerging of two singlets at 1.42 and 1.57 ppm for the newly formed acetyl groups (3 and 6 protons respectively). The spectrum also showed that there were different types of aromatic protons appearing as two singlets at 6.83 ppm (2 protons) and 6.99 ppm (2 protons) and another two singlets at 7.89 ppm (2 protons) and 7.91 ppm (2 protons). In line with what was seen in the ^{1}H-NMR spectral data for **26**, here also the more shielded protons at 6.83 and 6.99 ppm were *ortho* to the allyl groups, while the more de-shielded protons at 7.89 and 7.91 ppm suggested that our nitro groups were indeed not equivalent (the existence of only one multiplet signal for the CH group of allyl between 5.76-5.89 ppm also corroborated this theory). Thereby, in the light of this set of evidence, it was re-confirmed that the butylphthalimide spacer had been attached to a nitro-substituted phenol ring.

IR showed two different C=O stretches at 1702 cm^{-1} for the symmetric mode of phthalimide and also at 1752 cm^{-1}, which is presumably an overlapping one for the asymmetric mode of phthalimide and also the ester. In addition, the HRMS gave a signal at 939.3453 Da (calculated $[M+NH_4]^+$ value for our compound is 939.3435 Da).

Stellenbosch University https://scholar.sun.ac.za

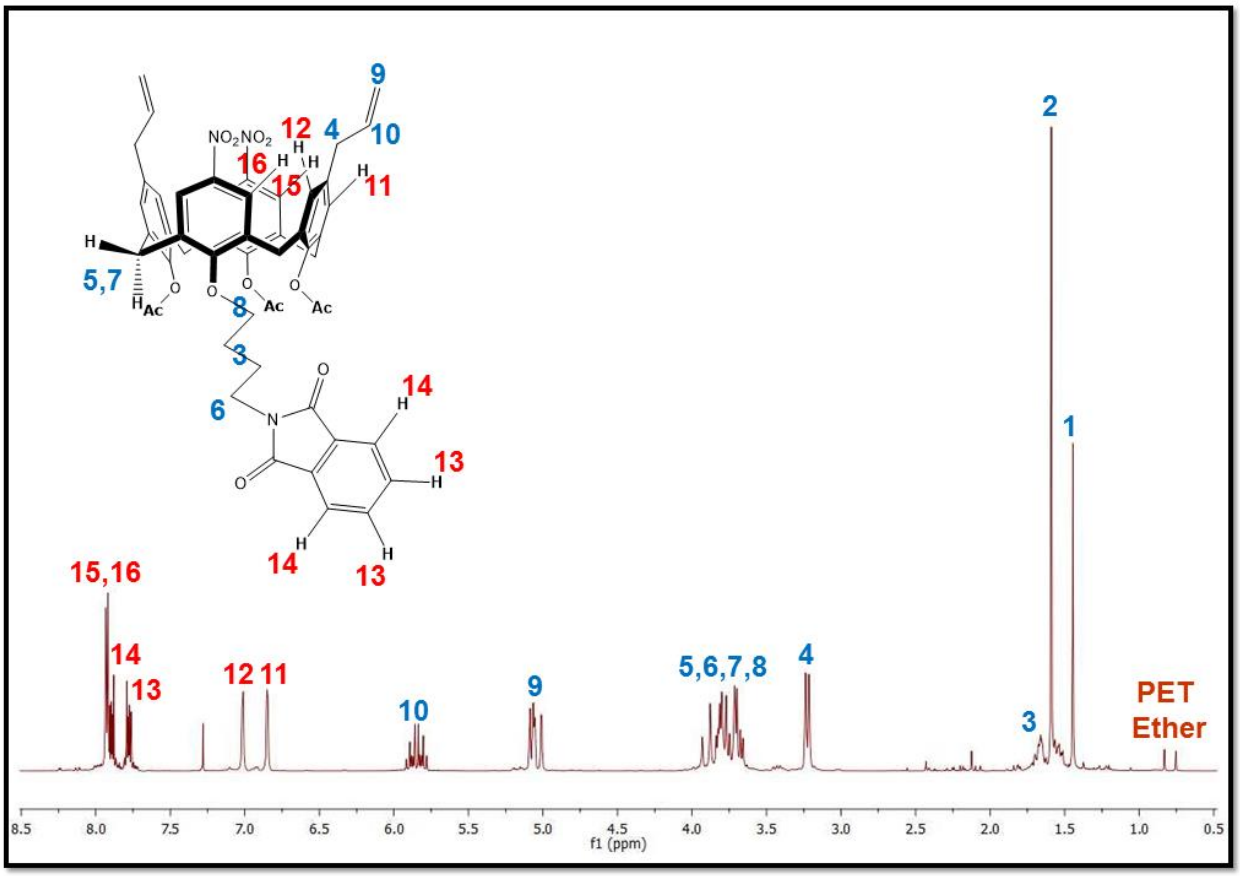

*Figure 4.10 ^{1}H-NMR spectrum (in $CDCl_3$) for **30***

Next, the fully lower rim-protected dinitrocalix[4]arene **30** was reduced in the same manner as before (Fe/HCl in EtOH/THF) to produce diamino **31** in a 90% yield (**Scheme 4.22**).

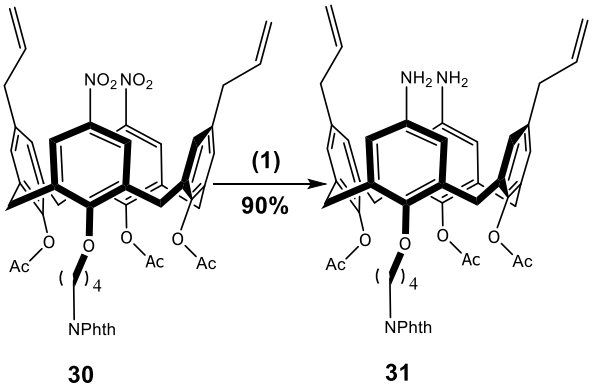

*Scheme 4.22 Synthesis of compound **31**. Reagents and conditions: (1) Iron powder (35.48 equiv.), 1 M HCl (38.71 equiv.) in EtOH/THF, reflux, 15 h*

Unlike the previous diamino calixarene, this compound's NMR spectra were very clean. As was the case for compound **27,** the strong hydrogen bonding between the upper rim NH_2 groups presumably results in the lack of amine protons on the ^{1}H-NMR spectrum for **31**, probably

Stellenbosch University https://scholar.sun.ac.za

being found around 3-4 ppm (**Figure 4.11**). Compared to **30**, the aromatic protons for nitro-substituted rings moved upfield to 6.31 ppm due to the strong electron-donating group (-NH_2).

In the IR spectrum of **31**, exhibits a bend for N-H at 1600 cm^{-1} was evident while HRMS not only showed the desired molecular ion 862.3705 Da (the calculated value for $[M+H]^+$: 862.3704 Da), but also two other fragments 661.2916 Da (our product minus butylphthalimide and acyl groups) and 431.6887 Da (for the double-charged ion). Overall, the compound **31** synthesis was achieved after another two steps.

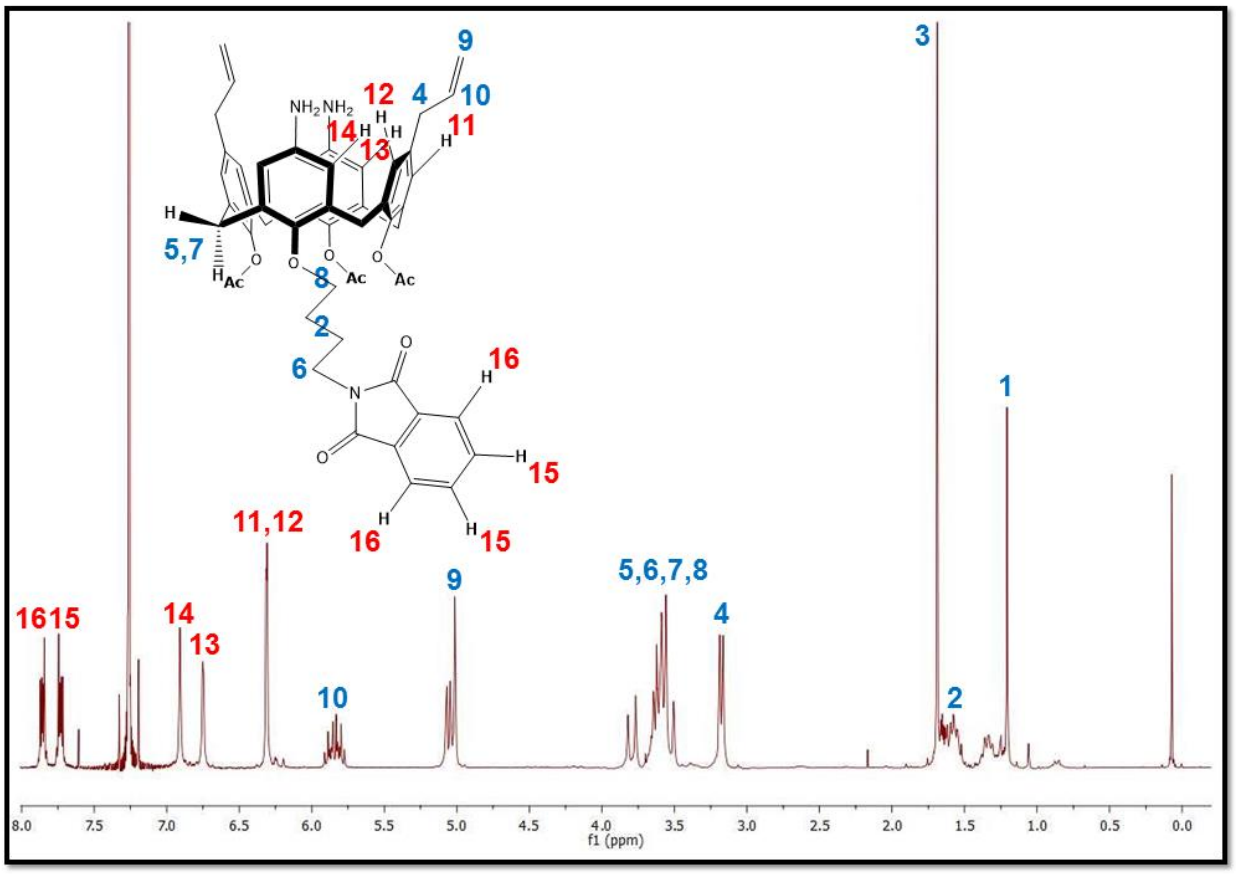

*Figure 4.11 ^{1}H-NMR spectrum (in $CDCl_3$) for **31***

Triacetyl-diamino-calixarene **31** was then subjected to a series of diazotization reactions. This time, phenol was the only nucleophilic source and 4 M HCl was the acid source, while the rest of the conditions were the same as the previous diazotization attempts. During the reactions, the TLC showed the formation of two spots and the crude products obtained were purified via column chromatography using EtOAc as the eluent. The first spot came off the column at 10% EtOAc/*n*-hexane, while the second spot was only collected when the polarity was increased to 25% EtOAc/*n*-hexane. The ^{1}H-NMR spectra of both spots were recorded, though, like the

Stellenbosch University https://scholar.sun.ac.za

previous diazotization attempt, the obtained spectra were not conclusive enough (complicated and unclear most likely due to decomposition of the products) (see the summary in **Table 4.6**).

*Table 4.6 Reagents and conditions of diazotization of a fully lower rim protected monoalkylated diallyl-diaminocalix[4]arene (**31**)*

Entry	Nucleophile (equiv.)	Acid (equiv.)	NaOAc (equiv.)	Solvent	Conc. (M)	Temp. (°C)	Time	Result
1	10.0	31.0	-	THF/Pyridine (4:1)	0.01	0→25	24 h	Two TLC spots for azo products
2	10.0	22.0	-	THF/Pyridine (4:1)	0.02	0→25	15 h	Two TLC spots for azo products
3	20.0	20.0	200.0	THF/MeOH/DMF (1:1.5:2.5)	0.01	0→25	1 h	Two TLC spots for azo products
4	20.0	20.0	-	THF/Pyridine (1.2:1)	0.01	0→25→50	24 h	Two TLC spots for azo products

Due to the complication of data analysis by ^{1}H-NMR spectroscopy, the samples were submitted for an HRMS experiment (see the related HRMS in **Figure 4.12**).

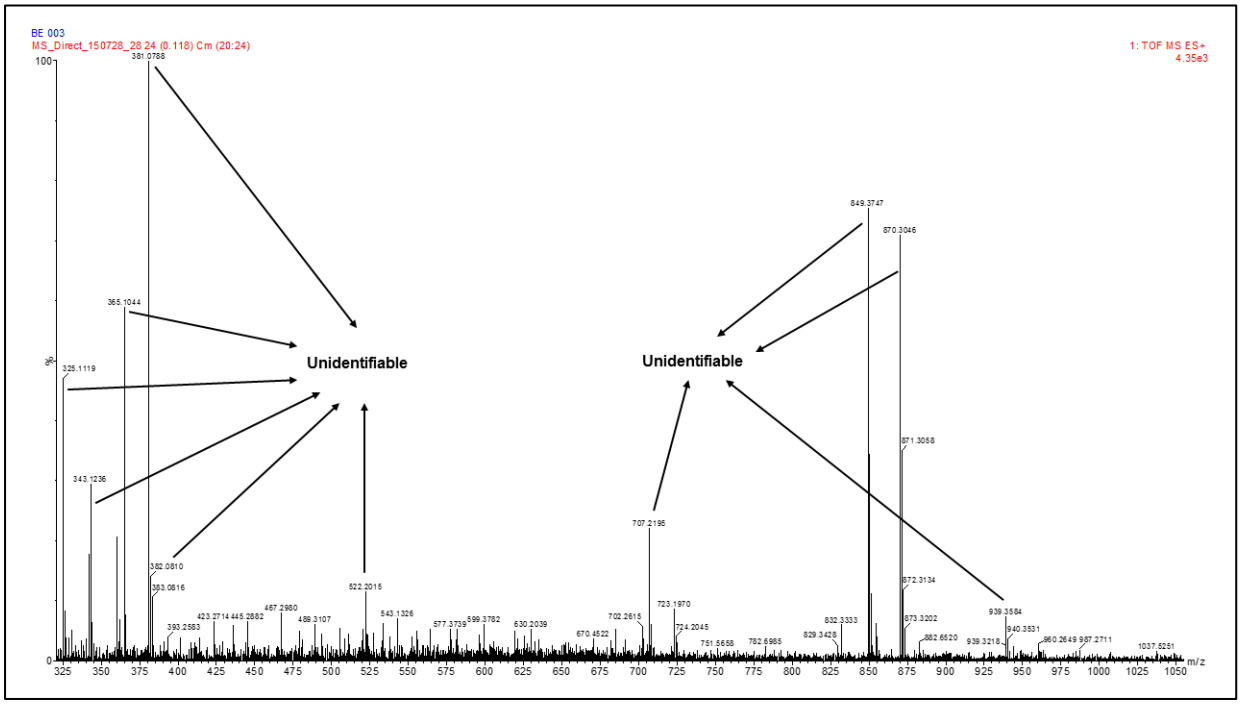

*Figure 4.12 HRMS results for the first product of diazotization on triacetyl-diamino-calixarene (**31**)*

According to these HRMS results, for the first spot (collected at 10% EtOAc/*n*-hexane), no molecular ion was found attributable to any possible structure resulted from the diazotization

Stellenbosch University https://scholar.sun.ac.za

reaction on our starting material (**31**). Therefore, it seemed that even HRMS was not capable of characterization of that compound.

On the other hand, for the second spot (collected at 25% EtOAc/*n*-hexane) HRMS was also obtained (the relevant HRMS can be seen in **Figure 4.13**).

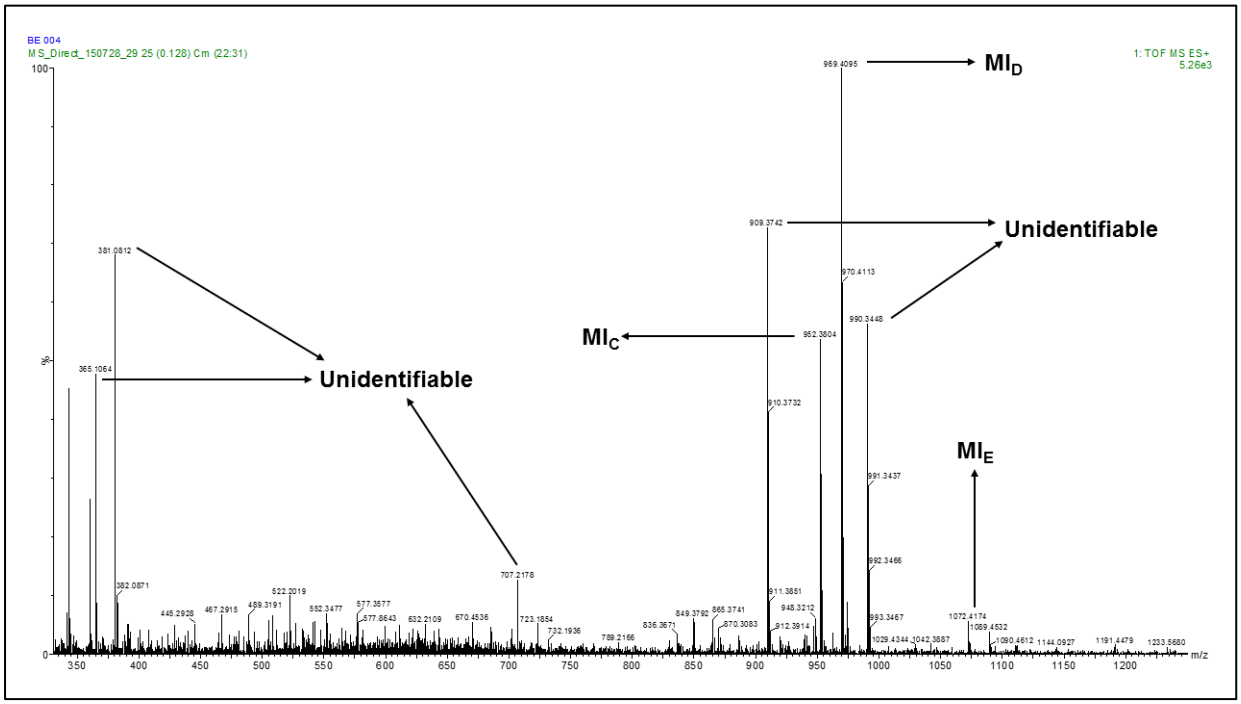

*Figure 4.13 HRMS results for the second product of diazotization on triacetyl-diamino-calixarene (**31**)*

This time, there were indications for the existence of both mono (**32$_x$** or **32$_y$**) and bis-diazotized derivatives (Triacylated version of **28**) of our azacalix[4]arene together. For the mono-diazotized derivatives: the molecular ion **MI$_C$** (952.3804 Da), was related to either of **32$_x$** or **32$_y$** regioisomers (the ideal calculated value for $[M+H]^+$ should be 952.3809 Da) in addition to the molecular ion **MI$_D$** (969.4095 Da) for the same couple of regioisomers (the ideal calculated value for $[M+NH_4]^+$ should be 969.4075 Da). With respect to the bis-diazotized derivative: the really low-intensity molecular ion **MI$_E$** (1072.4174 Da) was ascribable to the triacylated version of compound **28** (the ideal calculated value for $[M+H]^+$ should be 1072.4133 Da). The predicted structures for this diazotization attempt can be seen in **Figure 4.14**.

Overall, these results not only showed the unsuccessful purification approach for this reaction, but also proved that the obtained product was predominantly not the desired bis, but the undesired mono-azo derivative. Thus, unpromising NMR spectrum results and also vague indications from HRMS did not convince us to further this plan to the later stages.

Stellenbosch University https://scholar.sun.ac.za

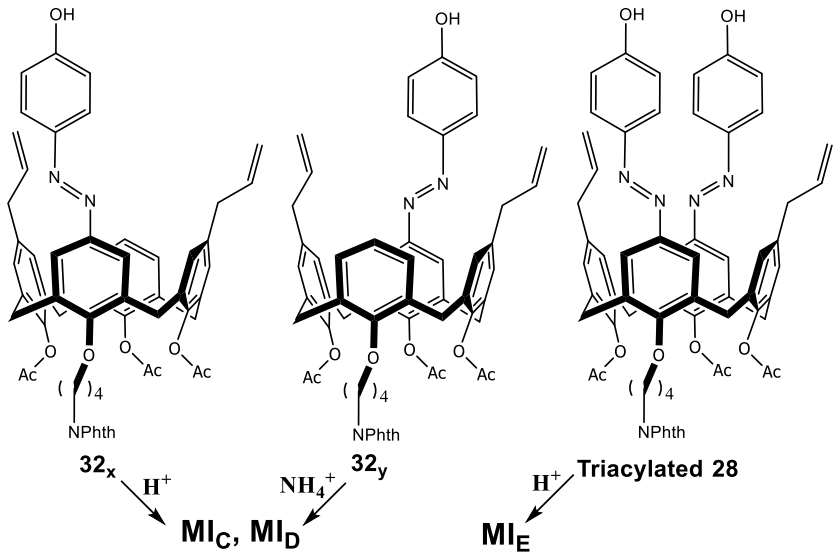

Figure 4.14 Predicted structures for MI_C, MI_D, and MI_E

4.6 Concluding remarks

Regrettably, in spite of all efforts and ideas dedicated to this chapter, our plan for making an azacalix[4]arene-grafted PSMA failed. The first stage of the plan was proven to be the most challenging one which had to be the formation of the modified Chung's sensor possessing a primary amine tether, whereas it was known from our experiments in chapter 3 that the second stage (PSMA and aminocalix[4]arene reaction) would be really straightforward to be done (The attachment was feasible even at room temperature). In some cases, the modified azacalix[4]arene did not form at all and in others, although HRMS confirmed the formation of our desired product, it was mixed with many other species. The ^{1}H-NMR spectrum also did not give us the ultimate proof for the product formation (complicated and impossible to interpret) which might be caused by the decomposition of the azacalix[4]arene scaffold under the reaction conditions, in addition to the presence of other regioisomers. Overall, under the attempted conditions, it was impossible to produce a pure modified Chung's sensor in high yield and use it for the next steps.

4.7 Experimental section

The same principles used for the experimental sections in previous chapters are applied to this section. Here only the synthesis and the characterization methods for all compounds studied in this chapter will be discussed.

Stellenbosch University https://scholar.sun.ac.za

25,27-Diallyloxy-26,28-dihydroxycalix[4]arene – 12

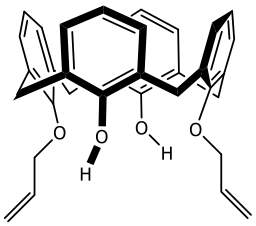

25,26,27,28-Tetrahydroxylcalix[4]arene **7** (2.12 g, 5.00 mmol), anhydrous K_2CO_3 (680 mg, 5.00 mmol) and allyl bromide (1.34 g, 11.1 mmol) were heated under reflux in acetonitrile (100 mL) for 4 hours under argon. After the removal of the solvent under the reduced pressure, 1 M HCl (100 mL) was added and the resulting white solid was recrystallized from $CHCl_3/CH_3OH$ to produce a colorless plate-like crystal (1.56 g, 62%). The spectral data were correlated with that from literature.[52] Mp 206 °C; R_f=0.46 (50% DCM/Petroleum ether); ^{1}H-NMR (300 MHz, $CDCl_3$) δ ppm 3.39 (d, *J*=13.0 Hz, 4H, $ArCH_2Ar$), 4.32 (d, *J*=13.0 Hz, 4H, $ArCH_2Ar$), 4.55 (d, *J*=5.0 Hz, 4H, OCH_2-C), 5.39-5.85 (m, 4H, CH_2=C), 6.18-6.37 (m, 2H, C=CH-C), 6.66 (t, *J*=7.5 Hz, 2H, ArH), 6.74 (t, *J*=7.5 Hz, 2H, ArH), 6.90 (d, *J*=7.5 Hz, 4H, ArH), 7.06 (d, *J*=7.5 Hz, 4H, ArH), 8.02 (s, 2H, ArOH).

5,17-Diallyl-25,26,27,28-tetrahydroxycalix[4]arene – 13

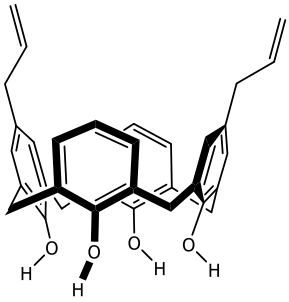

25,27-Diallyloxy-26,28-dihydroxycalix[4]arene **12** (1.00 g, 1.98 mmol) was heated under reflux in *N*,*N*-diethylaniline (10 mL) for 4 hours under argon. The reaction was cooled down and quenched with 1 M HCl (50 mL) to form a white solid. This crude was purified with a column chromatography (20% DCM/petroleum ether) and eventually recrystallized from $CHCl_3/CH_3OH$ to afford a pale-yellow needle-like crystal (840 mg, 84%). The spectral data were correlated with that from literature.[52] Mp 215 °C; R_f=0.46 (10% EtOAc/Petroleum ether); ^{1}H-NMR (300 MHz, $CDCl_3$) δ ppm 3.18 (d, *J*=7.0 Hz, 4H, $ArCH_2$-C), 3.52 (br. s, 4H, $ArCH_2Ar$), 4.27 (br. s, 4H, $ArCH_2Ar$), 5.00-5.10 (m, 4H, CH_2=C), 5.77-5.97 (m, 2H, C=CH-C), 6.74 (t, *J*=8.0 Hz, 2H, ArH), 6.86 (s, 4H, ArH), 7.06 (d, *J*=8.0 Hz, 4H, ArH), 10.21 (s, 4H, ArOH).

Stellenbosch University https://scholar.sun.ac.za

5,17-Diallyl-11,23-bis-(*p*-methoxyphenyl)azo-25,26,27,28-tetrahydroxycalix[4]arene – 14_x

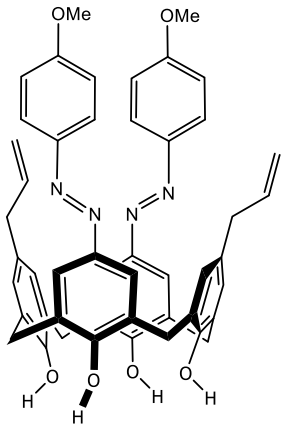

At 0 °C, *p*-anisidine (200 mg, 1.60 mmol) and $NaNO_2$ (170 mg, 2.46 mmol) were mixed in 4 M HCl (5.00 mL, 20.0 mmol) and acetone (5 mL) and added to a cold solution of 5,17-diallyl-25,26,27,28-tetrahydroxycalix[4]arene **13** (200 mg, 0.400 mmol) in pyridine (5 mL) resulted in the formation of a red-color solution. The reaction was warmed up to room temperature and stirring continued for an hour. The reaction was quenched with 1 M HCl (100 mL) to form a dark red solid and the solid was finally recrystallized from $CHCl_3/CH_3OH$ to produce a yellow powder (260 mg, 82%). The spectral data were correlated with that from literature.[52] Mp 264 °C; R_f=0.31 (10% EtOAc/Petroleum ether); ^{1}H-NMR (300 MHz, $CDCl_3$) δ ppm 3.22 (d, *J*=7.0 Hz, 4H, $ArCH_2$-C); 3.62 (br. s, 4H, $ArCH_2Ar$), 3.87 (s, 6H, $ArOCH_3$), 4.27 (br. s, 4H, $ArCH_2Ar$), 5.01-5.10 (m, 4H, CH_2=C), 5.78-5.98 (m, 2H, C=CH-C), 6.97 (s, 4H, ArH), 6.98 (d, *J*=9.0 Hz, 4H, ArH), 7.64 (s, 4H, ArH), 7.81 (d, *J*=9.0 Hz, 4H, ArH), 10.25 (br. s, 4H, ArOH).

25,27-Diallyloxy-26,28-calix[4]diquinone – 17

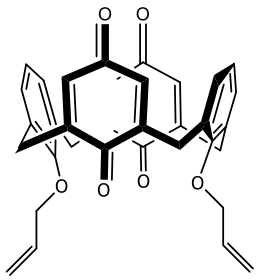

25,27-Diallyloxy-26,28-dihydroxycalix[4]arene **12** (2.52 g, 5.00 mmol) dissolved in acetonitrile (150 mL) and to that was added an aqueous solution of ClO_2 (100 mL).* The stirring continued for 4 hours and then the organic layer was removed under the reduced pressure to form a solid residue. The residue was purified with a column chromatography (20% EtOAc/petroleum ether) and eventually recrystallized from $CHCl_3/CH_3OH$ to yield an orange solid (540 mg, 20%). The spectral data were correlated with that from literature.[53] Mp 187 °C; R_f=0.12 (1% EtOH/DCM); ^{1}H-NMR (300 MHz, $CDCl_3$) δ ppm 3.35 (d, *J*=12.8 Hz, 4H, $ArCH_2Ar$), 3.69 (d, *J*=12.8 Hz, 4H, $ArCH_2Ar$), 4.22 (d, *J*=5.5 Hz, 4H, OCH_2-C), 5.24 (dd, *J*=10.4, 0.9 Hz, 2H, OCH_2-C), 5.32 (dd, *J*=17.1, 1.3 Hz, 2H, OCH_2-C), 5.96-6.11 (m, 2H, C=CH-C), 6.55 (s, 4H, quinone H), 6.45 (t, *J*=7.5 Hz, 2H, ArH), 6.82 (d, *J*=7.5 Hz, 2H, ArH).

*Aqueous ClO_2 preparation was achieved by mixing equal amounts of $NaClO_2$ (22.6 g, 0.250 mol) in water (500 mL) and $Na_2S_2O_8$ (29.7 g, 0.125 mol) in water (500 mL) and stored at 0 °C in a dark color bottle.

Stellenbosch University https://scholar.sun.ac.za

5,17-Diallyl-25-mono-phthalimidebutoxy-26,27,28-trihydroxycalix[4]arene and 5,17-Diallyl-26-mono-phthalimidebutoxy-25,27,28-trihydroxycalix[4]arene – 20_x, 20_y

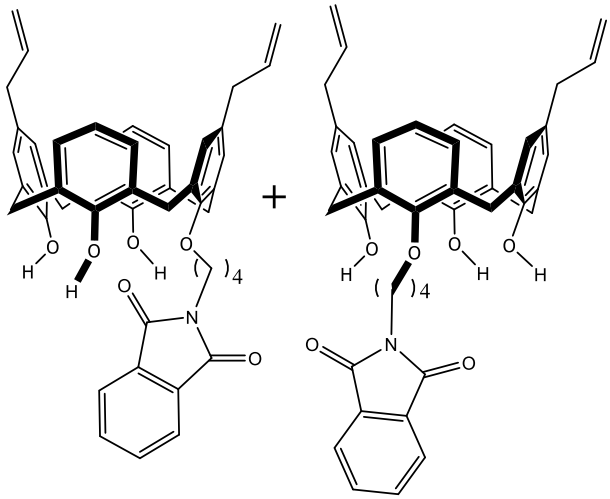

5,17-Diallyl-25,26,27,28-tetrahydroxycalix[4]arene **13** (210 mg, 0.420 mmol), NaH (60% in oil) (16.8 mg, 0.420 mmol) were suspended in dry DMF (7.2 mL) and the mixture was heated at 80 °C for 24 hours under argon. After that, *N*-(4-bromobutyl)phthalimide $\mathbf{4_b}$ (180 mg, 0.630 mmol) was added and the heating continued for another 24 hours. The reaction got cooled down and quenched with 10 mL of NH_4Cl (saturated solution). Ethyl acetate (3×50 mL) was added and then everything was transferred into a separation funnel. The organic phase was separated and washed with water (6×50 mL) and brine (50 mL) and dried over anhydrous $MgSO_4$. The EtOAc layer was removed under the reduced pressure and the crude left was purified via a column chromatography (10% EtOAc/petroleum ether) to afford a colorless oil as the mixture of 2 regioisomers (150 mg, 50%: recovered mass). R_f=0.23 (10% EtOAc/Petroleum ether); ^{1}H-NMR (300 MHz, $CDCl_3$) δ ppm 2.10-2.25 (m, 8H, C-CH_2-C), 3.16 (t, *J*=7.7 Hz, 8H, C-CH_2N), 3.38 (d, *J*=3.4 Hz, 4H, ArCH_2Ar), 3.41 (d, *J*=3.4 Hz, 4H, ArCH_2Ar), 3.92 (t, *J*=6.3 Hz, 4H, OCH_2-C), 4.19 (d, *J*=13.2 Hz, 4H, ArCH_2Ar), 4.30 (d, *J*=13.2 Hz, 4H, ArCH_2Ar), 4.99-5.07 (m, 8H, CH_2=C), 5.77-5.94 (m, 4H, C=CH-C), 6.63-6.69 (m, 3H, ArH), 6.80-6.89 (m, 9H, ArH), 6.97-7.07 (m, 8H, ArH), 7.68-7.71 (m, 4H, phthalimide ArH), 7.85-7.88 (m, 4H, phthalimide ArH), 9.20 (s, 2H, ArOH), 9.39 (s, 2H, ArOH), 9.59 (s, 1H, ArOH), 9.66 (s, 1H, ArOH) (*n*-hexane, ethyl acetate and water signals were not removed even after heating the product under vacuum at 100 °C).*

*The analytical data represented not one but two compounds.

Stellenbosch University https://scholar.sun.ac.za

25,27-Diallyloxy-26,28-diacetoxycalix[4]arene – 21

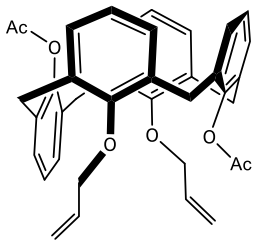

To a stirring solution of 25,27-diallyloxy-26,28-dihydroxycalix[4]arene **12** (200 mg, 0.400 mmol) and triethylamine (1.00 mL, 7.20 mmol) and DMAP (5 mol%) in dry DCM (5 mL) at 0 °C, was gently added acetic anhydride (0.680 mL, 7.20 mmol). The reaction was then warmed up to the room temperature and left for stirring for 15 hours. The reaction was washed with 10 mL of $NaHCO_3$ (saturated solution), extracted with DCM (3×50 mL) and ultimately washed with 1 M HCl (50 mL). The organic phase was dried over anhydrous $MgSO_4$ and the solvent was removed under the reduced pressure. The crude was purified with a column chromatography (10% EtOAc/ petroleum ether) to yield a colorless foam-like solid (100 mg, 43%). The spectral data were correlated with that from literature.[63] Mp 211 °C; R_f=0.46 (25% EtOAc/Petroleum ether); ^{1}H-NMR (300 MHz, $CDCl_3$) δ ppm 1.52 (s, 3H, CH_3-C), 1.89 (s, 3H, CH_3-C), 3.21 (d, *J*=13.2 Hz, 2H, $ArCH_2Ar$), 3.57 (d, *J*=13.2 Hz, 2H, $ArCH_2Ar$), 3.89 (d, *J*=13.2 Hz, 4H, $ArCH_2Ar$), 4.12-4.21 (m, 2H, OCH_2-C), 4.26-4.35 (m, 2H, OCH_2-C), 5.24-5.37 (m, 4H, CH_2=C), 6.06-6.19 (m, 2H, C=CH-C), 6.66-7.32 (m, 12H, ArH).

25,27-Diallyloxy-26,28-dihydroxy-5,17-dinitrocalix[4]arene – 24

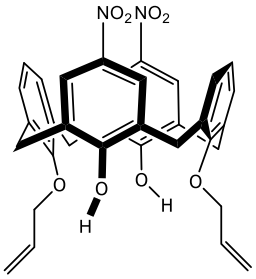

To a stirring solution of 25,27-diallyloxy-26,28-dihydroxycalix[4]arene **12** (1.00 g, 1.98 mmol) in DCM/AcOH (9 mL:12 mL) was added HNO_3 (70%, 2.25 mL, 35.5 mmol) dropwise at –10 °C. After 35 minutes, the reaction was poured into an ice/water beaker and then transferred to a separation funnel wherein the organic layer was separated. Then the aqueous layer was washed with DCM (5×50 mL) in order to extract the rest of our product. The combined organic phase was dried over anhydrous $MgSO_4$ and to that was added toluene (5 mL) as an azeotrope in order to remove the residual acetic acid. The solvent was removed under the reduced pressure and the resulting orange crude was purified with a column chromatography (50% DCM/petroleum ether) to afford a pale yellow solid (630 mg, 53%). Mp 215 °C DEC; R_f=0.31 (25% EtOAc/Petroleum ether); ^{1}H-NMR (300 MHz, $CDCl_3$) δ ppm 3.52 (d, *J*=13.2 Hz, 4H, $ArCH_2Ar$), 4.3 (d, *J*=13.2 Hz, 4H, $ArCH_2Ar$), 4.59 (dt, *J*=5.1, 1.5 Hz, 4H, OCH_2-C), 5.48 (dd, *J*=10.8, 1.2 Hz, 2H, CH_2=C), 5.78 (dd, *J*=17.4, 1.5 Hz, 2H, CH_2=C), 6.21-6.33 (m, 2H, C=CH-C), 6.86 (t, *J*=7.5 Hz, 2H, ArH), 6.99 (d, *J*=7.5 Hz, 2H, ArH), 8.05 (s, 4H, ArH), 9.18 (s, 2H, ArOH) (Water signal was not removed even after heating the product under vacuum at 100 °C). ^{13}C-NMR (75 MHz, $CDCl_3$) δ ppm 31.3 (4 × $ArCH_2Ar$),

Stellenbosch University https://scholar.sun.ac.za

76.5 (2 × OCH_2-C), 118.5 (2 × CH_2=C), 124.5 (4 × $C_{Ar}H$), 126.0 (2 × $C_{Ar}H$), 128.2 (4 × $C_{Ar}C$), 129.6 (4 × $C_{Ar}H$), 131.8 (2 × C=CH-C), 132.0 (4 × $C_{Ar}C$), 139.8 (2 × $C_{Ar}N$), 151.4 (2 × $C_{Ar}OC$), 159.4 (2 × $C_{Ar}O$).

FT-IR (ATR) cm^{-1}: 3083 (s, Aromatic C-H stretch), 2928 (m, Aliphatic C-H stretch), 1506 (s, Asymmetric N-O stretch), 1441 (m, C=C stretch), 1331 (s, Symmetric N-O stretch), 1275 (m, C-O stretch), 977 (s, C–H oop bend), 938 (m, C–H oop bend).

HRMS-TOF MS ESI^+: *m/z* $[M+NH_4]^+$ calculated for $C_{34}H_{34}N_3O_8$ 612.2346 Da; found: 612.2336 Da.

11,23-Diallyl-25,26,27,28-tetrahydroxy-5,17-dinitrocalix[4]arene – 25

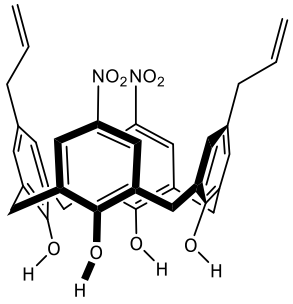

25,27-diallyloxy-26,28-dihydroxy-5,17-dinitrocalix[4]arene **24** (610 mg, 1.00 mmol) was heated at 150 °C under argon in diphenyl ether (10 mL) for 4 hours. Thereafter the reaction was cooled down to room temperature and triturated with petroleum ether (100 mL) which resulted in the appearance of some dark violet crude. The crude then was filtered off and the remaining solid dissolved in DCM (100 mL) and dried over anhydrous $MgSO_4$. The DCM was removed under the reduced pressure and the crude left was purified via a column chromatography (75% DCM/petroleum ether) to afford a pale pink solid (440 mg, 72%). Mp 205 °C DEC; R_f=0.15 (25% EtOAc/Petroleum ether); ^{1}H-NMR (300 MHz, $CDCl_3$) δ ppm 3.24 (d, *J*=6.6 Hz, 4H, $ArCH_2$-C), 3.65 (br. s, 4H, $ArCH_2Ar$), 4.25 (br. s, 4H, $ArCH_2Ar$), 5.04-5.06 (m, 2H, CH_2=C), 5.08-5.11 (m, 2H, CH_2=C), 5.79-5.93 (m, 2H, C=CH-C), 6.98 (s, 4H, ArH), 8.0 (s, 4H, ArH), 10.13 (br. s, 4H, ArOH) (Water and *n*-hexane signals were not removed even after heating the product under vacuum at 100 °C). ^{13}C-NMR (75 MHz, $CDCl_3$) δ ppm 31.7 (4 × $ArCH_2Ar$), 39.3 (2 × $ArCH_2$-C), 116.5 (2 × CH_2=C), 125.0 (4 × $C_{Ar}H$), 126.9 (4 × $C_{Ar}C$), 129.1 (4 × $C_{Ar}C$), 129.9 (4 × $C_{Ar}H$), 135.2 (2 × $C_{Ar}C$), 136.9 (2 × C=CH-C), 142.2 (2 × $C_{Ar}N$), 146.5 (2 × $C_{Ar}O$), 155.0 (2 × $C_{Ar}O$).

FT-IR (ATR) cm^{-1}: 3228 (b, O-H stretch), 1513 (s, Asymmetric N-O stretch), 1447 (m, C=C stretch), 1332 (s, Symmetric N-O stretch), 1264 (m, C-O stretch), 912 (s, C–H oop bend), 739 (m, C–H oop bend).

HRMS-TOF MS ESI^+: *m/z* $[M+NH_4]^+$ calculated for $C_{34}H_{34}N_3O_8$ 612.2346 Da; found: 612.2338 Da.

Stellenbosch University https://scholar.sun.ac.za

11,23-Diallyl-25-mono-phthalimidebutoxy-26,27,28-trihydroxy-5,17-dinitrocalix[4]arene – 26

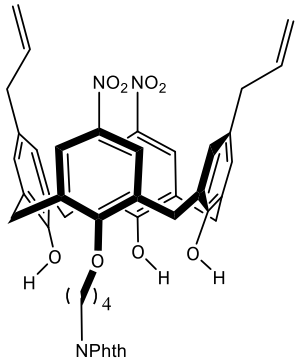

To a suspension of 11,23-diallyl-25,26,27,28-tetrahydroxy-5,17-dinitrocalix[4]arene **25** (290 mg, 0.480 mmol) and NaI (70.0 mg, 0.480 mmol) and anhydrous K_2CO_3 (270 mg, 1.92 mmol) in acetonitrile (6 mL), was added *N*-(4-bromobutyl)phthalimide **4b** (160 mg, 0.580 mmol) and the mixture was heated under reflux for 15 hours under argon. Then the reaction was cooled down and the solvent was removed under the reduced pressure. The remaining solid material was transferred into a separation funnel and washed with 1 M HCl (50 mL) and then re-extracted by DCM (5×50 mL). The resulting crude was purified via flushing with DCM in a short column chromatography to afford a pale pink solid (270 mg, 71%). Mp 181 °C DEC; R_f=0.69 (25% EtOAc/Petroleum ether); ^{1}H-NMR (300 MHz, $CDCl_3$) δ ppm 2.17-2.25 (m, 4H, C-CH_2-C), 3.23 (d, *J*=6.6 Hz, 4H, ArCH_2-C), 3.51 (d, *J*=4.4 Hz, 2H, ArCH_2Ar), 3.55 (d, *J*=4.4 Hz, 2H, ArCH_2Ar), 3.93 (t, *J*=6.3 Hz, 2H, C-CH_2N), 4.19-4.37 (m, 6H, ArCH_2Ar and OCH_2-C), 5.03-5.05 (m, 2H, CH_2=C), 5.07-5.10 (m, 2H, CH_2=C), 5.80-5.93 (m, 2H, C=CH-C), 6.92 (d, *J*=2.1 Hz, 2H, ArH), 6.96 (d, *J*=2.1 Hz, 2H, ArH), 7.70-7.72 (m, 2H, phthalimide ArH), 7.85-7.88 (m, 2H, phthalimide ArH), 7.92 (s, 2H, ArH), 7.94 (s, 2H, ArH), 8.66 (s, 2H, ArOH), 10.06 (s, 1H, ArOH) (Water signal was not removed even after heating the product under vacuum at 100 °C). ^{13}C-NMR (75 MHz, $CDCl_3$) δ ppm 25.3 (CH_2-C), 27.4 (CH_2-C), 31.6 (2 × ArCH_2Ar), 32.0 (2 × ArCH_2Ar), 37.5 (2 × ArCH_2-C), 39.3 (C-CH_2N), 77.3 (OCH_2-C), 116.1 (2 × CH_2=C), 123.5 (2 × C_{Ar}H), 124.9 (C_{Ar}H), 125.0 (C_{Ar}H), 126.8 (phthalimide C_{Ar}H), 127.0 (phthalimide C_{Ar}H), 129.2 (2 × C_{Ar}C), 129.5 (4 × C_{Ar}C), 129.6 (4 × C_{Ar}H), 132.2 (2 × C_{Ar}C), 133.6 (2 × phthalimide C_{Ar}H), 134.2 (2 × phthalimide C_{Ar}H), 135.9 (2 × C_{Ar}C), 137.3 (2 × C=CH-C), 142.1 (C_{Ar}N), 145.2 (C_{Ar}N), 148.9 (C_{Ar}O), 155.3 (C_{Ar}O), 156.5 (C_{Ar}OC), 168.7 (2 × C=O).

FT-IR (ATR) cm^{-1}: 3339 (b, O-H stretch), 1708 (s, Phthalimide C=O stretch), 1521 (s, Asymmetric N-O stretch), 1341 (s, Symmetric N-O stretch).

HRMS-TOF MS ESI$^+$: *m/z* $[M+NH_4]^+$ calculated for $C_{46}H_{45}N_4O_{10}$ 813.3136 Da; found: 813.3144 Da.

Stellenbosch University https://scholar.sun.ac.za

11,23-Diallyl-25-mono-phthalimidebutoxy-26,27,28-trihydroxy-5,17-diaminocalix[4]arene – 27

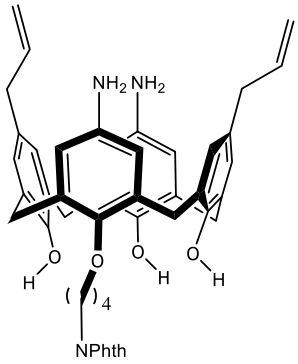

To a mixture of 11,23-diallyl-25-mono-phthalimidebutoxy-26,27,28-trihydroxy-5,17-dinitrocalix[4]arene **26** (440 mg, 0.550 mmol) and Iron powder (610 mg, 11.0 mmol) was added 1 M HCl solution in EtOH/THF (volume ratio: 1:1) (11 mL). The mixture was then heated under reflux for 15 hours under argon and cooled down to room temperature. The solvent was removed under the reduced pressure and the resulting crude was basified with a buffer solution with pH=9.6 (prepared by mixing 100 mL of the 0.05 M solution of $NaHCO_3$ and 10 mL of the 0.1 M solution of NaOH). To the basified mixture was added DCM (200 mL) and eventually everything was passed through a sintered funnel filled with Celite. The filtrate was dried over anhydrous $MgSO_4$ and the solvent was removed under the reduced pressure. The yellow-green crude was purified with a column chromatography (1% EtOH/DCM) to yield of a yellow foam-like solid (260 mg, 62%). Mp 168 °C; R_f=0.18 (1% EtOH/DCM); ^{1}H-NMR (300 MHz, $CDCl_3$) δ ppm 2.05-2.20 (m, 4H, C-CH_2-C), 3.19-3.51 (m, 8H, ArCH_2Ar and ArCH_2-C), 3.85-3.96 (m, 2H, C-CH_2N), 4.08-4.26 (m, 6H, ArCH_2Ar and OCH_2-C), 5.03-5.10 (m, 4H, CH_2=C), 5.83-5.98 (m, 2H, C=CH-C), 6.32 (s, 2H, ArH), 6.34 (s, 2H, ArH), 6.82 (s, 2H, ArH), 6.88 (s, 2H, ArH), 7.53-7.63 (m, 2H, phthalimide ArH), 7.74-7.82 (m, 2H, phthalimide ArH), 7.92 (Unknown impurity), 9.09-9.35 (sp. s,[nn] 3H, ArOH) (*n*-hexane signal was not removed even after heating the product under vacuum at 100 °C). ^{13}C-NMR (75 MHz, $CDCl_3$) δ ppm 25.2 (CH_2-C), 27.1 (CH_2-C), 31.4 (2 × ArCH_2Ar), 31.9 (2 × ArCH_2Ar), 37.5 (ArCH_2-C), 39.1 (ArCH_2-C), 39.3 (C-CH_2N), 76.2 (CH_2), 76.5 (OCH_2-C), 115.2 (2 × CH_2=C), 115.5 (C_{Ar}H), 115.6 (C_{Ar}H), 115.7 (C_{Ar}H), 115.8 (C_{Ar}H), 123.1 (2 × phthalimide C_{Ar}H), 124.5 (Ar), 126.6 (Ar), 128.0 (Ar), 128.1 (Ar), 128.3 (Ar), 128.6 (Ar), 128.7 (Ar), 128.9 (Ar), 129.3 (Ar), 129.7 (Ar), 131.5 (Ar), 131.9 (Ar), 132.5 (Ar), 133.7 (Ar), 134.4 (Ar), 137.5 (Ar), 137.9 (Ar), 140.1 (Ar), 141.6 (Ar), 143.6 (Ar), 148.7 (C_{Ar}O), 149.4 (C_{Ar}OC), 155.8 (C_{Ar}O), 168.4 (2 × C=O).

FT-IR (ATR) cm^{-1}: 3222 (b, O-H stretch), 2932 (b, Aliphatic C-H stretch), 1768 (m, Phthalimide asymmetric C=O stretch), 1704 (s, Phthalimide symmetric C=O stretch), 1603 (m, N-H bend), 1212 (m, C-O stretch), 909 (s, C–H oop bend), 852 (m, C–H oop bend).

[nn] It is a split singlet.

Stellenbosch University https://scholar.sun.ac.za

HRMS-TOF MS ESI$^+$: *m/z* $[M+H]^+$ calculated for $C_{46}H_{46}N_3O_6$ 736.3387 Da; found: 736.3392 Da. Also: 368.6735 Da (double-charged ion).

11,23-Diallyl-25-mono-phthalimidebutoxy-26,27,28-triacetoxy-5,17-dinitrocalix[4]arene – 30

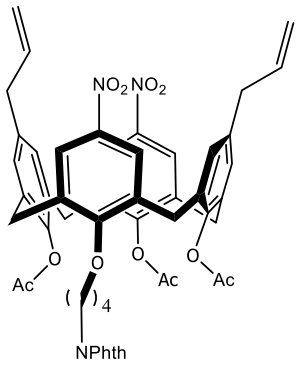

Acetic anhydride (0.580 mL, 6.12 mmol) was added gently to a solution of 11,23-diallyl-25-mono-phthalimidebutoxy-26,27,28-trihydroxy-5,17-dinitrocalix[4]arene **26** (270 mg, 0.340 mmol) and triethylamine (0.850 mL, 6.12 mmol) and DMAP (5 mol%) in dry DCM (4.5 mL) at 0 °C. The reaction was then warmed up to the ambient temperature and left for stirring for 15 hours. Afterward the reaction was transferred into a separation funnel and first washed with 50 mL of $NaHCO_3$ (saturated solution), extracted with DCM (5×50 mL) and ultimately washed with 1 M HCl (50 mL). The organic layer was dried over anhydrous $MgSO_4$ and the solvent was removed under the reduced pressure. The crude was purified with a column chromatography (25% EtOAc/ petroleum ether) yielded a white-yellow foam-like solid (200 mg, 68%). Mp 136 °C; R_f=0.61 (25% EtOAc/Petroleum ether); ^{1}H-NMR (300 MHz, $CDCl_3$) δ ppm 1.42 (s, 3H, $COOCH_3$), 1.57 (s, 6H, $COOCH_3$), 1.61-1.69 (m, 4H, C-CH_2-C), 3.20 (d, *J*=6.6 Hz, 4H, $ArCH_2$-C), 3.64-3.91 (m, 12H, $ArCH_2Ar$, C-CH_2N, and OCH_2-C), 4.99-5.07 (m, 4H, CH_2=C), 5.76-5.89 (m, 2H, C=CH-C), 6.83 (s, 2H, ArH), 6.99 (s, 2H, ArH), 7.74-7.77 (m, 2H, phthalimide ArH), 7.86-7.89 (m, 2H, phthalimide ArH), 7.90 (s, 2H, ArH), 7.91 (s, 2H, ArH) (*n*-hexane and glacial acetic acid signals were not removed even after heating the product under vacuum at 100 °C). ^{13}C-NMR (75 MHz, $CDCl_3$) δ ppm 20.1 (3 × CH_3-C), 25.2 (CH_2-C), 27.2 (CH_2-C), 37.4 ($ArCH_2$-C), 37.5 ($ArCH_2$-C), 37.6 (C-CH_2N), 39.3 (4 × $ArCH_2Ar$), 71.1 (OCH_2-C), 116.8 (2 × CH_2=C), 123.6 (2 × C_{Ar}H), 124.0 (2 × C_{Ar}H), 125.4 (2 × phthalimide C_{Ar}H), 129.4 (4 × C_{Ar}H), 130.3 (2 × phthalimide C_{Ar}=C_{Ar}), 131.4 (4 × C_{Ar}C), 132.0 (2 × C_{Ar}C), 132.3 (2 × phthalimide C_{Ar}H), 134.4 (2 × C_{Ar}C), 135.1 (C=CH-C), 135.5 (C=CH-C), 136.5 (C_{Ar}C), 137.2 (C_{Ar}C), 142.7 (C_{Ar}OC=O), 144.7 (C_{Ar}N), 146.3 (C_{Ar}N), 153.0 (C_{Ar}OC=O), 162.2 (C_{Ar}OC=O), 167.1 (C_{Ar}OC), 167.6 (2 × C=O), 168.4 (3 × C-COO).

FT-IR (ATR) cm^{-1}: 2915 (m, Aliphatic C-H stretch), 1752 (m, Ester and phthalimide asymmetric C=O stretch), 1702 (m, Phthalimide symmetric C=O stretch), 1525 (s, Asymmetric N-O stretch), 1461 (m, C=C stretch), 1341 (s, Symmetric N-O stretch), 1187.67 (m, C-O stretch), 909 (C–H oop bend), 721 (C–H oop bend).

Stellenbosch University https://scholar.sun.ac.za

HRMS-TOF MS ESI$^+$: *m/z* $[M+NH_4]^+$ calculated for $C_{52}H_{51}N_4O_{13}$ 939.3453 Da; found: 939.3435 Da.

11,23-Diallyl-25-mono-phthalimidebutoxy-26,27,28-triacetoxy-5,17-diaminocalix[4]arene – 31

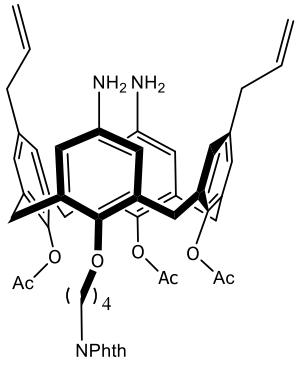

To a mixture of 11,23-diallyl-25-mono-phthalimidebutoxy-26,27,28-triacetoxy-5,17-dinitrocalix[4]arene **30** (290 mg, 0.310 mmol) and Iron powder (610 mg, 11.0 mmol) was added 1 M HCl solution in EtOH/THF (volume ratio: 1:1) (12 mL). The mixture was then heated under reflux for 15 hours under argon and cooled down to room temperature. The solvent was removed under the reduced pressure and the resulting crude was basified with a buffer solution with pH=9.6 (prepared by mixing 100 mL of the 0.05 M solution of $NaHCO_3$ and 10 mL of the 0.1 M solution of NaOH). To the basified mixture was added DCM (200 mL) and eventually everything was passed through a sintered funnel filled with Celite. The filtrate was dried over anhydrous $MgSO_4$ and the solvent was removed under the reduced pressure. The yellow-green crude was purified with a column chromatography (2% EtOH/DCM) to yield a yellow foam-like solid (240 mg, 90 %). Mp 147 °C; R_f=0.46 (5% EtOH/DCM); ^{1}H-NMR (300 MHz, $CDCl_3$) δ ppm 1.26 (s, 3H, $COOCH_3$), 1.52-1.64 (m, 4H, C-CH_2-C), 1.69 (s, 6H, $COOCH_3$), 3.17 (d, *J*=6.9 Hz, 4H, $ArCH_2$-C), 3.50-3.82 (m, 12H, $ArCH_2Ar$, C-CH_2N, and OCH_2-C), 5.01-5.07 (m, 4H, CH_2=C), 5.77-5.91 (m, 2H, C=CH-C), 6.31 (d, *J*=1.9 Hz, 4H, ArH), 6.75 (s, 2H, ArH), 6.91 (s, 2H, ArH), 7.72-7.74 (m, 2H, phthalimide ArH), 7.84-7.87 (m, 2H, phthalimide ArH). ^{13}C-NMR (75 MHz, $CDCl_3$) δ ppm 19.9 (3 × CH_3-C), 20.4 (CH_2-C), 25.4 (CH_2-C), 27.0 (4 × $ArCH_2Ar$), 37.6 ($ArCH_2$-C), 37.8 ($ArCH_2$-C), 39.4 (C-CH_2N), 70.2 (OCH_2-C), 76.6 (CH_2), 114.9 (2 × CH_2=C), 116.2 (2 × $C_{Ar}H$), 123.3 (2 × $C_{Ar}H$), 128.3 (2 × phthalimide $C_{Ar}H$), 129.3 (4 × $C_{Ar}H$), 132.0 (2 × phthalimide C_{Ar}=C_{Ar}), 132.2 (4 × $C_{Ar}C$), 133.3 (2 × phthalimide $C_{Ar}H$), 134.1 ($C_{Ar}C$), 134.4 ($C_{Ar}C$), 136.4 ($C_{Ar}C$), 136.9 ($C_{Ar}C$), 140.3 (2 × C=CH-C), 141.4 (2 × $C_{Ar}C$ and $C_{Ar}OC$=O), 143.6 ($C_{Ar}N$ and 2 × $C_{Ar}OC$=O), 146.4 ($C_{Ar}N$), 149.2 ($C_{Ar}OC$), 168.3 (2 × C=O), 168.8 (2 × $COOC_{Ar}$), 169.2 ($COOC_{Ar}$).

FT-IR (ATR) cm^{-1}: 3360 (b, O-H stretch), 2905 (b, Aliphatic C-H stretch), 1743 (m, Ester and phthalimide asymmetric C=O stretch), 1706 (s, Phthalimide symmetric C=O stretch), 1600 (m, N-H bend), 1222 (m, C-O stretch), 907 (s, C–H oop bend), 719 (m, C–H oop bend).

Stellenbosch University https://scholar.sun.ac.za

HRMS-TOF MS ESI$^+$: *m/z* $[M+H]^+$ calculated for $C_{52}H_{52}N_3O_9$ 862.3704 Da; found: 862.3705 Da.

Also: 661.2916 Da (minus butylphthalimide and acyl groups), 431.6887 Da (double-charged ion).

4.8 References

(1) Järup, L. *Br. Med. Bull.* **2003**, *68*, 167–182.

(2) Gustin, M. S.; Taylor, G. E.; Leonard, T. L. *Environ. Health Perspect.* **1994**, *102*, 772–778.

(3) David, R. L. *CRC Handbook of Chemistry and Physics*, Taylor & Francis, Abingdon, United Kingdom, **2005**, 86th ed.

(4) Greenwood, N. N.; Earnshaw, A. *Chemistry of the Elements*, Elsevier, Amsterdam, Netherlands, **2012**, 2nd ed.

(5) McAuliffe, C. A. *The Chemistry of Mercury*, Springer, Berlin, Germany, **2016**.

(6) Housecroft, C. E.; Sharpe, A. G. *Inorganic Chemistry*, Prentice Hall, Upper Saddle River, New Jersey, United States, **2004**, 2nd ed.

(7) Skoog, D. A.; Holler, F. J.; Nieman, T. A. *Principles of Instrumental Analysis*, Saunders College Pub. (Elsevier), Philadelphia, Pennsylvania, United States, **1998**, 5th ed.

(8) Klein, C.; Hurlbut, Cornelius S. J. *Manual of Mineralogy*, Wiley, Hoboken, New Jersey, United States, **1985**, 20th ed.

(9) King, R. J. *Geol. Today* **2002**, *18*, 195–199.

(10) Board on Environmental Studies and Toxicology, National Research Council (U.S.), *Toxicological Effects of Methylmercury*, National Academies Press, Washington, D.C., United States, **2000**.

(11) *Quantitative and Qualitative Analysis of Mercury Compounds in the List*, Food and Drug Administration (FDA), United States Department of Health and Human Services (HHS), **2009**.

(12) Suneja, T.; Belsito, D. V. *J. Am. Acad. Dermatol.* **2001**, *45*, 23–27.

(13) Pacyna, E. G.; Pacyna, J. M.; Steenhuisen, F.; Wilson, S. *Atmos. Environ.* **2006**, *40*,

Stellenbosch University https://scholar.sun.ac.za

4048–4063.

(14) *''What is EPA doing about mercury air emissions?'',* United States Environmental Protection Agency (EPA), **2007**.

(15) Maprani, A. C.; Al, T. A.; MacQuarrie, K. T.; Dalziel, J. A.; Shaw, S. A.; Yeats, P. A. *Environ. Sci. Technol.* **2005**, *39*, 1679–1687.

(16) Bernhoft, R. A. *J. Environ. Public Health* **2012**, *2012*, 1–10.

(17) Nabi, S. *Toxic Effects of Mercury,* Springer, New Delhi, India, **2014**.

(18) Grandjean, P.; Satoh, H.; Murata, K.; Eto, K. *Environ. Health Perspect.* **2010**, *118*, 1137–1145.

(19) Horowitz, Y.; Greenberg, D.; Ling, G.; Lifshitz, M. *Arch. Dis. Child.* **2002**, *86*, 453–455.

(20) Carvalho, C. M. L.; Chew, E-H.; Hashemy, S. I.; Lu, J.; Holmgren, A. *J. Biol. Chem.* **2008**, *283*, 11913–11923.

(21) Ou, Y.; Bloom, M. S.; Nie, Z.; Han, F.; Mai, J.; Chen, J.; Lin, S.; Liu, X.; Zhuang, J. *Environ Int.* **2017**, *106*, 127–134.

(22) el-Fawal, H. A.; Gong, Z.; Little, A. R.; Evans, H. L. *NeuroToxicology* **1996**, *17*, 267–276.

(23) Clarkson, T. W.; Magos, L. *Crit. Rev. Toxicol.* **2006**, *36*, 609–662.

(24) *Mercury Study Report to Congress*, United States Environmental Protection Agency (EPA), **1997**.

(25) Morell, P. *Myelin*, Springer Science & Business Media, Berlin, Germany, **2013**.

(26) *Toxicological Profile for Mercury,* Agency for Toxic Substances and Disease Registry (ATSDR), United States Department of Health and Human Services (HHS), **2011**.

(27) Langford, N. J.; Ferner, R. E. *J. Hum. Hypertens.* **1999**, *13*, 651–656.

(28) Emsley, J. *The Elements of Murder: A History of Poison*, Oxford University Press, Oxford, United Kingdom, **2005**.

(29) *Mercury Levels in Commercial Fish and Shellfish (1990-2012)*, Food and Drug

Stellenbosch University https://scholar.sun.ac.za

Administration (FDA), United States Department of Health and Human Services (HHS), **2012**.

(30) Newland, M. C.; Reed, M. N.; Rasmussen, E. *Behav. Processes* **2015**, *114*, 41–51.

(31) Djedjibegovic, J.; Larssen, T.; Skrbo, A.; Marjanovic, A.; Sober, M. *Food Chem.* **2012**, *131*, 469–476.

(32) Kenduzler, E.; Ates, M.; Arslan, Z.; McHenry, M.; Tchounwou, P. B. *Talanta* **2012**, *93*, 404–410.

(33) Jia, X.; Han, Y.; Liu, X.; T. Duan, T.; Chen, H. *Sens. Actuators, B* **2011**, *66*, 88–92.

(34) Rodrigues, J. L.; de Souza, S. S.; de Oliveira Souza, V. C.; Barbosa Jr, F. *Talanta* **2010**, *80*, 1158–1163.

(35) Zhao, Y.; Zheng, J.; Fang, L.; Lin, Q.; Wu, Y.; Xue, Z.; Fu, F. *Talanta* **2012**, *89*, 280–285.

(36) Gao, Y.; Shi, Z.; Long, Z.; Wu, P.; Zheng, C.; Hou, X. *Microchem. J.* **2012**, *103*, 1–14.

(37) Shah, A. Q.; Kazi, T. G.; Baig, J. A.; Afridi, H. I.; Arain, M. B. *Food Chem.* **2012**, *134*, 2345–2349.

(38) Coronado, E.; Galán-Mascarós, J. R.; Martí-Gastaldo, C.; Palomares, E.; Durrant, J. R.; Vilar, R.; Gratzel, M.; Nazeeruddin, M. K. *J. Am. Chem. Soc.* **2005**, *127*, 12351–12356.

(39) Singh, G.; Raj, P.; Singh, H.; Singh, N. *J. Mater. Chem. C* **2018**, *6*, 12728–12738.

(40) Hu, J.; Wu, T.; Zhang, G.; Liu, S. *Macromolecules* **2012**, *45*, 3939–3947.

(41) Li, Y.; Huang, H.; Li, Y.; Sua, X. *Sens. Actuators, B* **2013**, *188*, 772–777.

(42) Gupta, S.; Singh, R.; Anoop, M. D.; Kulshrestha, V.; Srivastava, D. N.; Ray, K.; Kothari, S. L.; Awasthi, K.; Kumar, M. *Appl. Phys. A: Mater. Sci. Process.* **2018**, *124*, 737, 1–6.

(43) Aswathia, R.; Sandhya, K. Y. *J. Mater. Chem. A* **2018**, *6*, 14602–14613.

(44) Dong, Z-M.; Zhao, G-C. *J. Sensors* **2002**, *12*, 7080–7094.

(45) Sabri, Y. M.; Ippolito, S. J.; O'Mullane, A. P.; Tardio, J.; Bansal, V.; Bhargava, S. K. *Nanotechnology* **2011**, *22*, 1–9.

(46) Shimizu, H.; Iwamoto, K.; Fujimoto, K.; Shinkai, S. *Chem. Lett.* **1991**, *20*, 2147–2150.

Stellenbosch University https://scholar.sun.ac.za

(47) McCarrick, M.; Harris, S. J.; Diamond, D. *J. Mater. Chem.* **1994**, *4*, 217–221.

(48) Gordon, J. L. M.; Bo¨hmer, V.; Vogt, W. *Tetrahedron Lett.* **1995**, *36*, 2445–2448.

(49) Yamamoto, H.; Ueda, K.; Sandanayake, K. R. A. S.; Shinkai, S. *Chem. Lett.* **1995**, *24*, 497–498.

(50) Kao, T-L.; Wang, C-C.; Pan, Y-T.; Shiao, Y-J.; Yen, J-Y.; Shu, C-M.; Lee, G-H.; Peng, S- M.; Chung, W-S. *J. Org. Chem.* **2005**, *70*, 2912–2920.

(51) Ho, I-T.; Lee, G-H.; Chung, W-S. *J. Org. Chem.*, **2007**, *72*, 2434–2442.

(52) Shu, C.; Yuan, T.; Ku, M.; Ho, Z.; Liu, W.; Tang, F.; Lin, L. *Tetrahedron* **1996**, *52*, 9805– 9818.

(53) Lin, Y. L.; Yu, T. S.; Wang, W. Y.; Lin, L. G. *Tetrahedron* **2006**, *62*, 6082–6089.

(54) Reddy, P. A.; Kashyap, R. P.; Watson, W. H.; Gutsche, C. D. *Isr. J. Chem.* **1992**, *32*, 89–96.

(55) Reddy, P. A.; Gutsche, C. D. *J. Am. Chem. Soc.* **1993**, *58*, 3245–3251.

(56) Chawla, H. M.; Singh, S. P.; Sahu, S. N.; Upreti, S. *Tetrahedron* **2006**, *62*, 7854–7865.

(57) Shinkai, S.; Araki, K.; Iwamoto, K. *J. Org. Chem.* **1991**, *56*, 4955–4962.

(58) Arena, G.; Casnati, A.; Contino, A.; Lombardo, G. G.; Sciotto, D.; Ungaro, R. *Chem. Eur. J.* **1999**, *5*, 738–744.

(59) Sharma, K.; Gutsche, C. D. *J. Org. Chem.* **1996**, *61*, 2564–2568.

(60) Galán, H.; Hennrich, G.; de Mendoza, J.; Prados, P. *Eur. J. Org. Chem.* **2010**, 1249–1257.

(61) Ali, Y.; Bunnori, N, M.; Susanti, D.; Alhassan, A. M.; Abd Hamid, S. *Front. Chem. (Lausanne, Switz.)* **2018**, *6*.

(62) Ryu, E.; Zhao, Y. *J. Org. Chem.* **2006**, *71*, 9491–9494.

(63) Wu, F. Y.; Chang, K. F.; Kuo, C. H.; Chen, K. C.; Lee, K. C.; Huang, C. S.; Chiang, Y. S.; Lin, L. G. *Tetrahedron* **2011**, *67*, 3238–3247.

Stellenbosch University https://scholar.sun.ac.za

Chapter 5. Synthesis of a PSMA polymer containing a sulfonated calix[4]arene for hydrogel formation studies

5.1 Chapter overview

In this chapter, the rationale for selecting *p*-sulfonated calix[4]arenes as our compound of interest, and a brief review on its synthesis and its reported applications, will be presented. Then, a short section focusing on the concept of hydrogel and the requirements for its formation will be presented. After that, following the lessons learned from chapter 3 regarding different ways of modifying PSMA with functionalized calix[4]arene, a series of water-soluble calix[4]arene-grafted PSMAs will be synthesized. These PSMA-modified grafts will be investigated in terms of their ability to form a hydrogel in the presence of bis-quaternary amines, which are known to bind to *p*-sulfonated calix[4]arenes. These crosslinkers will be synthesized in accordance with the literature methods. Various parameters in order to facilitate hydrogel formation will be assessed (i.e. temperature, concentration, etc.). In the case of the PSMA-made grafts, failure to produce a crosslinked network resulted in several alternative compounds to be considered and synthesized using the same calix[4]arene scaffold. Having tried all these approaches for hydrogel formation, the possible reasons for the failure of these attempts will be thoroughly discussed.

5.2 Study rationale

Due to the failure of the plan to synthesize a highly functionalized mercury sensor in the previous chapter, it was decided to choose a simpler calix[4]arene target with an interesting potential application. After careful considerations, *p*-sulfonated calix[4]arenes were found to exhibit these desired features and were reportedly easy to synthesize. The following short review explains the synthetic methods and the common applications of this set of compounds through literature.

5.3 A short review on the synthesis and applications of *p*-sulfonated calixarenes

In 1984, Shinkai *et al*. were the first to report the successful synthesis of the sodium salt of a *p*-sulfonated calix[6]arene using concentrated sulfuric acid on calix[6]arene (**Scheme 5.1**). According to their spectral data, this compound was capable of encapsulating a naphthalene molecule proving its role as the first reported calix[6]arene water-soluble host.[1]

Stellenbosch University https://scholar.sun.ac.za

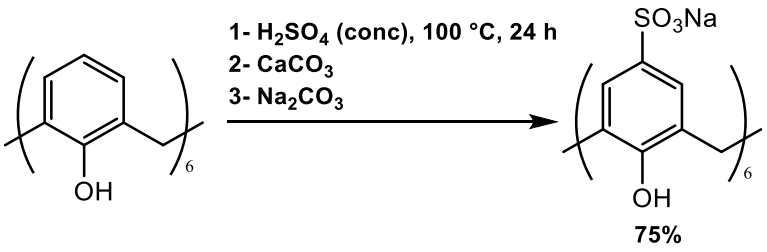

Scheme 5.1 First report on the synthesis of a p-sulfonated calixarene based on the work of Shinkai et al.[1]

Two years later Shinkai *et al*. implemented a comprehensive study on a series of substituted sulfonated calix[6]arenes. The conformational status of these compounds and their aggregation behavior were evaluated with various analytical methods. In addition, their kinetic study suggested some potential for a catalysis effect of water-soluble calix[6]arenes (**Figure 5.1**).[2]

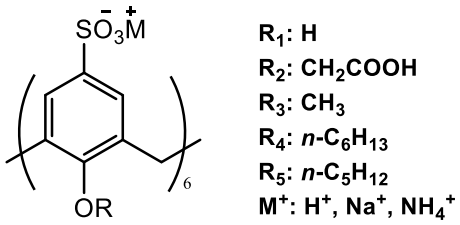

Figure 5.1 p-sulfonated calix[6]arene library used for catalysis study based on the work of Shinkai et al.[2]

In 1987, the same group published a paper on the sulfonation of plain calixarenes for calix[4]arene, calix[6]arene and even calix[8]arene. (**Scheme 5.2**).[3]

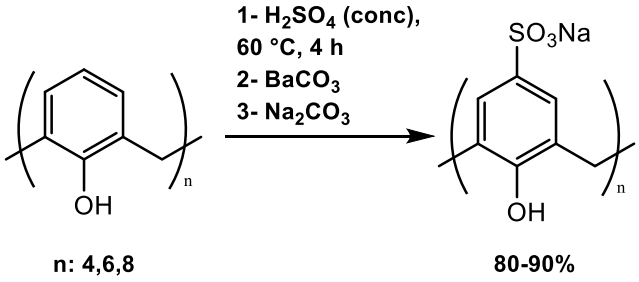

Scheme 5.2 Synthesis of a series of the p-sulfonated calixarene based on the work of Shinkai et al.[3]

More interestingly, in 2003 Kumar *et al*. suggested a Shinkai-like approach for *ipso*-sulfonation of tertiary butylated calixarenes. This approach made the one-pot synthesis of these compounds possible with no need for a pre-de-butylation (**Scheme 5.3**).[4]

Stellenbosch University https://scholar.sun.ac.za

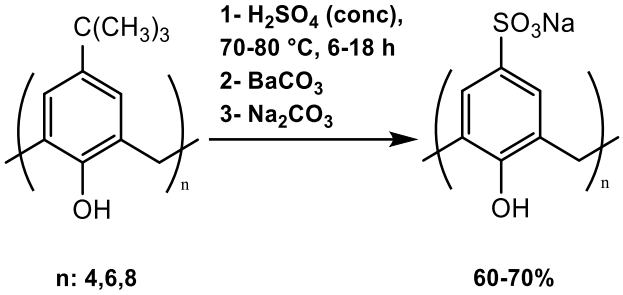

Scheme 5.3 The approach to synthesize p-sulfonated calixarene via ipso-sulfonation based on the work of Kumar et al.[4]

In this later approach, apart from employing different types of calixarenes (*para* butylated or plain) and the cavity size (n=4, 6 or 8), overall the calixarene should be heated at 70-80 °C in concentrated sulfuric acid, until there is no water-insoluble material left. Then the acidic crude should be neutralized with a Ba^{2+} source to precipitate $BaSO_4$, and the filtrate basified with a Na^+ source, triturated with ethanol to afford the desired sodium salt of *p*-sulfonated calixarene in an appropriate yield.

There have been many applications of *p*-sulfonated calixarenes and their derivatives. *p*-Sulfonated calixarenes have been used as biological catalysts,[5] doping agents for polymerizations,[6] for preparation of potentiometric sensors[7] and even for autopolymerization of pyrrole.[8] Regardless of these applications, *p*-sulfonated calixarenes are renowned for their notable ability for forming inclusion complexes with cations and even neutral molecules. This feature, in conjunction with their water-solubility, has made them one of the more important receptors in supramolecular science.[9] An early example of this kind of complexation was a report by Shinkai *et al*. investigating the interaction of Ce^{3+} and *p*-sulfonated calix[4]arene in an alkaline environment (color change from colorless to red-brown), and the calculation of its stability constants using UV-Vis experiments.[10]

Later Dalgarno and Raston used the same sulfonated calix[4]arene, not only with Ce^{3+}, but also with other lanthanides (Nd^{3+}, Sm^{3+}, and Eu^{3+}) for capturing a [2.2.2]-cryptand at an acidic pH. It was the first time that a [2.2.2]-cryptand was encapsulated by calixarenes in the solid state and it was found to form a two dimensional bi-layer coordination polymer (**Scheme 5.4**).[11]

Stellenbosch University https://scholar.sun.ac.za

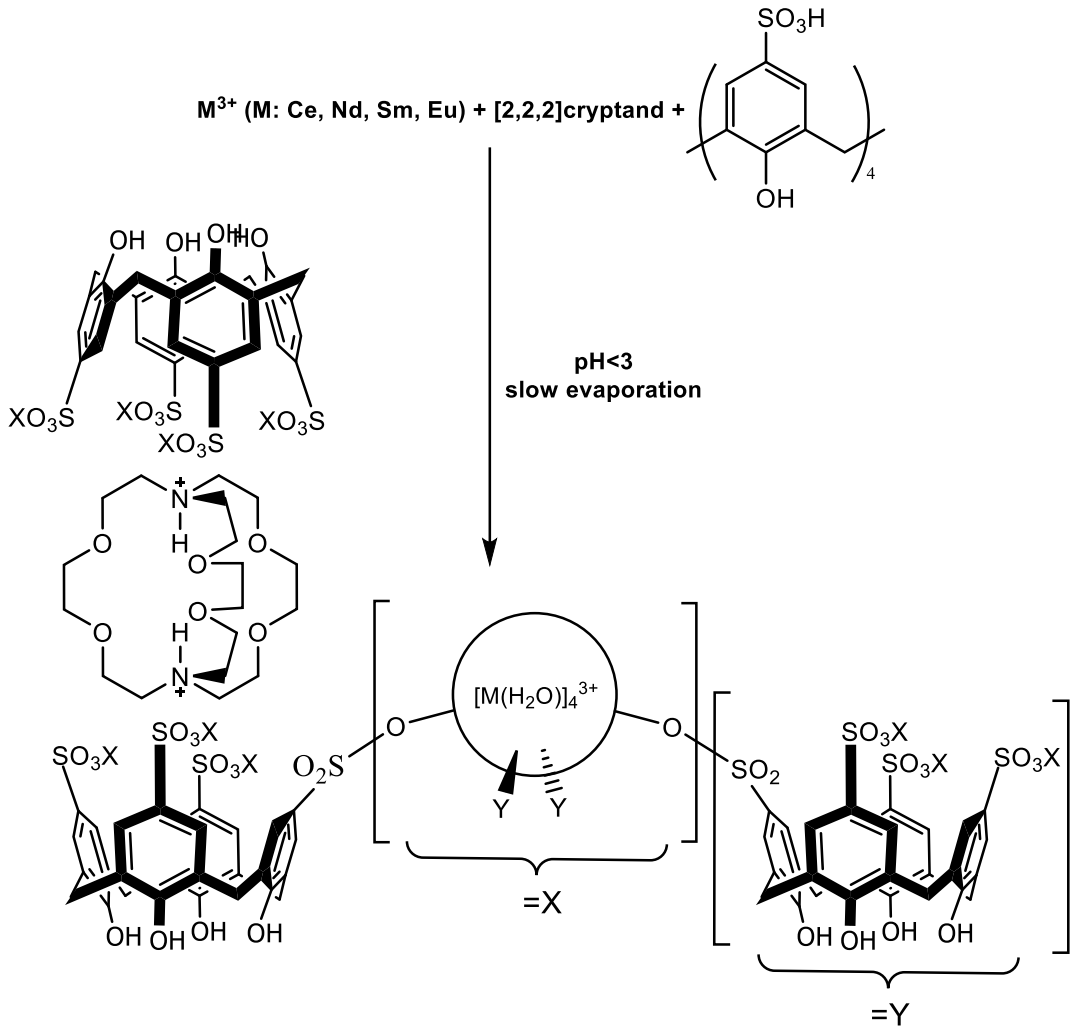

Scheme 5.4 [2.2.2]-cryptand solid state encapsulation by p-sulfonated calix[4]arene in the presence of lanthanides, based on the work of Dalgarno and Raston[11]

Other coordination polymers were also synthesized in a similar manner, for example, Ma and Yang reported a couple of coordination polymers made up of sulfonated calix[4]arene and bis(triazolyl) ligands with Cu(II).[12]

In the same respect, Thuery's work on complexation of uranyl and other lanthanides cations with the same calix[4]arene is also worth mentioning. As a continuation of Shinkai's work on producing uranophilic calixarenes,[13] these were the first examples of the *p*-sulfonated calixarene uranyl complexes.[14]

The complexation of L-α-aminoacids with water-soluble calix[4]arenes (including SO_3H, COOH functionalities) has also been investigated. For example, a comprehensive study was published by Sciotto and co-workers, using ^{1}H-NMR spectroscopic titrations in D_2O at pD=7.3 (phosphate buffer) to determine the binding constants. Plotting the chemical shift change versus

Stellenbosch University https://scholar.sun.ac.za

concentration enabled them to obtain the binding constants values. For the most part, obtaining relatively large values for these constants proved the strong interaction between the calix[4]arene hosts and their L-α-aminoacids guests [oo] (**Figure 5.2**).[15]

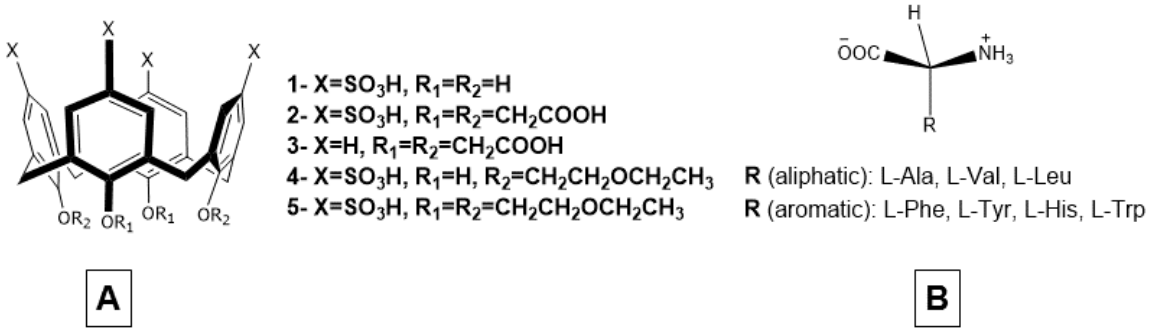

Figure 5.2 A: Water-soluble calix[4]arene library studied by [1]H-NMR spectroscopic titrations for complexation purposes; B: L-α-aminoacids for [1]H-NMR spectroscopic titrations with water-soluble calix[4]arenes based on the work of Sciotto and co-workers[15]

Later the same group published an article regarding the binding behavior of neutral molecules with the same calix[4]arenes using similar analytical methods. Like their previous paper, large-value binding constants were acquired for most calix[4]arene-neutral molecule complexes as an indication of the strong interaction between the host and the guest.[16]

Of greater interest to us though was the reported complexation of *p*-sulfonated calixarenes with quaternary ammonium groups, and their ability to form supramolecular amphiphiles. One of the first reported studies was by the Nobel prize-winning chemist, Jean-Marie Lehn, who studied the interactions of acetylcholine, choline and a series of other quaternary ammonium groups on sulfonated versions of calix[4]arene and calix[6]arene. The association constants determined for acetylcholine and choline were interestingly close to the values taken from the recognition sites in living tissues.[17] A similar approach was used by Wang and Liu in order to evaluate the molecular binding behavior of several sulfonatocalixarenes with 5,6-dihydropyrazion[1,2,3,4-lmn][1,10]phenanthroline-4,7-diium (DP^{2+}) in both liquid and solid states (**Figure 5.3A**).[18] In another report, Liu *et al*. studied the effect of viologen guests[pp] on *p*-sulfonated calix[4]arene. It was found that benzyl viologen formed a polymeric capsule with

[oo] In the [1]H-NMR spectra, the guest protons dramatically shifted upfield as a result of the strong complexation.[15]

[pp] Viologens are an important category of redox couples[19] used for many research-related purposes such as producing herbicides,[20] redox indication of biological systems,[21] zeolite study probes,[22] and several other applications.[23,24,25] Nonetheless, their toxicity limits their uses[26,27,28] and to resolve that, their inhibition through encapsulation by supramolecular hosts is pivotal.[29,30,31,32,33]

Stellenbosch University https://scholar.sun.ac.za

p-sulfonated calix[4]arene, while methyl viologen formed a 2:1 complex with its calix[4]arene host (**Figure 5.3B**).[34]

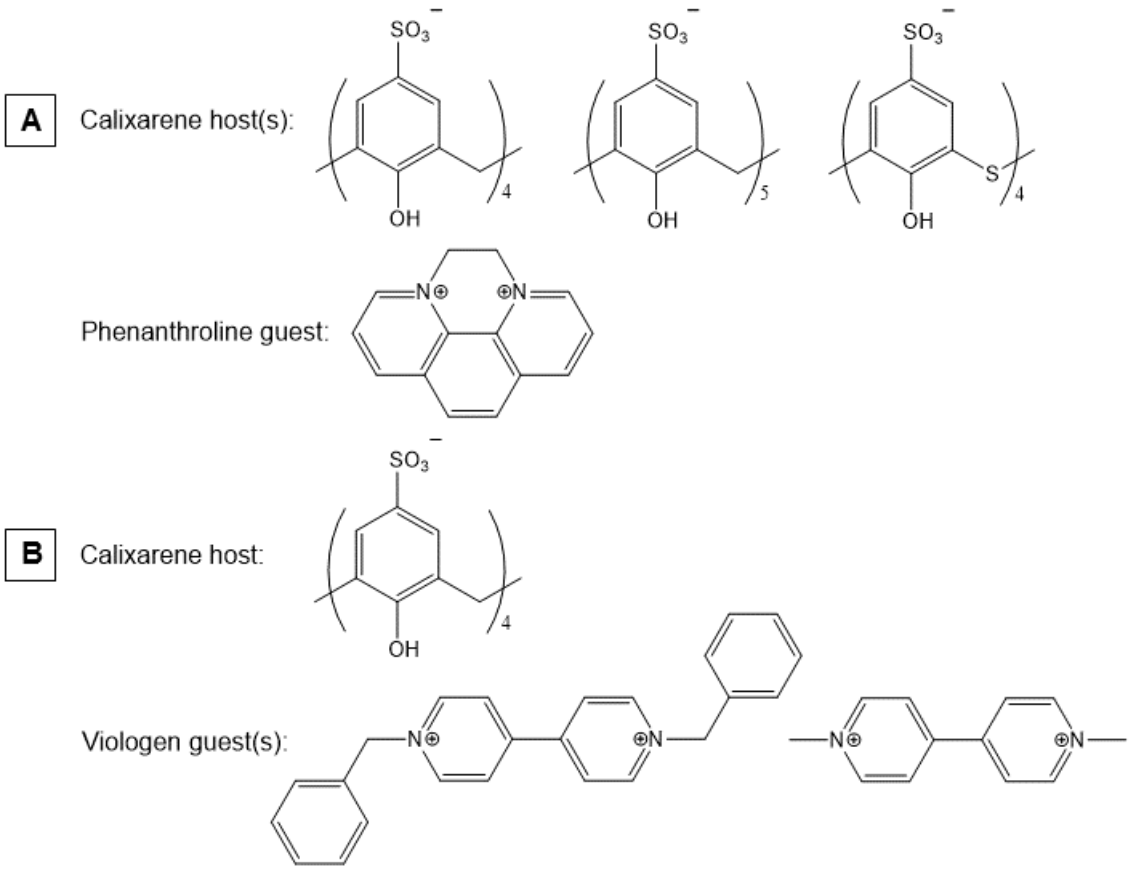

Figure 5.3 A: Phenanthroline agents solid state study with p-sulfonated calixarene based on the work of Lehn et al.;[18] B: Viologen-based calix[4]arene complexes based on the work of Wang and Liu[34]

Finally, the last noteworthy application of sulfonated calixarenes presented in this section is in the formation of hydrogels as a result of their interactions (particularly non-covalent) in solution with specific types of stimuli. For example, Liu *et al*. published a report regarding a fully lower rim-protected sulfonated calix[4]arene gelation phenomenon facilitated by a randomly modified poly(vinyl alcohol) with viologen (**Figure 5.4**). In short, initially, the amphiphilic calix[4]arene assembly turned into a spherical micelle and then the micelle transformed into a hydrogel by the addition of a cationic polymer gelating agent. The reversibility of the process was the fascinating aspect of this study. Through this research, heating to 75 °C resulted in a gel to sol transition (thermal stimulus) as well as using a sodium chloride solution (ionic strength stimulus) or adding hydrazine monohydrate (redox stimulus). Cooling to at least 25 °C resulted in the reverse transition (sol to gel). The resulting hydrogel was the first example of a hydrogel prepared involving a *p*-sulfonated calix[4]arene derivative.[35]

Stellenbosch University https://scholar.sun.ac.za

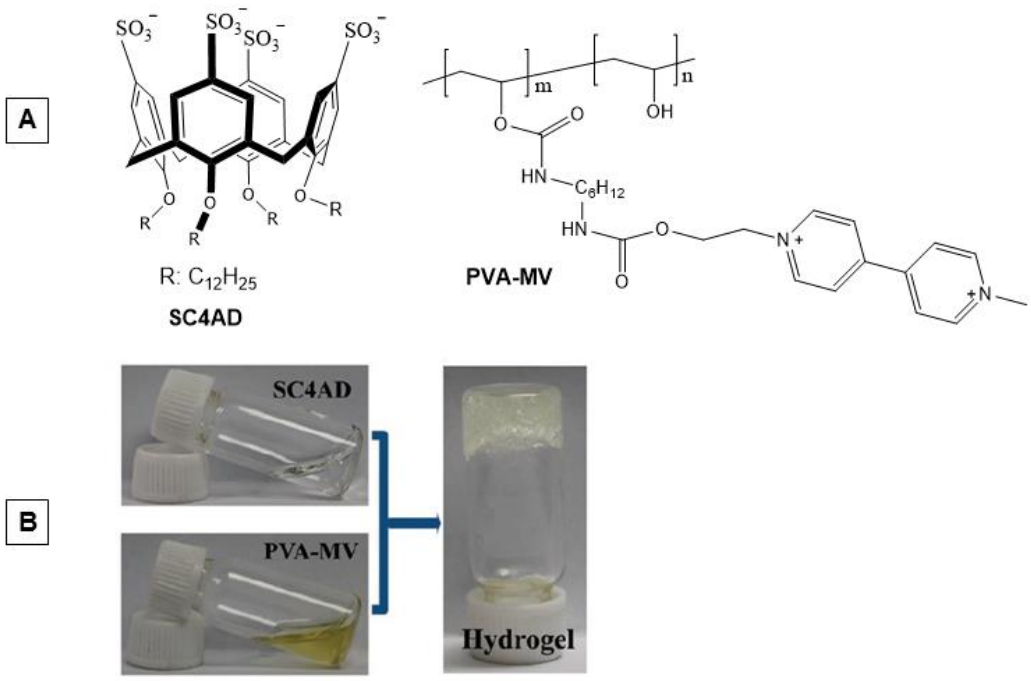

Figure 5.4 A: Water-soluble calix[4]arene host versus its viologen-modified polymeric guest; B: Formation of a hydrogel by a calix[4]arene-viologen system (this picture was taken from reference[35])

The formation of hydrogels has led to the discovery of applications in many fields, and interestingly, the development of hydrogels has not been limited to calixarene as other supramolecular systems have also been involved including cyclodextrins,[36] cucurbiturils,[37] and even crown ethers.[38] Considering this background, the idea of creating a hydrogel employing a calix[4]arene-grafted PSMA scaffold (based on the results obtained in the previous chapters) will be the center of our discussion in this chapter. Thus, for a better understanding of the hydrogel concept, the next section will provide the reader with some insights.

5.4 Hydrogel: Definition, classification, and application

In accordance with IUPAC definition, a gel is a nonfluid colloidal network or a polymer network which is expanded through its entire volume by a fluid.[39] A hydrogel (also known as a hydrophilic gel) possesses a three-dimensional crosslinked network (commonly a polymer network[qq]) capable of swelling as a result of retaining a considerable amount of water.[39] The hydrogel concept was first introduced by Wichterle and Lím in 1960.[40] Upon swelling as a result of water absorption, the hydrogel volume can massively increase. For example, wound-dressing hydrogels can achieve a 90% water content (the polymer only constitutes 10% of their volume).[41] The hydrophilicity of hydrogels is due to the existence of hydrophilic functionalities

[qq] In case of having a colloidal network, the term aquagel can be used as well.[39]

Stellenbosch University https://scholar.sun.ac.za

such as amides,[42] carboxylic acids,[43] sulfonic acids,[44] and other polar substituents[45-48] (see an example in **Scheme 5.5**).

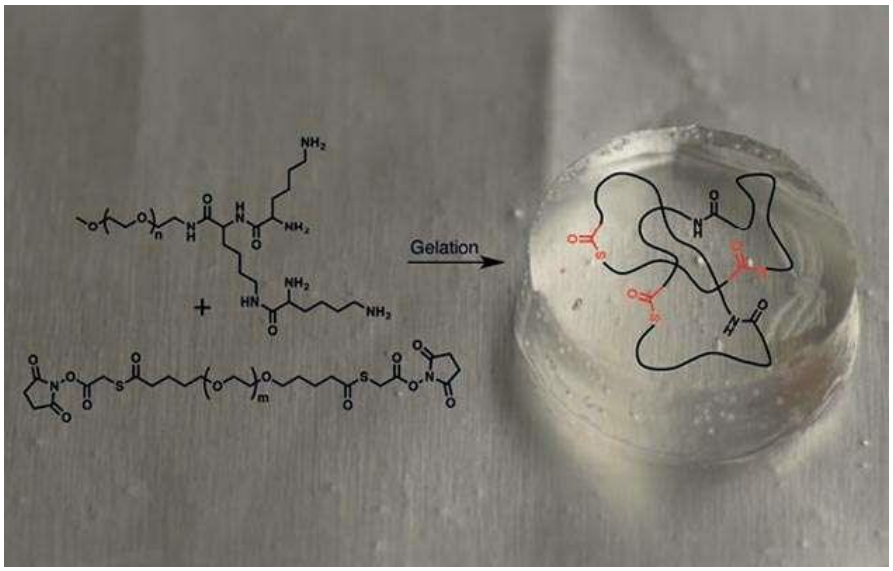

Scheme 5.5 A wound-dressing hydrogel produced through a thiol–thioester exchange reaction based on the work of Konieczynska and Villa-Camacho[49] (the picture has also been taken from reference[49])

There are numerous ways of classifying hydrogels. One of them is based on their preparation method which determines their polymeric composition. In this regard, hydrogels can be prepared as a homopolymer,[50] a copolymer[51] or even an inter-penetrating network (IPN)[rr].[52]

The second feature considered for the classification of a hydrogel is its source. The source of a polymer hydrogel can be a naturally-occurring polymer,[53] or a synthetic polymer[54] or even a hybrid system.[55]

The third parameter used for hydrogel classification is its electric charge. A hydrogel can either be neutral (non-ionic),[56] ionic (cationic[57] or anionic[58]), amphoteric electrolyte (with both acidic and basic functionalities)[59] or even zwitterionic (with both cationic and anionic functionalities in the polymer repeating unit).[60]

The fourth way of classifying a hydrogel relies on its network morphology. Taking this approach, a hydrogel can be seen non-crystalline (amorphous),[61] semi-crystalline (including both crystalline and amorphous phases)[62] or crystalline.[63]

[rr] According to IUPAC, an inter-penetrating network exists when a polymer comprises two or more interlaced networks (which are not bonded to each other covalently) and the only way to separate the networks from each other is through breaking their chemical bonds.[39]

Stellenbosch University https://scholar.sun.ac.za

The fifth factor regarding the classification of a hydrogel is its physical appearance. A hydrogel can be either observed as a macrosphere[64] or a microsphere (also known as microgel)[65] depending on its preparation technique.

The last, and in fact the most common method for the classification of hydrogels is the crosslinking approach facilitated their formation. The crosslinking can occur through a covalent or a non-covalent manner. The covalent crosslinking (also known as chemical crosslinking) is achieved via chemical reactions such as Michael addition,[66] formation of Schiff base,[67] enzyme-assisted reactions[68] and many other examples.[69-71] The hydrogelation process for the chemical hydrogel is irreversible due to the existence of permanent bonds between its polymer chains. The non-covalent crosslinking (also known as physical crosslinking) happens either as a result of the dynamic supramolecular species becoming entangled or the non-covalent interactions[ss] between supramolecular polymer chains. In such a case, the crosslink between polymer chains is transient, and consequently the process is reversible. In addition, since self-assembly of the molecules is the driving force of the hydrogel formation, sol to gel transition does not lead to a substantial volume change (see different types of crosslinking in **Scheme 5.6**).[72]

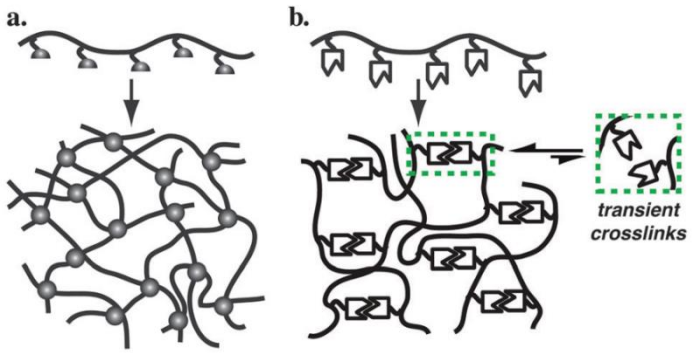

Scheme 5.6 Different crosslinking approaches for a supramolecular polymer in solution: a. covalent crosslinking for producing a chemical hydrogel. b. non-covalent crosslinking for producing a physical hydrogel (the scheme has been taken from the review published by Appel and Del Barrio).[72]

The chemical hydrogel is useful when a hydrogel with a high degree of stability and toughness is required. However, for the most part, this type of hydrogel is usually non-transparent, brittle and incapable of self-healing[tt] (when the crosslink breaks) which restricts its applications.[73] On the contrary, due to its weaker crosslinking, a physical hydrogel is not as resistant as the

[ss] These interactions include electrostatic interaction (such as hydrogen bonding and charge transfer interaction), van der Waals interaction, hydrophobic interactions, and π-stacking.[74]

[tt] Self-healing is a mechanism initiated by a material to repair its microdamage.[75]

Stellenbosch University https://scholar.sun.ac.za

chemical hydrogel to mechanical forces. Nonetheless, in this case, the reversibility of sol to gel process potentially endows the hydrogel with features like self-healing (see an example in **Figure 5.7**)[36] or responsiveness to many stimuli such as pH,[76] temperature[77] or even shear force[uu].[78] Due to their stimuli-responsive nature, physical hydrogels are sometimes called ‘‘smart hydrogels’’ or ‘‘intelligent hydrogels’’ and their modeling and synthesis has been a subject of utmost interest for researchers.[79,80] Physical hydrogels have been found useful with regards to drug delivery,[81] tissue engineering,[82] biosensing,[83] and many other applications.[84-88]

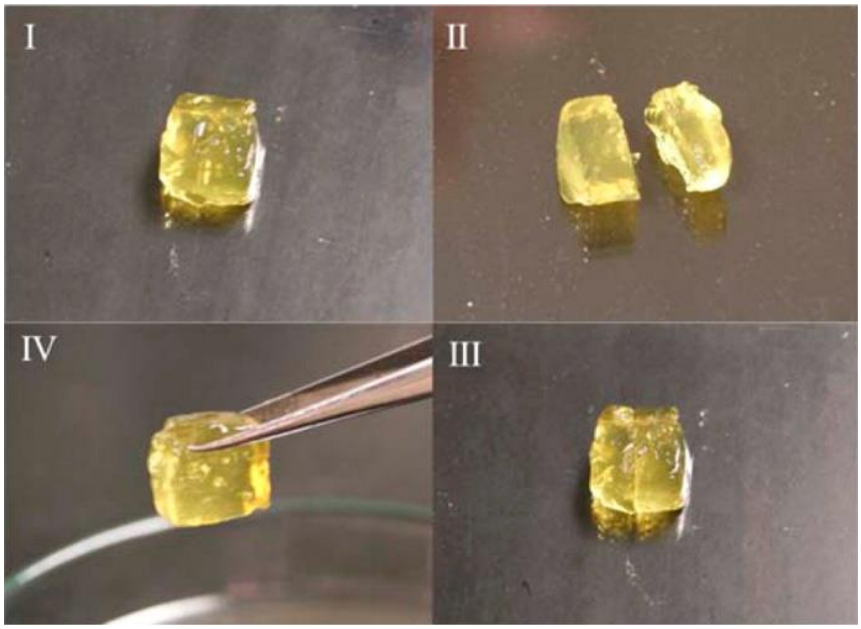

Figure 5.5 Slicing, re-joining, and finally self-healing of a β-cyclodextrin-based polymer hydrogel based on the work of Zhu et al.[36](the picture has also been taken from reference[36])

Considering the literature example from the previous section[35] and the advantages of employing a non-covalent approach (which have been argued in this section), a similar approach will be the taken in this dissertation for the production of the calix[4]arene-based hydrogel. In the next section, the plan and the requirements for achieving the desired hydrogel will be discussed.

5.5 Chapter plan including the requirements for the hydrogel formation

Drawing from the literature example related to the hydrogel formation,[35] it was decided to design an experiment with similar elements (*p*-sulfonated calix[4]arene and a viologen salt), but on a new system.

[uu] According to literature, ‘‘If a plane is passed through a body, a force acting along this plane is called a shear force or shearing force’’.[89]

Stellenbosch University https://scholar.sun.ac.za

Undoubtedly, the first requirement for the hydrogel formation is a supramolecular polymer. As discussed in section 5.3, numerous examples of strong complexation between *p*-sulfonated calix[4]arene and quaternary amines have been reported in literature, but none of these cases has ever resulted in the formation of a hydrogel.[17,18,34] Obviously, a system with a low molar mass (such as our *p*-sulfonated calix[4]arene) is simply not capable of generating a massive crosslinked network. Thus, a supramolecular polymer version of *p*-sulfonated calix[4]arene is required. Additionally, to form the above-mentioned crosslinked network through a non-covalent approach, a crosslinker is necessary to make the polymer chains link to one another through strong inter-molecular forces.[vv] In this case, with regards to Liu's paper[20] and other literature reports on strong complexation of quaternary-amines (especially the viologen derivatives) with *p*-sulfonated calix[4]arene,[17,18,34,90,91] one or a series of quaternary amines can be examined in our experiments as potential crosslinkers.[ww]

Considering all these requirements, the new system was designed which involved a PSMA-grafted version of the *p*-sulfonated calix[4]arene with a primary-amine tether (based on the model mono-substituted calix[4]arene-grafted PSMA made in chapter 3, but with sulfonate groups solubilizing it in water).[xx] Then, instead of using a water-soluble viologen-grafted polymer (the gelating agent), an aqueous solution of a viologen salt would be added to a highly-concentrated solution of the water-soluble polymeric calix[4]arene to facilitate the hydrogel formation. The purpose of this study was to see if it would be possible to achieve crosslinking using a water-soluble calix[4]arene-grafted PSMA in the presence of a chemical stimulus (here the viologen salt) (**Figure 5.6**). To do so, a primary amine-tethered sulfonated calix[4]arene should be synthesized and later modified with PSMA to form a water-soluble graft.[yy] Second,

---

[vv] Regarding Liu's paper, in addition to the electrostatic interaction between the cationic moiety (viologen group) and the anionic moiety (sulfonate functionalities), it seemed that the π-stacking interaction between the calix[4]arene ring and the viologen conjugated system also played a major role in facilitating the hydrogel formation.[35]

[ww] As was the case in section 5.3, the strong complexation of *p*-sulfonated calix[4]arenes and viologen derivatives has been verified by the literature examples using ^{1}H-NMR spectroscopic titration studies.[90,91]

[xx] In accordance with literature, due to its hydrophobic nature, PSMA is not capable of forming a hydrogel unless it is modified with hydrophilic groups.[92,93]

[yy] The direct sulfonation of a *p*-*t*-butylated calix[4]arene-grafted PSMA (the model graft made in chapter 3) to achieve the desired *p*-sulfonated calix[4]arene-grafted PSMA was not a viable option. It was due to the harsh reaction conditions (using concentrated sulfuric acid) which would certainly result in the uncontrolled over-sulfonation of every subunit of the polymer (even the styrene units) and more importantly the decomposition of

Stellenbosch University https://scholar.sun.ac.za

by a series of bis-quaternary amines (preferably the viologen derivatives) must be prepared in accordance with the literature-based approaches. Finally, the hydrogel formation employing the water-soluble grafts and the bis-quaternary amines will be put to the test.

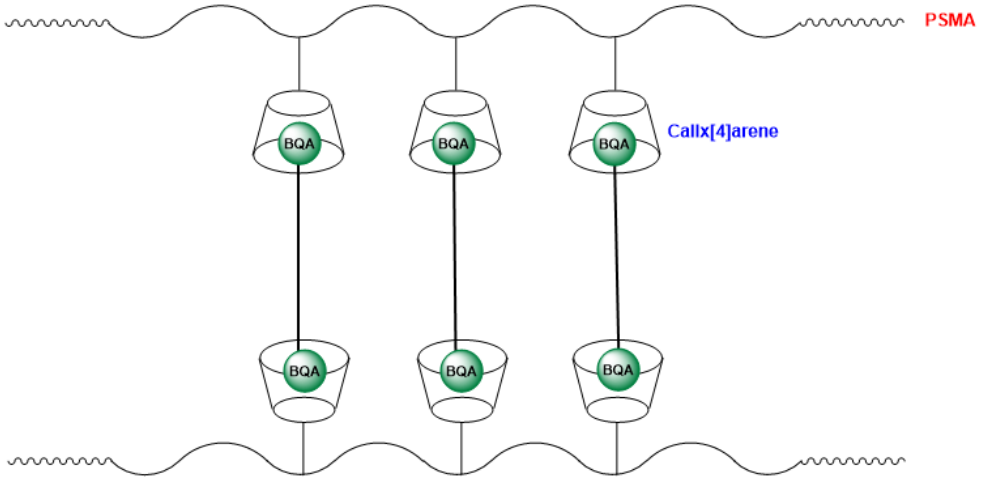

Figure 5.6 Crosslinking between PSMA chains through the encapsulated units of amines (B.Q.A: bis-quaternary amine)

5.6 Synthesis of a primary-amine tethered *p*-sulfonated calix[4]arene

The model study performed in chapter 3 indicated that PSMA could achieve the highest degree of modification upon grafting with mono-substituted butylamine-tethered *p*-*t*-butyl-calix[4]arene **10$_b$** (78% in glacial acetic acid and 32% in DMF). Following the same pattern, the *p*-sulfonated version of the same calix[4]arene was targeted to be synthesized.

As discussed earlier, there were two options for the synthesis of a sulfonated calixarene: 1) sulfonation of a de-butylated calixarene, or 2) *ipso*-sulfonation of a *p*-*t*-butylated calixarene. Due to the shorter synthetic route for *ipso*-sulfonation, the second approach was chosen for making our desired target molecule. In addition, in accordance with the results taken from chapters 2 and 3, compound **10$_b$** (the monofunctionalized amine-tethered *t*-butylated calix[4]arene with butyl spacer) was chosen for the sulfonation reaction.

The original approach to make a sulfonated calixarene was Shinkai's method.[1] The first involved heating the calixarene in concentrated sulfuric acid at a temperature range between 70-80 °C until an aliquot taken from the reaction was found completely water-soluble (the starting material was highly insoluble in water). Then after cooling, the acid was neutralized

---

the polymeric backbone. This is why it was necessary for the sulfonate groups to be introduced before the calix[4]arene attachment onto PSMA.

Stellenbosch University https://scholar.sun.ac.za

by a basic Ba^{2+} source ($BaCO_3$ or $Ba(OH)_2.8H_2O$) to form insoluble $BaSO_4$ which was removed from the water-soluble product (the newly-formed *p*-sulfonated calixarene) via suction filtration. Thereafter, the barium salt of the *p*-sulfonated calix[4]arene (in the filtrate) underwent a metal exchange upon adding a Na^+ source (Na_2CO_3 or NaOH) until 8<pH<9. The aqueous phase was dried *in vacuo* and the resulting solid dissolved in the minimum amount of water. To this solution, was added ethanol to afford a sodium salt of *p*-sulfonated calixarene.

As expected, for neutralizing x mmol of sulfuric acid, x mmol of Ba^{2+} should be used. In practice, 0.300 mmol of amine-tethered *t*-butylated calix[4]arene **10_b** (220 mg) was heated in 36.0 mmol of concentrated sulfuric acid (2.00 mL) at 70 °C for 24 hours. After cooling, in order to neutralize the acid, 36.0 mmol of $Ba(OH)_2.8H_2O$ was added. After that, the insoluble $BaSO_4$ was removed by way of filtration and the aqueous phase was basified with a Na^+ source. Many different attempts, using both solid and solution forms of both NaOH and Na_2CO_3, still resulted in 3-5 grams of salt being produced after trituration with ethanol (**Scheme 5.7**). The yield was always more than 100%, suggesting a work-up problem for the basification step. It demonstrated that the material obtained was predominantly an inorganic salt as no important analytical data was acquired from ^{1}H-NMR spectroscopy and HRMS.

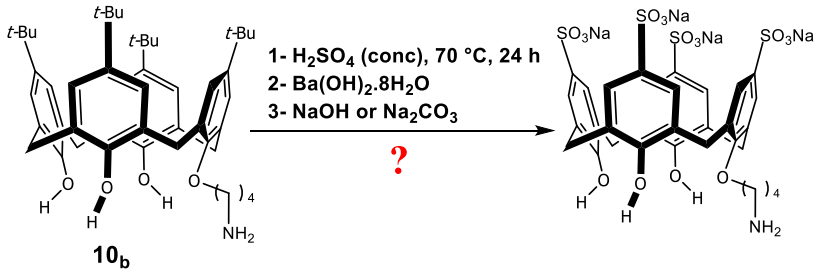

Scheme 5.7 Failed attempt to produce an amine-tethered p-sulfonated calix[4]arene, followed by an aqueous work-up

Thus, another approach was sought to sulfonate our calix[4]arene; however, most literature examples were associated with an aqueous work-up procedure similar to Shinkai's approach.[94,95,96] Of interest to us was that, Da Silva and Coleman have reported a sulfonation reaction in which several mono-alkylated calix[4]arenes were heated in sulfuric acid, and the compounds undergoing a sulfonation reaction at 50 °C overnight, with the products being precipitated using cold diethyl ether (yields>80%).[97] This approach appeared to work in our hands, producing an 86% yield for the desired *p*-sulfonated calix[4]arene, proving the advantage of employing a non-aqueous work-up over an aqueous one. To improve the yield even more, the temperature was decreased to room temperature and the reaction was stopped

Stellenbosch University https://scholar.sun.ac.za

after 17 hours (decreasing the possibility of the product decomposition under harsh acidic conditions). This time an excellent yield (95%) for the product was achieved (**Scheme 5.8**).

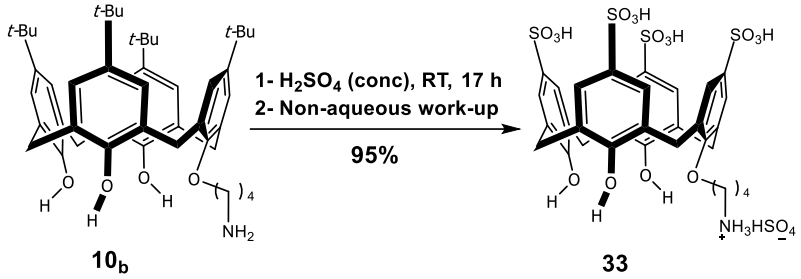

*Scheme 5.8 The final approach to synthesize the desired amine-tethered p-sulfonated calix[4]arene (**33**)*

FT-IR spectrum revealed the existence of two very strong stretches at 1151 cm^{-1} and 1116 cm^{-1} respectively, for the asymmetric and symmetric stretching modes of S=O groups, suggesting the successful sulfonation of our calix[4]arene.

In the ^{1}H-NMR spectrum of the product (**Figure 5.7**), the most important indication thus confirming the synthesis of the desired product was the disappearance of the tertiary butyl signals, the successful de-butylation by the sulfonate groups. In addition, dramatic peak-broadening, especially in the aliphatic region, confirmed the strong hydrogen-bonding caused by the sulfonic acid groups. This phenomenon complicated the interpretation of the aliphatic region of the spectrum, making the precise assignments of the signals to the compound protons almost impossible, which is why the aromatic region was the main focus of this analysis. The presence of three aromatic signals at 7.02 ppm (2H), 7.06 ppm (4H),[zz] and 7.08 ppm (2H) proved the dissymmetry caused by the existence of the tether, as another indication for the successful synthesis of our desired product. However, due to the imperfect NMR spectral results, HRMS data would be required as compelling evidence for further confirmation of compound **33**'s existence.

Fortunately, HRMS data showed a species with molecular ion of 816.0772 Da (the calculated molecular ion for $[M+H]^{+}$ was 816.0760 Da) confirming the successful synthesis of compound **33**.

[zz] Apparently, due to some conformational issue for the product, two of the signals (each one with two protons) merged with each other and showed up as one signal (with four protons). The conformational status of this compound will later be explained in detail in section 5.10.

Stellenbosch University https://scholar.sun.ac.za

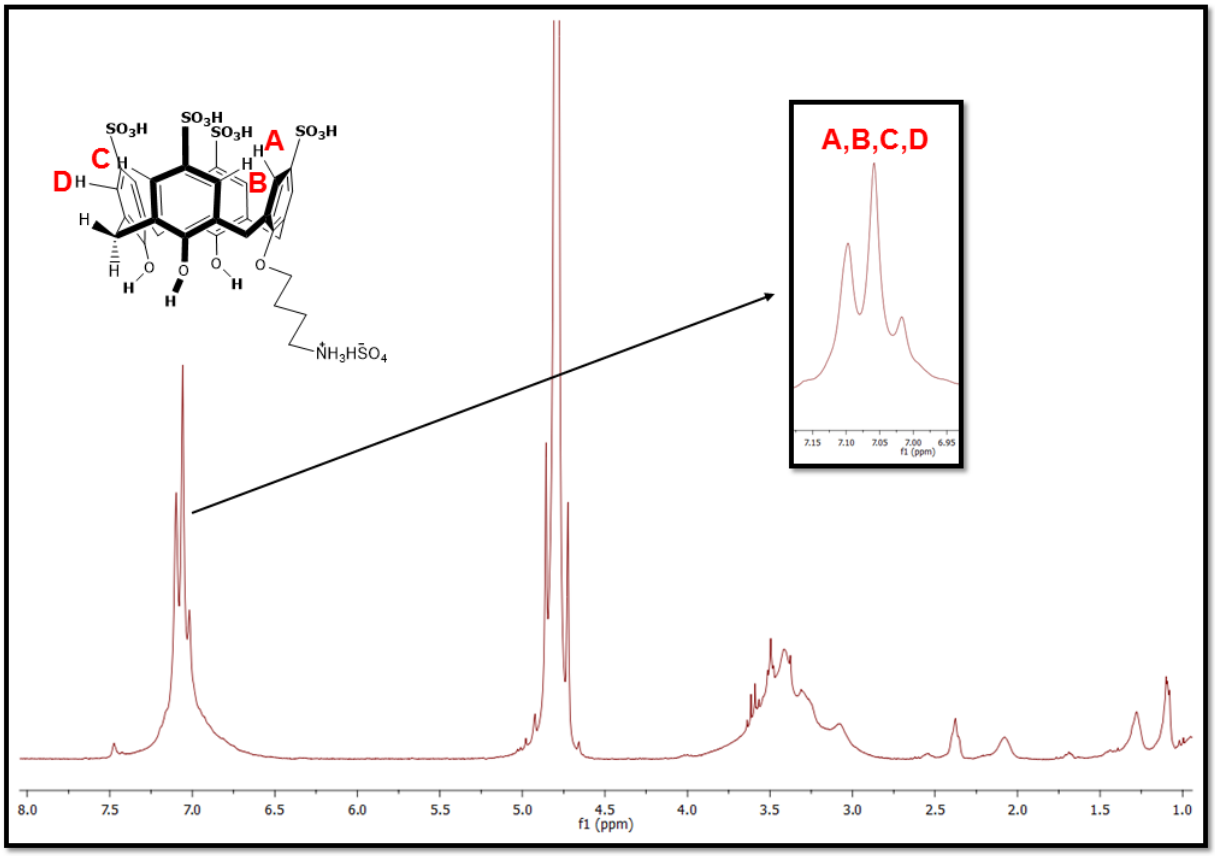

*Figure 5.7 ^{1}H-NMR spectrum (in D_2O) for the desired amine-tethered p-sulfonated calix[4]arene (**33**)*

5.7 Synthesis of the bis-quaternary ammonium salts as crosslinkers

Simulating the viologen moiety of Liu's study,[35] (1,1'-dimethyl-[4,4'-bipyridine]-1,1'-diium iodide) **34** was chosen and synthesized following a literature report by Kuang and co-workers.[98] To do so, 4,4'-bipyridine and a large excess of iodomethane were mixed together in dry acetonitrile and heated under reflux overnight to produce the desired methyl viologen salt (96%) (**Scheme 5.9**). This reagent was later utilized as a titrating agent[aaa] and not for the actual hydrogel formation study. It was due to some literature evidence which suggested that methyl viologen monomer could produce a complex with *p*-sulfonated calix[4]arene with a far smaller binding constant than its corresponding dimer did. The ^{1}H-NMR spectral data ascribed this matter to the axial orientation of the methyl group of the viologen monomer upon immersing into the *p*-sulfonated calix[4]arene cavity.[90,99] As another piece of evidence to support this notion, Liu *et al*. also claimed that methyl viologen **34** could only form a simple host-guest

[aaa] In the following sections, several ^{1}H-NMR spectroscopic titration experiments were conducted to determine the real degree of functionalization of our polymers after reaction with the amine-tethered *p*-sulfonated calix[4]arene (**33**), when FT-IR spectroscopy failed to indicate those values accurately.

Stellenbosch University https://scholar.sun.ac.za

complex with *p*-sulfonated calix[4]arenes, while it was unable to form part of any supramolecular polymer in its monomeric form.[34]

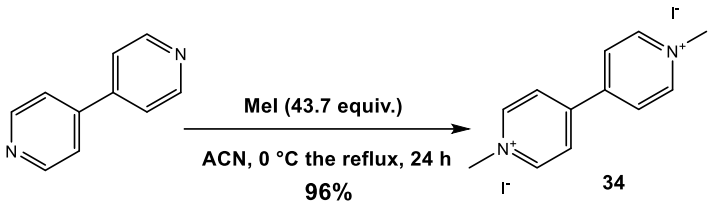

*Scheme 5.9 Synthesis of the bis-quaternary amine **34** based on the work of Kuang and co-workers*[98]

As mentioned earlier, the dimerized version of the viologen salts has shown potential in forming strong intermolecular interactions with *p*-sulfonated calix[4]arenes. As an example, a paper by Liu *et al*. described some exciting finding of the supramolecular polymerization of a bis-*p*-sulfonated calix[4]arene upon complexation with a dimerized methyl viologen possessing an ethyl bridge, namely **36** (**Scheme 5.10**).[90]

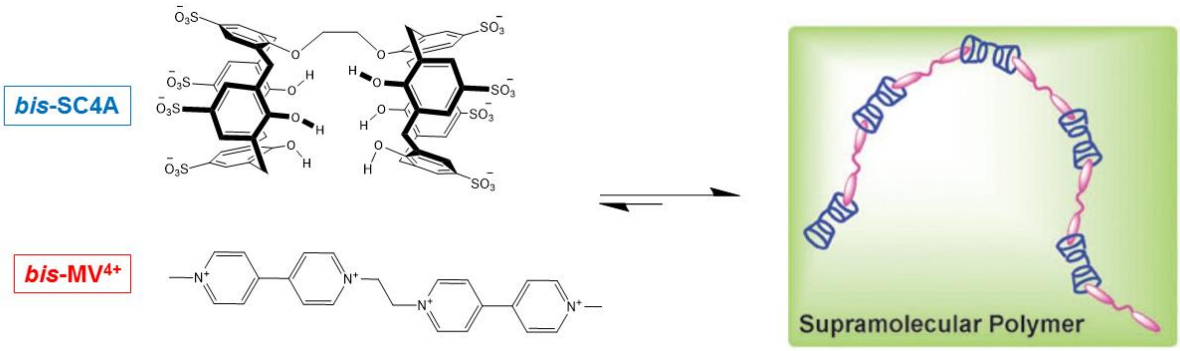

Scheme 5.10 Supramolecular polymer construction using a bis p-sulfonated calix[4]arene and a viologen dimer (the right-hand side structure was taken from reference[90]*)*

This work suggested that to achieve hydrogel formation for our system, a diammonium species with a longer spacer could also be employed. Thus, as our first crosslinker, compound **36** (which is the dimerized version of the methyl viologen salt **34** was synthesized. To do so, 4,4'-bipyridine was first dimerized through an ethyl linker chain using 1,2-dibromoethane in DMF, following the approach reported in literature to form the dimer **35** (1,1''-(ethane-1,2-diyl)bis(([4,4'-bipyridin]-1-ium)) bromide) in 20% yield (**Scheme 5.11**).[100]

Thereafter, the methylated version of the dimer **36** (1',1'''-(ethane-1,2-diyl)bis(1-methyl-[4,4'-bipyridine]-1,1'-diium) dibromide diiodide) was synthesized using an excess of iodomethane in DMF in an excellent yield (94%), exactly as the literature-based method suggested (**Scheme 5.12**).[90]

Stellenbosch University https://scholar.sun.ac.za

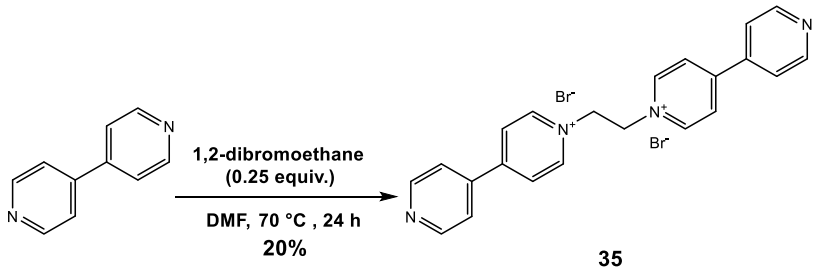

*Scheme 5.11 Synthesis of the dimer **35** based on the work of Summers et al.*[100]

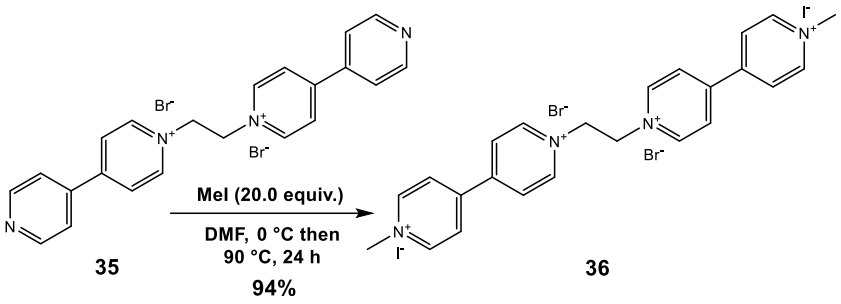

*Scheme 5.12 Synthesis of the dimer **36** based on the work of Liu et al.*[90]

Another study by the same researchers on another bis-*p*-sulfonated calix[4]arene, utilizing a dimerized methyl viologen with a much longer bridge, also demonstrated the construction of a supramolecular polymer (**Scheme 5.13**).[91] Therefore, the chain length of the bridge was also considered as a possibly determining factor in the hydrogel formation study and a viologen dimer with a longer bridge (**38**) was synthesized to put this effect to the test (due to the availability of chemicals in the lab, only a simple hexyl tether was targeted for the crosslinker synthesis).

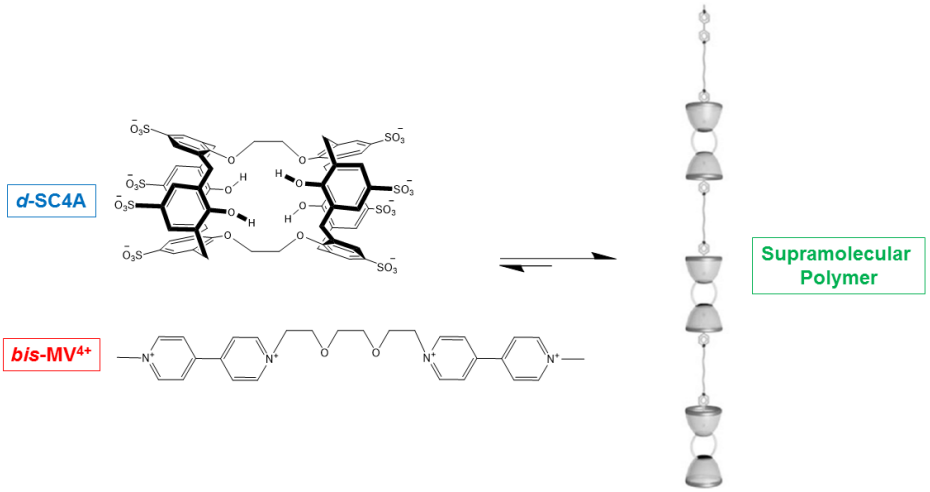

Scheme 5.13 Supramolecular polymer construction using a double-bridged bis p-sulfonated calix[4]arene and a longer-bridged viologen dimer (the right-hand side structure was taken from reference[91]*)*

Stellenbosch University https://scholar.sun.ac.za

To begin with, the dimer with a 6-member chain (1,1''-(hexane-1,6-diyl)bis(([4,4'-bipyridin]-1-ium)) bromide **37**) was synthesized under exactly the same conditions explained for the previous dimer. The first reaction in this matter suffered from a lower yield (49%) compared to the reported value in literature (75%) (**Scheme 5.14**).[101]

The second reaction (methylation with iodomethane) was also performed according to the method described above to produce the novel dimer 1',1'''-(hexane-1,6-diyl)bis(1-methyl-[4,4'-bipyridine]-1,1'-diium) dibromide diiodide **38** in a good yield (80%) (**Scheme 5.15**).

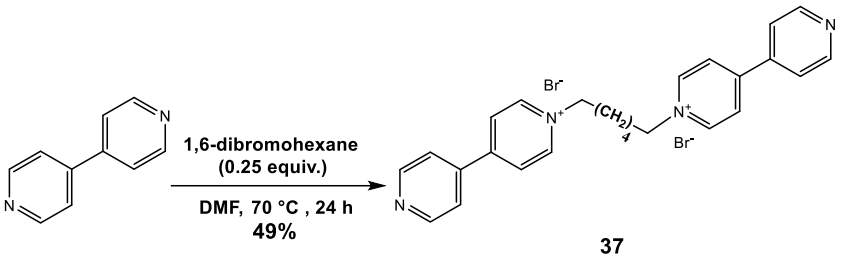

*Scheme 5.14 Synthesis of the dimer **37** based on the work of Tazuke et al.*[101]

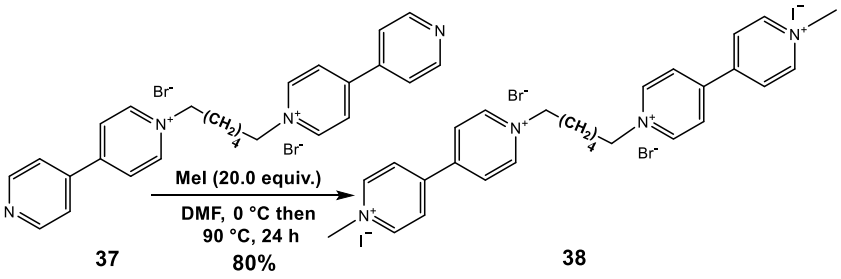

*Scheme 5.15 Synthesis of the dimer **38***

FT-IR spectrum revealed the most important indication for the successful methylation of the starting material (**37**) which was the existence of two medium bends characteristic for our product's aliphatic methyl groups at 1349 cm^{-1} and 1440 cm^{-1}.

In the ^{1}H-NMR spectrum (**Figure 5.8**), aside from the hexyl tether protons (between 1.52 ppm and 4.76 ppm) and the aromatic protons (between 8.56 ppm and 9.14 ppm), which were common for both starting material (**37**) and the product (**38**), the existence of a singlet at 4.52 ppm was the proof for the successful methylation resulting compound **38**.

HRMS data exhibited two molecular ions: 1) a 554.1863 Da molecular ion ($[M+H]^+$) for our compound molar mass without Br_2I (the calculated molecular ion for that was 554.1906 Da), and 2) a 681.0914 Da molecular ion ($[M+H]^+$) for our compound molar mass without Br_2 (the

Stellenbosch University https://scholar.sun.ac.za

calculated molecular ion for that was 681.0951 Da). Overall, the analytical evidence strongly supported the formation of bis-quaternary amine **38**.

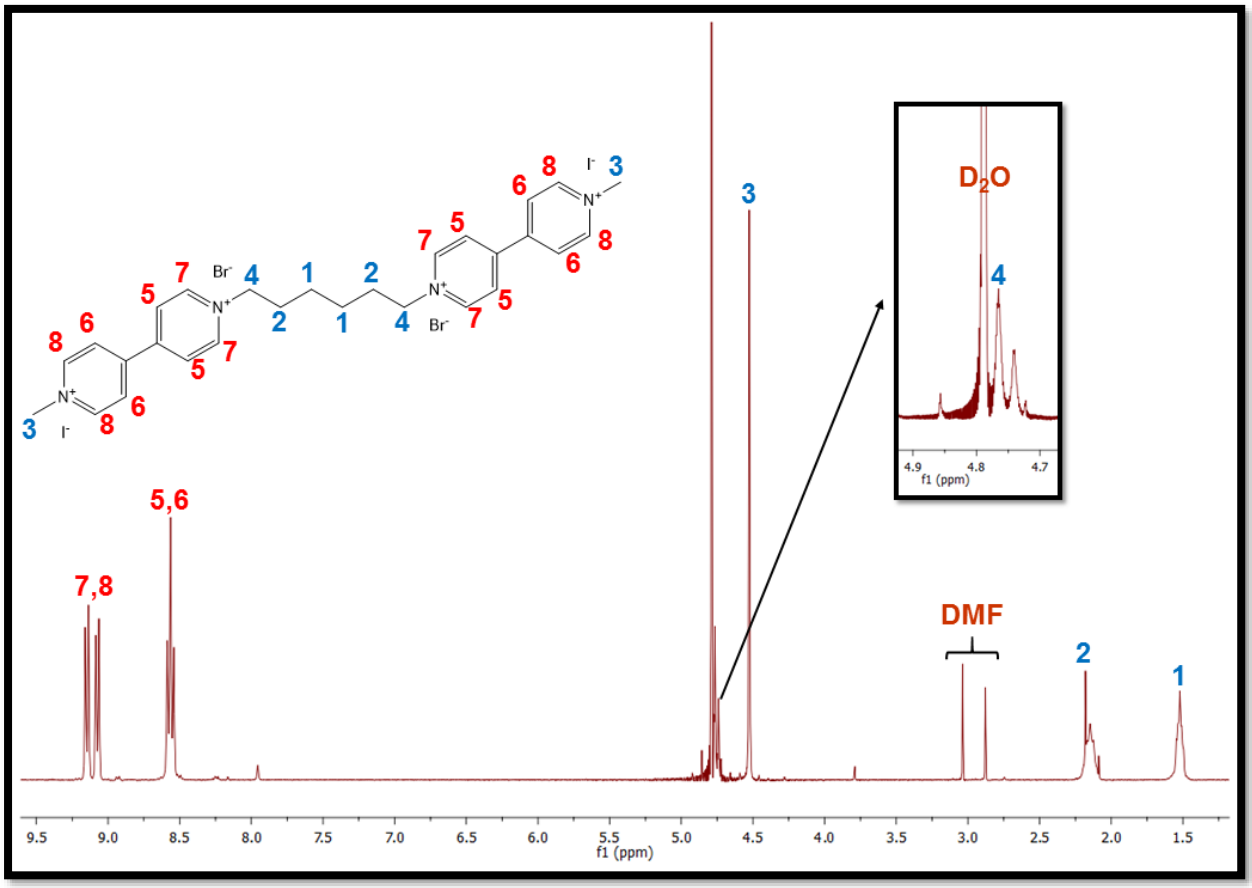

*Figure 5.8 ^{1}H-NMR spectrum (in D_2O) for the novel viologen dimer (**38**)*

As alternatives, in case of the above-mentioned bis-quaternary amines failure to act as the crosslinkers for the *p*-sulfonated calix[4]arene-modified polymer, several simple aliphatic bis-quaternary ammonium salts were also prepared.[bbb] For example, following an old procedure by Zaimis,[102] bis-quaternary ammonium salts *N,N,N,N′,N′,N′*-hexamethylethane-1,2-diaminium iodide **39**, 2,2'-(methylazanediyl)bis(*N,N,N*-trimethylethan-1-aminium) iodide **40**[ccc] and *N,N,N,N′,N′,N′*-hexamethylhexane-1,6-diaminium iodide **41** were synthesized through heating their corresponding bis-tertiary amine parents with an excess of iodomethane and sodium

[bbb] Due to forming strong complexes, these compounds had been found useful for biological purposes[102] and catalytic studies.[103]

[ccc] ^{1}H-NMR spectrum suggested that the middle nitrogen for this compound did not become quaternized. An old report by Marxer and Miescher also confirmed the possibility of this matter.[104] It might be due to the strong electric repulsion caused by the like charges of the quaternized terminal nitrogen atoms.

Stellenbosch University https://scholar.sun.ac.za

hydroxide under reflux in methanol (respectively 58%, 81%, and 77% yields were achieved respectively) (see **Scheme 5.16**).

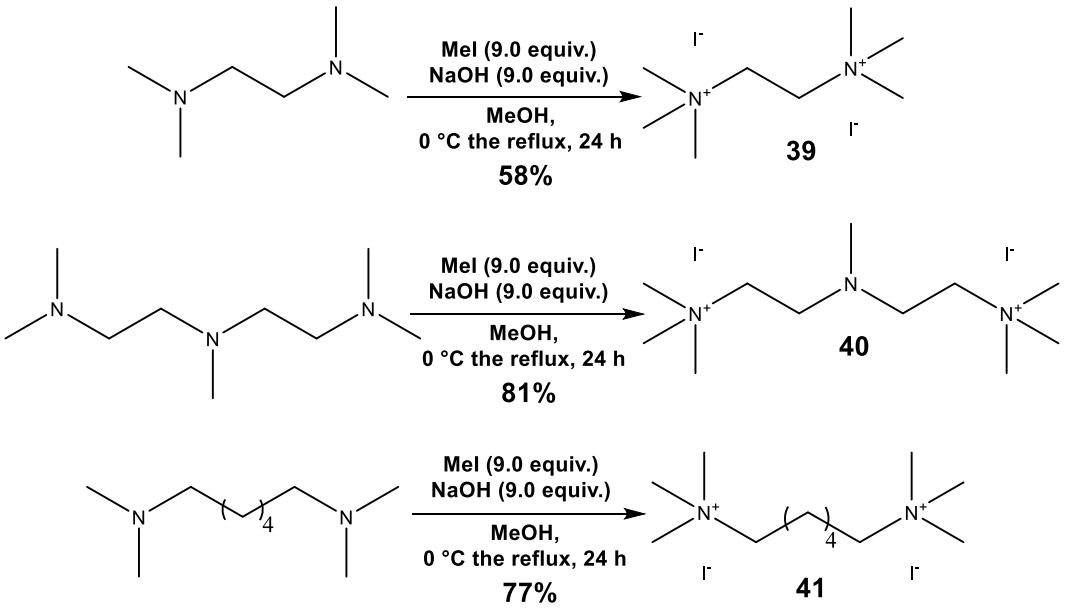

*Scheme 5.16 Synthesis of a series of monomer bis-quaternary amines (**39**, **40**, **41**) based on the work of Zaimis et al.*[102]

The last bis-quaternary ammonium salt synthesized in this regard was *N,N,N,N′,N′,N′*-hexaethylhexane-1,6-diaminium bromide **42**. According to a previously reported approach by Bhaumik and Sasidharana, 1,6-dibromohexane and an excess of triethylamine were heated under reflux in dry acetone to produce the desired product in 57% yield (**Scheme 5.17**).[103]

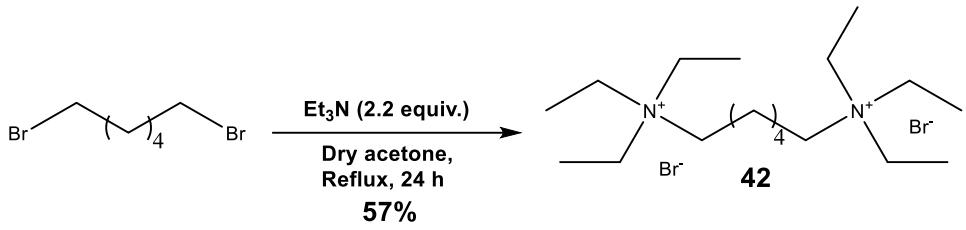

*Scheme 5.17 Synthesis of the monomer bis-quaternary amine (**42**) based on the work of Bhaumik et al.*[103]

5.8 Synthesis of a water-soluble calix[4]arene-grafted PSMA

After the successful synthesis of the desired tethered *p*-sulfonated calix[4]arene **33**, the synthesis of a water-soluble calix[4]arene-grafted polymer was pursued. Thus, a series of PSMA grafts of the tethered *p*-sulfonated calix[4]arene were synthesized (**Scheme 5.18**).

Stellenbosch University https://scholar.sun.ac.za

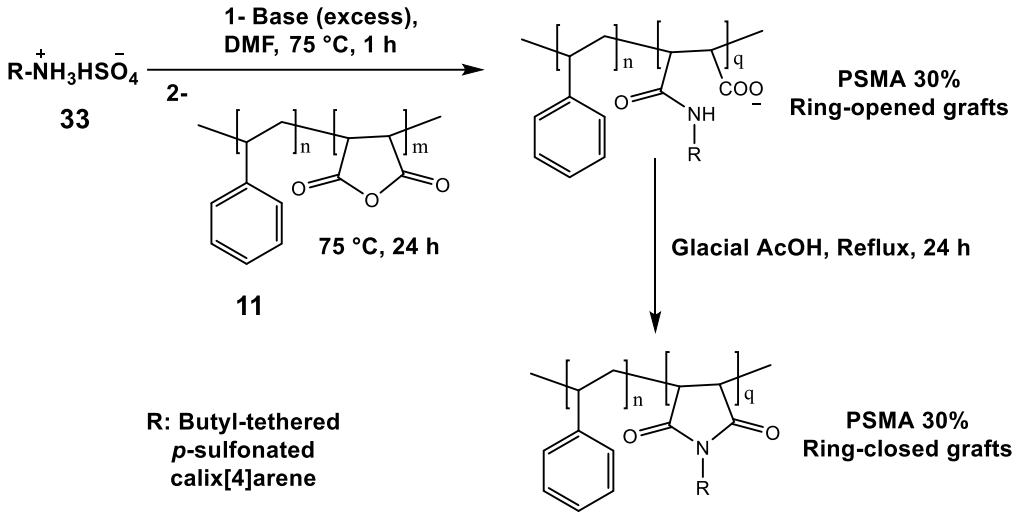

*Scheme 5.18 Modification of PSMA 30% (**11**) with an amine-tethered p-sulfonated calix[4]arene (**33**)*

Overall, to synthesize a *p*-sulfonated calix[4]arene-grafted PSMA, the tethered *p*-sulfonated calix[4]arene **33** had to be deprotonated first (since it was an amine salt) with a base in the reaction solvent (here DMF) via heating (75 °C). The reason for applying mild heating in the grafting step in DMF (as opposed to the room temperature reaction described in chapter 3 for the neutral amine) was to increase the degree of functionalization (in case of PSMA 30%, according to FT-IR spectrum, reaction at room temperature only afforded a graft with a 10% degree of functionalization). Thereafter, PSMA (with 30% of maleic anhydride content) **11**[ddd] was added and stirred overnight (at the same temperature) to form the desired polymeric graft with the water-soluble calix[4]arene. The work-up for these reactions comprised of dilution of the reaction with water, dialysis (to remove DMF, unreacted calix[4]arene and extra base) and subsequently freeze-drying to afford a hygroscopic solid. Obviously, this approach resulted in the formation of a ring-opened product (possessing maleamic functionality with tethered *p*-sulfonated calix[4]arene as the pendant group). As learned from chapter 3, in order to determine the degree of functionalization for the grafts, the ring-closed versions had to be synthesized and analyzed via FT-IR spectroscopy (see **Table 5.1** and the experimental section). To make the graft with ring-closed functionality (maleimide), the ring-opened compound was heated under reflux in glacial acetic acid and then the solvent was removed to yield the desired product.

[ddd] As was the case in chapter 3, PSMA 30% **11** was commercially available and therefore it was not synthesized.

Stellenbosch University https://scholar.sun.ac.za

*Table 5.1 FT-IR spectroscopy speculated values for functionalization degrees of PSMA 30% **11** with the amine-tethered p-sulfonated calix[4]arene **33***

Entry	Base (equiv.)	Compound name[eee]	Degree of functionalization (%)[fff]	Water solubility
1	NaH (10.0)	**A_{30}-S_{10}-33**	35	Slightly soluble[ggg]
2	Et_3N (5.0)	**A_{30}-T_5-33**	54	Slightly soluble[hhh]

In practice, the PSMA 30%-originated grafts showed poor solubility in water. In order to increase the water-solubility, PSMA with more maleic anhydride content was required. Thus, to generate a more water-soluble polymer upon grafting with *p*-sulfonated calix[4]arene, PSMA 50% (with 50% maleic anhydride content) was also synthesized and tested.

PSMA 50% **43** was synthesized by mixing freshly distilled styrene and sublimed maleic anhydride (respective mole ratio: 1.0 to 1.1) in dry methyl ethyl ketone (MEK) at 65 °C using AIBN (2 mole % based on the monomer feed) as the free radical initiator (**Scheme 5.19**). The molar mass data were determined by GPC.[iii] The alternate nature of the polymer was verified using FT-IR and ^{13}C-NMR spectroscopies (for more details, including the GPC elugram see the experimental section).

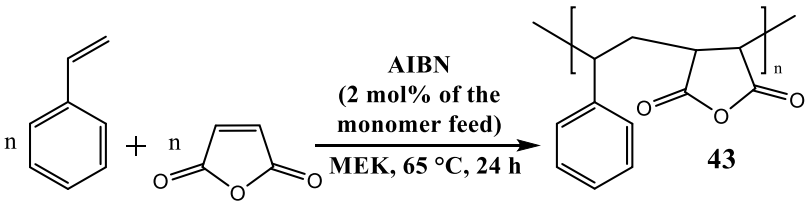

*Scheme 5.19 Radical polymerization for producing PSMA 50% **43***

Exactly, the same synthetic procedures used to produce PSMA 30%-originated grafts, were applied to PSMA50% (employing a wider range of base choices such as carbonate sources)

[eee] In addition to the coding protocols explained in chapter 3, here, the middle letters S, T, P and C respectively refer to NaH, Triethylamine, K_2CO_3 and Cs_2CO_3 (the base choice) while their subscripts show their number of equivalents used in the reaction (q: Number of reacted maleic anhydride units).

[fff] These degrees of functionalization belong to the ring-closed versions of the mentioned products.

[ggg] Maximum solubility was approximately 5.0 mg/mL.

[hhh] Maximum solubility was also approximately 5.0 mg/mL.

[iii] M_n = 17 683 g.mol^{-1}, M_w = 104 220 g.mol^{-1}, Đ = 5.89.

Stellenbosch University https://scholar.sun.ac.za

and the desired grafts were made accordingly. This time, several grafts with notable degrees of solubility were obtained (see **Scheme 5.20** and **Table 5.2**).

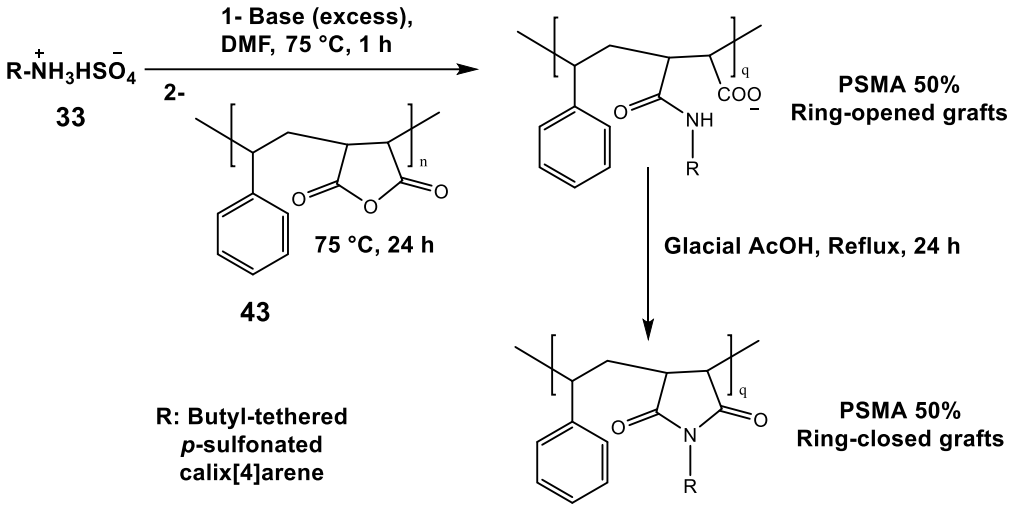

*Scheme 5.20 Modification of PSMA 50% **43** with an amine-tethered p-sulfonated calix[4]arene **33**[jjj]*

*Table 5.2 Speculated values for functionalization degrees of PSMA 50% **43** with the amine-tethered p-sulfonated calix[4]arene **33** by FT-IR spectroscopy*

Entry	Base (equiv.)	Compound name	Degree of functionalization (%)	Water solubility
1	NaH (10.0)	**A_{50}-S_{10}-33**	46	Soluble[kkk]
2	Et_3N (5.0)	**A_{50}-T_5-33**	13	Slightly soluble[lll]
3	Et_3N (10.0)	**A_{50}-T_{10}-33**	46	Soluble
4	Et_3N (20.0)	**A_{50}-T_{20}-33**	71	Soluble
5	K_2CO_3 (10.0)	**A_{50}-P_{10}-33**	20	Slightly soluble
6	Cs_2CO_3 (10.0)	**A_{50}-C_{10}-33**	30	Soluble

In addition to the calix[4]arene and PSMA signals discussed in chapter 3, both grafts bore strong stretches between 1100 cm^{-1} and 1200 cm^{-1} on their FT-IR spectra which were characteristic signals for S=O for the sulfonate groups. Unlike C=O stretches, these signals could not provide any evidence of attachment, but only justified the water-soluble nature of the grafts (see an example in **Figure 5.9**).

[jjj] q: Number of reacted styrene-maleic anhydride units.

[kkk] Maximum solubility was approximately 50 mg/mL.

[lll] Maximum solubility was approximately 5.0 mg/mL.

Stellenbosch University https://scholar.sun.ac.za

No solution analysis could be carried out for the ring-closed grafts due to their lack of solubility in any solvent. In addition, due to the hydrophilic nature of our ring-opened grafts and their poor solubility in DMF and THF (our only available size-exclusion chromatography solvent systems), no GPC analysis was performed on them. Consequently, the remaining solution analysis (including UV-Vis and NMR spectroscopies) were done for the ring-opened grafts.

Generally in the ^{1}H-NMR spectra (see an example on **Figure 5.10**), aside from the PSMA backbone protons and the butyl tether protons (between 0.50 ppm and 2.50 ppm), a characteristic signal for the calix[4]arene methylene bridges (around 4.00 ppm) together with aromatic protons of both calix[4]arene and styrene (between 6.00 ppm and 8.00 ppm) were observable.

Very similar to the results obtained for the grafts in chapter 3 for UV-Vis spectroscopy, 0.1 mg/mL aqueous solutions of the grafts (or their soluble fractions in water) showed an absorption band between 280 nm to 290 nm, indicative of the attachment of a strong chromophore (here *p*-sulfonated calix[4]arene). Finally, thermal studies (DSC) were performed applying the same protocols utilized in chapter 3 for determining the glass transition temperature and other related parameters.

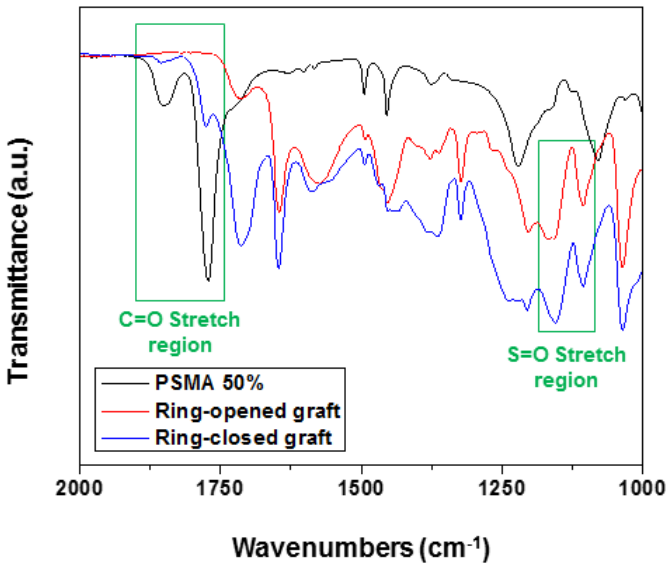

*Figure 5.9 Overlayed FT-IR spectra for PSMA 50% **43** and a ring-opened p-sulfonated calix[4]arene-grafted PSMA 50% example (**A_{50}-S_{10}-33**) and its corresponding ring-closed graft (**C_{50}-S_{10}-33**) (Transmittance values were normalized to styrene bend at 700 cm^{-1}, a.u: arbitrary unit)*

Stellenbosch University https://scholar.sun.ac.za

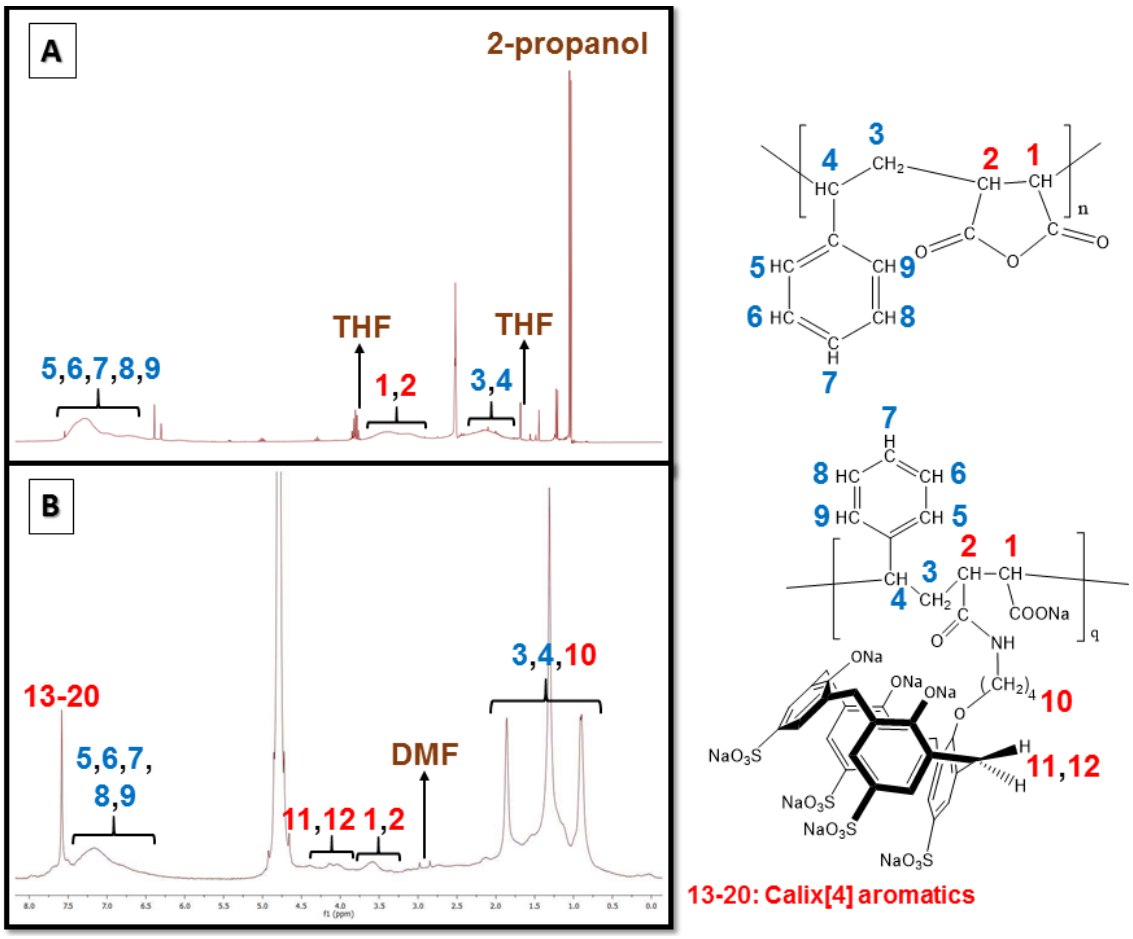

*Figure 5.10 A: ^{1}H-NMR spectrum (in DMSO-d_6) for PSMA 50% **43**; B: An example of the ^{1}H-NMR spectrum (in D_2O) for a ring-opened p-sulfonated calix[4]arene grafted PSMA 50% (here **A$_{50}$-S$_{10}$-33**)*[mmm]

5.9 Possible applications for the water-soluble grafts

As mentioned in the literature review section, Liu *et al*. suggested an approach for the production of a gel using a viologen-based polyvinyl alcohol and a multi-substituted *p*-sulfonated calix[4]arene.[35] In this section, our attempts at producing a gel with a similar approach with a *p*-sulfonated calix[4]arene-grafted PSMA will be evaluated.

5.9.1 Gelation attempt on a *p*-sulfonated calix[4]arene-grafted PSMA

Naturally, a bis-quaternary amine as a bidentate ligand can complex with a calix[4]arene in a 1 to 2 ratio. That marks the maximum amount of ligand that can be accommodated by its calix[4]arene host, otherwise exceeding that limit will result in the calix[4]arene cavity being swamped by the guest and most likely undoing the interaction between the host and the guest. As a result of that, no hydrogel will form. Thus, the starting point for every hydrogel study

[mmm] The interpretation of signals appearing between 3.0 to 4.5 ppm is based on the best speculation we could come up with (q: Number of reacted styrene-maleic anhydride units).

Stellenbosch University https://scholar.sun.ac.za

experiment should be a ratio very far from the above-mentioned 1 to 2 (e.g. 1 to 100). In addition, the solubility of the ring-opened grafts and the quaternary amines were considered before performing the experiments. All our quaternary amines were only soluble in water (they also showed some degree of solubility in methanol and ethanol). Out of all PSMA-based grafts, only a few of the PSMA 50% grafts showed significant solubility in water (the rest were only slightly soluble in water or alcoholic solvents), which is why it was decided that the experiments were only run in aqueous media.

To determine the hypothetical number of mmols for the graft versus the number of mmols for the amine, firstly, the repeating unit of the grafts had to be specified individually (based on the degree of functionalization by the calix[4]arene). Then, the molecular weight for that repeating unit could be used to ascertain the number of mmols for it. Amongst all water-soluble grafts synthesized in this section, the PSMA 50% grafted by *p*-sulfonated calix[4]arene-amine (**33**) in the case of using 20 equivalents of triethylamine showed a 71% degree of functionalization (the maximum FT-IR spectroscopy speculated value in **Table 5.2**). This graft was considered as the best host due to the fact that approximately three out of every four of its parent styrene-maleic anhydride units were modified by the water-soluble calix[4]arene **A_{50}-T_{20}-33** (**Figure 5.11**). For this graft, after careful calculations, the hypothetical molecular weight of the graft was found to be 7731.02 g/mol (with approximately 70% modification of PSMA, 7 units of calix[4]arene was added to 10 units of styrene-maleic anhydride). In this case, a 50.0 mg/mL solution of the graft (the highest concentration prepared) amounted to be 0.0450 mmol (effective mmol was calculated by dividing 50.0 mg by 7731.02 mg/mmol giving 0.006467 mmol, and then multiplying that figure by 7 for the calix[4]arene units to yield 0.0450 mmol) and obviously to test the hydrogel formation with a 2 to 1 ratio, a maximum of 0.0225 mmol of the amine (here **38**) was required. As mentioned earlier, the starting point for the study (host:guest ratio) was changed in a way that minimized the possibility of the calix[4]arene host being swamped by the amine guest. For example, the first ratio attempted for the graft **A_{50}-T_{20}-43** could be 100 to 1 (0.00045 mmol of the amine should be added to 0.0450 mmol of the graft) and then gradually after every failure the ratio was changed to increase the amine portion until it finally reached a system with a 2 to 1 ratio. To follow the literature suggestion (mentioned in section 5.7), the preferred amine source was the dimer possessing the longest tether possible (here compound **38**). To avoid dilution of the samples upon addition of the amine (which might act as a counter-gelating parameter), the amine

Stellenbosch University https://scholar.sun.ac.za

solution was prepared as concentrated as possible (here 0.01 M), and as a result, only a minute volume of amine was added (here 2.25 μL).

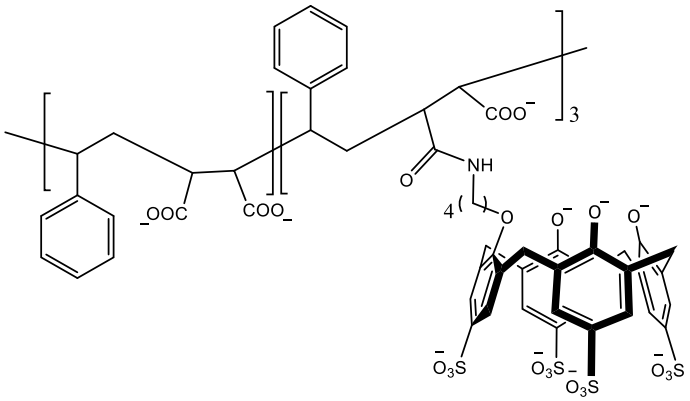

Figure 5.11 FT-IR spectroscopy speculated repeating unit for the ring-opened graft of amine-tethered p-sulfonated calix[4]arene and PSMA 50% (base choice: Et_3N 20.0 equiv.)

After all, no hydrogel formation was achieved for graft **A_{50}-T_{20}-33** using the conditions explained above nor even a tangible increase in the viscosity of the solutions. Thus, various parameters were considered to address this. As stated before, other amine sources were also prepared in case the preferred crosslinker (**38**) would not produce a hydrogel. Therefore, in addition to the dimeric amines (**36** and **38**), the monomeric ones (**39**, **40**, **41**, and **42**) were also employed as the alternative crosslinkers. Unfortunately, none of them produced the desired hydrogel sate.

Aside from the amine concentration discussed before, the graft concentration itself could play a role in the failure to achieve the hydrogel. The fact of the matter was that practically the graft concentration could not go further than 50.0 mg/mL. As an idea, to increase the possibility of hydrogel formation, a polymeric film of the graft was developed by spreading the graft solution on a very small watch glass and slowly evaporating the solvent under the fume hood. After this, the quaternary amine was added onto the film surface in the previously mentioned manner. Unfortunately, this approach was also unable to facilitate any hydrogel formation.

The other influential parameter studied was temperature. In accordance with the paper our study was based on (Liu *et al.*), normally hydrogel formation could happen at room temperature.[35] Following that rule, the first option of change was from room temperature; therefore, cooling (down to 5 °C) and heating with sonication (up to 70 °C) were also tried to examine any unusual behavior of the grafts in the presence of the quaternary amine. Regrettably, all these preparations did not contribute to any observable crosslinking.

Stellenbosch University https://scholar.sun.ac.za

One of the other parameters whose role was considered was the pH of the aqueous solution in which the hydrogel formation study was conducted. Some literature suggested that the interaction between the amine and the *p*-sulfonated calix[4]arene could occur at neutral or basic pHs.[99] Considering the Liu *et al*. hydrogel formation conditions, the first option attempted was hydrogel formation at neutral pHs.[35] To do that, both de-ionized water and even phosphate buffer with exact pH=7 (prepared by mixing 29.1 mL of 0.1 M NaOH and 50.0 mL of 0.1 M KH_2PO_4) were employed. For the basic conditions, the pH was varied from pH~10 (using $NaHCO_3$ saturated solution) to pH~14 (using 2 M NaOH solution), but as was the case for the neutral pHs, no hydrogel formation was observed. To cover every angle on this subject, acidification of the graft solutions was also looked at and changing the pH from mildly acidic (pH~5 for NH_4Cl saturated solution) to highly acidic (pH<1 for HCl 35% and H_2SO_4 95-97%) were performed. Unfortunately, in case of our graft (**A_{50}-T_{20}-33**), the graft precipitated out without any gel formation.

After all these failures, it was also considered that probably the real degree to which our polymer (**A_{50}-T_{20}-33**) was modified did not match the FT-IR spectroscopy speculated value. As known, FT-IR spectroscopy could be an efficient tool for determining PSMA functionalization degree by amines (see the experimental section of chapters 3). However, to double check the accuracy of the FT-IR spectroscopy speculated value, a ^{1}H-NMR spectroscopic titration experiment was designed.[nnn] To do so, a 50.0 mg/ml solution of the graft **A_{50}-T_{20}-33** in D_2O (equal to 0.0450 mmol in the FT-IR based assumption, which led us to believe that the hypothetical molecular weight of the graft was 7731.02 g/mol) was prepared. As explained in section 5.7, the methyl viologen salt **34** was used as the titrating agent to determine the real degree of functionalization of PSMA. Unlike other viologen salts, it only possessed two aromatic signals (4 protons each) and was obviously much easier to be analyzed after the titration with the graft. Hence, it was decided to set up an experiment on a 2 to 1 mmol ratio in favor of the graft for the titration. Thus, to maintain that ratio, versus 8 aromatic protons of *p*-sulfonated calix[4]arene moiety of the graft, 4 aromatic protons of viologen (0.5 equivalent) had to be seen. To examine that, 112.5 µL (0.0225 mmol) from a 0.2 M solution of methyl viologen salt **34** was added. In practice, the ^{1}H-NMR spectral data

[nnn] The approach taken for the non-sulfonated grafts prepared in chapter 3 cannot be used here for corroborating the FT-IR spectroscopy speculated degree of functionalization. Due to the massive peak-broadening in the aliphatic region, the methylene bridges of calix[4]arene are very difficult to be seen and analyzed. This is why a titration experiment targeting the aromatic region of our graft was recommended to solve this problem.

Stellenbosch University https://scholar.sun.ac.za

showed some serious deviation from the real value of functionalization degree. The ^{1}H-NMR spectrum suggested that 48 aromatic protons existed for viologen in this case, suggesting that the real degree of functionalization must be $\frac{1}{12}$ of the FT-IR spectroscopy speculated value which became 5.9% (all spectra can be seen in **Figure 5.12**). This deviation could be attributed to the *p*-sulfonated calix[4]arene effect on the baseline of PSMA FT-IR spectrum after grafting (probably due to its strong hydrogen bonding). Learning from this error, the real degree of functionalization was used for the hydrogel formation study and accordingly less amine solution was used. Despite adhering to the corrected value, the hydrogel formation was still not achieved. However, the observation of the viologen protons shifting upfield proved the interaction between the graft and the quaternary amine.

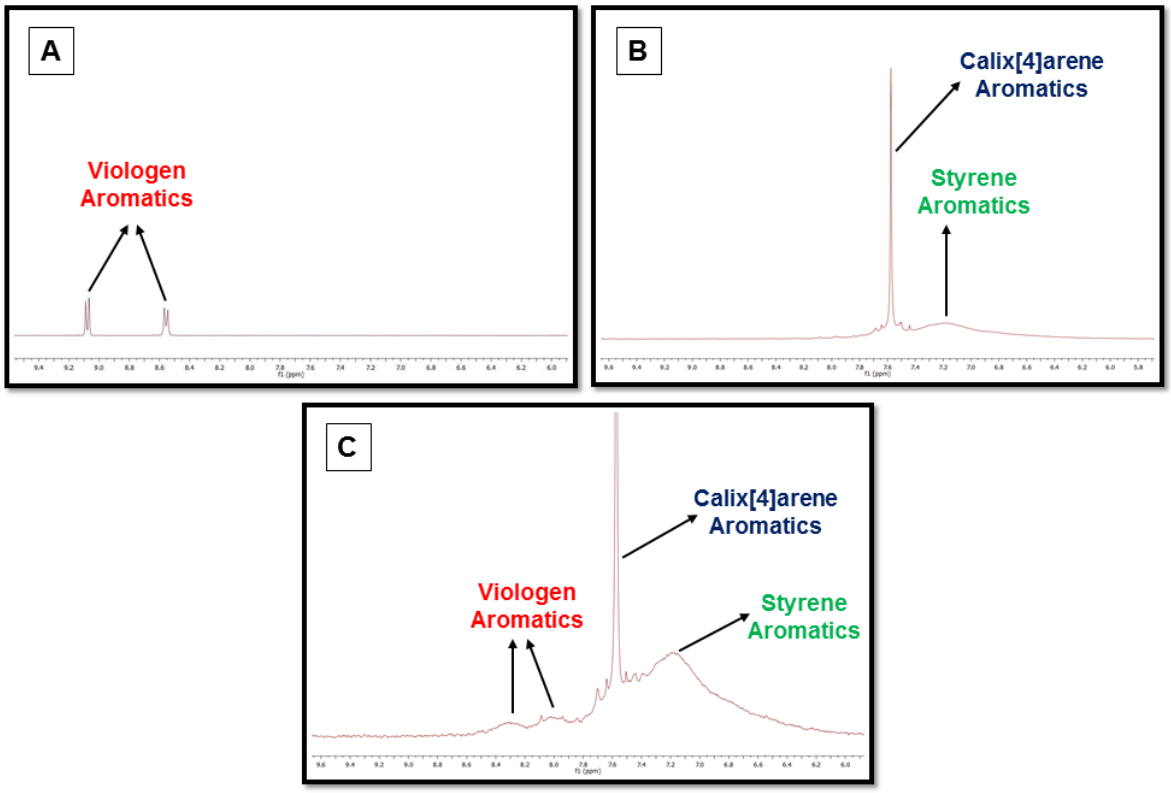

*Figure 5.12 ^{1}H-NMR spectroscopic titration (in D_2O) on a p-sulfonated calix[4]arene-grafted PSMA 50% (**A_{50}-T_{20}-33**) using methyl viologen salt **34**; A: Blank methyl viologen salt **34**; B: Blank graft (**A_{50}-T_{20}-33**); C: methyl viologen salt **34** plus graft (**A_{50}-T_{20}-33**)[ooo]*

Following the same titration approach, the real degrees of functionalization were calculated for other grafts as well (see **Table 5.3**).

[ooo] The drastic broadening of viologen aromatic signals on **Figure 5.12C** is more likely due to kinetics that are similar to the timescale of NMR acquisition. As a result, a blurry average of these aromatic signals is seen.

Stellenbosch University https://scholar.sun.ac.za

*Table 5.3 Corrected values for PSMA functionalization degrees with p-sulfonated calix[4]arene **33***

Entry	Base (equiv.)	Compound name	PSMA type	Corrected degree of functionalization (%)
1	NaH (10.0)	**A_{30}-S_{10}-33**	30%	NA[ppp]
2	Et_3N (5.0)	**A_{30}-T_5-33**	30%	NA
3	NaH (10.0)	**A_{50}-S_{10}-33**	50%	**5.7**
4	Et_3N (5.0)	**A_{50}-T_5-33**	50%	NA
5	Et_3N (10.0)	**A_{50}-T_{10}-33**	50%	**5.7**
6	Et_3N (20.0)	**A_{50}-T_{20}-33**	50%	**5.9**
7	K_2CO_3 (10.0)	**A_{50}-P_{10}-33**	50%	NA
8	Cs_2CO_3 (10.0)	**A_{50}-C_{10}-33**	50%	**4.8**

However, in the case of the grafts with poor water solubility whose ^{1}H-NMR spectra were recorded in DMSO-d_6, the determination of the functionalization degree via this approach was not possible. Those compounds could not be titrated in DMSO-d_6 due to the insolubility of our bis-quaternary amines in that solvent, and as a result, there would be no viologen signal in their ^{1}H-NMR spectra to be compared with other signals of the graft (see an example in **Figure 5.13**). Using a co-solvent system (e.g. DMSO-d_6/D_2O) did not resolve the solubility issue either. Overall for these grafts, there was no ^{1}H-NMR spectroscopy approach to corroborate the FT-IR spectroscopy speculated functionalization degree of PSMA.

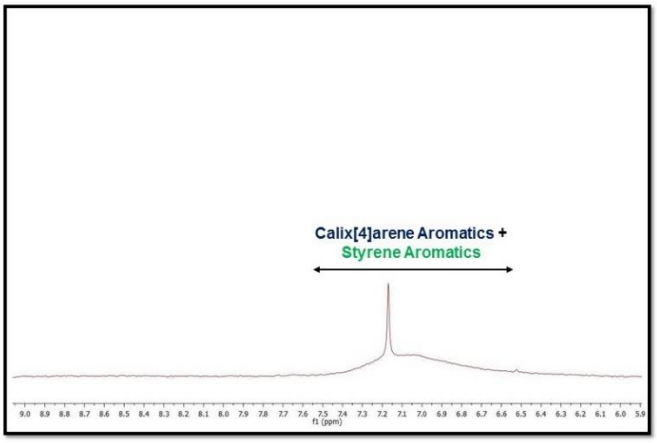

*Figure 5.13 An example of a ^{1}H-NMR spectrum (in DMSO-d_6) of p-sulfonated calix[4]arene-grafted PSMA (here **A_{50}-P_{10}-33**)*

[ppp] Not assigned, due to the impossibility of conducting ^{1}H-NMR spectroscopic titration.

Stellenbosch University https://scholar.sun.ac.za

Owing to the failure of all hydrogel studies on the graft **A_{50}-T_{20}-33**, a hypothesis regarding the possible negative effect of Et_3NH^+ species on the encapsulation of the injected possible crosslinker (the bis-quaternary amine) was also considered. It was suggested that after PSMA grafting with *p*-sulfonated calix[4]arene assisted by Et_3N, presumably the produced Et_3NH^+ species could be encapsulated by the calix[4]arene cavity in a way which would make further encapsulation of other species very difficult. The motive for this hypothesis was a paper published by Coleman and co-workers about the formation of a supramolecular assembly between *p*-sulfonated calix[4]arene and Et_3NH^+.[105] Despite no triethylammonium species being detected in the NMR spectra of the polymers, it was put to the test. For this reason, our other water-soluble calix[4]arene-grafted PSMAs (produced not by Et_3N, but by NaH and Cs_2CO_3) were tested for hydrogel formation using their corrected degrees of functionalization. However, these experiments gave the same negative results and so the failure could not be attributed to the possibility of triethylammonium being present.

It must also be noted that the hydrogel formation study was not carried out on the ring-closed *p*-sulfonated calix[4]arene-grafted PSMAs owing to their extremely poor solubility in all solvents. Given the explained circumstances, the hydrogel formation idea was pursued through other approaches.

5.9.2 Gelation attempt on a *p*-sulfonated calix[4]arene-grafted PVP-MA

It was assumed that the failure of the PSMA-modified grafts to achieve gelation, could possibly be ascribed to their poor solubility in water (it was impossible to prepare very concentrated aqueous solutions of them). Therefore, it was decided that the study required some copolymer which could easily turn into a highly water-soluble product upon grafting with the calix[4]arene. Since the project was based on the succinic anhydride unit modification, a similar copolymer was suggested, namely poly[(*N*-vinylpyrrolidone)-*alt*-(maleic anhydride)] (**Figure 5.14**).

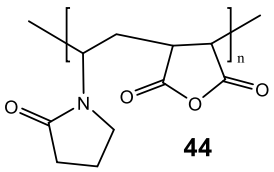

44

Figure 5.14 Poly[(N-vinylpyrrolidone)-alt-(maleic anhydride)] ***44***

Stellenbosch University https://scholar.sun.ac.za

This compound was supplied to us by Dr. Rueben Pfukwa's research group from the Polymer Science Division of the Department of Chemistry and Polymer Science at Stellenbosch University.[qqq]

Following the synthetic method presented in section 5.8, the PVP-MA 50% **44** was successfully modified with amine-tethered *p*-sulfonated calix[4]arene **33** (reaction in DMF at 75 °C overnight) (**Scheme 5.21**). This time only one inorganic base, NaH, was used for the deprotonation of the *p*-sulfonated calix[4]arene-amine (Et_3N was discarded to remove the possibility of any detrimental effect on the hydrogel formation). Additionally, as was the case for PSMA, the ring-closure of the graft was also attempted via heating the ring-opened one under reflux in glacial acetic (the analytical data for the second step; however, could not conclusively suggest the complete conversion of the ring-opened graft to the ring-closed one) (also **Scheme 5.21**).

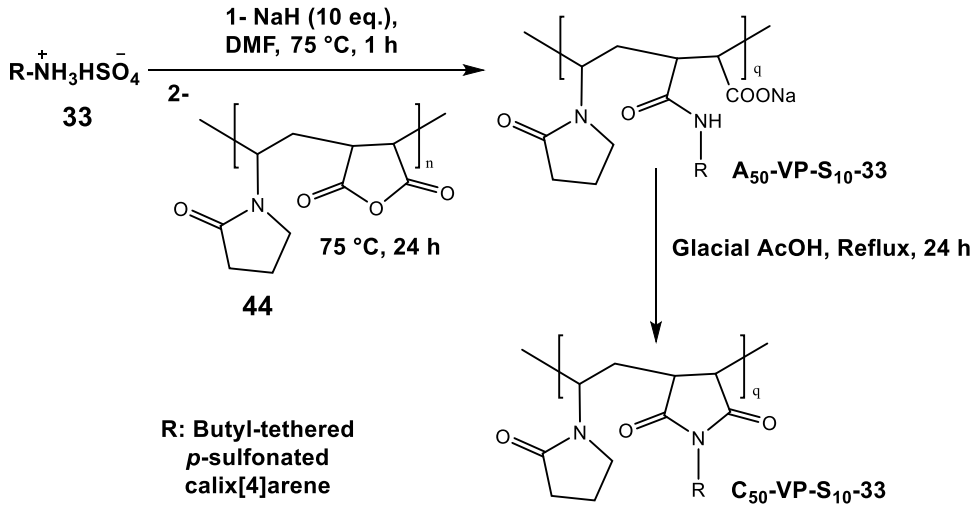

*Scheme 5.21 Modification of PVP-MA 50% **44** with an amine-tethered p-sulfonated calix[4]arene (**33**)*[rrr]

As was the case for PSMA, PVP-MA FT-IR spectrum also showed signals corresponding to its succinic anhydride moiety (such as symmetric and asymmetric stretches for anhydride carbonyl). Even so, the *N*-vinylpyrrolidone moiety exhibited another stretch for a carbonyl, this time for the amide C=O. After modification, as was the case for PSMA, PVP-MA also revealed evidence of sulfonate groups via characteristic S=O stretches (see an example in **Figure 5.15**).

[qqq] Its molar mass data are as determined by Dr. Pfukwa: M_n = 11 286 g.mol^{-1}, M_w = 38 984 g.mol^{-1}, Đ = 3.45.

[rrr] The middle letters VP refer to *N*-vinylpyrrolidone (q: Number of reacted *N*-vinylpyrrolidone-maleic anhydride).

Stellenbosch University https://scholar.sun.ac.za

Owing to the lack of solubility in THF and DMF, PVP-MA grafts of calix[4]arene were not submitted for GPC analysis.

Similar to the modified PSMA, PVP-MA modification with the calix[4]arene could be confirmed by the appearance of its methylene bridge in the ^{1}H-NMR spectrum (~4 ppm), in addition to the presence of aromatic protons of calix[4]aren (7-8 ppm) (see **Figure 5.16**).

UV-Vis spectra for the products were also obtained in water (concentration: 0.1 mg/mL) exhibiting an absorption band between 280 nm and 290 nm for the calix[4]arene attachment. DSC experiments were also performed with the protocols explained earlier in chapter 3.

As explained in the experimental section of this chapter, the FT-IR spectroscopy speculated functionalization degree for our graft was 24%. Therefore, approximately only one out of every four *N*-vinylpyrrolidone-maleic anhydride unit was modified by the calix[4]arene and consequently the hypothetical molecular weight of the graft was found to be 4151.85 g/mol (with approximately 25% modification of PVP-MA, 2.5 units of calix[4]arene was added to 10 units of *N*-vinylpyrrolidone -maleic anhydride) (see **Figure 5.17**).

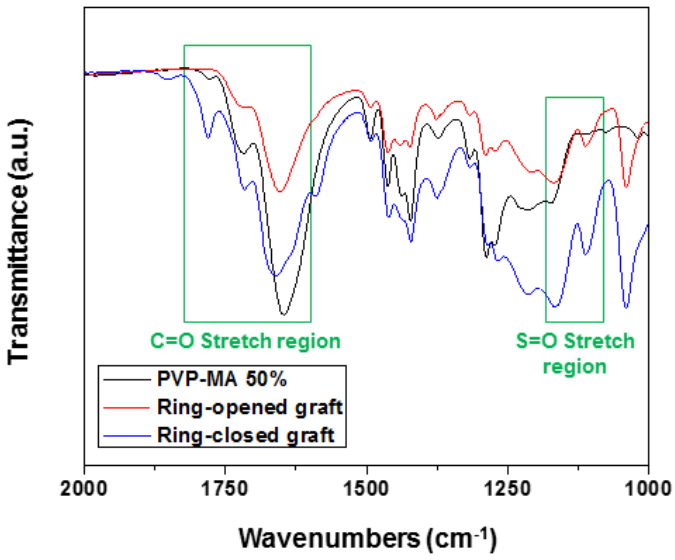

*Figure 5.15 Overlayed FT-IR spectra for PVP-MA 50% **44** and a ring-opened p-sulfonated calix[4]arene-grafted PVP-MA 50% example (**A_{50}-VP-S_{10}-33**) and its corresponding attempted ring-closed graft (**C_{50}-VP-S_{10}-33**) (Transmittance values were normalized to pyrrolidone bend at 1373 cm^{-1}, a.u: arbitrary unit)*

Stellenbosch University https://scholar.sun.ac.za

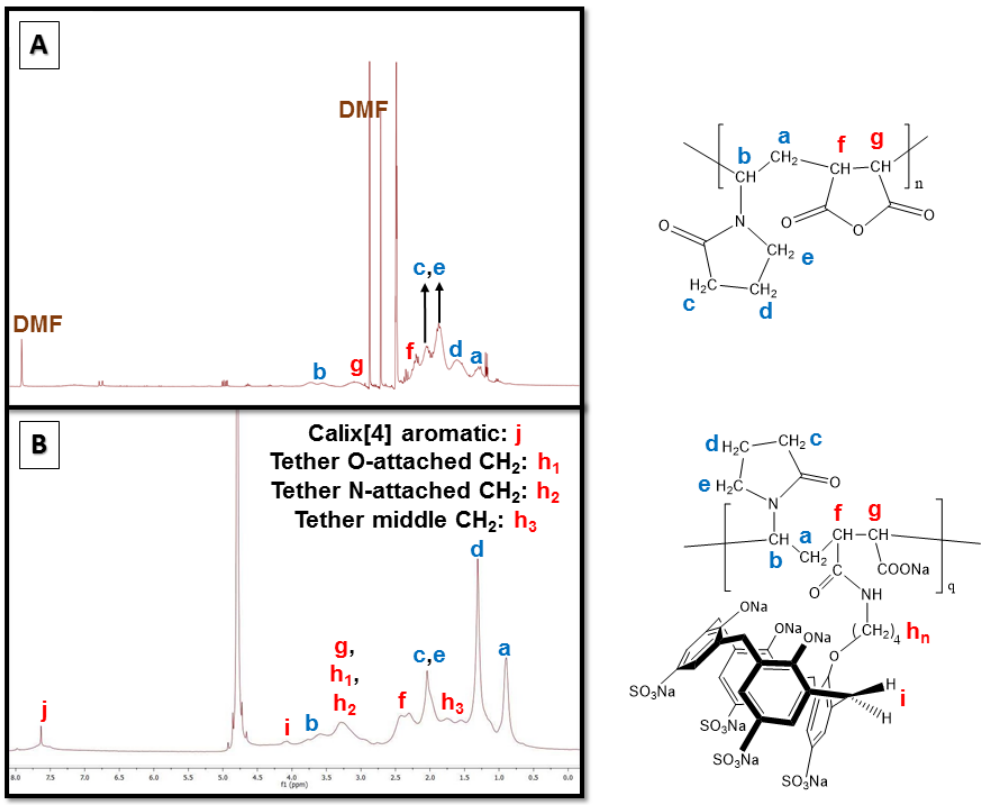

*Figure 5.16 A: ^{1}H-NMR spectrum (in DMSO-d_6) for PVP-MA 50% **44**; B: ^{1}H-NMR spectrum (in D_2O) for PVP-MA modified p-sulfonated calix[4]arene ring-opened graft (**A_{50}-VP-S_{10}-33**)*[sss]

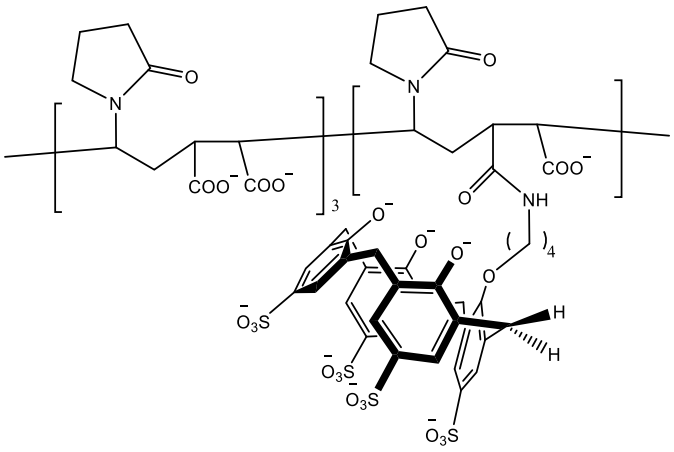

Figure 5.17 FT-IR spectroscopy speculated repeating unit for the ring-opened graft of amine-tethered p-sulfonated calix[4]arene and PVP-MA 50% (base choice: NaH 10.0 equiv.)

However, with knowledge from the previous section, the probability of fault in the measurement of the degree of functionalization was considered as a serious challenge.

[sss] The same speculation issue explained for PSMA-grafted compounds (section 5.8) regarding the aliphatic region interpretation is also true for PVP-MA-grafted compounds here (q: Number of reacted *N*-vinylpyrrolidone-maleic anhydride).

Stellenbosch University https://scholar.sun.ac.za

Following the same ^{1}H-NMR spectroscopic titration approach, a 50.0 mg/mL solution of the graft **A_{50}-VP-S_{10}-33** in D_2O amounted to be 0.030 mmol (effective mmol was calculated by dividing 50 mg by 4151.85 mg/mmol, giving 0.012042 mmol and then multiplying that figure by 2.5 for calix[4]arene units to yield 0.030 mmol) was prepared. Then, this solution was titrated with 75 µL (0.015 mmol) from a 0.2 M solution of methyl viologen salt **34** to fulfill a 2 to 1 host:guest mmol ratio. The same fault observed in measuring the functionalization degree of the PSMA-originated graft, occurred this time for the PVP-MA modified graft. Instead of witnessing 8 aromatic protons for the calix[4]arene versus 4 aromatic protons of the methyl viologen salt **34**, 20 aromatic protons were seen for the methyl viologen salt **34**. This suggested that our polymer had only been 4.8% modified and to achieve a 2 to 1 ratio between the graft and the amine, only $\frac{1}{5}$ of the initial amine amount must have been added. As was the case for the PSMA grafts, the PVP-MA graft also made the viologen protons move upfield as an indication of its interaction with the quaternary amine (all spectra can be seen in **Figure 5.18**).

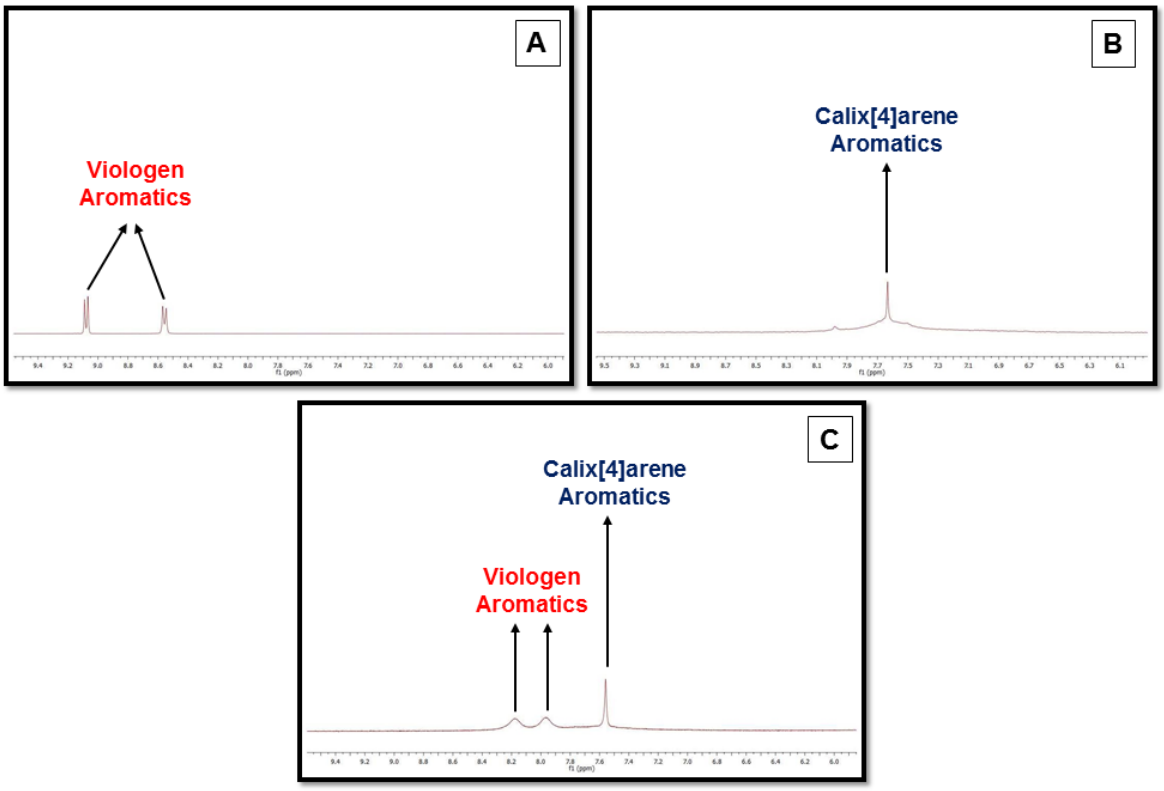

*Figure 5.18 ^{1}H-NMR spectroscopic titration (in D_2O) on a p-sulfonated calix[4]arene-grafted PVP-MA 50% (**A_{50}-VP-S_{10}-33**) using methyl viologen salt **34**; A: Blank methyl viologen salt **34**; B: Blank graft (**A_{50}-VP-S_{10}-33**); C: methyl viologen salt **34** plus graft (**A_{50}-VP-S_{10}-33**)*

Due to the extremely highly soluble nature of this ring-opened graft (**A_{50}-VP-S_{10}-33**), it was possible to prepare an aqueous solution with a maximum concentration of 1 g/1 mL. As an example, a 0.1 g/0.1 mL (1 g/1 mL) solution of the graft amounted to be 0.0191 mmol (the

Stellenbosch University https://scholar.sun.ac.za

corrected value for the degree of functionalization was used) and obviously to start the hydrogel formation study with a 100 to 1 ratio, 0.000191 mmol of the amine was required. As was the case for PSMA section, a concentrated solution of the amine had to be prepared (here 0.05 M) and a tiny amount of amine needed to be added (here 3.8 μL for 100 to 1 ratio). Unfortunately, despite employing all approaches and playing with every parameter mentioned for PSMA, the hydrogel formation was not achieved for this ring-opened graft either (**A_{50}-VP-S_{10}-33**).[ttt]

5.10 Possible role of the calix[4]arene conformation on the failure of hydrogel formation study

The only remaining parameter which might have some effect on our gelation failure was the issue of conformation for our amine-tethered *p*-sulfonated calix[4]arene (**33**) and also for the calix[4]arene moiety of the graft. It is highly critical to know that according to some studies the adoption of the partial cone conformation by the calix[4]arene can lead to a significant decrease in its encapsulation potency toward different species.[106,107] Just recently, a paper by Crowley and co-workers on *p*-sulfonated calix[4]arenes tethered with mono- and bis-substituents of polyethylene glycol (PEG) encapsulating proteins was published. It was claimed in this work that in the case of the mono-substituted calix[4]arene, the graft adopted the partial cone conformation affecting its encapsulation ability (**Figure 5.19**).[108]

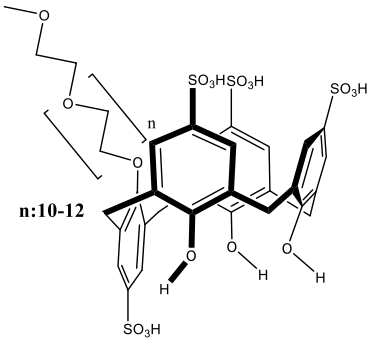

Figure 5.19 Partial cone mono-substituted p-sulfonated calix[4]arene with a long polyethylene glycol chain used by Crowley and co-workers[108]

Thus, the assumption of our *p*-sulfonated calix[4]arene (**33**) adopting a partial cone conformation as a possible reason for perturbing the hydrogel formation process for our water-soluble grafts must be investigated. In line with the literature examples,[109] and what was presented in chapter 2, in case of the mono-alkylated *t*-butyl-calix[4]arene upon adopting the

[ttt] However, the synthesis of the ring-closed graft (**C_{50}-VP-S_{10}-33**) was not conclusively confirmed, it was also subjected to the hydrogel formation study. The result was also a failure.

Stellenbosch University https://scholar.sun.ac.za

cone conformation, the methylene bridge can show up as four doublets including two equatorial (4 protons) and two axial (4 protons) while for the partial cone conformation typically two doublets (2 protons each) and one multiplet (4 protons) can be seen at room temperature. Also, the aromatic protons of calix[4]arene can appear as two singlets (2 protons each) and two doublets (2 protons each) for the cone conformation, while for the partial cone one they can be seen as three sharp singlets at room temperature (two of them with 2 protons and one with 4 protons). Unfortunately, due to the significant peak-broadening observable in the ^{1}H-NMR spectrum of our *p*-sulfonated calix[4]arene (**Figure 5.7**), it was not possible to determine its conformations at room temperature with confidence (none of the splitting patterns explained above was observed). To see some possible change in the appearance of the signals in the ^{1}H-NMR spectrum of our *p*-sulfonated calix[4]arene (**33**), an experiment was run at a high temperature (90 °C), so that a more clear splitting pattern could be witnessed for the signals of interest (through changing the relaxation time of the protons).[uuu] Despite this, the new aliphatic region still remained for the complex (methylene bridge status was unknown) and though the aromatic region splitting pattern changed again, it did not produce either of the patterns clarified earlier. The aromatic region exhibited four doublets with unequal integrations. In fact, this may suggest that our calix[4]arene did not adopt a fixed conformation (**Figure 5.20**).

To understand this, a comprehensive study by Sciotto and co-workers regarding the recognition of aromatic ammonium cations by water-soluble sulfonated and carboxylated calix[4]arenes is worth mentioning.[110] The purpose of that study (employing combined NMR spectroscopy, calorimetry and also molecular mechanics calculations) was the specific recognition of the guests by their calix[4]arene hosts via different binding modes. For example, it was discovered that calix[4]arenes **1a** and **1b** exhibited selective binding behavior (**1a** only binds R–NMe_3^+ moiety of the quaternary amines, while **1b** co-ordinates with the aromatic ring of the quaternary amine), while calix[4]arene **1c** did not have any selective binding behavior toward either of the quaternary amine guests. The notable aspect of this study was that the researchers attributed this phenomenon to the conformational feature of the hosts. They found that host **1c** possessed a mobile conformation, while hosts **1a** and **1b** had fixed conformations (**Figure 5.21**).

[uuu] This experiment was performed using a 400 MHz instrument. The room temperature spectrum performed by the same instrument did not show any different result compared to what obtained by the 300 MHz instrument at room temperature.

Stellenbosch University https://scholar.sun.ac.za

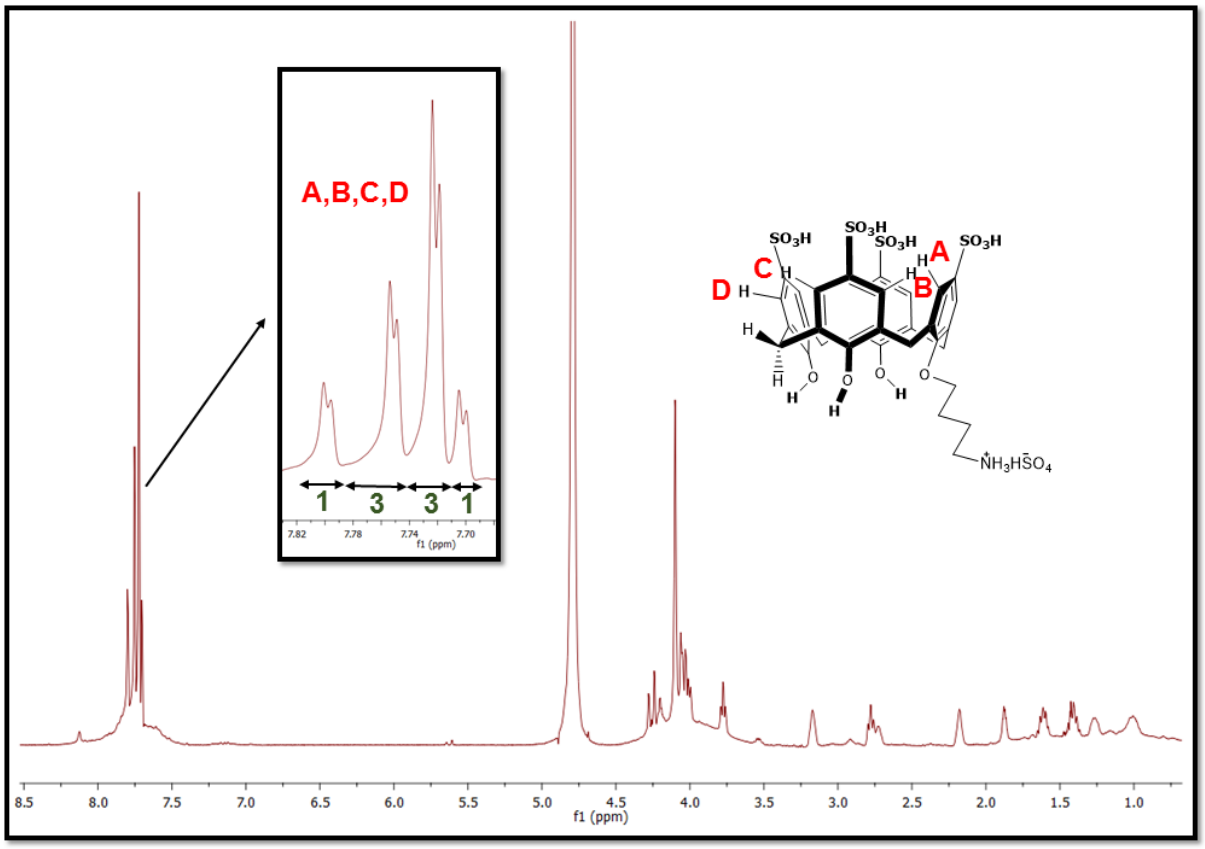

*Figure 5.20 ^{1}H-NMR spectrum (in D_2O) for the desired amine-tethered p-sulfonated calix[4]arene **33** at 90 °C*

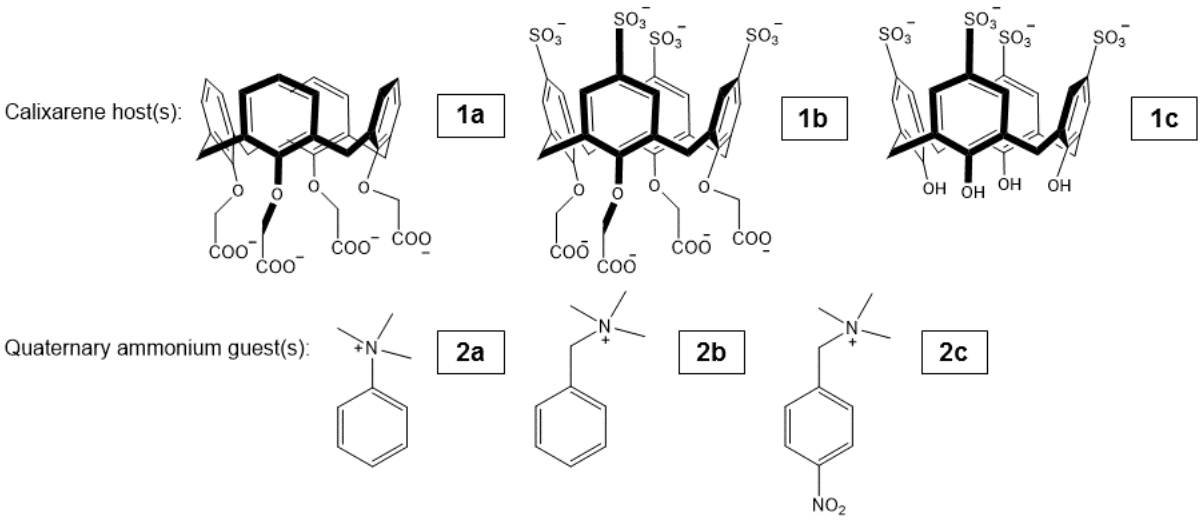

Figure 5.21 Water-soluble calix[4]arenes used for encapsulation of the quaternary ammonium guests based on the work of Sciotto and co-workers[110]

This may well justify our challenge to get the gelation study to work. Our choice of *p*-sulfonated calix[4]arene (**33**), which resembles host **1c** the most (except for its amine tether), possibly suffers from the same disadvantage that the mentioned host does. It is possible that it cannot remain in the favored cone formation (with maximum potential for encapsulation) and

Stellenbosch University https://scholar.sun.ac.za

rapidly transforms into the disfavored partial cone conformation (the worst choice for encapsulation) back and forth (an equilibrium state). Overall, our ^{1}H-NMR spectral data and the literature suggestions magnify the importance of having the calix[4]arene host in a fixed cone conformation.

5.11 Concluding remarks

In total, the synthesis of a water-soluble calix[4]arene using a previously made amine-tethered parent was successfully carried out through the sulfonation reaction at temperatures lower than that suggested by the Shinkai's approach.[1] The work-up troubles experienced in Shinkai's approach were also resolved by employing non-aqueous procedures. In respect with some literature reports on the strong interaction between bis-quaternary amines and water-soluble calix[4]arenes (the existence of a large-value association constant for calix[4]arene-amine complex), the prospect of a crosslinked network formation on a supramolecular scaffold was considered. Looking at a paper by Liu *et al*. in which a crosslinked network was constructed using a *p*-sulfonated calix[4]arene and a viologen-modified polyvinyl alcohol,[35] the formation of a hydrogel via mixing a polymeric *p*-sulfonated calix[4]arene with a bis-quaternary amine (the chemical stimulus) was followed. In achieving that goal, the knowledge obtained from chapter 3 (grafting PSMA 30% with calix[4]arene-amines) was used to produce water-soluble PSMA grafts with the help of the amine-tethered *p*-sulfonated calix[4]arene **33**. Due to the low water-solubility of these PSMA 30% grafts, a radical polymerization approach was planned to prepare PSMA 50%, so that after its grafting with water-soluble calix[4]arene, grafts with higher water-solubility could be produced. Despite managing to make the desired PSMA 50% grafts and improvement of water-solubility, the idea of hydrogel formation on PSMA-originated grafts did not contribute to any success. The alternative to the PSMA method was to use a similar copolymer with a higher prospect of becoming water-soluble upon modification. In doing so, PVP-MA was chosen and used for producing the desired water-soluble graft. In spite of having a lower degree of functionalization (compared to PSMA), a highly water-soluble graft was synthesized. Unfortunately, the hydrogel formation study failed again, even though a much more concentrated aqueous solution of the graft was used. For both grafts (PSMA and PVP-MA originated ones), the possible parameters causing failure were investigated. Amongst these parameters, the temperature, the pH, a possibly inappropriate base choice (such as Et_3N), the quaternary amine nature could be ruled out as the reasons for failure due to the fact that the study failed even with trying many alternative options for them and covering numerous possible angles. It is believed that most likely two matters could result in

Stellenbosch University https://scholar.sun.ac.za

the failure of this study. The first was the degree of functionalization. The ^{1}H-NMR spectroscopic titration study on our grafts (using viologen methyl iodide **34** as the titrating agent) gave us both positive and negative results. The positive result was the confirmation of our water-soluble calix[4]aren-grafted polymer interaction with the quaternary amine through the large upfield chemical shift for the viologen aromatic protons (an indication that at least the amine guests had been encapsulated by the calix[4]arene host). The negative result was disproving the high degrees of functionalization speculated by FT-IR spectroscopy. Unlike what FT-IR spectroscopy predicted, the maximum degree to which our pristine polymers became functionalized in this study was 5.9% for PSMA and 4.8% for PVP-MA.[vvv] Possibly, the low reactivity of the *p*-sulfonated calix[4]arene-amine **33** was the reason for this result. It is very unlikely that the deactivating effect of the sulfonate groups on the aromatic ring, could cause an electronic withdrawal on the tether resulting in the dramatic decrease of the primary amine nucleophilicity. That is due to the long distance between the sulfonate groups and the amine nucleophile on the calix[4]arene scaffold. Instead, it appears more rational that the sulfonate groups facilitated some sort of a self-encapsulation process through which the amine tale of the calix[4]arene became entangled within the calix[4]arene cavity. Due to this undesired phenomenon, only a few *p*-sulfonated calix[4]arene molecules managed to react with the polymer. That is why, unlike its corresponding model amine discussed in chapter 3 (*t*-butylated calix[4]arene-amine $\mathbf{10_b}$), our *p*-sulfonated calix[4]arene-amine **33** was not capable of forming a polymeric graft with a high degree of modification. As a result, it cannot be stated with certainty that the number of *p*-sulfonated calix[4]arene per polymer subunit was enough to encapsulate a large number of the amine guests and facilitate crosslinking efficiently. The second matter which also remained unclear, was the issue of conformation for the *p*-sulfonated calix[4]arene **33**. It seemed highly likely that adopting a partial cone conformation (as a result of sulfonation reaction on our butylamine-tethered *t*-butylated calix[4]arene $\mathbf{10_b}$), drastically decreased the calix[4]arene capability to encapsulate and eventually form a hydrogel employing the amine units. That is by far the most probable cause of the failure for hydrogel formation study, even though the ^{1}H-NMR spectra were unable to identify the precise conformational status of the *p*-sulfonated calix[4]arene (**33**) due to its conformationally mobile nature.

[vvv] FT-IR spectroscopy suggested that those values should respectively be 71% and 24% for PSMA and PVP-MA.

Stellenbosch University https://scholar.sun.ac.za

5.12 Experimental section

Following the points explained in the previous sections and the rules applied in chapter 3, the synthesis and the characterization of several *p*-sulfonated calix[4]arene-grafted PSMAs will be presented in this section. It must be noted that all these examples are the water-soluble grafts stemmed from PSMA 50% and the rest will be covered in the appendix of this dissertation. However, first of all, the synthesis and the characterization of the primary-amine tethered *p*-sulfonated calix[4]arene **33**, all our bis-quaternary ammonium salts and eventually PSMA 50% will be discussed. Having finished the PSMA-related grafts synthesis, the synthesis and the characterization of the PVP-MA-related grafts will be presented.

5.12.1 Synthesis of 25-mono-(4-aminobutoxy)-26,27,28-trihydroxy-calix[4]arene-5,11,17,23-tetrasulfonic acid (the ammonium hydrogen sulfate salt) – 33

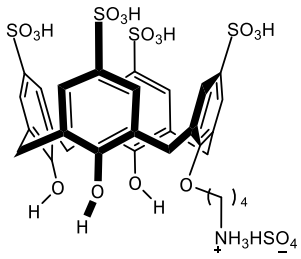

5,11,17,23-Tetra-*t*-butyl-25-mono-(4-aminobutoxy)-26,27,28-trihydroxy-calix[4]arene **10b** (280 mg, 0.410 mmol) was stirred in concentrated sulfuric acid (95-97%) (2.00 mL) in a round-bottom flask at room temperature for 17 hours. The reaction was then poured into ice-cold diethyl ether (100 mL) and the resulting solid was collected. After that, this solid was dissolved in methanol (50 mL) and precipitated by adding ethyl acetate (200 mL) forming a hygroscopic green-brown powder. Thereafter, the powder was freeze dried for 24 hours (to remove most of the encapsulated solvent by the calix[4]arene during the work-up). In the end, this resulting solid underwent a post-heating process at 100 °C under vacuum for 24 hours (to eliminate the remnants of diethyl ether and methanol not removed by the freeze dryer) to yield a green-brown product (360 mg, 95%). Mp 252 °C DEC; ^{1}H-NMR (300 MHz, D_2O) δ ppm 1.00-4.50 (a collection of broad signals: 4H, C-CH_2-C + 2H, C-CH_2N + 2H, C-NH_2 + 2H, OCH_2-C + 8H, ArCH_2Ar), 7.01 (br. s, 2H, ArH), 7.06 (br. s, 4H, ArH), 7.10 (br. s, 2H, ArH). ^{13}C-NMR (75 MHz, D_2O) δ ppm 22.9 (CH_2), 24.9 (CH_2), 30.2 (CH_2), 38.6 (CH_2), 43.9 (C-CH_2N), 68.1 (OCH_2-C), 126.0 (Ar), 126.8 (Ar), 127.8 (Ar), 133.7 (Ar), 134.8 (Ar), 135.6 (Ar), 151.0 (3 × C_{Ar}O), 153.0 (C_{Ar}OC).[www]

FT-IR (ATR) cm^{-1}: 3177 (b, O-H stretch), 1646 (m, N-H bend), 1151 (s, asymmetric S=O stretch), 1116 (s, symmetric S=O stretch), 1026 (m, C-O stretch), 868 (m, C–H oop bend), 785 (m, C–H oop bend).

[www] These results were all obtained at room temperature.

Stellenbosch University https://scholar.sun.ac.za

HRMS-TOF MS ESI$^+$: *m/z* $[M+H]^+$ calculated for $C_{32}H_{34}NO_{16}S_4$ 816.0760 Da; found: 816.0772 Da.[xxx]

5.12.2 Synthesis of 1,1'-dimethyl-[4,4'-bipyridine]-1,1'-diium iodide – 34

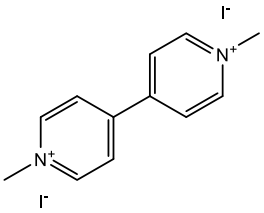

To a round-bottom flask containing 4,4'-bipyridine (100 mg, 0.640 mmol) in dry acetonitrile (20 mL) in an ice-bath, was gently added iodomethane (4.00 g, 1.75 mL, 28.0 mmol). Then, the ice-bath was removed, the flask was equipped with a condenser and the system was heated under reflux for 24 hours. Afterward, the heating was stopped and the solvent was removed under the reduced pressure. Finally, the resulting orange solid was dried under vacuum to yield 270 mg of the bis-quaternary amine (96%). The spectral data were correlated with that from literature;[98] ^{1}H-NMR (300 MHz, D_2O) δ ppm 4.51 (s, 6H, CH_3), 8.53 (d, *J*=6.3 Hz, 4H, ArH), 9.06 (d, *J*=6.3 Hz, 4H, ArH).

5.12.3 Synthesis of 1,1''-(ethane-1,2-diyl)bis(([4,4'-bipyridin]-1-ium)) bromide – 35

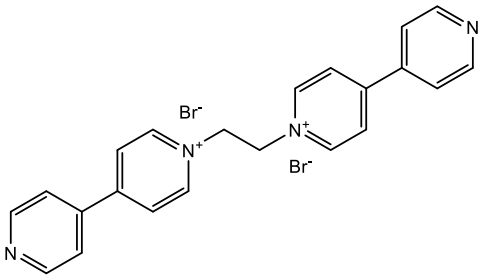

4,4'-Bipyridine (2.50 g, 16.0 mmol) was dissolved in DMF (20 mL) and to that solution was added 1,2-dibromoethane (0.740 g, 0.340 mL, 4.00 mmol). This solution was heated at 70 °C for 24 hours and then the resulting yellowish solid was filtered off. This slimy solid was treated with diethyl ether (50 mL) to produce 410 mg of a brown-yellow fine powder (20%). The spectral data were correlated with that from literature;[100] ^{1}H-NMR (300 MHz, D_2O) δ ppm 5.48 (s, 4H, CH_2-CH_2), 7.97 (d, *J*=6.4 Hz, 4H, ArH), 8.54 (d, *J*=6.9 Hz, 4H, ArH), 8.81 (d, *J*=6.2 Hz, 4H, ArH), 9.06 (d, *J*=7.0 Hz, 4H, ArH).

[xxx] H_2SO_4 was not involved in the calculations since it was removed from the molecule through the ionization process.

Stellenbosch University https://scholar.sun.ac.za

5.12.4 Synthesis of 1',1'''-(ethane-1,2-diyl)bis(1-methyl-[4,4'-bipyridine]-1,1'-diium) dibromide diiodide – 36

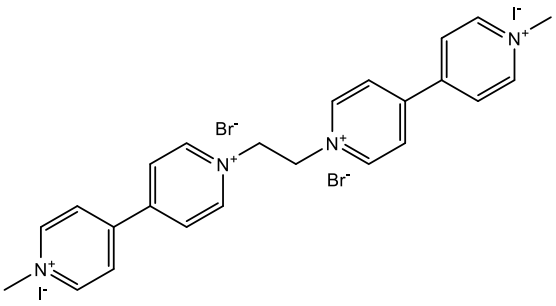

The dimerized 4,4'-bipyridine **35** (400 mg, 0.800 mmol) was placed in DMF (8 mL) at 0 °C. To that, iodomethane (2.28 g, 1.00 mL, 16.0 mmol) was gently added and then the reaction vessel was equipped with a reflux condenser and heated at 90 °C for 24 hours. After that, the solid crude was collected via suction and rinsed with acetonitrile (50 mL) to yield a 590 mg of an orange powder (94%). The spectral data were correlated with that from literature;[90] ^{1}H-NMR (300 MHz, D_2O) δ ppm 4.54 (s, 6H, CH_3), 5.58 (s, 4H, CH_2-CH_2), 8.60 (d, *J*=6.8 Hz, 4H, ArH), 8.71 (d, *J*=6.8 Hz, 4H, ArH), 9.10 (d, *J*=6.8 Hz, 4H, ArH), 9.28 (d, *J*=6.8 Hz, 4H, ArH).

5.12.5 Synthesis of 1,1''-(hexane-1,6-diyl)bis(([4,4'-bipyridin]-1-ium)) bromide – 37

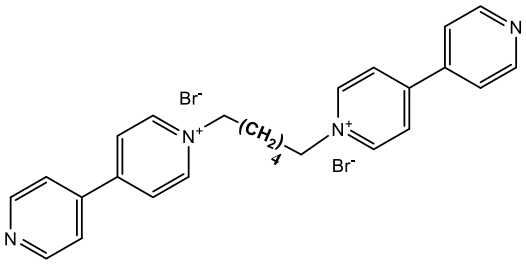

This compound was synthesized following the method used for compound **35** using 4,4'-bipyridine (2.50 g, 16.0 mmol) in DMF (20 mL) plus 1,6-dibromohexane (970 mg, 0.610 mL, 4.00 mmol). After filtration, followed by trituration with diethyl ether (50 mL), the resulting orange-yellow crude was recrystallized with the minimum amount of water producing 1.09 g of a pale yellow crystal (49%). The spectral data were correlated with that from literature;[101] ^{1}H-NMR (300 MHz, D_2O) δ ppm 1.42-1.52 (m, 4H, C-CH_2-C), 2.04-2.16 (m, 4H, C-CH_2-C), 4.68 (t, *J*=7.1 Hz, 4H, CH_2N), 7.88 (d, *J*=6.3 Hz, 4H, ArH), 8.38 (d, *J*=7.0 Hz, 4H, ArH), 8.74 (d, *J*=6.3 Hz, 4H, ArH), 8.97 (d, *J*=7.0 Hz, 4H, ArH).

5.12.6 Synthesis of 1',1'''-(hexane-1,6-diyl)bis(1-methyl-[4,4'-bipyridine]-1,1'-diium) dibromide diiodide – 38

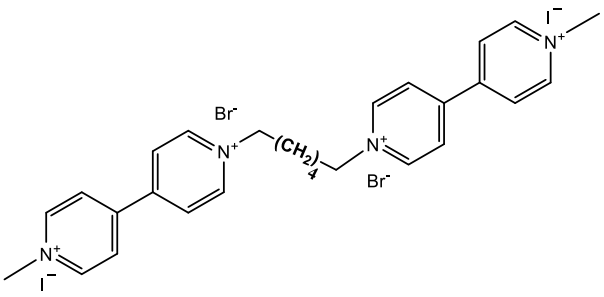

Following the approach employed for compound **36**, this compound was produced via the dimerized 4,4'-bipyridine **37** (1.07 g, 1.92 mmol) in DMF (19.2 mL) and iodomethane (5.47 g, 2.40 mL, 38.4 mmol). After filtration, followed by trituration with

Stellenbosch University https://scholar.sun.ac.za

acetonitrile (50 mL), 1.25 g of an orange powder was collected (80%). Mp 270 °C DEC; ^{1}H-NMR (300 MHz, D_2O) δ ppm 1.48-1.57 (m, 4H, C-CH_2-C), 2.09-2.21 (m, 4H, C-CH_2-C), 4.52 (s, 6H, CH_3), 4.76 (t, *J*=7.2 Hz, 4H, CH_2N), 8.52-8.61 (m, 8H, ArH), 9.07 (d, *J*=6.7 Hz, 4H, ArH), 9.14 (d, *J*=6.8 Hz, 4H, ArH). ^{13}C-NMR (75 MHz, $CDCl_3$) δ ppm 24.8 (2 × C-CH_2-C), 30.4 (2 × C-CH_2-C), 48.4 (2 × CH_3N), 61.9 (2 × C-CH_2N), 126.7 (Ar), 127.1 (Ar), 145.4 (Ar), 146.2 (Ar), 149.7 (Ar), 150.0 (Ar).

FT-IR (ATR) cm^{-1}: 3490 (b, residual water stretch), 3002 (m, Aromatic C-H stretch), 2856 (m, Aliphatic C-H stretch), 1635 (s, Aromatic C=C stretch), 1557 (m, Aromatic C=C stretch), 1440 (m, Aliphatic CH_3 bend), 1349 (m, Aliphatic CH_3 bend), 1183 (m, C-N stretch), 813 (m, C–H oop bend), 708 (m, C–H oop bend).

HRMS-TOF MS ESI$^+$: *m/z* $[M–Br_2I+H]^+$ calculated for $C_{28}H_{35}IN_4$ 554.1906 Da; found: 554.1863 Da.

Also: 681.0914 Da (calculated for $[M–Br_2+H]^+$: 681.0951 Da).

5.12.7 General procedure for the synthesis of quaternary ammonium salts 39, 40, 41

According to the method devised by Zaimis, the amine was dissolved in methanol together with sodium hydroxide pellets (9.0 equiv.) in an ice bath. Then iodomethane (9.0 equiv.) was added slowly and the tube was sealed and heated under reflux for 24 hours. Afterward, the heating was stopped and the solvent evaporated under the reduced pressure. The residue was triturated with boiling acetone (50 mL) to dissolve and remove sodium iodide. Thereafter the insoluble material was washed with cold acetone (50 mL) and collected to afford our desired quaternary ammonium salt.[102]

5.12.7.1 Synthesis of *N,N,N′,N′,N′,N′*-hexamethylethane-1,2-diaminium iodide – 39

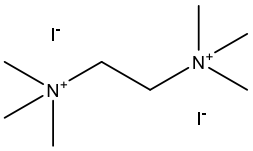

Following the general procedure, *N,N,N′,N′*-tetramethylethane-1,2-diamine (TMEDA) (500 mg, 0.645 mL, 4.30 mmol) and NaOH (1.55 g, 38.7 mmol) and iodomethane (5.49 g, 2.41 mL, 38.7 mmol) were heated under reflux in methanol (6 mL) to yield a pale-yellow powder (1.00 g, 58%); The spectral data were correlated with that from literature;[102] Mp 250 °C DEC; ^{1}H-NMR (300 MHz, D_2O) δ ppm 3.37 (s, 18H, $N^+(CH_3)_3$), 4.10 (s, 4H, CH_2). ^{13}C-NMR (75 MHz, $CDCl_3$) δ ppm 53.8 (6 × CH_3), 57.8 (2 × CH_2).

Stellenbosch University https://scholar.sun.ac.za

5.12.7.2 Synthesis of 2,2'-(methylazanediyl)bis(*N*,*N*,*N*-trimethylethan-1-aminium) iodide – 40

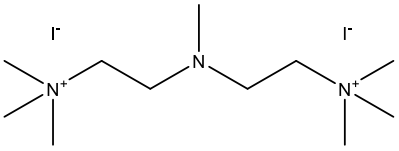

Following the general procedure, *N*,*N*,*N*′,*N*″,*N*″-pentamethyldiethylenetriamine (PMDTA) (300 mg, 0.360 mL, 1.73 mmol) and NaOH (620 mg, 15.6 mmol) and iodomethane (2.26 g, 0.990 mL, 15.6 mmol) were heated under reflux in methanol (6 mL) to yield a pale-yellow powder (640 mg, 81%); The spectral data were correlated with that from literature;[102,104] Mp 228 °C; ^{1}H-NMR (300 MHz, D_2O) δ ppm 2.41 (s, 3H, N-CH_3), 3.07 (t, *J*=7.5 Hz, 4H, N-CH_2-C), 3.24 (s, 18H, $N^+(CH_3)_3$), 3.59 (t, *J*=6.9 Hz, 4H, N^+-CH_2-C). ^{13}C-NMR (75 MHz, $CDCl_3$) δ ppm 40.8 (CH_3), 50.5 (6 × CH_3), 53.7 (2 × N-CH_2-C), 62.5 (2 × N^+-CH_2-C).

5.12.7.3 Synthesis of *N*,*N*,*N*,*N*′,*N*′,*N*′-hexamethylhexane-1,6-diaminium iodide – 41

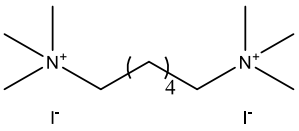

Following the general procedure, hexane-1,6-diamine (250 mg, 2.15 mmol) and NaOH (770 mg, 19.3 mmol) and iodomethane (2.75 g, 1.20 mL, 19.3 mmol) were heated under reflux in methanol (6 mL) to yield a pale-yellow powder (760 mg, 77 %); The spectral data were correlated with that from literature;[102] Mp 270 °C; ^{1}H-NMR (300 MHz, D_2O) δ ppm 1.44-1.54 (m, CH_2-CH_2, 4H), 1.78-1.95 (m, C-CH_2-C, 4H), 3.16 (s, 18H, $N^+(CH_3)_3$), 3.33-3.43 (m, 4H, N-CH_2-C). ^{13}C-NMR (75 MHz, $CDCl_3$) δ ppm 22.1 (2 × C-CH_2-C), 25.0 (2 × C-CH_2-C), 52.8 (6 × CH_3), 66.3 (2 × C-CH_2N).

5.12.8 Synthesis of *N*,*N*,*N*,*N*′,*N*′,*N*′-hexaethylhexane-1,6-diaminium bromide – 42

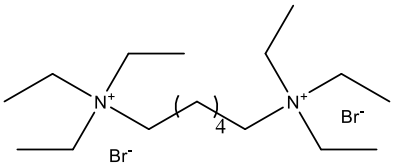

According to a previously reported approach by Sasidharana and Bhaumik, 1,6-dibromohexane (240 mg, 0.150 mL, 1.00 mmol) and triethylamine (220 mg, 0.310 mL, 2.20 mmol) were heated under reflux in a sealed tube containing dry acetone (2.5 mL) overnight. After that, the reaction was cooled and filtered and the product was washed with acetone (5×10 mL) several times to produce a pale-yellow powder (310 mg, 57%); The spectral data were correlated with that from literature;[103] Mp 268 °C; ^{1}H-NMR (300 MHz, D_2O) δ ppm 1.29 (bt, 18H, CH_3-C), 1.42-1.51 (m, C-CH_2-C, 4H), 1.65-1.81 (m, CH_2-CH_2, 4H), 3.14-3.24 (m, N-CH_2-C, 4H), 3.31 (q, *J*=7.5 Hz, 12H, C-CH_2-N). ^{13}C-NMR (75 MHz, $CDCl_3$) δ ppm 6.6 (6 × CH_3-C), 20.8 (2 × C-CH_2-C), 25.2 (2 × C-CH_2-C), 52.4 (6 × C-CH_2N), 56.2 (2 × C-CH_2N).

Stellenbosch University https://scholar.sun.ac.za

5.12.9 Synthesis of poly(styrene-*alt*-maleic anhydride) or P(St-*alt*-MA) – 43

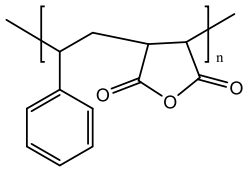

Freshly distilled styrene (2.00 g, 19.2 mmol) was added to a solution of freshly sublimed maleic anhydride (2.07 g, 21.1 mmol) and 2,2′-azobis(2-methylpropionitrile) (AIBN) (133 mg, 0.810 mmol) in dry methyl ethyl ketone (4 mL). The reaction was degassed with argon for 30 minutes, sealed and heated at 65 °C overnight. Thereafter, the viscous sticky crude dissolved in acetone (20 mL) and poured in 2-propanol (250 mL). The white solid formed was filtered using a Buchner funnel and the product was dried at room temperature under vacuum for 24 hours to afford 4.00 g of the desired copolymer.

5.12.9.1 Characterization of PSMA 50%

5.12.9.1.1 ATR-FTIR spectroscopy

In the FT-IR spectrum (**Figure 5.22**), several characteristic signals are observable.[yyy]

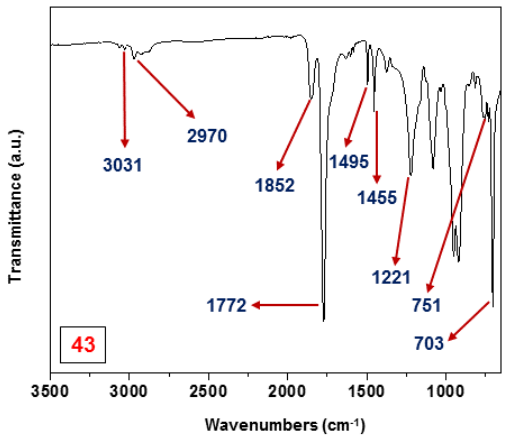

*Figure 5.22 PSMA 50% **43** FT-IR spectrum (Transmittance values were normalized to styrene bend at 700 cm^{-1}, a.u: arbitrary unit)*

Two bends related to out of plane modes of C-H (styrene) can be seen at 703 cm^{-1} (strong) and 751 cm^{-1} (weak). C-O stretch shows up as a medium signal at 1221 cm^{-1}. A bend at 1455 cm^{-1} (medium) belongs to C-H (polymer chain) and also a bend at 1495 cm^{-1} attributable to the aromatic C=C (styrene) are available. More importantly, the anhydride group reveals itself as a symmetric stretch at 1772 cm^{-1} (strong) and an asymmetric stretch at 1852 cm^{-1} (weak). Moreover, there are two very weak stretches at 2970 cm^{-1} (sp^2 aromatic C-H for styrene) and 3031 cm^{-1} (sp^3 aliphatic C-H for polymer chain). The final worthwhile point is

[yyy] These signals can be interpreted very much like the ones observed for PSMA 30% (**11**) in chapter 3.

Stellenbosch University https://scholar.sun.ac.za

the intensity of the styrene signal at 703 cm^{-1} compared to the maleic anhydride one at 1772 cm^{-1}. These two signals relatively have equal intensities which denote the existence of an alternate PSMA (unlike PSMA 30% with the relative ratio of 2 to 1 in favor of the styrene unit)

5.12.9.1.2 NMR spectroscopy

The spectrum was obtained in the deuterated dimethyl sulfoxide (DMSO-d_6).

5.12.9.1.2.1 ^{1}H-NMR spectroscopy

The solvent impurities can be seen at 1.10 ppm (2-propanol), and 1.76 ppm and 3.60 ppm (THF). The CH_2 and CH groups of the backbone (originated from styrene vinyl) are observable between 1.79 ppm to 2.40 ppm while CH groups of the backbone (stemmed from maleic anhydride) can be witnessed between 2.90 ppm to 3.64 ppm. In the end, the aromatic protons (styrene CHs) can be found between 6.17 ppm to 7.55 ppm (**Figure 5.23**).[zzz]

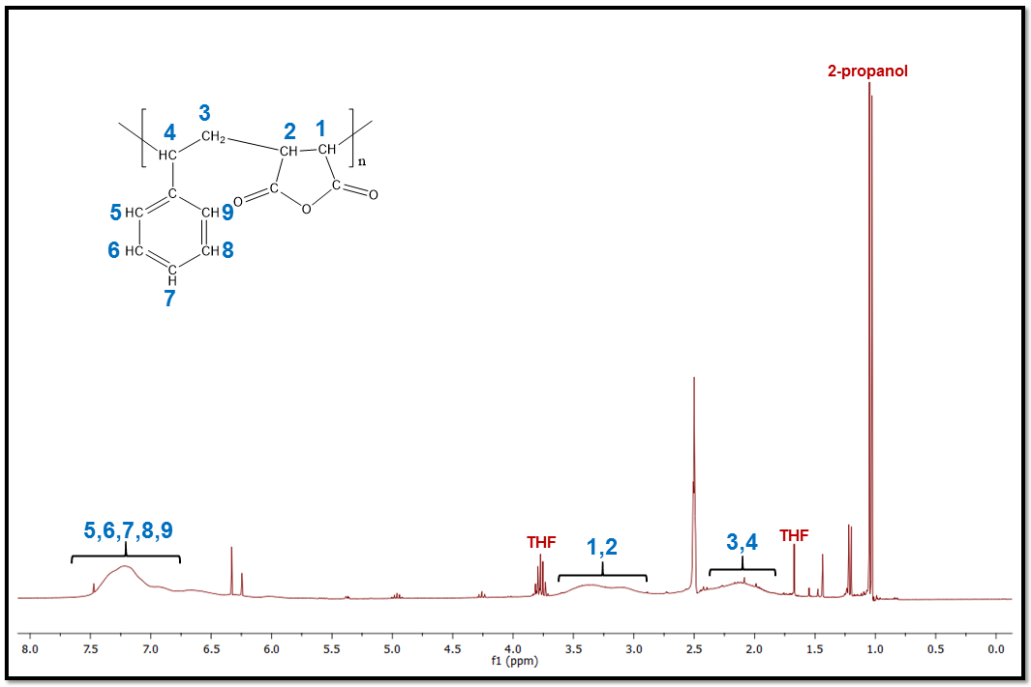

*Figure 5.23 PSMA 50% **43** ^{1}H-NMR spectrum (in DMSO-d_6)*

5.12.9.1.2.2 ^{13}C-NMR spectroscopy

The solvent impurities can be seen at 25.4 ppm and 64.9 ppm (2-propanol) and 25.1 ppm and 67.0 ppm (THF). The CH_2 group of the backbone (originated from styrene vinyl), the CH group of the backbone (originated from styrene vinyl), the CHs group of the backbone (stemmed from maleic anhydride), the aromatic CHs of styrene, the quaternary carbon of styrene and finally

[zzz] The 300 MHz instrument was used.

Stellenbosch University https://scholar.sun.ac.za

the carbonyls of maleic anhydride can be found respectively at ranges: 30.4 ppm to 35.5 ppm, 40.7 ppm to 43.9 ppm, 48.5 ppm to 52.7 ppm, 125.0 ppm to 130.6 ppm, 135.2 ppm to 140.0 ppm, 170.1 ppm to 174.2 ppm (**Figure 5.24**).[aaaa]

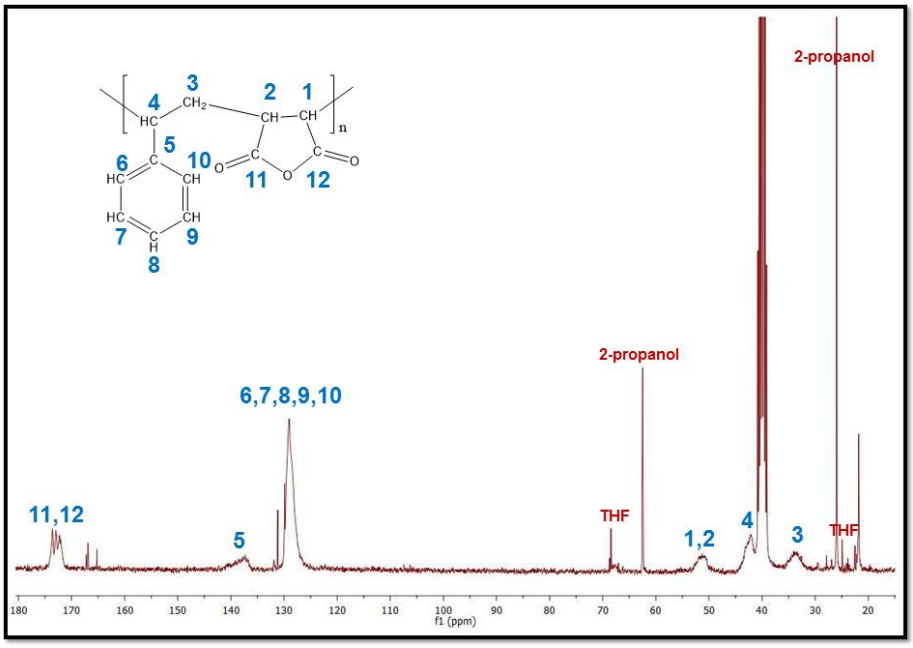

*Figure 5.24 PSMA 50% **43** ^{13}C-NMR spectrum (in DMSO-d_6)*

In addition to the point mentioned in the FT-IR section, in accordance with literature, it is also possible to prove the existence of a perfectly alternating PSMA through ^{13}C-NMR spectrum results. The determination of the triad sequence of styrene (S) and maleic anhydride (M), suggests whether the copolymer is actually alternating (SMS) or not. Two predominant markers for that are respectively: 1- The CH_2 group of the backbone (originated from styrene) which can be seen between 33 ppm to 37 ppm. 2- The quaternary carbon of styrene unit (the closest carbon to the backbone) which shows up between 137 ppm to 140 ppm.[111,112] In the case of our copolymer, the literature values can be correlated with the ones obtained for our compound suggesting a perfectly alternating PSMA (SMS).

5.12.9.1.3 UV-Vis spectroscopy

A 0.1 mg/ml solution of the copolymer was used to perform this experiment. Later with the tethered *p*-sulfonated calix[4]arene as the pendant group, the change in the absorption band of PSMA graft will be witnessed (**Figure 5.25**).

[aaaa] The 75 MHz instrument was used.

Stellenbosch University https://scholar.sun.ac.za

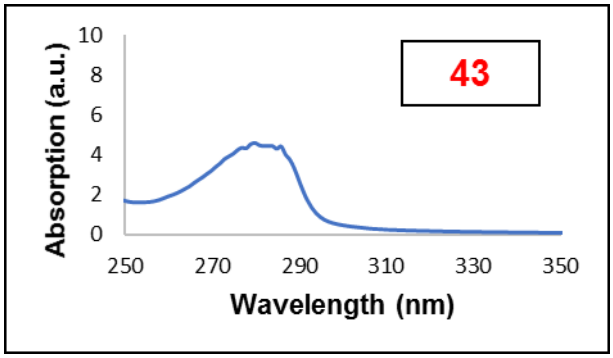

*Figure 5.25 PSMA 50% **43** UV-Vis spectrum*

5.12.9.1.4 SEC (GPC)

Following the previously mentioned protocols, the size-exclusion experiment was performed on the synthesized PSMA 50% **43** in DMF (**Figure 5.26**). Unfortunately, due to the solubility problems, these results cannot be compared for the grafts synthesized by PSMA 50% and amine-tethered *p*-sulfonated calix[4]arene.

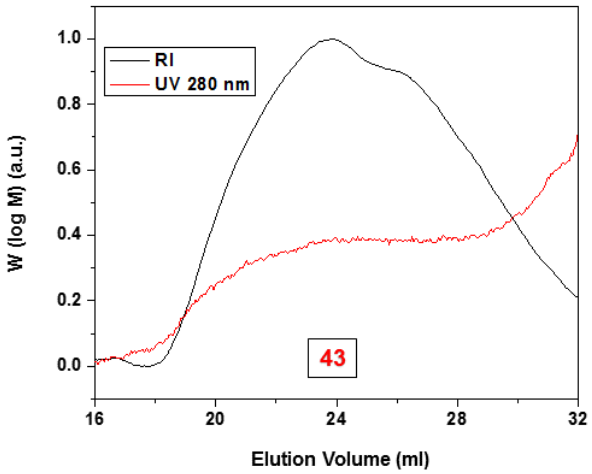

*Figure 5.26 PSMA 50% **43** GPC elugram*

5.12.9.1.5 DSC

Following the protocols explained in chapter 3, the DSC experiment was run to study the thermal behavior of the copolymer. The greater T_g value for PSMA 50% **43** compared to PSMA 30% **11** could stem from the higher degree of maleic anhydride strengthening the intermolecular interactions between the polymer chains (see **Table 5.4** for DSC data and the appendix section for the thermogram).

Stellenbosch University https://scholar.sun.ac.za

*Table 5.4 PSMA 50% **43** thermal data*

T_g (°C)	Height ($W.g^{-1}$)	Delta $C_{P\ (J.g^{-1}.°C^{-1})}$
204.04	0.04769	0.1437

5.12.9.1.6 Final analysis

After all analysis carried out on our copolymer, it can be said with certainty that PSMA 50% **43** (the perfectly alternating PSMA) has been successfully synthesized.

5.12.10 Synthesis of the *p*-sulfonated calix[4]arene-grafted PSMAs

5.12.10.1 General procedure for the synthesis of the ring-opened *p*-sulfonated calix[4]arene-grafted PSMAs (GP.A)

The amine-tethered *p*-sulfonated calix[4]arene **33** and an excess amount of base (5 to 20 equivalents) were mixed with each other in dry DMF in a round-bottom flask under argon. After one hour of stirring at 75 °C, PSMA was added and the stirring continued under the same conditions overnight (the calix[4]arene to PSMA weight ratio: 4 to 1). Thereafter, the reaction was cooled down and the crude was diluted with de-ionized water. This solution was dialyzed against de-ionized water at 10 KDalton MWCO (molecular weight cut-off) (the tubing was supplied by Thermo Fisher Scientific, USA) for 72 hours (the dialysate was replaced three times per day, i.e. nine times in total). The remaining solution in the tubing was freeze-dried to produce a hygroscopic solid.[bbbb]

5.12.10.1.1 The ring-opened *p*-sulfonated calix[4]arene-grafted PSMA made by triethylamine (20.0 equiv.) – A_{50}-T_{20}-33

Following **GP.A**, **33** (720 mg, 0.800 mmol), triethylamine (2.27 mL, 16.0 mmol) and PSMA 50% **43** (180 mg) were mixed in DMF (16 mL). The product was made as a brown solid **A_{50}-T_{20}-33** (180 mg).

[bbbb] In the case of the calix[4]arene attachment to the polymer, the massive loss of the product is another indication for the very low degree of polymer modification by the calix[4]arene. Logically, since only a small amount of the calix[4]arene had reacted with the polymer, the unreacted calix[4]arene would be washed out of the tubing upon dialysis. Moreover, because the experiment was conducted on such a small scale, it is very likely that some product was lost as a result of the conditions by which the dialysis operation was performed and these experimental errors caused a significant deviation from the expected recovery of mass.

Stellenbosch University https://scholar.sun.ac.za

5.12.10.1.2 The ring-opened *p*-sulfonated calix[4]arene-grafted PSMA made by sodium hydride (10.0 equiv.) – A_{50}-S_{10}-33

Following **GP.A**, **33** (250 mg, 0.270 mmol), sodium hydride (60% suspension in oil) (108 mg, 2.70 mmol) and PSMA 50% **43** (62.0 mg) were mixed in DMF (5.4 mL). The product was made as a light brown powder **A_{50}-S_{10}-33** (62.0 mg).

5.12.10.1.3 The ring-opened *p*-sulfonated calix[4]arene-grafted PSMA made by cesium carbonate (10.0 equiv.) – A_{50}-C_{10}-33

Following **GP.A**, **33** (400 mg, 0.440 mmol), anhydrous cesium carbonate (1.43 g, 4.40 mmol) and PSMA 50% **43** (100 mg) were mixed in DMF (8.8 mL). The product was made as a dark brown solid **A_{50}-C_{10}-33** (100 mg).

5.12.10.2 General procedure for the synthesis of the ring-closed *p*-sulfonated calix[4]arene-grafted PSMAs (GP.C)

The ring-opened graft obtained from **GP.A** was heated under reflux in glacial acetic acid in a sealed vial for 24 hours. After cooling, the solvent was removed under the reduced pressure (with toluene as an azeotrope) to produce a highly insoluble solid.

5.12.10.2.1 The ring-closed *p*-sulfonated calix[4]arene-grafted PSMA made by triethylamine (20.0 equiv.) – C_{50}-T_{20}-33

Following **GP.C**, the ring open graft **A_{50}-T_{20}-33** (50.0 mg) was placed in glacial acetic acid (5 mL). The product was obtained as a dark brown powder **C_{50}-T_{20}-33** (50.0 mg).

5.12.10.2.2 The ring-closed *p*-sulfonated calix[4]arene-grafted PSMA made by sodium hydride (10.0 equiv.) – C_{50}-S_{10}-33

Following **GP.C**, the ring open graft **A_{50}-S_{10}-33** (50.0 mg) was placed in glacial acetic acid (5 mL). The product was obtained as a dark brown powder **C_{50}-S_{10}-33** (50.0 mg).

5.12.10.2.3 The ring-closed *p*-sulfonated calix[4]arene-grafted PSMA made by cesium carbonate (10.0 equiv.) – C_{50}-C_{10}-33

Following **GP.C**, the ring open graft **A_{50}-C_{10}-33** (50.0 mg) was placed in glacial acetic acid (5 mL). The product was obtained as a dark brown powder **C_{50}-C_{10}-33** (50.0 mg).

Stellenbosch University https://scholar.sun.ac.za

5.12.10.3 Characterization of *p*-sulfonated calix[4]arene-grafted PSMAs

5.12.10.3.1 ATR-FTIR spectroscopy

Considering all the infrared data, the ring-opened graft made by triethylamine (**A_{50}-T_{20}-33** in **Figure 5.27b**) exhibited a medium stretch at 1708 cm^{-1} (carboxylic acid) and disappearance of the maleic anhydride carbonyl stretches of PSMA 50% at 1772 cm^{-1} (symmetric C=O) and 1852 cm^{-1} (asymmetric C=O) proving the formation of a ring-opened graft. Also, sulfonate groups showed two strong stretches at 1115 cm^{-1} and 1158 cm^{-1}. The ring-closed graft of the same compound (**C_{50}-T_{20}-33** in **Figure 5.27c**) demonstrated the attenuated stretches of maleic anhydride carbonyl at 1776 cm^{-1} (symmetric C=O) and 1856 cm^{-1} (asymmetric C=O) in addition to the appearance of a strong maleimide carbonyl stretch at 1705 cm^{-1} confirming the formation of a ring-opened graft. The sulfonate group stretches also were found at 1116 cm^{-1} and 1159 cm^{-1}.

The ring-opened graft made by sodium hydride (**A_{50}-S_{10}-33** in **Figure 5.27d**) exhibited a medium stretch at 1715 cm^{-1} (carboxylic acid) and disappearance of the maleic anhydride carbonyl stretches of PSMA 50% at 1772 cm^{-1} (symmetric C=O) and 1852 cm^{-1} (asymmetric C=O) proving the formation of a ring-opened graft. Also, sulfonate groups showed two strong stretches at 1106 cm^{-1} and 1168 cm^{-1}. The ring-closed graft of the same compound (**C_{50}-S_{10}-33** in **Figure 5.27e**) demonstrated the attenuated stretches of maleic anhydride carbonyl at 1776 cm^{-1} (symmetric C=O) and 1855 cm^{-1} (asymmetric C=O) in addition to the appearance of a strong maleimide carbonyl stretch at 1714 cm^{-1} confirming the formation of a ring-opened graft. The sulfonate group stretches also were found at 1106 cm^{-1} and 1155 cm^{-1}.

The ring-opened graft made by cesium carbonate (**A_{50}-C_{10}-33** in **Figure 5.27f**) exhibited a medium stretch at 1709 cm^{-1} (carboxylic acid) and disappearance of the maleic anhydride carbonyl stretches of PSMA 50% at 1772 cm^{-1} (symmetric C=O) and 1852 cm^{-1} (asymmetric C=O) proving the formation of a ring-opened graft. Also, sulfonate groups showed two strong stretches at 1102 cm^{-1} and 1162 cm^{-1}. The ring-closed graft of the same compound (**C_{50}-C_{10}-33** in **Figure 5.27g**) demonstrated the attenuated stretches of maleic anhydride carbonyl at 1776 cm^{-1} (symmetric C=O) and 1849 cm^{-1} (asymmetric C=O) in addition to the appearance of a strong maleimide carbonyl stretch at 1708 cm^{-1} confirming the formation of a ring-opened graft. The sulfonate group stretches also were found at 1113 cm^{-1} and 1165 cm^{-1}.

Stellenbosch University https://scholar.sun.ac.za

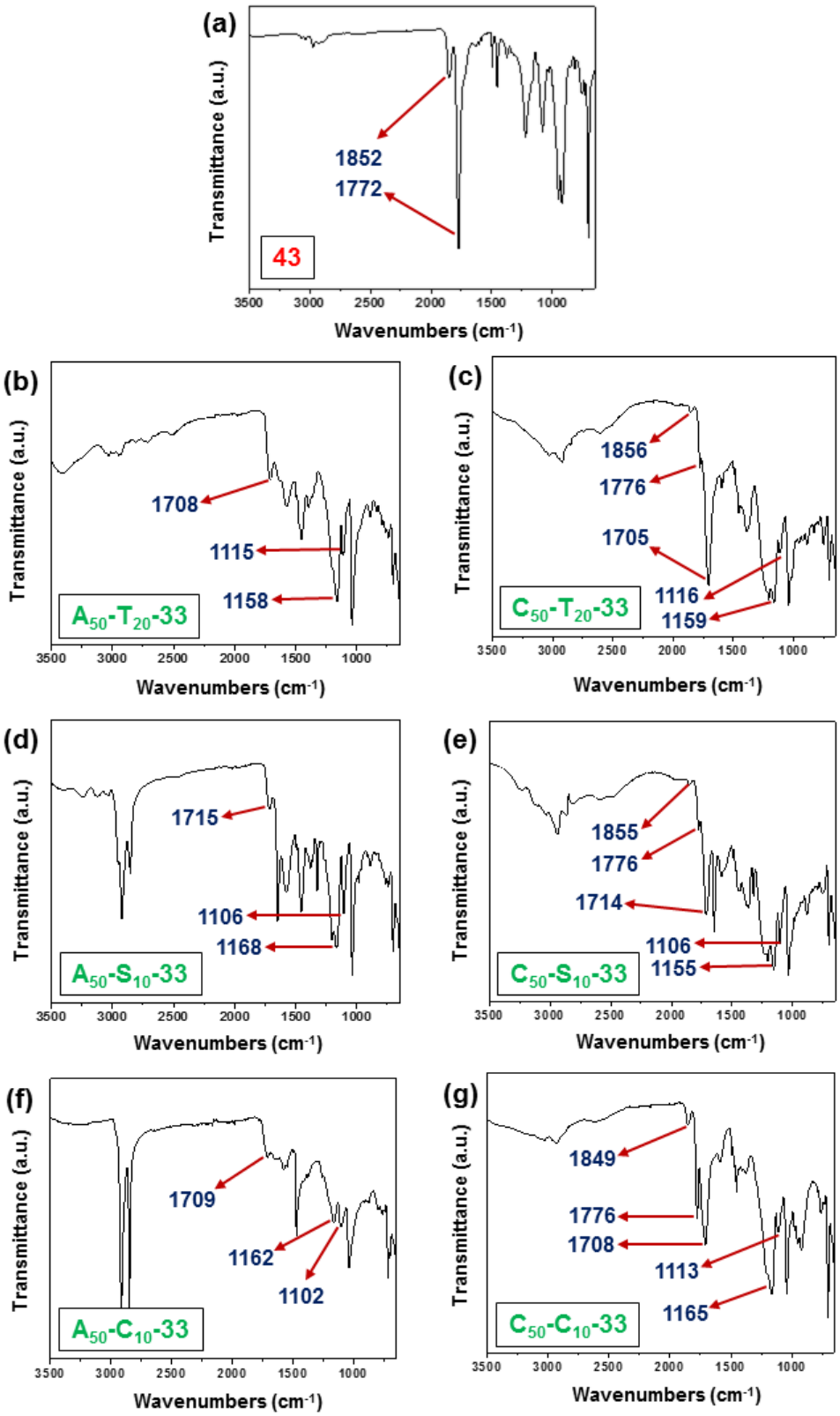

*Figure 5.27 FT-IR spectra for PSMA 50% modification with p-sulfonated calix[4]arene **33** (Transmittance values were normalized to styrene bend at 700 cm^{-1}, a.u: arbitrary unit)*

Stellenbosch University https://scholar.sun.ac.za

5.12.10.3.2 NMR spectroscopy

5.12.10.3.2.1 ^{1}H-NMR spectrum for the ring-opened graft made by triethylamine – A_{50}-T_{20}-33

^{1}H-NMR (300 MHz, D_2O) δ ppm 0.72-3.02 (butyl tether + PSMA backbone), 3.47-3.73 (calix[4]arene methylene bridge), 3.87-4.21 (PSMA backbone), 4.29-4.52 (calix[4]arene methylene bridge), 6.00-8.00 (aromatic protons for styrene and calix[4]arene).

5.12.10.3.2.2 ^{1}H-NMR spectrum for the ring-opened graft made by sodium hydride – A_{50}-S_{10}-33

^{1}H-NMR (300 MHz, D_2O) δ ppm 0.38-2.14 (butyl tether + PSMA backbone), 3.39-3.76 (PSMA backbone), 2.89-3.08 (PSMA backbone), 3.89-4.24 (calix[4]arene methylene bridge), 6.00-8.00 (aromatic protons for styrene and calix[4]arene).

5.12.10.3.2.3 ^{1}H-NMR spectrum for the ring-opened graft made by cesium carbonate – A_{50}-C_{10}-33

^{1}H-NMR (300 MHz, D_2O) δ ppm 0.64-3.02 (butyl tether + PSMA backbone), 3.48-3.74 (calix[4]arene methylene bridge), 3.93-4.18 (PSMA backbone), 4.32-4.50 (calix[4]arene methylene bridge), 6.00-8.00 (aromatic protons for styrene and calix[4]arene).

As mentioned earlier, the insoluble ring-closed grafts were not analyzed with NMR spectroscopy.

5.12.10.3.3 UV-Vis spectroscopy

Having followed the protocols used earlier for UV-Vis experiments, PSMA 50% **43** spectrum was obtained in THF (**Figure 5.28a**); however, due to the solubility issue, the ring-opened grafts spectra were acquired in water. These grafts demonstrated a much smoother absorption band compared to their parent PSMA 50% (**Figures 5.28b, 5.28c, 5.28d**). Presumably, it was caused by the presence of the sulfonate groups of calix[4]arene while back in chapter 3 the non-sulfonated calix[4]arene-grafted PSMA did not show such a massive band-broadening effect. As mentioned earlier, the insoluble ring-closed grafts were not subjected to any UV-Vis experiment in this section.

Stellenbosch University https://scholar.sun.ac.za

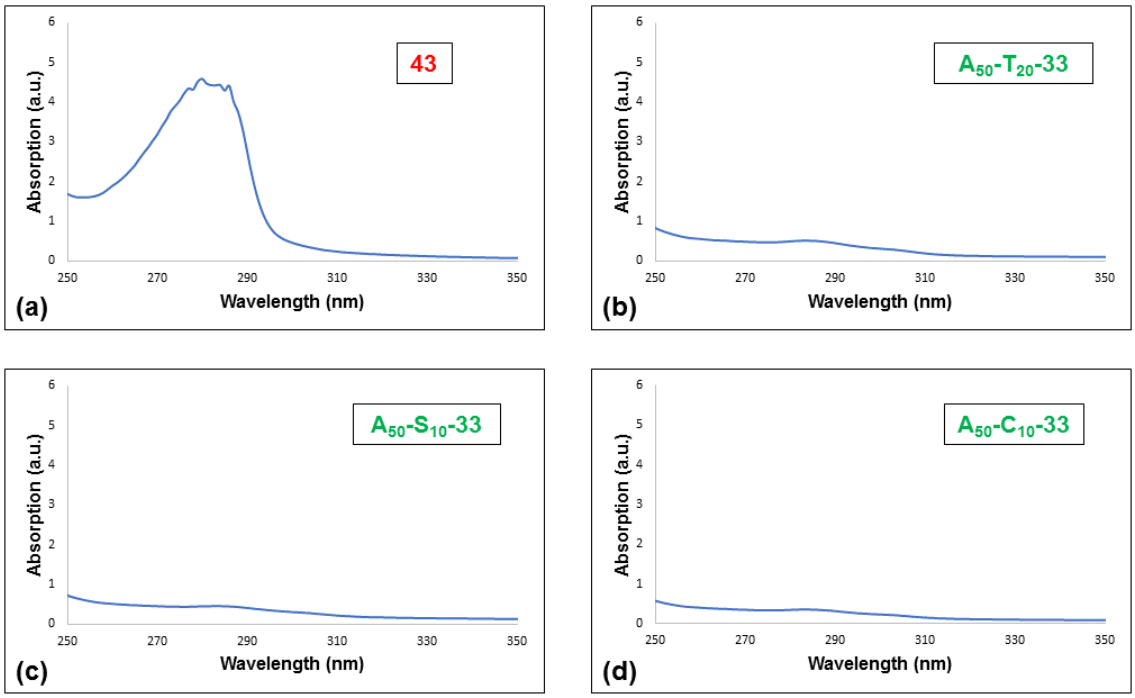

*Figure 5.28 UV-Vis spectra for PSMA 50% modification with p-sulfonated calix[4]arene **33***

5.12.10.3.4 SEC (GPC)

As mentioned earlier, due to the lack of solubility for our grafts in the available GPC solvents (DMF and THF), unfortunately, no sample was run for size exclusion chromatography analysis.

5.12.10.3.5 DSC

Unlike what observed for the grafts made up of *t*-butylated calix[4]arene and PSMA 30% in chapter 3, there was very little change for T_g values in all cases for the grafts made up of the tethered *p*-sulfonated calix[4]arene and PSMA 50%. The T_g value for PSMA 50% **43** (204.14 °C) was much higher than PSMA 30% **11** (158.82 °C) in way that even adding a bulky pendant group like a *p*-sulfonated calix[4]arene could not change it drastically (see **Table 5.5** for DSC data and the appendix section for the thermograms). In addition, the low degree of functionalization for the *p*-sulfonated calix[4]arene grafts compared to the model *t*-butylated calix[4]arene grafts (made in chapter 3) may be another reason for this negligible change in T_g for these compounds. This problem could also be caused by a fault in measurement by the DSC instrument.

Stellenbosch University https://scholar.sun.ac.za

*Table 5.5 Thermal data for PSMA 50% modification with p-sulfonated calix[4]arene **33**[cccc]*

Entry	Compound name	T_g (°C)	Height ($W.g^{-1}$)	Delta C_P ($J.g^{-1}.°C^{-1}$)
1	**43**	204.14	0.06281	0.1889
2	**A_{50}-T_{20}-33**	198.08	0.2695	0.8102
3	**A_{50}-S_{10}-33**	-	-	-
4	**A_{50}-C_{10}-33**	203.58	0.2782	0.8374
5	**C_{50}-T_{20}-33**	203.61	0.1877	0.5642
6	**C_{50}-S_{10}-33**	206.43	0.09707	0.2918
7	**C_{50}-C_{10}-33**	195.09	0.1747	0.5247

5.12.10.3.6 Final analysis

Despite the lack of GPC results, all other analytical evidence suggests the successful formation of the water-soluble *p*-sulfonated-grafted PSMAs.

5.12.11 Synthesis of the *p*-sulfonated calix[4]arene-grafted PVP-MAs

Precisely following the approaches taken for the synthesis of the *p*-sulfonated calix[4]arene-grafted PSMA, the PVP-MA calix[4]arene grafts were produced.

5.12.11.1 The ring-opened *p*-sulfonated calix[4]arene-grafted PVP-MA – A_{50}-VP-S_{10}-33

The amine-tethered *p*-sulfonated calix[4]arene **33** (870 mg, 0.930 mmol) was heated with sodium hydride (60% suspension in oil) (372 mg, 9.30 mmol) in dry DMF (18.6 mL) at 75 °C under argon for one hour. Then, PVP-MA 50% **44** (217 mg) was added and the heating continued under the same conditions overnight. After cooling, the reaction was diluted by water and the solution was dialyzed against de-ionized water (the tubing molecular weight cut-off: 10 KDalton) for 72 hours. Meanwhile, the dialysate was replaced three times a day and when the dialysis finished, the tubing solution was freeze-dried to yield a brown solid **A_{50}-VP-S_{10}-33** (250 mg).

5.12.11.2 The attempted ring-closed *p*-sulfonated calix[4]arene-grafted PVP-MA – C_{50}-VP-S_{10}-33

The ring-opened product **A_{50}-VP-S_{10}-33** (50.0 mg) was heated under reflux in glacial acetic acid (5 mL) for 24 hours. After the evaporation of the solvent, the product was attained as a brown solid **C_{50}-VP-S_{10}-33** (50.0 mg).

[cccc] The accuracy of these T_g values are in question. As observed in chapter 3, upon grafting PSMA 30% **11** with calix[4]arene as a bulky pendant group, the T_g increased for all the grafts. Overall, there should always be a regular pattern for T_g values of a polymer upon grafting with a specific group of compounds such as *p*-sulfonated calix[4]arenes (either increase or decrease in T_g value).

Stellenbosch University https://scholar.sun.ac.za

5.12.11.3 Characterization of *p*-sulfonated calix[4]arene-grafted PVP-MAs

5.12.11.3.1 ATR-FTIR spectroscopy

As was the case for PSMA, the FT-IR spectra were also recorded this time for PVP-MA-originated compounds (see **Figure 5.29**).

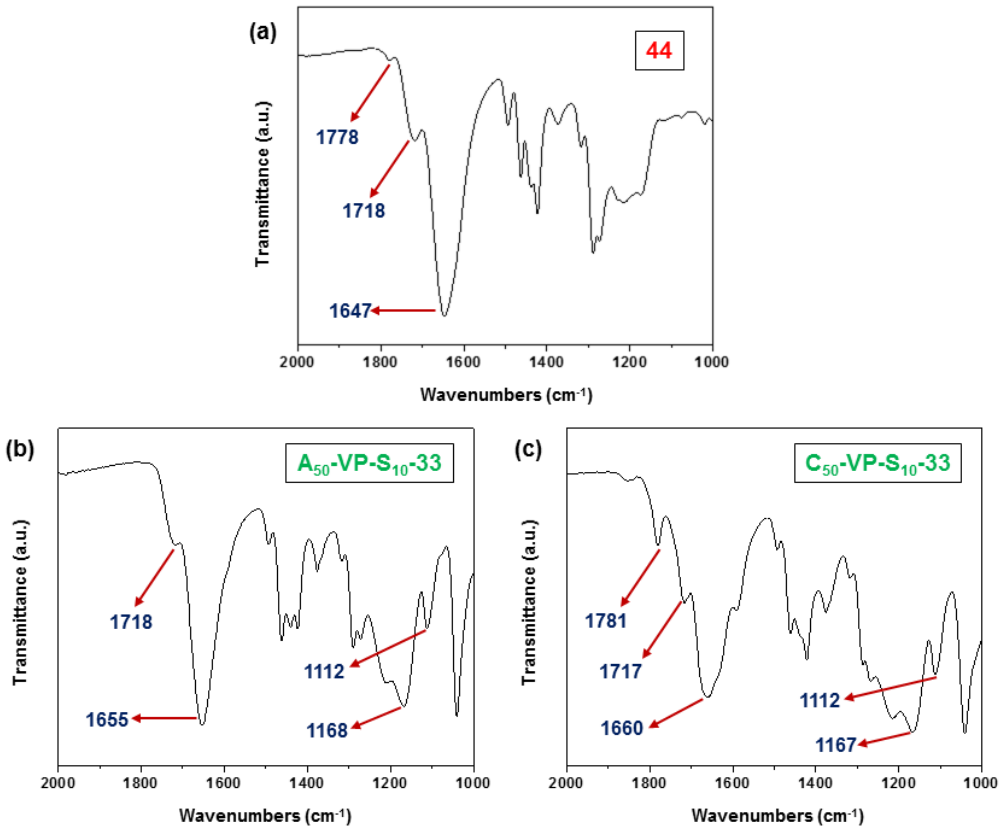

*Figure 5.29 FT-IR spectra for PVP-MA 50% modification with p-sulfonated calix[4]arene **33** (Transmittance values were normalized to pyrrolidone bend at 1373 cm^{-1}, a.u: arbitrary unit)*

In the FT-IR spectrum of PVP-MA (**44** in **Figure 5.29a**), two maleic anhydride carbonyl stretches were observable respectively at 1718 cm^{-1} (symmetric) and 1778 cm^{-1} (asymmetric). In addition, there was another carbonyl stretch representing amide at 1647 cm^{-1}. After ring-opening with the *p*-sulfonated calix[4]arene-amine **33**, as expected for the newly formed graft (**A_{50}-VP-S_{10}-33** in **Figure 5.29b**), the carbonyl region was affected and the asymmetric carbonyl disappeared. Also, the symmetric signal at 1718 cm^{-1} got broadened thanks to the formation of the carboxylate group. The amide carbonyl signal (exhibiting stretches for both pyrrolidone and maleic anhydride moieties) was seen at 1655 cm^{-1}. More importantly, the presence of two sulfonate stretches at 1112 cm^{-1} (medium) and 1168 cm^{-1} (strong) proved the existence of the sulfonate groups. After attempted ring-closure (compound **C_{50}-VP-S_{10}-33** in

Stellenbosch University https://scholar.sun.ac.za

Figure 5.29c), a changed version of symmetric and asymmetric maleimide carbonyls could be witnessed at 1717 cm^{-1} and 1781 cm^{-1}. The combining stretch for amide was also observed at 1660 cm^{-1} and finally, the sulfonate signals were found at 1112 cm^{-1} and 1167 cm^{-1}. Unfortunately, due to the lack of a new carbonyl signal for imide (probably because of the existence of a lot of ring-opened maleic anhydride moieties resulted in peak-broadening in the region between 1660 and 1717 cm^{-1}), the successful full closure of the ring for this graft is still in question.

The degree of functionalization was suggested to be determined using C-H bend of the pyrrolidone group (1373 cm^{-1}) as the internal standard (since it did not take part in the reaction, the intensity of this signal was not supposed to change). As known from PSMA modification, the decrease in the intensity of maleic anhydride for the attempted ring-closed modified polymer compared to the pristine polymer would ascertain the degree of functionalization (normalization of IR data with the internal standard was a crucial part of this process). Employing the same approach for the *p*-sulfonated calix[4]arene-grafted PVP-MA, suggested that the degree of functionalization was 24%.

5.12.11.3.2 NMR spectroscopy

5.12.11.3.2.1 ^{1}H-NMR spectrum for the ring-opened *p*-sulfonated calix[4]arene-grafted PVP-MA – A_{50}-VP-S_{10}-33

^{1}H-NMR (300 MHz, D_2O) δ ppm 0.73-1.03 (backbone CH_2), 1.05-1.45 (heterocycle middle CH_2), 1.49-1.83 (tether middle CH_2), 1.89-2.19 (heterocycle carbonyl-attached CH_2 + heterocycle N-attached CH_2), 2.20-2.76 (backbone amide-attached CH), 2.93-3.45 (backbone carboxylate-attached CH + tether O-attached CH_2 + tether N-attached CH_2), 3.48-3.90 (backbone N-attached CH), 3.95-4.18 (calix[4]arene methylene bridge), 7.35-7.94 (calix[4]arene aromatic protons).

5.12.11.3.2.2 ^{1}H-NMR spectrum for the attempted ring-closed *p*-sulfonated calix[4]arene-grafted PVP-MA – C_{50}-VP-S_{10}-33

^{1}H-NMR (300 MHz, D_2O) δ ppm 0.5-2.5 (backbone CH_2 + tether middle CH_2 + all heterocycle CH_2 + backbone carbonyl-attached CH), 3.05-3.49 (backbone carbonyl-attached CH + tether O-attached CH_2 + tether N-attached CH_2), 3.51-3.94 (backbone N-attached CH), 3.96-4.29 (calix[4]arene methylene bridge), 7.37-8.08 (calix[4]arene aromatic protons).

Stellenbosch University https://scholar.sun.ac.za

5.12.11.3.3 UV-Vis spectroscopy

Employing the same protocols used for PSMA 50%, PVP-MA 50% UV spectrum was obtained in THF (**Figure 5.30a**) while for the water-soluble calix[4]arene grafts of that, the experiments were performed in water (**Figure 5.30b, 5.30c**).

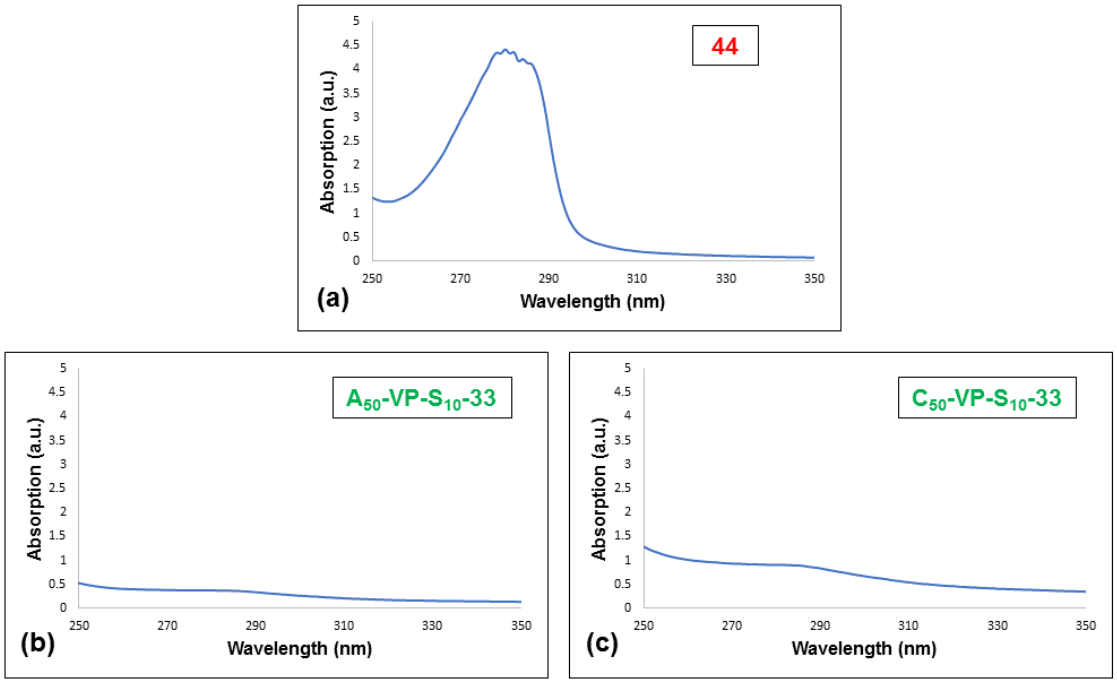

*Figure 5.30 UV-Vis spectra for PVP-MA 50% modification with p-sulfonated calix[4]arene **33***

Like the modified PSMA 50%, these grafts demonstrated an extremely smooth absorption band in comparison to the parent PVP-MA 50% **44**. It is believed that it was caused by the presence of the sulfonate groups of calix[4]arene resulting in the occurrence of such a massive band-broadening effect.

5.12.11.3.4 SEC (GPC)

Due to the lack of solubility for the grafts in GPC solvents, no experiment was carried out on our samples.

5.12.11.3.5 DSC

DSC experiments were run following the previously mentioned protocols. PVP-MA 50% **44** did not show any glass transition (only a melting point was observed at 231.61 °C). Both the ring-opened and attempted ring-closed modified PVP-MA grafts exhibited very similar thermal features (especially T_g values were very close) as an indication that probably the closure was

Stellenbosch University https://scholar.sun.ac.za

not achieved as a result of the second reaction (heating the ring-opened graft under reflux in glacial acetic acid) (see **Table 5.6** for DSC data and the appendix section for the thermograms).

*Table 5.6 Thermal data for PVP-MA 50% modification with p-sulfonated calix[4]arene **33***

Entry	Compound name	T_g (°C)	Height ($W.g^{-1}$)	Delta $C_{P\ (J.g^{-1}.°C^{-1})}$
1	**44**	-	-	-
2	**A_{50}-VP-S_{10}-33**	212.85	0.07685	0.2306
3	**C_{50}-VP-S_{10}-33**	211.98	0.06340	0.1900

5.12.11.3.6 Final analysis

Despite the lack of GPC results, the rest of the analytical data suggested the formation of our desired grafts in its ring-opened form. Overall, since very insignificant negligible differences were shown in the analysis between the ring-opened graft and the attempted ring-closed one, there was no compelling evidence suggesting the formation of the desired ring-closed product.

5.13 References

(1) Shinkai, S.; Mori, S.; Tsubaki, T.; Sone, T.; Manabe, O. *Tetrahedron Lett.* **1984**, *25*, 5315–5318.

(2) Shinkai, S.; Mori, S.; Koreishi, H.; Tsubaki, T.; Manabe, O. *J. Am. Chem. Soc.* **1986**, *108*, 2409–2416.

(3) Shinkai, S.; Tsubaki, T.; Arimura, T.; Manabe, O. *J. Chem. Soc., Perkin Trans. I* **1987**, 2297–2299.

(4) Kumar, S.; Chawla, H. M.; Varadarajan, R. *Indian J. Chem.* **2003**, *428*, 2863–2865.

(5) Shinkai, S.; Isaka, K.; Komiyama, M. *Chem. Lett.* **1991**, *20*, 937–940.

(6) Davey, J. M.; Too, C. O.; Ralph, S. F.; Kane-maguire, L. A. P.; Wallace, G. G.; Partridge, A. C. *Macromolecules* **2000**, *33*, 7044–7050.

(7) Mousavi, Z.; Bobacka, J.; Ivaska, A. *Electroanalysis* **2005**, *17*, 1609–1615.

(8) Reece, D. A.; Pringle, J. M.; Ralph, S. F.; Wallace, G. G. *Solutions* **2005**, *38*, 1616–1622.

(9) Basilio, N.; Francisco, V.; Garcia-Rio, L. *Int. J. Mol. Sci.* **2013**, *14*, 3140–3157.

(10) Shinaki, S.; Yoshida, I.; Yamamoto, M.; Sagara, F.; Ueno, K.; Ishii, D. *Chem. Lett.* **1991**, *20*, 2105–2108.

Stellenbosch University https://scholar.sun.ac.za

(11) Dalgarno, S. J.; Raston, C. L. *Chem. Commun.* **2002**, *19*, 2216–2217.

(12) Chen, C.; Ma, J.; Liu, B.; Yang, J.; Liu, Y. *Cryst. Growth. Des.* **2011**, *11*, 4491–4497.

(13) Shinkai, S.; Koreishi, H.; Ueda, K.; Manabe, O. *J. Chem. Soc., Chem. Commun.* **1986**, 233–234.

(14) Thuéry, P. *CrystEngComm.* **2012**, *14*, 6369–6373.

(15) Arena, G.; Contino, A.; Gulino, G.; Magrı, A.; Sansone, F.; Sciotto, D.; Ungaro, R. *Tetrahedron. Lett.* **1999**, *40*, 1597–1600.

(16) Arena, G.; Contino, A.; Gulino, F. G.; Magrı, A.; Sciotto, D.; Ungaro, R. *Tetrahedron Lett.* **2000**, *41*, 9327–9330.

(17) Lehn, J-M.; Meric, R.; Vigneron, J-P.; Cesario, M.; Guilhem, J.; Pascard, C.; Asfari, Z.; Vicens, J. *Supramol. Chem.* **1995**, *5*, 97–103.

(18) Wang, K.; Yang, E.; Zhao, X.; Dou, H.; Liu, Y. *Cryst. Growth. Des.* **2014**, *14*, 4631−4639.

(19) Bird, C. L.; Kuhn, A. T. *Chem. Soc. Rev.* **1981**, *10*, 49–82.

(20) Summers, L. A. *The Bipyridinium Herbicides*, Academic Press, New York, United States, **1980**.

(21) Brun, A. M.; Harriman, A. *J. Am. Chem. Soc.* **1991**, *113*, 8153–8159.

(22) Clennan, E. L.; Harriman, A. *Coord. Chem. Rev.* **2004**, *248*, 477–492.

(23) Monk, P. M. S. *The Viologens. Physicochemical Properties, Synthesis and Applications of the Salts of 4,4'-Bipyridine*, John Wiley & Sons, Chichester, United Kingdom, **1998**.

(24) Balzani, V.; Credi, A.; Raymo, F. M.; J. F. Stoddart, J. F.; *Angew. Chem. Int. Ed.* **2000**, *39*, 3348–3391.

(25) Migliaccio, E.; Giorgio, M.; Mele, S.; Pelicci, G.; Reboldi, P.; Pandolfi, P. P.; Lanfrancone, L.; Pelicci, P. G. *Nature* **1999**, *402*, 309–313.

(26) Bismuth, C.; Hall, A. H.; *Paraquat Poisoning: Mechenvironanisms, Prevention, Treatment*, Dekker, New York, United States, **1995**.

(27) Vale, J. A.; Meredith, T. J.; Buckley, B. M.; *Hum. Toxicol.* **1987**, *6*, 41–47.

Stellenbosch University https://scholar.sun.ac.za

(28) Saibara, T.; Toda, K.; Wakatsuki, A.; Ogawa, Y.; Ono, M.; Onishi, S.; *Toxicol. Lett.* **2003**, *143*, 51–54.

(29) Wang, K.; Guo, D-S.; Zhang, H-Q.; Li, D.; Zheng, X-L.; Liu, Y.; *J. Med. Chem.* **2009**, *52*, 6402–6412.

(30) Moon, K.; Kaifer, A. E. *Org. Lett.* **2004**, *6*, 185–188.

(31) Li, C-J.; Shu, X-Y.; Li, J.; Chen, S-H.; Han, K.; Xu, M.; Hu, B-J.; Yu, Y-H.; Jia, X-S.; *J. Org. Chem.* **2011**, *76*, 8458–8465.

(32) Li, C-J.; Xu, Q-Q.; Li, J.; Yao, F-N.; Jia, X-S.; *Org. Biomol. Chem.* **2010**, *8*, 1568–1576.

(33) Chen, H-Q.; Fan, J-Z.; Hu, X-S.; Ma, J-W.; Wang, S-L.; Li, J.; Yu, Y-H.; Jia, X-S.; Li, C-J.; *Chem. Sci.* **2015**, *6*, 197–202.

(34) Liu, Y.; Guo, D-S.; Suo, X. *Cryst. Growth. Des.* **2008**, *8*, 3514–3517.

(35) Wang, K.; Chen, Y.; Liu, Y. *Chem. Commun.* **2015**, *51*, 1647–1649.

(36) Jia, Y. G.; Zhu, X. X. *Chem. Mater.* **2015**, *27*, 387–393.

(37) Park, K. M.; Yang, J. A.; Jung, H.; Yeom, J.; Park, J. S.; Park, K. H.; Hoffman, A. S.; Hahn, S. K.; Kim, K. *ACS Nano* **2012**, *6*, 2960–2968.

(38) Zhang, M.; Xu, D.; Yan, X.; Chen, J.; Dong, S.; Zheng, B.; Huang, F. *Angew. Chem. Int. Ed.* **2012**, *51*, 7011–7015.

(39) Nic, M.; Jirat, J.; Kosata, B. *IUPAC Compendium of Chemical Terminology: The Gold Book, International Union of Pure and Applied Chemistry (IUPAC)*, **2014**, Version 2.3.3 (online: https://goldbook.iupac.org/).

(40) Wichterle, O.; Lím, D. *Nature* **1960**, *185*, 117–118.

(41) Rajendran, S. *Advanced Textiles for Wound Care*, Elsevier, Amsterdam, Netherlands, **2009**.

(42) Schauenburg, D.; Gálvez, A. O.; Bode, J. W. *J. Mater. Chem. B* **2018**, *6*, 4775–4782.

(43) Zhang, M.; Waldron, K. C.; Zhu, X. X. *RSC Adv.* **2016**, *6*, 35436–35440.

(44) Durmaz, S.; Okay, O. *Polymer* **2000**, *41*, 3693–3704.

(45) Hassan, E.; Deshpande, P.; Claeyssens, F.; Rimmer, S.; MacNeil, S. *Acta Biomater.*

Stellenbosch University https://scholar.sun.ac.za

2014, *10*, 3029–3037.

(46) Ma, S.; Wang, S.; Li, Q.; Leng, Y.; Wang, L.; Hu, G. H. *Ind. Eng. Chem. Res.* **2017**, *56*, 7971–7976.

(47) Wang, L. S.; Du, C.; Chung, J. E.; Kurisawa, M. *Acta Biomater.* **2012**, *8*, 1826–1837.

(48) Qiu, B.; Stefanos, S.; Ma, J.; Lalloo, A.; Perry, B. A.; Leibowitz, M. J.; Sinko, P. J.; Stein, S. *Biomaterials* **2003**, *24*, 11–18.

(49) Konieczynska, M. D.; Villa-Camacho, J. C.; Ghobril, C.; Perez-Viloria, M.; Tevis, K. M.; Blessing, W. A.; Nazarian, A.; Rodriguez, E. K.; Grinstaff, M. W. *Angew. Chem. Int. Ed.* **2016**, *55*, 9984–9987.

(50) Moghadam, M. N.; Pioletti, D. P. *J. Biomed. Mater. Res., Part B* **2016**, *104*, 1161–1169.

(51) Şolpan, D.; Kölge, Z.; Torun, M. *J. Macromol. Sci., Part A: Pure Appl. Chem.* **2006**, *43*, 129–152.

(52) Cui, L.; Jia, J.; Guo, Y.; Liu, Y.; Zhu, P. *Carbohydr. Polym.* **2014**, *99*, 31–38.

(53) Kabir, S. M. F.; Sikdar, P. P.; Haque, B.; Rahman Bhuiyan, M. A.; Ali, A.; Islam, M. N. *Prog. Biomater.* **2018**, *7*, 153–174.

(54) Zhang, H.; Patel, A.; Gaharwar, A. K.; Mihaila, S. M.; Iviglia, G.; Mukundan, S.; Bae, H.; Yang, H.; Khademhosseini, A. *Biomacromolecules* **2013**, *14*, 1299–1310.

(55) Liu, Z.; Xia, Z.; Fan, L.; Xiao, H.; Cao, C. *Chem. Commun.* **2017**, *53*, 5842–5845.

(56) Zhang, S.; Alvarez, D. J.; Sofroniew, M. V.; Deming, T. J. *Biomacromolecules*, **2015**, *16*, 1331–1340.

(57) Wei, W.; Qi, X.; Li, J.; Zhong, Y.; Zuo, G.; Pan, X.; Su, T.; Zhang, J.; Dong, W. *Int. J. Biol. Macromol.* **2017**, *101*, 474–480.

(58) Liang, J.; Struckhoff, J. J.; Du, H.; Hamilton, P. D.; Ravi, N. *J. Biomed. Mater. Res., Part B* **2017**, *105*, 977–988.

(59) Kozlovskaya, V.; Sukhishvili, S. A. *Macromolecules* **2006**, *39*, 6191–6199.

(60) Ye, L.; Zhang, Y.; Wang, Q.; Zhou, X.; Yang, B.; Ji, F.; Dong, D.; Gao, L.; Cui, Y.; Yao, F. *ACS Appl. Mater. Interfaces* **2016**, *8*, 15710–15723.

Stellenbosch University https://scholar.sun.ac.za

(61) Agren, M. S. *Acta Derm. Venereol.* **1998**, *78*, 119–122.

(62) Wei, D.; Yang, J.; Zhu, L.; Chen, F.; Tang, Z.; Qin, G.; Chen, Q. *ACS Appl. Mater. Interfaces* **2018**, *10*, 2946–2956.

(63) Zhou, J.; Wang, G.; Marquez, M.; Hu, Z. *Soft Matter.* **2009**, *5*, 820–826.

(64) Lewis, G.; Coughlan, D. C.; Lane, M. E.; Corrigan, O. I. *J. Microencapsul.* **2006**, *23*, 677–685.

(65) He, X.; Liu, L.; Han, H.; Shi, W.; Yang, W.; Lu, X. *Macromolecules* **2019**, *52*, 72–80.

(66) Pritchard, C. D.; O'Shea, T. M.; Siegwart, D. J.; Calo, E.; Anderson, D. J.; Reynolds, F. M.; Thomas, J. A.; Slotkin, J. R.; Woodward, E. J.; Langer, R. *Biomaterials* **2011**, *32*, 587–597.

(67) Zhang, H.; Qadeer, A.; Mynarcik, D.; Chen, W. *Biomaterials* **2011**, *32*, 890–898.

(68) Kurisawa, M.; Chung, J. E.; Yang, Y. Y.; Gao, S. J.; Uyama, H. *Chem. Commun.* **2005**, 4312–4314.

(69) Rydholm, A. E.; Bowman, C. N.; Anseth, K. S. *Biomaterials* **2005**, *26*, 4495–4506.

(70) Pathak, C. P.; Sawhney, A. S.; Hubbell, J. A. *J. Am. Chem. Soc.* **1992**, *114*, 8311–8312.

(71) DeForest, C. A.; Polizzotti, B. D.; Anseth, K. S. *Nat. Mater.* **2009**, *8*, 659–664.

(72) Appel, E. A.; Del Barrio, J.; Loh, X. J.; Scherman, O. A. *Chem. Soc. Rev.* **2012**, *41*, 6195–6214.

(73) Peppas, N.A.; Bures, P.; Leobandung, W.; Ichikawa, H. *Eur. J. Pharm. Biopharm.* **2000**, *50*, 27–46.

(74) Schalley, C. A. *Analytical Methods in Supramolecular Chemistry*, John Wiley & Sons, Hoboken, New Jersey, United States, **2007**.

(75) Wypych, G. *Self-Healing Materials: Principles and Technology*, Elsevier, Amsterdam, Netherlands, **2017**.

(76) Wang, K.; Fu, Q.; Chen, X.; Gao, Y.; Dong, K. *RSC Adv.* **2012**, *2*, 7772–7780.

(77) Gong, C.; Qi, T.; Wei, X.; Qu, Y.; Wu, Q.; Luo, F.; Qian, Z. *Curr. Med. Chem.* **2013**, *20*, 79–94.

Stellenbosch University https://scholar.sun.ac.za

(78) Liu, Z.; Xu, G.; Wang, C.; Li, C.; Yao, P. *Int. J. Pharm.* **2017**, *530*, 53–62.

(79) Li, H. *Smart Hydrogel Modelling*, Springer Science & Business Media, Berlin, Germany, **2010**.

(80) Sadowski, G.; Richtering, W. *Intelligent Hydrogels*, Springer, Berlin, Germany, **2014**.

(81) Neufeld, L.; Bianco-Peled, H. *Int. J. Biol. Macromol.* **2017**, *101*, 852–861.

(82) Ryan, M. D.; Nilsson, B. L. *Polym. Chem.* **2012**, *3*, 18–33.

(83) Culver, H. R.; Clegg, J. R.; Peppas, N. A. *Acc. Chem. Res.* **2017**, *50*, 170–178.

(84) Sun, T. L.; Kurokawa, T.; Kuroda, S.; Ihsan, A. B.; Akasaki, T.; Sato, K.; Haque, A.; Nakajima, T.; Gong, J. P. *Nat. Mater.* **2013**, *12*, 932–937.

(85) Farris, S.; Schaich, K. M.; Liu, L. S.; Piergiovanni, L.; Yam, K. L. *Trends Food Sci. Technol.* **2009**, *20*, 316–332.

(86) Wong Po Foo, C. T. S.; Lee, J. S.; Mulyasasmita, W.; Parisi-Amon, A.; Heilshorn, S. C. *Proc. Natl. Acad. Sci. U. S. A.* **2009**, *106*, 22067–22072.

(87) Bayat, N.; Zhang, Y.; Falabella, P.; Menefee, R.; Whalen, J. J.; Humayun, M. S.; Thompson, M. E. *Sci. Transl. Med.* **2017**, *9*, 1–14.

(88) Xu, Y.; Yang, X.; Thomas, A. K.; Patsis, P. A.; Kurth, T.; Kräter, M.; Eckert, K.; Bornhäuser, M.; Zhang, Y. *ACS Appl. Mater. Interfaces* **2018**, *10*, 14418–14425.

(89) Nash, W.; Potter, M. *Schaum's Outline of Strength of Materials*, McGraw Hill Professional, New York, United States, **2010**, 5th ed.

(90) Guo, D-S.; Chen, S.; Qian, H.; Zhang, H.; Liu, Y. *Chem. Commun.* **2010**, *46*, 2620–2622.

(91) Wang, K-P.; Guo, D-S.; Zhao, H-X.; Liu, Y. *Chem. Eur. J.* **2014**, *20*, 4023–4031.

(92) Xi, H.; Yang, L.; Chen, J. *J. Macromol. Sci. B* **2013**, *52*, 1198–1211.

(93) Kim, S-H.; Lee, H. R.; Yu, S. J.; Han, M-E.; Lee, D. Y.; Kim, S. Y.; Ahn, H-J.; Han, M-J.; Lee, T-I.; Kim, T-S.; Kwon, S-K.; Im, S. G.; Hwang, N. S. *Proc. Natl. Acad. Sci. U. S. A.* **2015**, *112*, 15426–15431.

(94) Maity, D.; Bhatt, M.; Paul, P. *Microchim. Acta.* **2015**, *182*, 377–384.

Stellenbosch University https://scholar.sun.ac.za

(95) Baghbanian, S. M.; Khanzad, G.; Vahdat, S. M.; Tashakkorian, H. *Res. Chem. Intermed.* **2015**, *41*, 9951–9966.

(96) Arena, G.; Contino, A.; Lombardo, G. G.; Sciotto, D. *Thermochimica Acta.* **1995**, *264*, 1–11.

(97) Da Silva, E.; Coleman, A. W. *Tetrahedron* **2003**, *59*, 7357–7364.

(98) Yin, J.; Hu, Y.; Wang, H.; Jin, Z.; Zhang, Y.; Kuang, G. *Chem. Asian J.* **2017**, *12*, 3088–3095.

(99) Guo, D-S.; Wang, L.; Liu, Y. *J. Org. Chem.* **2007**, *72*, 7775–7778.

(100) Summers, L. A.; McAlpine, N. S.; Attalla, M. I. *Z. Naturforsch.* **1984**, *39b*, 74–78.

(101) Tazuke, S.; Kitamura, N.; Imabayashi, S-I. *J. Electroanal. Chem.* **1988**, *243*, 143–160.

(102) Zaimis, E. J. *Br. J. Pharmacol. Chemother.* **1950**, *5*, 424–430.

(103) Bhaumic, A.; Sasidharan. M. *Phys. Chem. Chem. Phys*. **2011**, *13*, 16282–16294.

(104) Marxer, A.; Miescher, K. *Helv. Chim. Acta* **1996**, *34*, 924–931.

(105) Danylyuk, O.; Suwinska, K.; Perret, F.; Coleman, A. W.; Gue´ret, S. *J. Mol. Struct.* **2006**, *797*, 1–4.

(106) Zhu, H.; Liu, D.; Gega, J.; Surowiec, K.; Purkiss, D. W.; Bartsch, R. A. *Org. Biomol. Chem.* **2007**, *5*, 324–332.

(107) Zhang, D.; Cao, X.; Purkiss, D. W.; Bartsch, R. A. *Org. Biomol. Chem.* **2007**, *5*, 1251–1259.

(108) Mummidivarapu, S.; Rennie, M.; Doolan, A.; Crowley, P. B. *Bioconjugate Chem.* **2018**, *29*, 3999–4003.

(109) Gutsche, C. D. *Acc. Chem. Res.* **1983**, *16*, 161–170.

(110) Arena, G.; Casnati, A.; Contino, A.; Lombardo, G. G.; Sciotto, D.; Ungaro, R. *Chem. Eur. J.* **1999**, *5*, 738–744.

(111) Hieu Ha, N. T. *Polymer* **1999**, *40*, 1081–1086.

(112) Lessard, B.; Maric', M. *Macromolecules* **2010**, *43*, 879–885.

Stellenbosch University https://scholar.sun.ac.za

Overall conclusion

To summarize, in the course of this research, the idea of functionalizing PSMA with calix[4]arenes and some their potential applications were investigated.

To further this idea, a simple calix[4]arene-grafted PSMA model was required which could later be modified into a more elaborate system with potential for many applications. Considering the literature examples in the matter of producing calix[4]arene-polymer grafts,[1-3] the ‘‘grafting onto approach’’, due to its more convenient conditions, was chosen as our preferred method for synthesizing the model compounds.[2,4-7]

Moving forward with that method, a functionalized calix[4]arene with a strong nucleophilic linker capable of opening the succinic anhydride moiety of PSMA had to be synthesized. In accordance with the literature, the best possible linker was a primary amine tether,[8-10] but first the calix[4]arene needed to be mono-functionalized with an alkyl halide (with different chain lengths) possessing the amine precursor. Among all attempted options in this regard, the phthalimide precursor gave us the best results for monoalkylation (52% yield in the case of $\mathbf{5_h}$ for *t*-butylated calixarene and 59% yield in the case of $\mathbf{9_b}$ for de-butylated calixarene). Next, the mono-alkylated calix[4]arenes underwent different phthalimide deprotection methods to produce the final calix[4]arene-amine model. Gabriel synthesis using hydrazine monohydrate was shown to be the best approach for producing the amine model (86% yield in the case of $\mathbf{10_h}$ for *t*-butylated calixarene).

Then, the above-mentioned ‘‘grafting onto approach’’ was put to the test and the grafting of the amines to PSMA was attempted through multiple synthetic methods. The attachment of calix[4]arene to PSMA was performed via conducting the experiment in both DMF (at room temperature or heating at 150 °C) and glacial acetic acid (heating under reflux); in the case of using glacial acetic acid, the ring-closed form was obtained in all cases. Overall, the best degree of modification for PSMA with the calix[4]arene-amine pedant group was achieved via heating the polymer with *t*-butylated calixarene-butylamine ($\mathbf{10_b}$) under reflux in glacial acetic acid (78%). Nevertheless, due to the poor solubility of other amines in glacial acetic acid, for those amines the two-step process (the attachment in DMF at room temperature followed by the closure in glacial acetic acid via heating under reflux) was applied which resulted in the considerable decrease of the degree of modification for PSMA (from 78% to 20-30%).

Stellenbosch University https://scholar.sun.ac.za

Having established *t*-butylated calixarene-grafted PSMA (**B_{30}-10_b**) as the framework for our future studies, the focus of research was placed on producing a sensing instrument for mercury (an important contaminant of aqueous media).[11,12] This sensing instrument was inspired by Chung and co-workers paper on the synthesis and use of the distal diallyl-bis(*p*-methoxyphenylazo)calix[4]arene (**14_x** also known as the Chung's sensor) as a host for Hg^{2+}.[13,14] Our plan was to synthesize a butylamine-tethered version of the Chung's sensor, graft it onto PSMA and finally create a durable sensing instrument for Hg^{2+} employing the calix[4]arene-PSMA graft. Following the approach taken to make the model calix[4]arene-grafted PSMA, the Chung's sensor had to be mono-alkylated via an alkylphthalimide which could later be transformed into an amine for PSMA grafting. The initial attempt to produce the desired amine-tethered Chung's sensor via the direct alkylation of the Chung's sensor failed resulting in many alternative approaches being designed to resolve this problem. Unfortunately, these approaches did not work and no pure diazotized product was collected. In the future work section, several solutions to this problem will be presented.

Next, the focus of our research moved to producing a hydrogel.[15-19] This part of the study was based on a paper by Liu *et al.* on the synthesis of a reversible stimulus-responsive hydrogel using a *p*-sulfonated calix[4]arene and a randomly viologen -modified poly(vinyl alcohol).[20] The idea was to replace the model *t*-butylated calixarene-grafted PSMA (**B_{30}-10_b**) with its water-soluble sulfonated version and achieve gelation upon complexation of bis-viologen-based quaternary amines (**36** and **38**) or several other bis-quaternary amines (**39-42**). Despite successful synthesis of the desired butylamine-tethered *p*-sulfonated calix[4]arene (**33**) and its corresponding PSMA grafts (made with PSMA 30%), the products only showed slight solubility in water and therefore they were unable to be tested for gelation. To increase the solubility, the commercially available PSMA 30% was replaced with PSMA 50% (**43**) and the grafting was performed using the same *p*-sulfonated calix[4]arene (**33**). Pleasingly, the newly-formed grafts exhibited better solubility (made with PSMA 50%), but unfortunately the gelation was not achieved. To increase the solubility of the functionalized polymer further, PSMA 50% was replaced with PVP-MA 50% (**44**). As was the case for PSMA, the hydrogel formation was not observed; however, in all these cases, the complexation between the host (the sulfonated calix[4]arene-supported polymer) and the guest (the viologen-based quaternary amine) was confirmed by ^{1}H-NMR spectroscopic titrations. In order to discover the cause for gelation failure, every possible parameter affecting the gelation process was considered. These parameters include the concentration, the temperature, the pH, the base choice, the

Stellenbosch University https://scholar.sun.ac.za

calix[4]arene conformation, and the degree of modification of the polymer. Amongst all these parameters, the status of two of them remained concerning including the conformationally mobile nature of the *p*-sulfonated calix[4]arene and also the low degree of modification of the polymer. To eliminate the possible disruption of gelation by these factors, several solutions will be offered in the future work section.

Overall conclusion references

(1) Erdemir, S.; Yilmaz, M. *J. Mol. Catal. B Enzym.* **2009**, *58*, 29–35.

(2) Memon, S.; Akceylan, E.; Sap, B.; Tabakci, M.; Roundhill, D. M.; Yilmaz, M. *J. Polym. Environ.* **2003**, *11*, 67–74.

(3) Blanda, M. T.; Adou, E. *Chem. Commun.* **1998**, 139–140.

(4) Deligöz, H.; Yilmaz, M. *React. Funct. Polym.* **1996**, *31*, 81–88.

(5) Kang, Y.; Rudkevich, D. M. *Tetrahedron* **2004**, *60*, 11219–11225.

(6) Engrand, P.; Regnouf-de-Vains, J. B. *Tetrahedron Lett.* **2002**, *43*, 8863–8866.

(7) Sayin, S.; Ozcan, F.; Memon, S.; Yilmaz, M. *J. Incl. Phenom. Macrocycl. Chem.* **2010**, *67*, 385–391.

(8) Cronje, L.; Klumperman, B. *Eur. Polym. J.* **2013**, *49*, 3814–3824.

(9) Lee, S. J.; Tatavarty, R.; Gu, M. B. *Biosens. Bioelectron.* **2012**, *38*, 302–307.

(10) Li, P.; Zhang, Y.; Zhang, S.; Wang, P.; Wang, M. *Adv. Chem. Eng. Pts 1-3*, **2012**, *396–398*, 1394–1397.

(11) Järup, L. *Br. Med. Bull.* **2003**, *68*, 167–182.

(12) Gustin, M. S.; Taylor, G. E.; Leonard, T. L. *Environ. Health Perspect.* **1994**, *102*, 772–778.

(13) Kao, T-L.; Wang, C-C.; Pan, Y-T.; Shiao, Y-J.; Yen, J-Y.; Shu, C-M.; Lee, G-H.; Peng, S-M.; Chung, W-S. *J. Org. Chem.* **2005**, *70*, 2912–2920.

(14) Ho, I-T.; Lee, G-H.; Chung, W-S. *J. Org. Chem.*, **2007**, *72*, 2434–2442.

(15) Nic, M.; Jirat, J.; Kosata, B. *IUPAC Compendium of Chemical Terminology: The Gold Book, International Union of Pure and Applied Chemistry (IUPAC)*, **2014**, Version 2.3.3

Stellenbosch University https://scholar.sun.ac.za

(online: https://goldbook.iupac.org/).

(16) Lee, K. Y.; Mooney, D. J. *Chem. Rev.* **2001**, *101*, 1869–1880.

(17) Langer, R.; Tirrell, D. A. *Nature* **2004**, *428*, 487–492.

(18) Lutolf, M. P. *Nat. Mater.* **2009**, *8*, 451–453.

(19) Harada, A.; Kobayashi, R.; Takashima, Y. Hashidzume, A.; Yamaguchi, H. *Nat. Chem.* **2011**, *3*, 34–37.

(20) Wang, K.; Chen, Y.; Liu, Y. *Chem. Commun.* **2015**, *51*, 1647–1649.

Stellenbosch University https://scholar.sun.ac.za

Future work

This section briefly provides the reader with several suggestions regarding the two main fields of research in this project i.e. the synthesis of the modified Chung's sensor for grafting onto PSMA (for mercury detection purposes) and also the synthesis of an alternative water-soluble polymeric graft of *p*-sulfonated calix[4]arene (for hydrogel formation studies). Employing these ideas may contribute to circumventing the challenges discussed in this dissertation. However, before addressing these matters, some potential future work for the model grafts made in chapter 3 will be presented.

Part A. Suggested future work for the *t*-butylated calix[4]arene-grafted PSMA

As shown in chapter 3, several *t*-butylated calix[4]arene-grafted PSMAs were successfully synthesized. In this case, the best modification degree was achieved for the butylamine-tethered calix[4]arene via heating under reflux in glacial acetic acid (78%). As future work, this graft (**B_{30}-10_b**) can be used as a potential colorimetric sensor for NO_2. As observed in chapter 1, *t*-butylated calix[4]arenes anchored to the polymeric support could be employed as potent agents for sensing and conversion of NO_2 (see Kang and Rudkevich work on using a *t*-butylated calix[4]arene with poly(ethylene glycol) as the support).[1] It should be pointed out that Rudkevich's PEG-supported calix[4]arene was in the 1,3-alternate conformation, whereas the graft **B_{30}-10_b** is in the cone conformation. However, in accordance with literature, different conformations of calix[4]arene will give no substantial difference in colorimetric response toward NO_2.[2] For that reason, the use of graft **B_{30}-10_b** as a colorimetric NO_2 sensor is highly recommended (**Figure FW.1**).

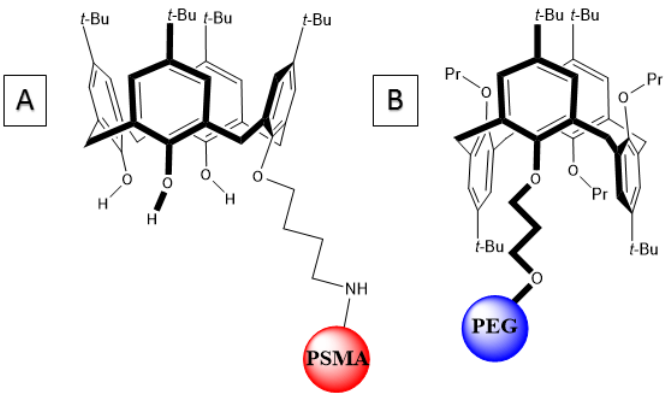

*Figure FW.1 A: Graft **B_{30}-10_b** (cone conformation), B: Kang and Rudkevich's PEG-supported calix[4]arene (1,3-alternate conformation) for NO_2 sensing and conversion[1]*

Stellenbosch University https://scholar.sun.ac.za

Part B. Suggested future work for the diazotization studies

As concluded in chapter 4, the synthesis of the mono butylamine-tethered distal diallyl-bis(*p*-methoxyphenylazo)calix[4]arene failed, despite some initially positive results (including the mercury test). One of the main challenges faced in that chapter was the issue of regioselectivity which resulted in the formation of many regioisomers of the azo products which ended up being inseparable. According to chapter 4, compound **20$_x$** (**Figure FW.2**) was our preferred regioisomer of butylphthalimide-tethered distal diallylcalix[4]arene, since two of its diazotized product azophenol moieties could tautomerize upon complexation with mercury. For that purpose, a new synthetic route was suggested to resolve the above-mentioned regioselectivity issue yielding only compound **20$_x$**.

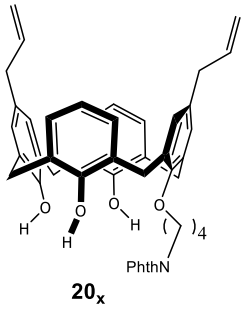

20$_x$

Figure FW.2 Precursor to the final modified Chung's sensor

Employing a distal dibrominated calix[4]arene (**47**) may solve the above-mentioned regioselectivity problem (see the retrospect synthesis in **Scheme FW.1**). After the formation of this compound (**47**), based on what was seen in chapter 4 for a distal dinitrated calix[4]arene (**25**), upon a mono-alkylation reaction with the alkyl halide (which is *N*-(4-bromobutyl)phthalimide **4$_b$**)), the alkyl will only go for one of the calix[4]arene rings with a strongly electronegative functionality (nitro in chapter 4 and bromo here) forming compound **48**.[dddd] Finally, compound **48** can undergo a transmetallation reaction, followed by an S_N2 reaction (with allyl bromide) to substitute the bromine functionalities of compound **48** with the allyl group giving the desired regioisomer of butylphthalimide-tethered distal diallylcalix[4]arene (**20$_x$**).

To begin with, dibenzoylation can be carried out on the non-butylated calix[4]arene (**7**) using benzoyl chloride and K_2CO_3 in acetonitrile (heating under reflux) to produce the distal dibenzoylated calix[4]arene (**45**). This dibenzoylated product (**45**) then can be dibrominated

[dddd] Bromine facilitates the formation of a stronger nucleophile.

Stellenbosch University https://scholar.sun.ac.za

using molecular bromine/chloroform solution in chloroform (at 0 °C then room temperature) to produce the distal dibrominated-dibenzoylated calix[4]arene (**46**).[eeee] After that, de-benzoylation of this compound can be done using KOH in aqueous ethanol/THF (heating under reflux) to yield the distal dibrominated calix[4]arene (**47**). Next, the dibrominated product (**47**) should be mono-alkylated by *N*-(4-bromobutyl)phthalimide (**4$_b$**) with K_2CO_3 in acetonitrile (heating under reflux) forming the butylphthalimide-tethered distal dibrominated calix[4]arene (**48**) (see the summary in **Scheme FW.2**).

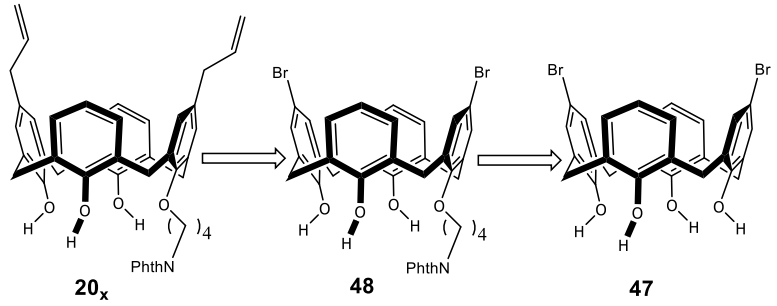

Scheme FW.1 Retrospect synthesis for the precursor to the final modified Chung's sensor

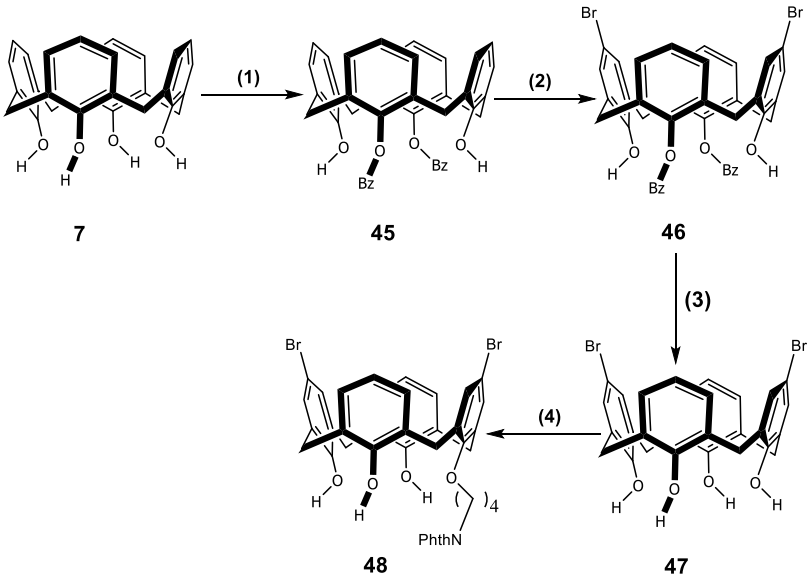

*Scheme FW.2 Formation of the butylphthalimide-tethered distal dibrominated calix[4]arene (**48**). Reagents and conditions: (1) K_2CO_3 (1.0 equiv.), benzoyl chloride (2.0 equiv.), CH_3CN, reflux; (2) $Br_2/CHCl_3$ (2.0 equiv.), $CHCl_3$, 0 °C then RT; (3) KOH (20.0 equiv.), aqueous EtOH/THF, reflux (4) K_2CO_3 (0.6 equiv.), N-(4-bromobutyl)-phthalimide (3.3 equiv.), CH_3CN, reflux*

[eeee] One-step bromination on the non-butylated calix[4]arene (**7**) might result in forming multiple products resulting in purification problems. To avoid that, the approach taken in another paper for producing a distal dibrominated calix[4]arene was considered. In that paper, the non-butylated calix[4]arene (**7**) was first dimethylated and then dibrominated.[3] Unlike their plan, our plan was to remove the extra group after dibromination via an alkaline hydrolysis.

Stellenbosch University https://scholar.sun.ac.za

Thereafter, the butylphthalimide-tethered distal dibrominated calix[4]arene (**48**) can be protected by chloromethyl methyl ether upon mild heating (at 50 °C) with NaH in DMF producing the MOM-protected[ffff] dibrominated calix[4]arene (**49**).[gggg] Now, the transmetallation reaction can be performed employing *i*-PrMg.LiCl$_2$ (Grignard reagent) in THF (at room temperature) followed by an S$_N$2 reaction upon adding allyl bromide (the nucleophile) to the same reaction vial (heating under reflux). The resulting MOM-protected diallyl calix[4]arene (**50**) can then be deprotected by TFA[hhhh] in DCM (at room temperature) to give the desired butylphthalimide-tethered distal diallylcalix[4]arene **20$_x$** (see the summary in **Scheme FW.3**).

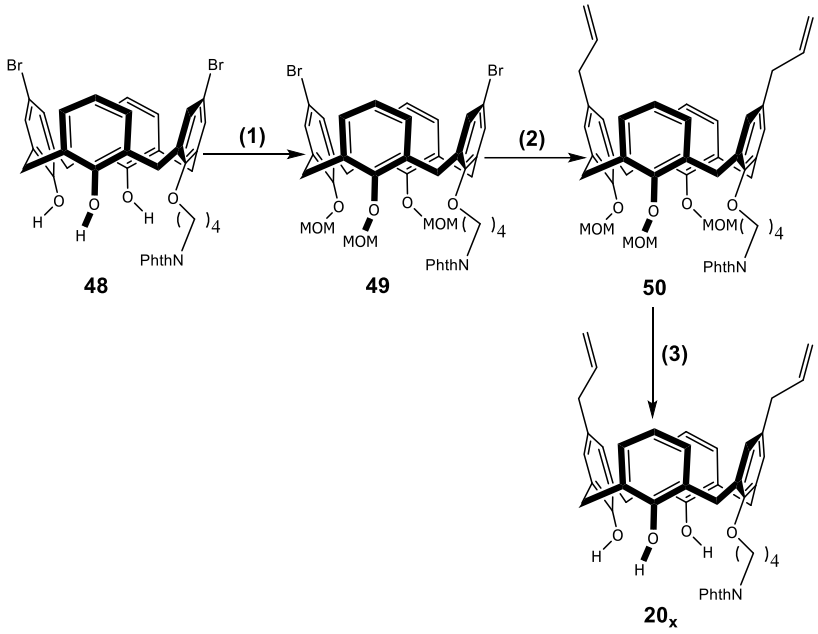

*Scheme FW.3 Formation of the butylphthalimide-tethered distal diallyl calix[4]arene (**20$_x$**). Reagents and conditions: (1) NaH (60% in oil) (3.0 equiv.), MOM-Cl (3.0 equiv.), DMF, 50 °C; (2) (a) i-PrMg.LiCl$_2$ (2.0 equiv.), THF, 0 °C then RT (b) allyl bromide (2.0 equiv.), THF, reflux; (3) TFA (3.0 equiv.), DCM, RT*

After the successful synthesis of the calix[4]arene nucleophile for the diazotization reaction (**20$_x$**), this compound can be subjected to the diazotization alongside *p*-anisidine, NaNO$_2$ and 4 M HCl in acetone/pyridine (at 0 °C then room temperature). Having achieved the desired diazotized calix[4]arene (**16**), the product phthalimide group needs to be deprotected to form the final modified Chung's sensor. Caution must be taken so that the deprotection takes place

[ffff] MOM: Methoxymethyl ether.

[gggg] According to literature, a safe and easy way to conduct this kind of synthesis is using a MOM-protected starting material.[4] It would prevent the side reactions such as the lower rim hydroxyls deprotonation by the carbanion.

[hhhh] TFA: Trifluoroacetic acid.

Stellenbosch University https://scholar.sun.ac.za

at room temperature and not at high temperatures due to the possible decomposition of azo groups under harsh thermal conditions (which occurred for several of our azo compounds in chapter 4). Thus, instead of hydrazine monohydrate used in chapter 2 for phthalimide deprotection, the alkaline hydrolysis can be attempted by KOH in aqueous ethanol/THF (at room temperature) (see the summary in **Scheme FW.4**).

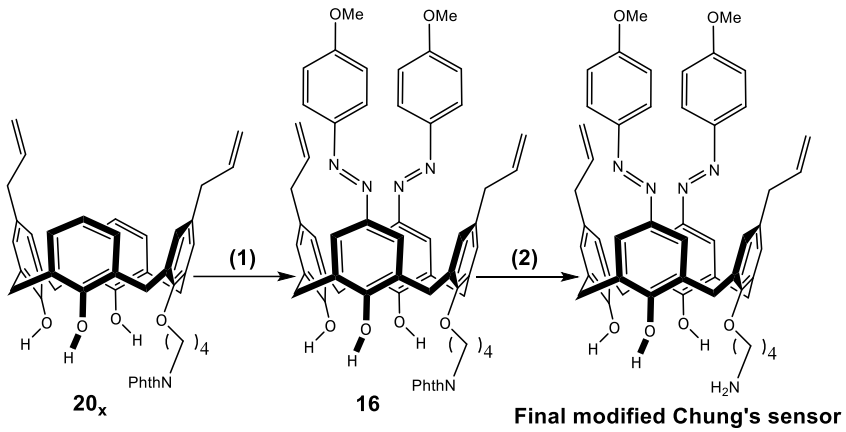

Scheme FW.4 Formation of the final modified Chung's sensor. Reagents and conditions: (1)(a) pyridine, 0 °C (b) p-anisidine (5.0 equiv.), $NaNO_2$ (5.0 equiv.), 4 M HCl (50.0 equiv.), acetone, 0 °C then RT; (2) KOH (10.0 equiv.), aqueous EtOH/THF, RT

This product can then be grafted onto PSMA employing the approaches explained in chapter 3.

Part C. Suggested future work for the hydrogel formation studies

In chapter 5 our attempts to facilitate the hydrogel formation on the polymeric scaffold of *p*-sulfonated calix[4]arene (with either of PSMA or PVP-MA as its polymeric moieties) failed to achieve any favorable result despite proving the interaction between the graft and the potential crosslinker (through ^{1}H-NMR spectroscopic titration studies).

As mentioned in chapter 5, one possible reason for that failure could be the conformational status of the calix[4]arene. Since our calix[4]arene has a conformationally mobile nature (apparently there is an equilibrium between the cone and the partial cone conformations), locking the cone conformer may be a solution to our problem. According to Shinkai *et al.*, the easiest way to do that is through the protection of the lower rim with propyl groups.[5] To avoid the alkylation of amine, it is not possible to start from the amine-tethered *p*-sulfonated calix[4]arene (**33**) and trialkylate it. Thus, a trialkylated *t*-butylated calix[4]arene (**51**) should be produced following a previously reported approach by Shinkai *et al.*[5] In order to regioselectively trialkylate a calix[4]arene, the parent *t*-butylated calix[4]arene (**7**) and

Stellenbosch University https://scholar.sun.ac.za

iodopropane (excess) should be stirred in DMF at room temperature using $BaO/Ba(OH)_2.8H_2O$ forming compound **51** in cone conformation.[iiii] Thereafter, this compound can be monoalkylated with the alkyl halide (*N*-(4-bromobutyl)phthalimide $\mathbf{4_b}$) exactly the same way described in chapter 2 (with K_2CO_3 in acetonitrile via heating under reflux) to afford compound **52**. Next, this compound should be transformed into amine using the hydrazinolysis approach discussed in chapter 2 (with hydrazine monohydrate in ethanol/THF (heating under reflux) to yield compound **53**. After that, this compound can be sulfonated with concentrated sulfuric acid at room temperature resulting in compound **54**. This ammonium salt (**54**) should be grafted onto the polymer[jjjj] with the method explained in chapter 5 (with a large excess of NaH at 75 °C) to afford the *p*-sulfonated calix[4]arene-grafted polymer (**55**). This graft (**55**) can be subjected to the gelation study and if it forms a hydrogel upon mixing with the crosslinker, it will verify the conformation role in the failure of our previous gelation attempts (see the summary in **Scheme FW.5**).

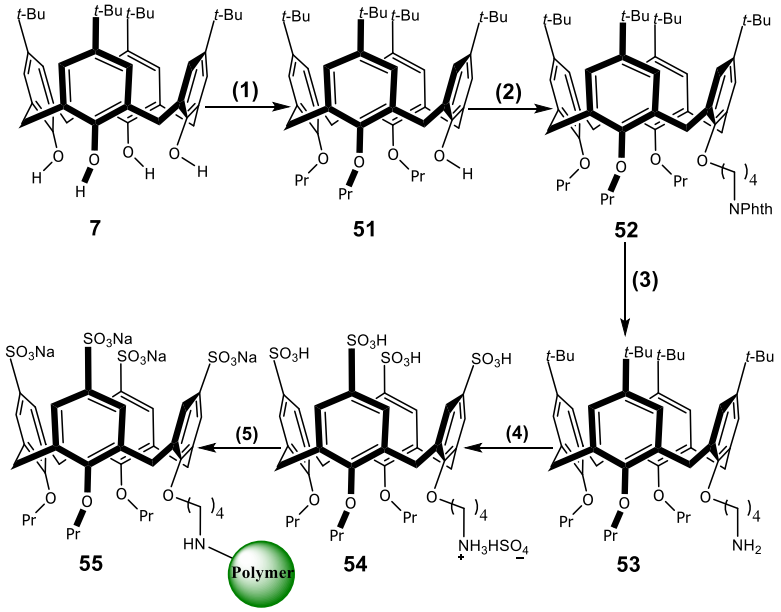

*Scheme FW.5 Formation of p-sulfonated calix[4]arene-grafted polymer (in cone conformation) (**55**). Reagents and conditions: (1) BaO (1.5 equiv.), $Ba(OH)_2.8H_2O$ (3.5 equiv.), iodopropane (30.0 equiv.), DMF; (2) K_2CO_3 (0.6 equiv.), N-(4-brombutyl)-phthalimide (3.3 equiv.), CH_3CN, reflux; (3) $N_2H_4{\cdot}H_2O$ (10.0 equiv.), EtOH/THF, reflux; (4) H_2SO_4 (Conc.), RT; (5) Polymer, NaH (60% in oil) (10.0 equiv.), DMF, 75 °C*

Another possible reason for the failure of the gelation study was presumed to be the low modification degree of the polymer. As mentioned in chapter 5, due to the deactivating effect

[iiii] According to Shinkai *et al.*, the product was obtained in 63% yield.[5]

[jjjj] PVP-MA is the preferable choice, due to the fact that its calix[4]arene-modifed graft will possess better solubility in water than that of PSMA.

Stellenbosch University https://scholar.sun.ac.za

of the sulfonate groups which is reducing the nucleophilicity of the amine, it does not seem possible to achieve a high modification degree upon grafting the calix[4]arene onto the polymer. As a possible solution to this problem, instead of a ‘‘grafting onto approach’’, a ‘‘grafting through approach’’ can be employed. By using this approach, the calix[4]arene content of the graft can be drastically increased through carefully adjusting the mmol ratio between the calix[4]arene macromonomer and the other monomer.[kkkk] In order to do so, a macromonomer of the amine-tethered *p*-sulfonated calix[4]arene (**33**) should be prepared and then copolymerized with another water-soluble monomer (here *N*,*N*-dimethylacrylamide) so that an extremely water-soluble copolymer with a high calix[4]arene content can be obtained. As a suggestion, the macromonomer of compound **33** can possess an acrylamide substituent for the purpose of copolymerization. Therefore, acryloyl chloride must react with compound **33** to produce the desired macromonomer. In doing so, this compound (**33**) can be acylated with acryloyl chloride (in DMF at –10 °C then room temperature) to yield compound **56**. This compound can eventually go through an ion-exchange column (Na^+ will be replaced with H^+)[llll] to afford the macromonomer **57** (see the summary in **Scheme FW.6**).

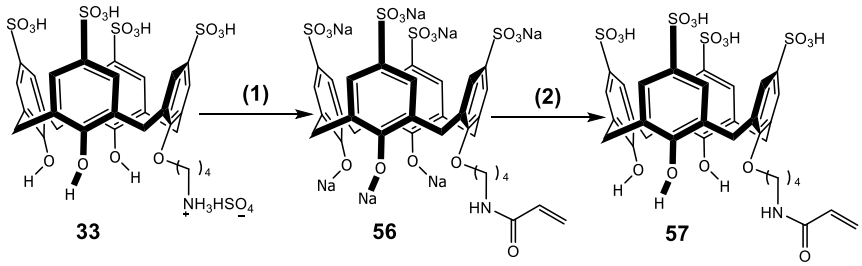

*Scheme FW.6 Formation of p-sulfonated calix[4]arene-acrylated monomer (**57**). Reagents and conditions: (1) (a) NaH (60% in oil) (8.0 equiv.), DMF, 75 °C (b) acryloyl chloride (1.0 equiv.), DMF, –10 °C then RT; (2) Ion exchange column*

After the synthesis of the macromonomer **57**, it can be copolymerized with another monomer such as *N*,*N*-dimethylacrylamide. The copolymerization could be performed by a redox system (e.g. ammonium persulfate and tetramethylethylenediamine) at low temperatures (0 °C to room temperature) in de-ionized water or by a radical initiator like AIBN in methanol or ethanol via mild heating or even by a UV-assisted polymerization (see the general plot in **Scheme FW.7**).

[kkkk] For example, when 1.0 mmol of the calix[4]arene macromonomer is copolymerized with 1.0 mmol of the other monomer, ideally a calix[4]arene-grafted polymer with a 50% calix[4]arene content can form.

[llll] This solution was suggested by Shinkai *et al.* as the first approach ever attempted to make the sulfonic acid version of the calixarenes.[6]

Stellenbosch University https://scholar.sun.ac.za

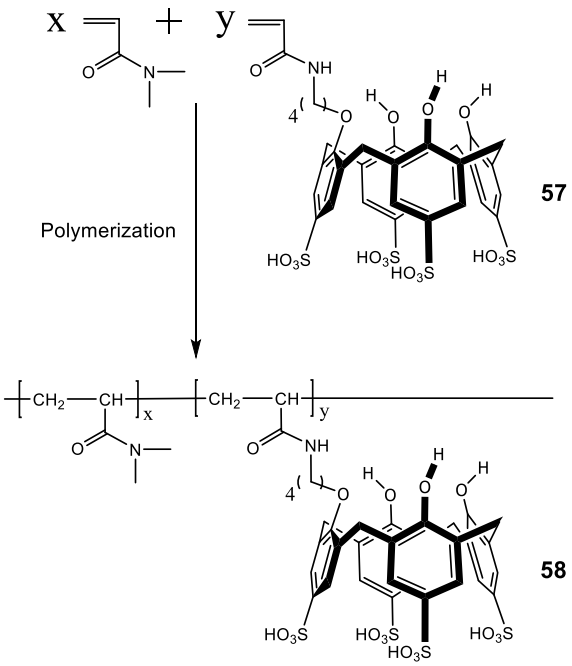

*Scheme FW.7 General plot to copolymerize p-sulfonated calix[4]arene-acrylated macromonomer (**57**) with N,N-dimethylacrylamide*

This copolymer might be able to form a hydrogel upon mixing with a crosslinker. The success of the gelation experiment, in this case, will prove the importance of the modification degree of the polymer in the formation of a hydrogel.

Future work references

(1) Kang, Y.; Rudkevich, D. M. *Tetrahedron* **2004**, *60*, 11219–11225.

(2) Ohira, S-I; Wanigasekara, E.; Rudkevich, D. M.; Dasgupta, P. K. *Talanta* **2009**, *77*, 1814–1820.

(3) Yang, Y.; Arora, G.; Fernandez, F. A.; Crawford, J. D.; Surowiec, K.; Lee, E. K.; Bartsch, R. A. *Tetrahedron* **2011**, *67*, 1389–1397.

(4) Agharahimi, M. R.; Lebel, N. A. *J. Org. Chem.* **1995**, *60*, 1856–1863.

(5) Shinkai, S.; Araki, K.; Iwamoto, K. *J. Org. Chem.* **1991**, *56*, 4955–4962.

(6) Shinkai, S.; Mori, S.; Koreishi, H.; Tsubaki, T.; Manabe, O. *J. Am. Chem. Soc*. **1986**, *108*, 2409–2416.

Stellenbosch University https://scholar.sun.ac.za

Appendix

In this section, the remaining analytical data of our experiments will be presented. The summary of these experiments and the produced grafts with their corresponding codes can be seen in **Table A.1**. The samples with the solubility issues were not subjected to the solution analysis.

Table A.1 Synthesized grafts for the project and the conditions to make them

Entry	Graft code	Polymeric backbone	Pendant group (calix[4]arene)	Base (equiv.)	Graft status
1	**A_{30}-10_b**	PSMA 30%	**10_b**	-	Ring-opened
2	**B_{30}-10_b**	PSMA 30%	**10_b**	-	Ring-closed
3	**C_{30}-10_b**	PSMA 30%	**10_b**	-	Ring-closed
4	**D_{30}-10_b**	PSMA 30%	**10_b**	-	Ring-opened
5	**E_{30}-10_b**	PSMA 30%	**10_b**	-	Ring-opened
6	**A_{30}-10_e**	PSMA 30%	**10_e**	-	Ring-opened
7	**C_{30}-10_e**	PSMA 30%	**10_e**	-	Ring-closed
8	**A_{30}-10_h**	PSMA 30%	**10_h**	-	Ring-opened
9	**C_{30}-10_h**	PSMA 30%	**10_h**	-	Ring-closed
10	**A_{30}-S_{10}-33**	PSMA 30%	**33**	NaH (10.0)	Ring-opened
11	**C_{30}-S_{10}-33**	PSMA 30%	**33**	NaH (10.0)	Ring-closed
12	**A_{30}-T_5-33**	PSMA 30%	**33**	Et_3N (5.0)	Ring-opened
13	**C_{30}-T_5-33**	PSMA 30%	**33**	Et_3N (5.0)	Ring-closed
14	**A_{50}-S_{10}-33**	PSMA 50%	**33**	NaH (10.0)	Ring-opened
15	**C_{50}-S_{10}-33**	PSMA 50%	**33**	NaH (10.0)	Ring-closed
16	**A_{50}-T_5-33**	PSMA 50%	**33**	Et_3N (5.0)	Ring-opened
17	**C_{50}-T_5-33**	PSMA 50%	**33**	Et_3N (5.0)	Ring-closed
18	**A_{50}-T_{10}-33**	PSMA 50%	**33**	Et_3N (10.0)	Ring-opened
19	**C_{50}-T_{10}-33**	PSMA 50%	**33**	Et_3N (10.0)	Ring-closed
20	**A_{50}-T_{20}-33**	PSMA 50%	**33**	Et_3N (20.0)	Ring-opened
21	**C_{50}-T_{20}-33**	PSMA 50%	**33**	Et_3N (20.0)	Ring-closed
22	**A_{50}-P_{10}-33**	PSMA 50%	**33**	K_2CO_3 (10.0)	Ring-opened
23	**C_{50}-P_{10}-33**	PSMA 50%	**33**	K_2CO_3 (10.0)	Ring-closed
24	**A_{50}-C_{10}-33**	PSMA 50%	**33**	Cs_2CO_3 (10.0)	Ring-opened
25	**C_{50}-C_{10}-33**	PSMA 50%	**33**	Cs_2CO_3 (10.0)	Ring-closed
26	**A_{50}-VP-S_{10}-33**	PVP-MA 50%	**33**	NaH (10.0)	Ring-opened
27	**C_{50}-VP-S_{10}-33**	PVP-MA 50%	**33**	NaH (10.0)	Unknown

Stellenbosch University https://scholar.sun.ac.za

Appendix A: FT-IR extras

1. Chapter 3 FT-IR spectra

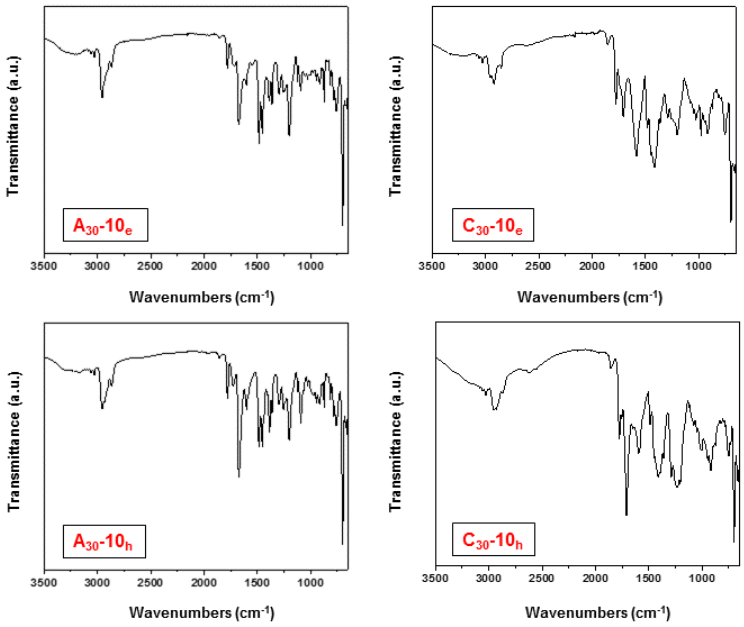

Figure A.1 Chapter 3 FT-IR spectra

Stellenbosch University https://scholar.sun.ac.za

2. Chapter 5 FT-IR spectra

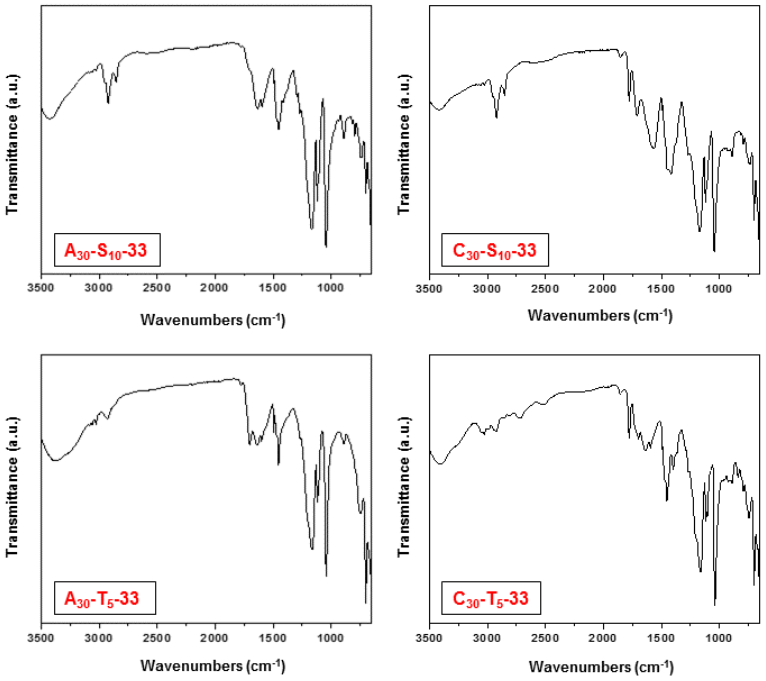

Figure A.2 Chapter 5 FT-IR spectra (part 1)

Stellenbosch University https://scholar.sun.ac.za

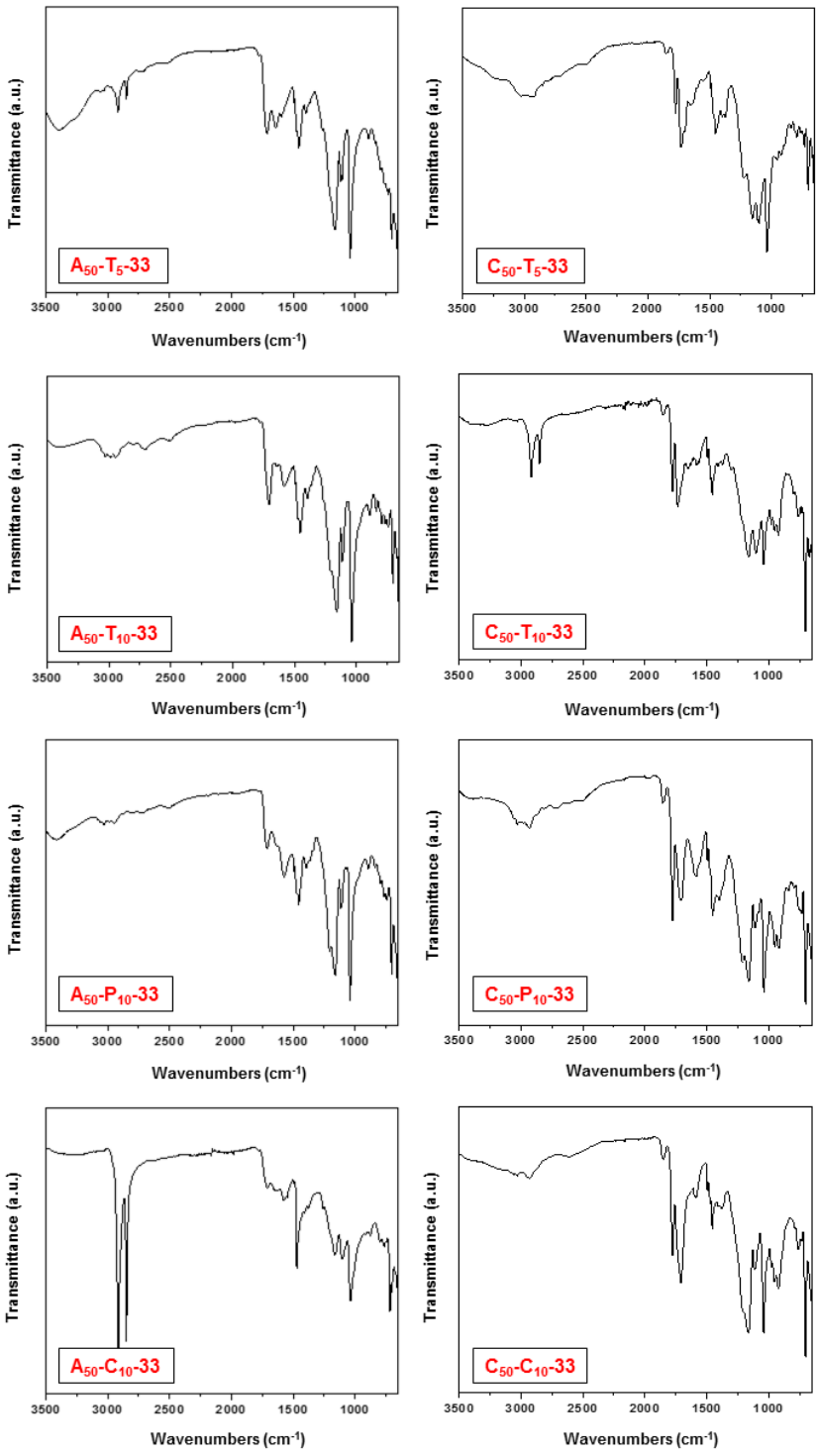

Figure A.3 Chapter 5 FT-IR spectra (part 2)

Stellenbosch University https://scholar.sun.ac.za

Appendix B: UV-Vis extras

1. Chapter 3 UV-Vis spectra

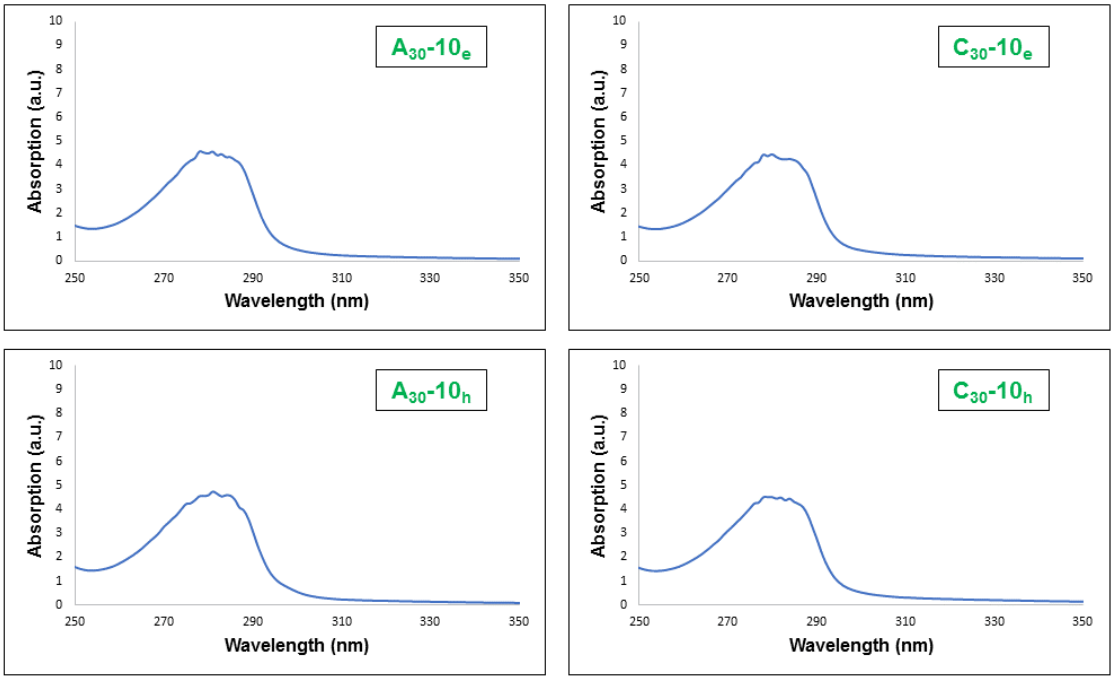

Figure A.4 Chapter 3 UV-Vis spectra

Stellenbosch University https://scholar.sun.ac.za

2. Chapter 5 UV-Vis spectra

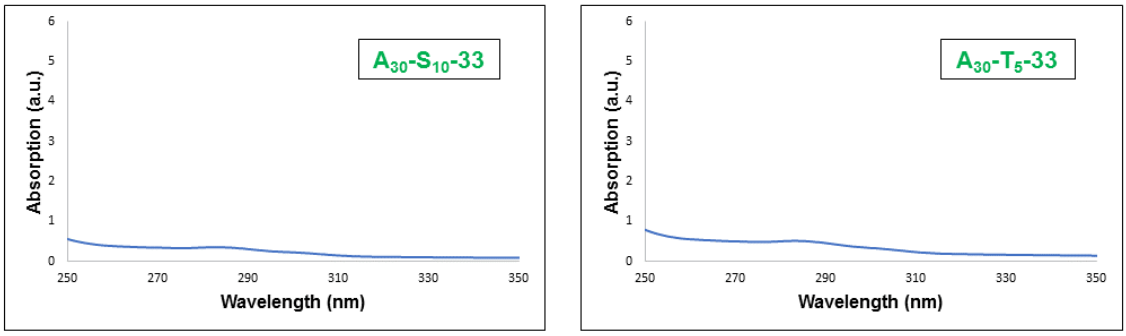

Figure A.5 Chapter 5 UV-Vis spectra (part 1)

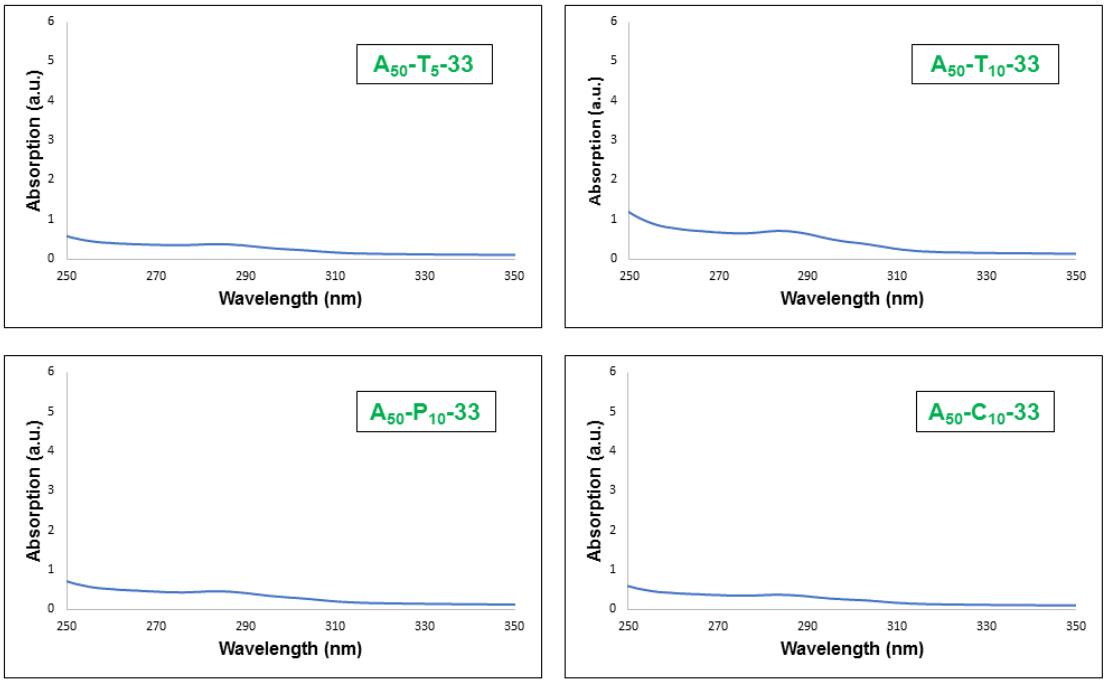

Figure A.6 Chapter 5 UV-Vis spectra (part 2)

Stellenbosch University https://scholar.sun.ac.za

Appendix C: ^{1}H-NMR extras

1. Chapter 3 ^{1}H-NMR spectra

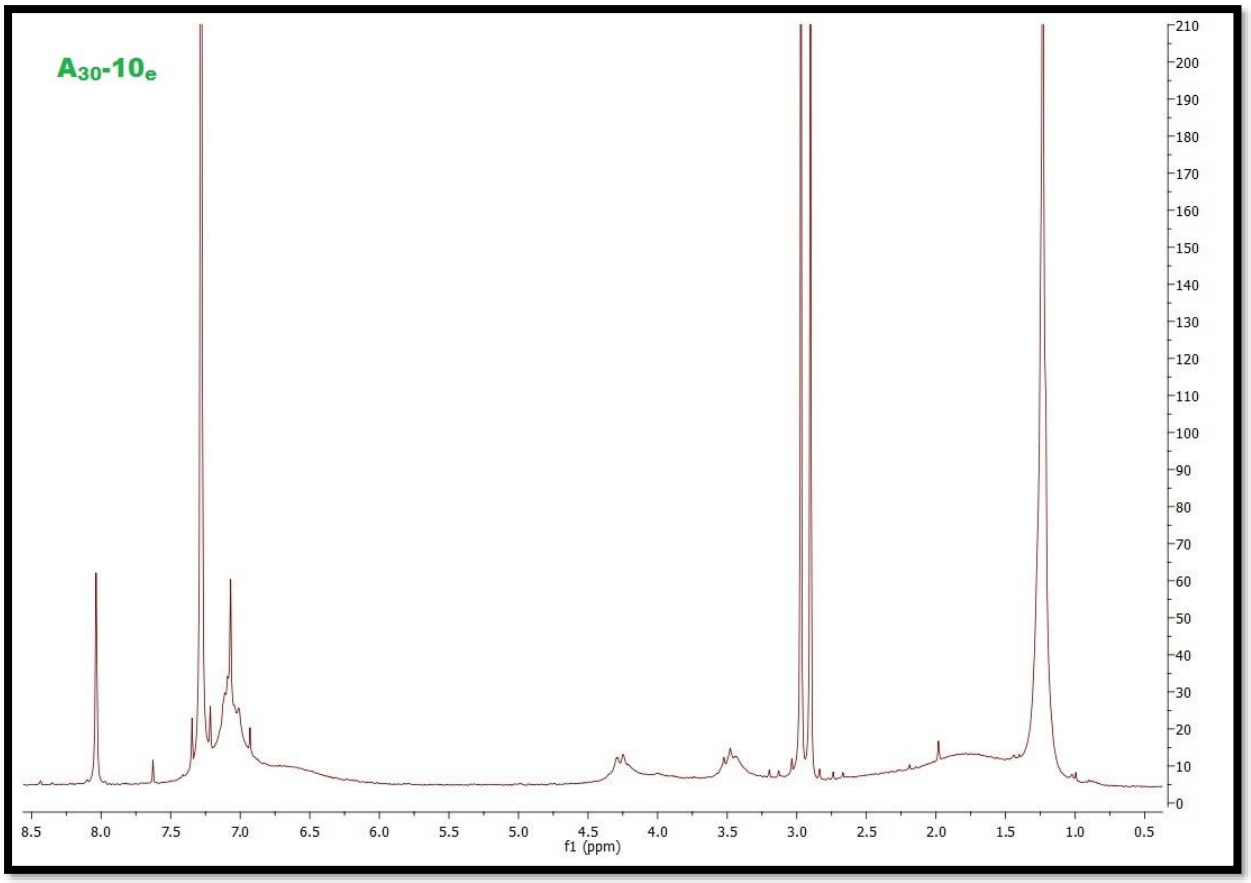

Figure A.7 ***A$_{30}$-10$_{e}$*** *^{1}H-NMR spectrum (in $CDCl_3$)*

Stellenbosch University https://scholar.sun.ac.za

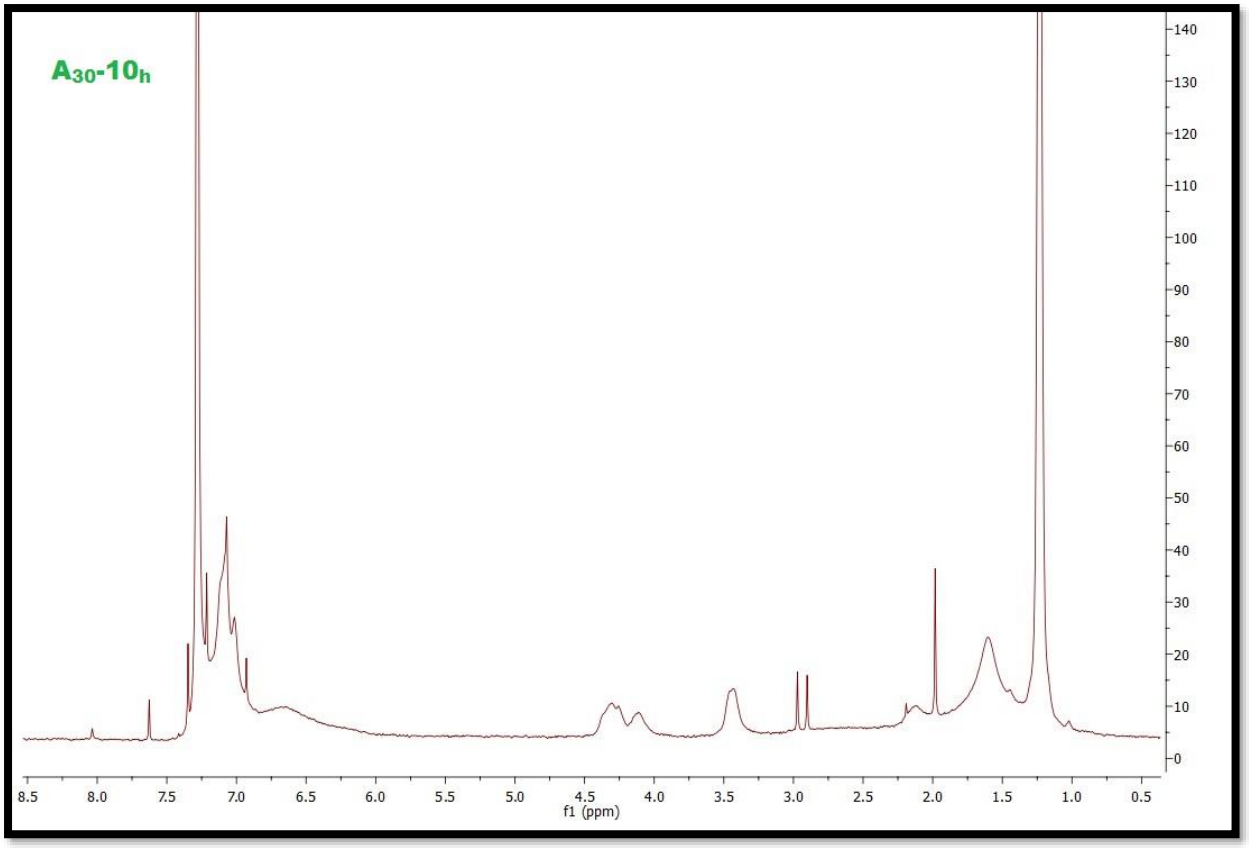

Figure A.8 ***A30-10h*** *^{1}H-NMR spectrum (in $CDCl_3$)*

Stellenbosch University https://scholar.sun.ac.za

2. Chapter 5 ^{1}H-NMR spectra

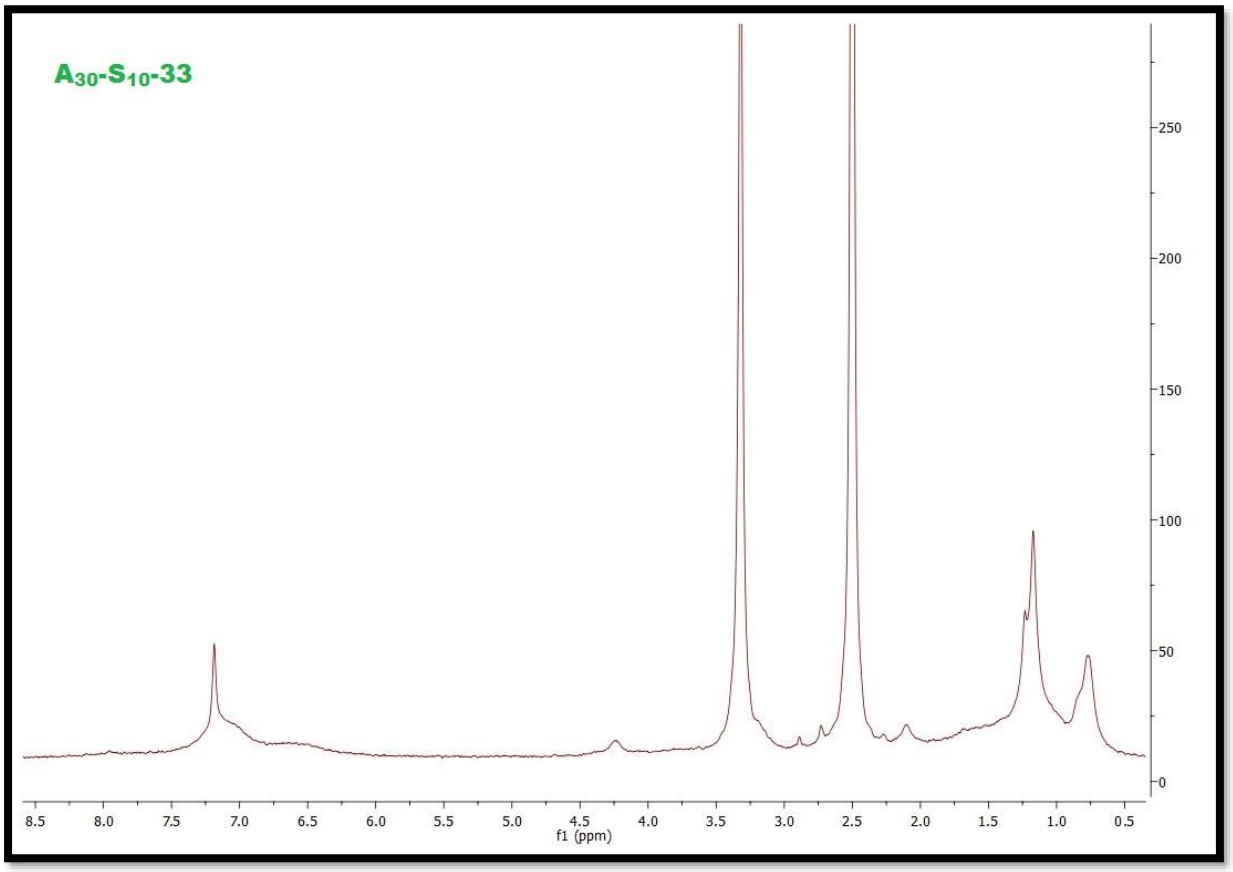

Figure A.9 ***A$_{30}$-S$_{10}$-33*** *^{1}H-NMR spectrum (in DMSO-d$_6$)*

Stellenbosch University https://scholar.sun.ac.za

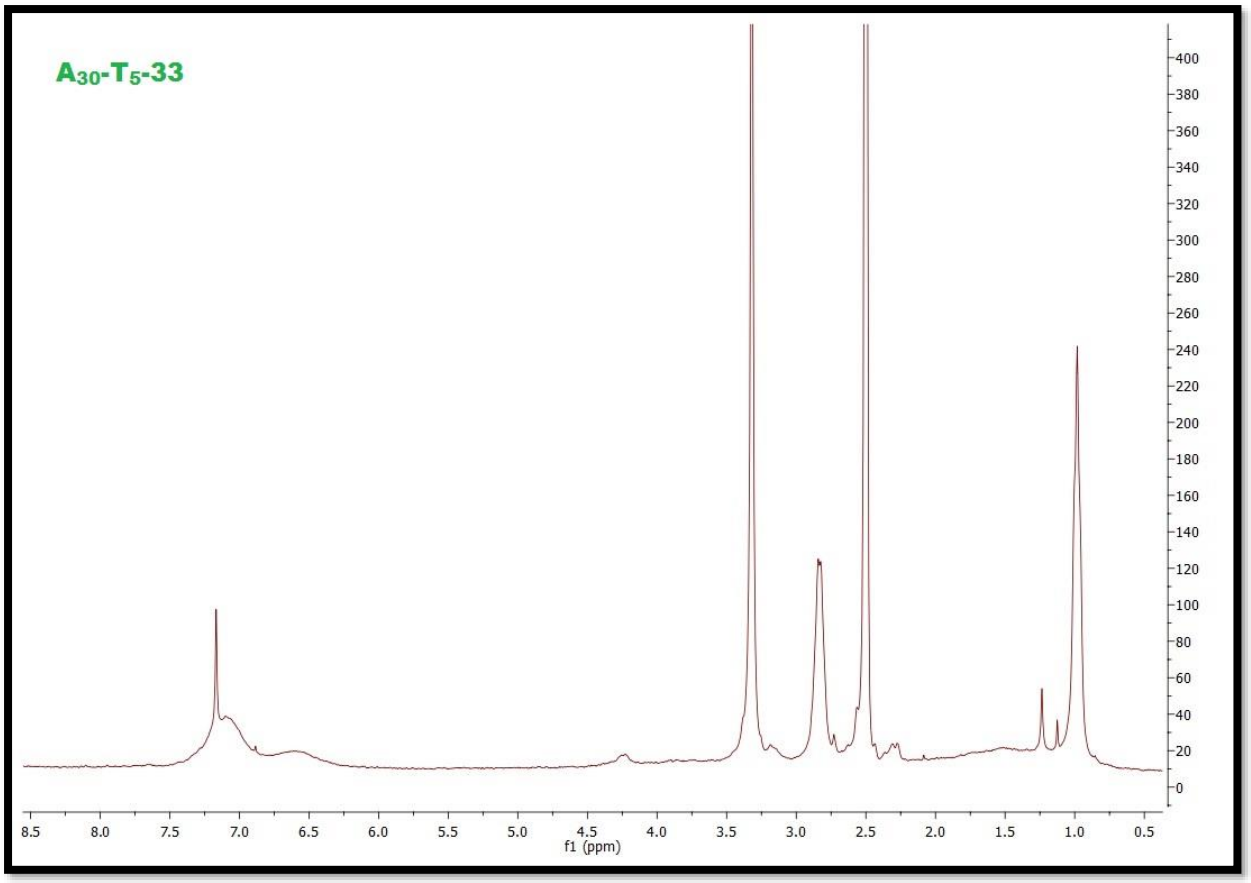

Figure A.10 ***A30-T5-33*** *^{1}H-NMR spectrum (in DMSO-d_6)*

Stellenbosch University https://scholar.sun.ac.za

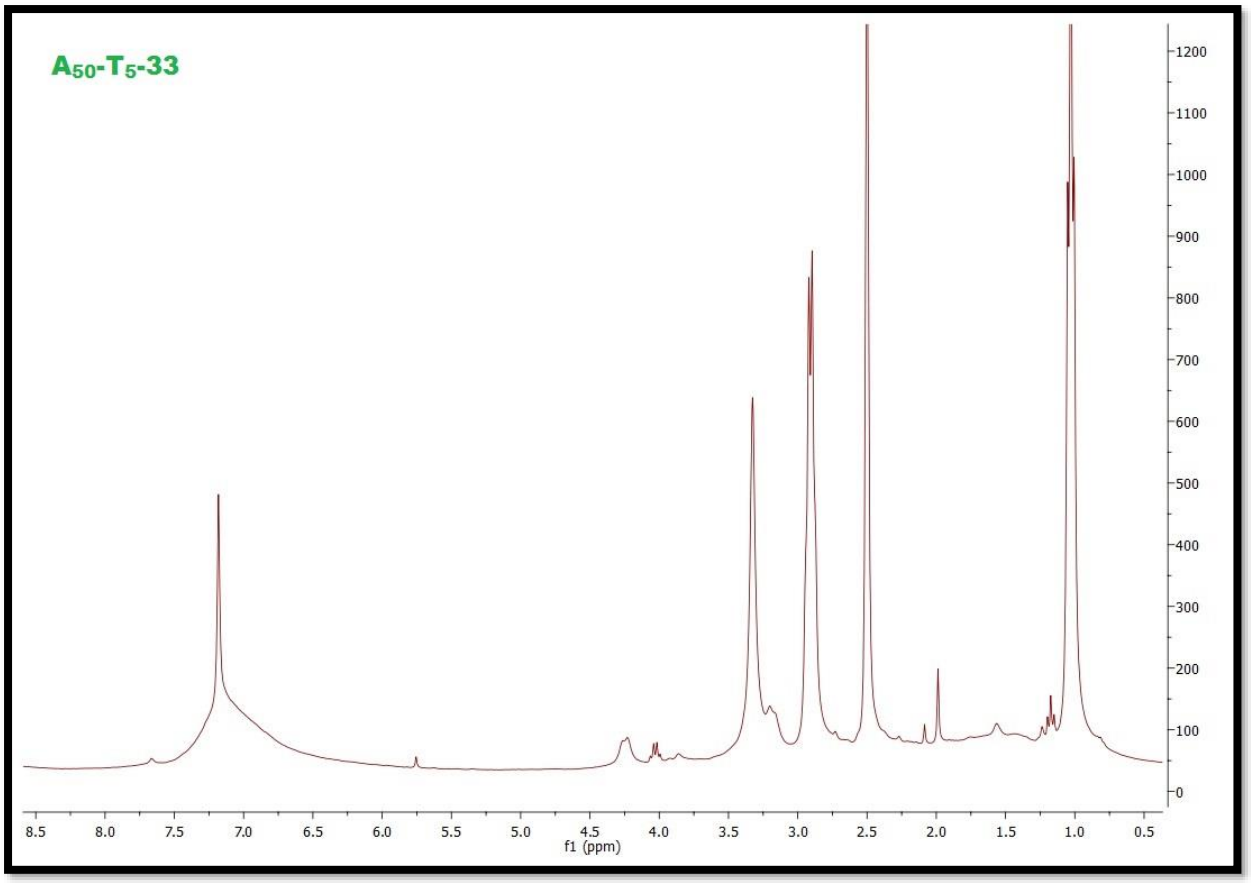

Figure A.11 ***A*$_{50}$-*T*$_{5}$-33** *^{1}H-NMR spectrum (in DMSO-d$_{6}$)*

Stellenbosch University https://scholar.sun.ac.za

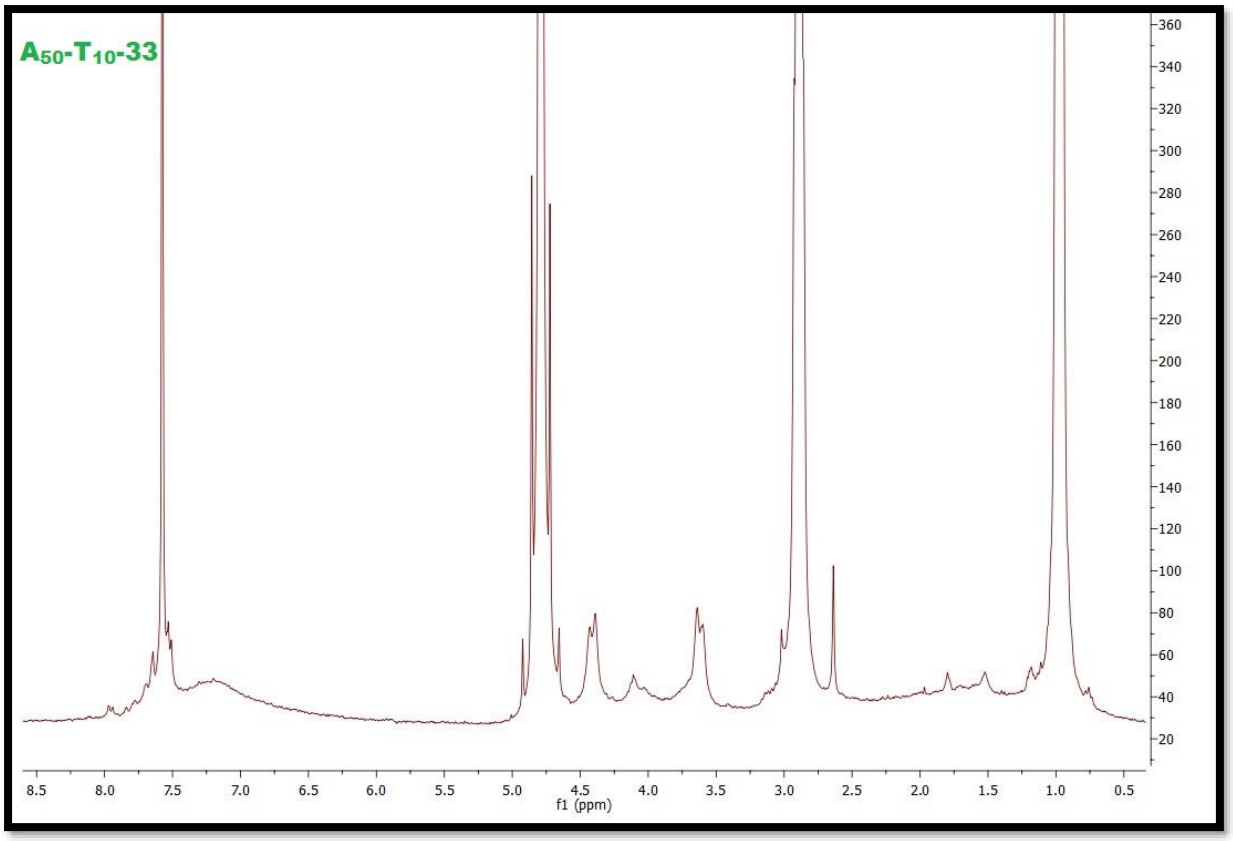

Figure A.12 ***A_{50}-T_{10}-33*** *^{1}H-NMR spectrum (in D_2O)*

Stellenbosch University https://scholar.sun.ac.za

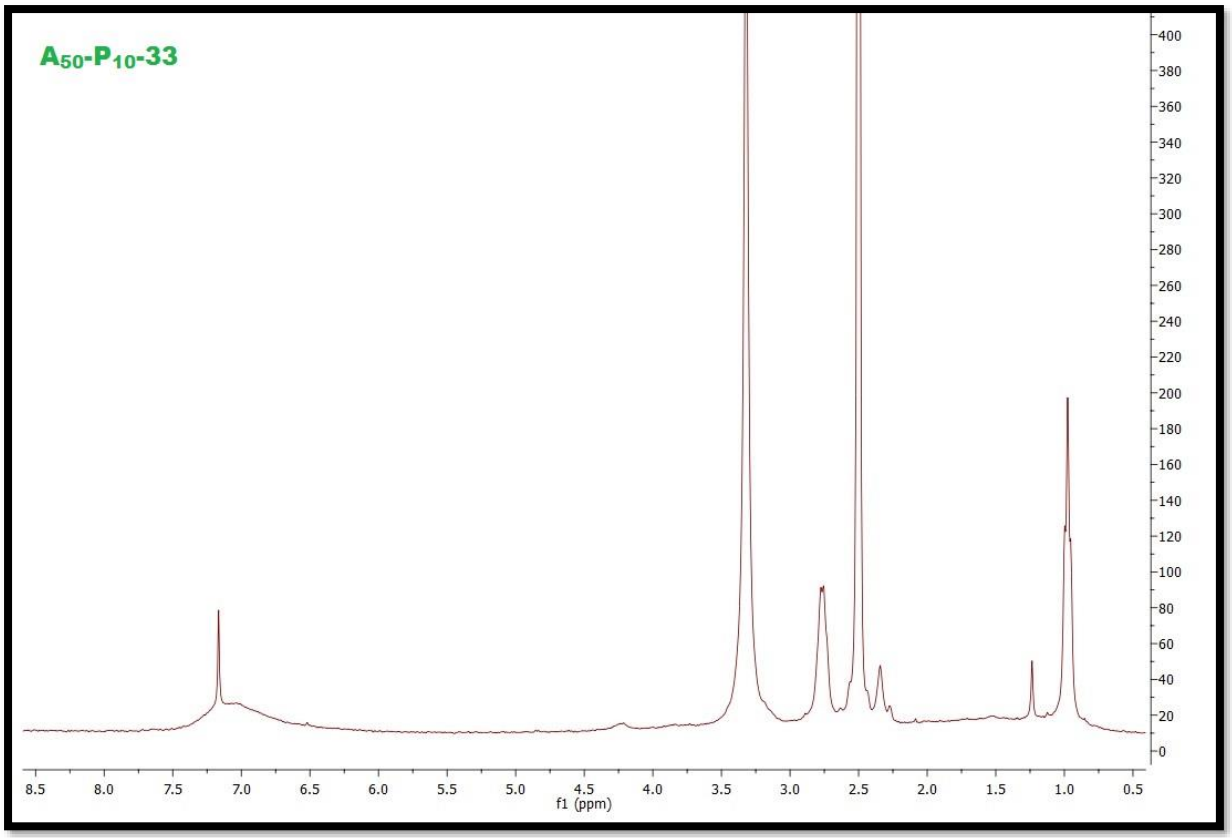

Figure A.13 ***A_{50}-P_{10}-33*** *^{1}H-NMR spectrum (in DMSO-d_6)*

Stellenbosch University https://scholar.sun.ac.za

Appendix D: SEC (GPC) extras

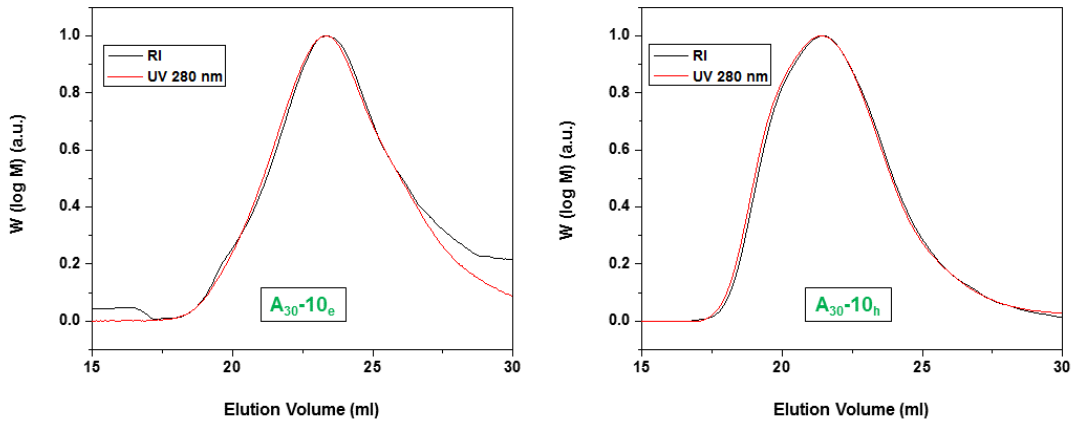

Figure A.14 SEC (GPC) results for ***A_{30}-10$_e$*** *and* ***A_{30}-10$_h$***

Table A.2 SEC data for ***A_{30}-10$_e$*** *and* ***A_{30}-10$_h$***

Entry	Compound name	M_n (g.mol^{-1})	M_w (g.mol^{-1})	Đ
1	**A_{30}-10$_e$**	6.7781×10^4	1.3495×10^5	1.99
2	**A_{30}-10$_h$**	1.6061×10^5	3.2315×10^5	2.01

Stellenbosch University https://scholar.sun.ac.za

Appendix B: DSC extras

1. Chapter 3 DSC thermograms

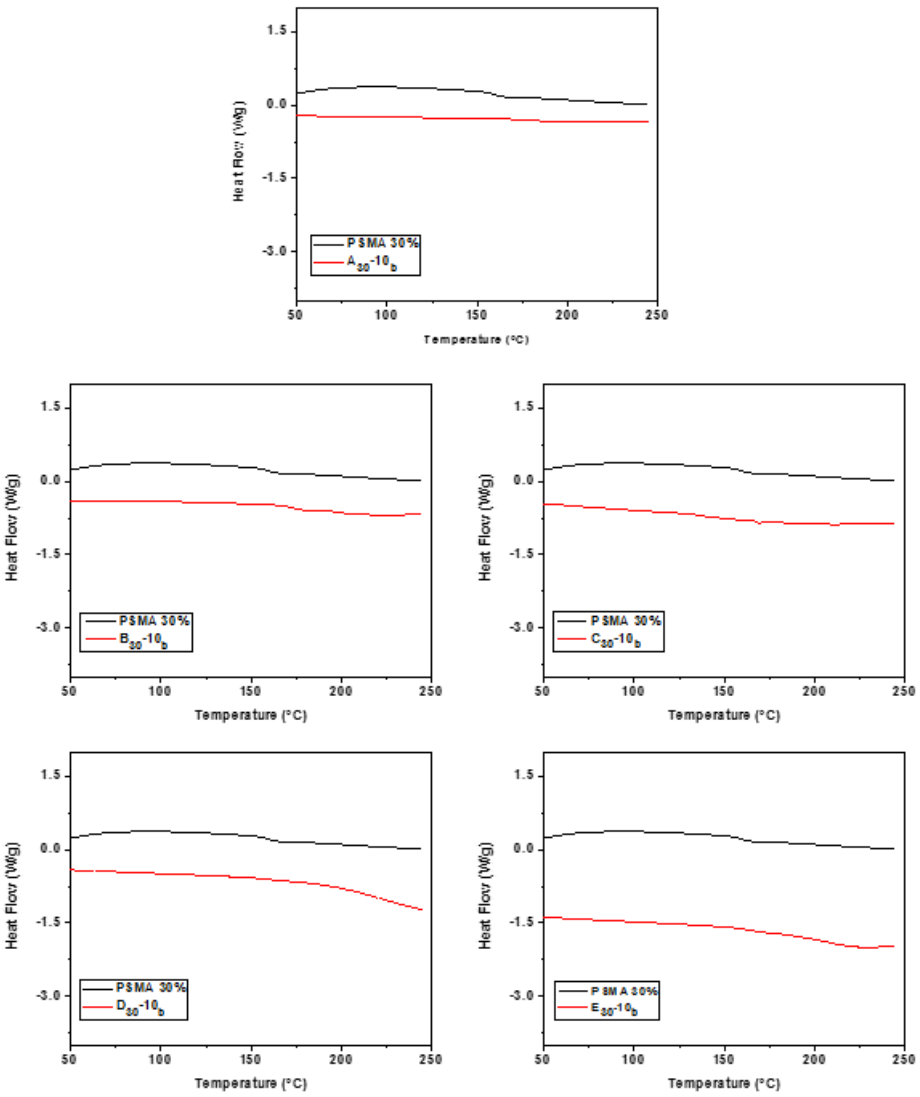

Figure A.15 Chapter 3 DSC thermograms (part 1)

Stellenbosch University https://scholar.sun.ac.za

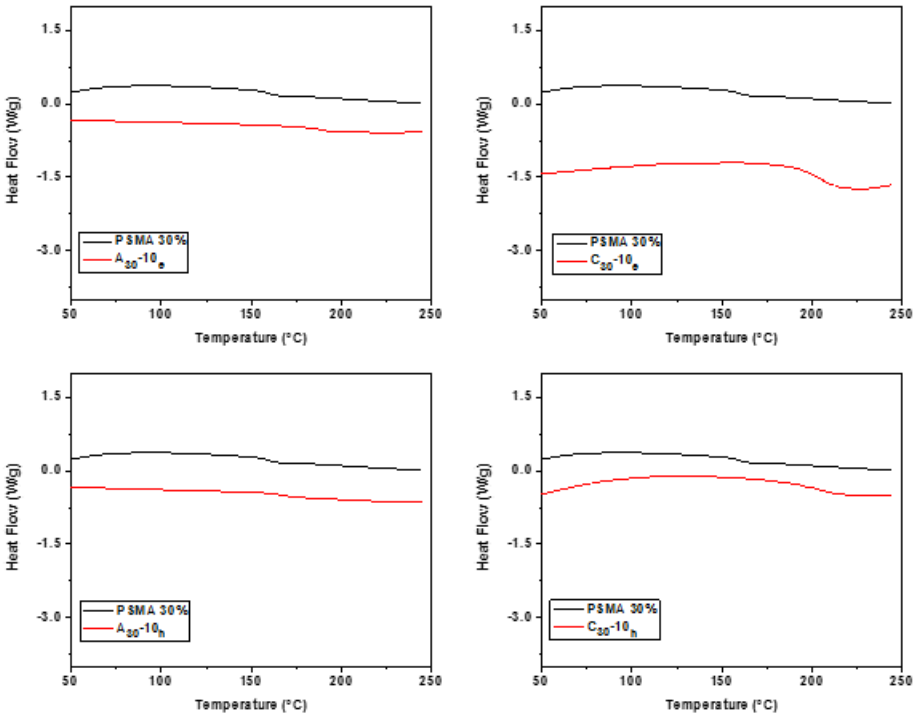

Figure A.16 Chapter 3 DSC thermograms (part 2)

Stellenbosch University https://scholar.sun.ac.za

2. Chapter 5 DSC thermograms

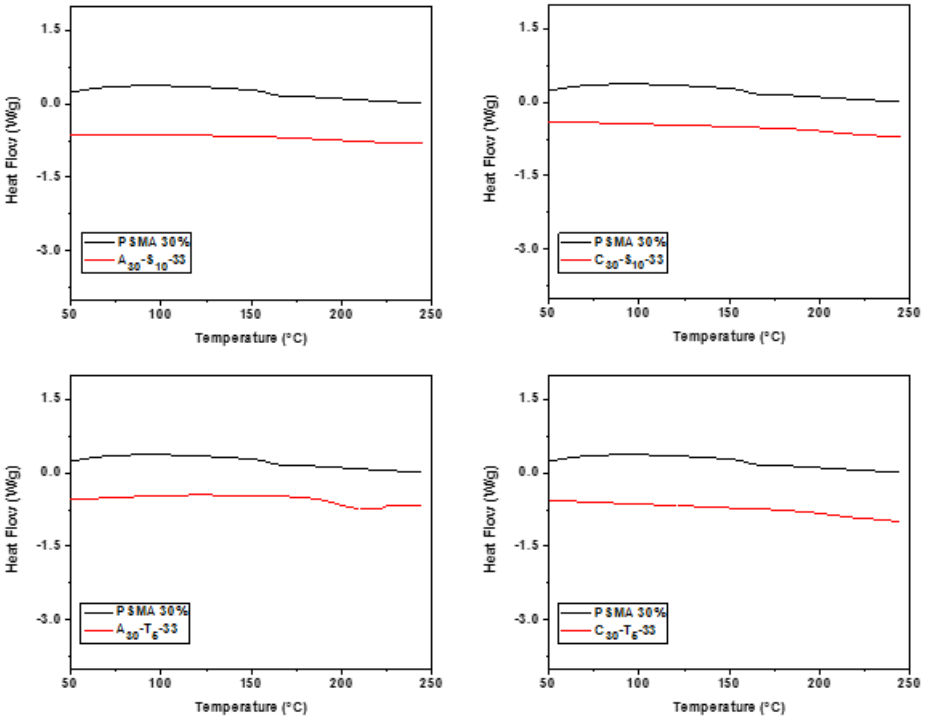

Figure A.17 Chapter 5 DSC thermograms (part 1)

Stellenbosch University https://scholar.sun.ac.za

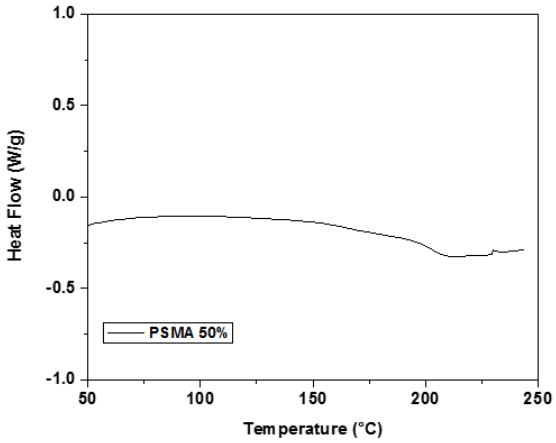

Figure A.18 Chapter 5 DSC thermograms (part 2)

Stellenbosch University https://scholar.sun.ac.za

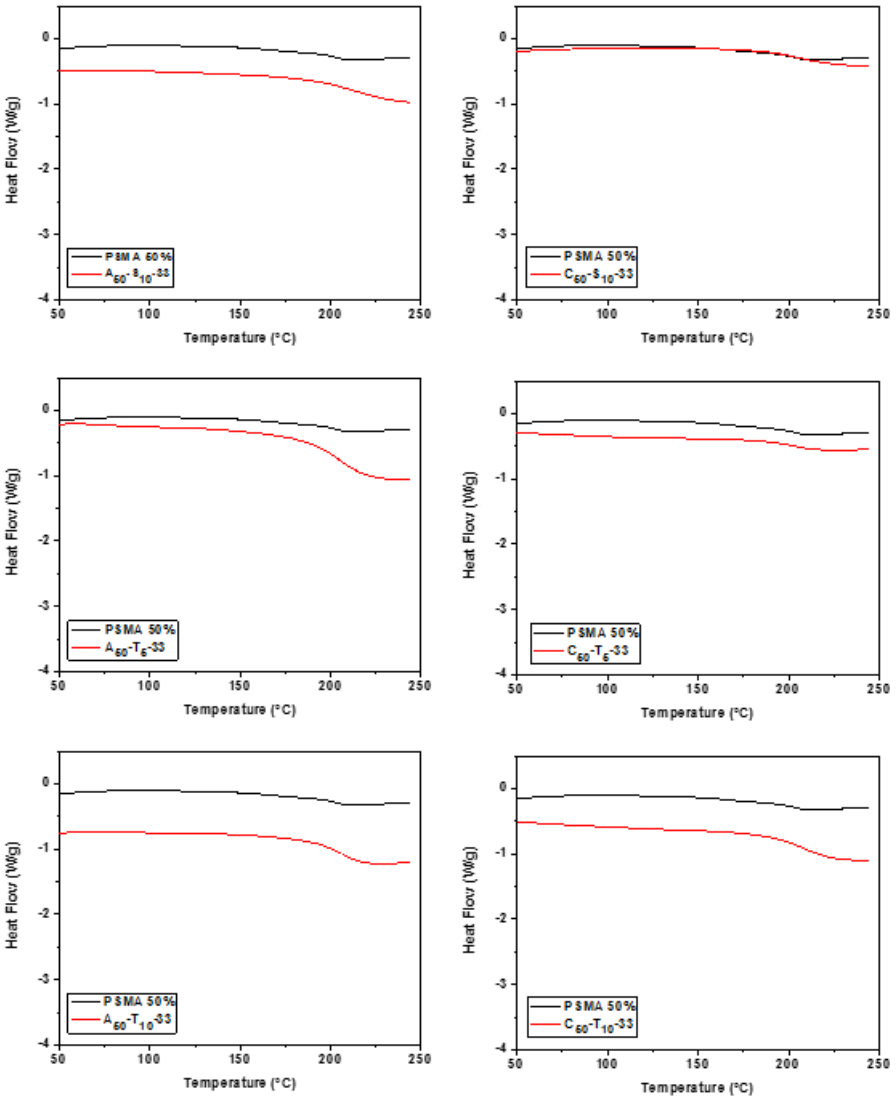

Figure A.19 Chapter 5 DSC thermograms (part 3)

Stellenbosch University https://scholar.sun.ac.za

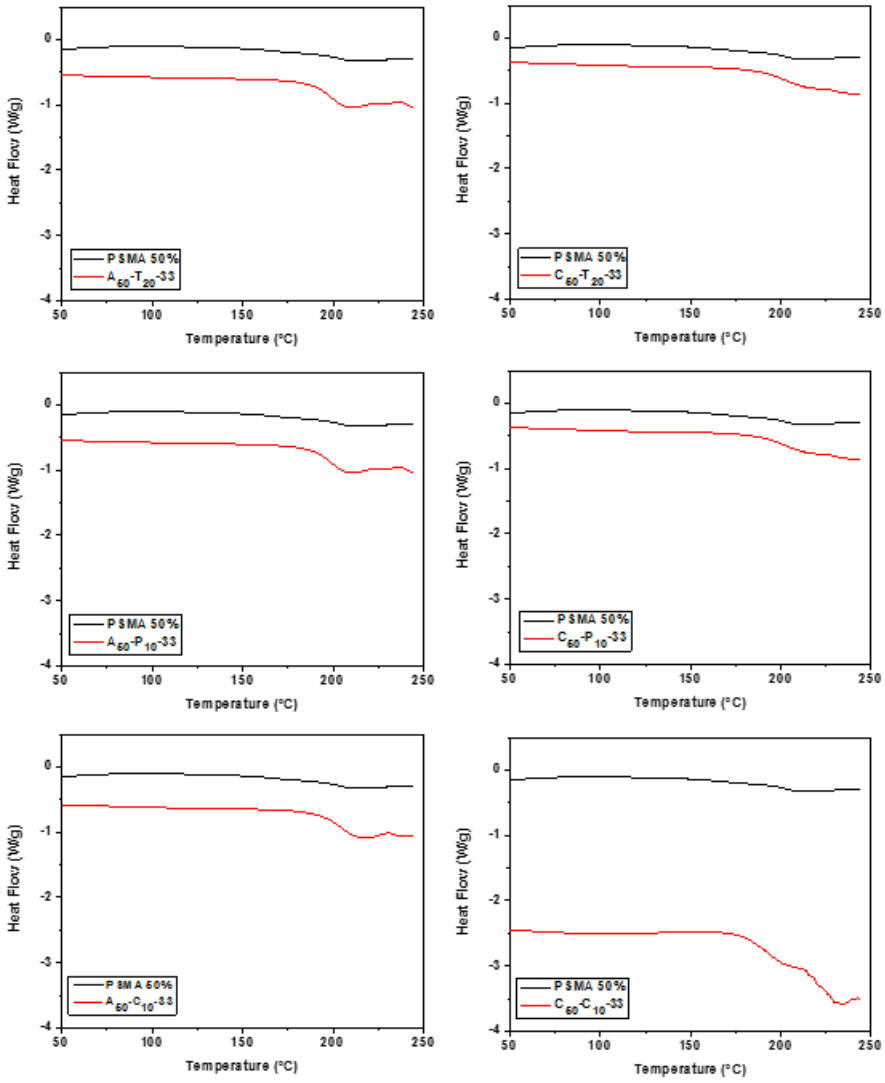

Figure A.20 Chapter 5 DSC thermograms (part 4)

Stellenbosch University https://scholar.sun.ac.za

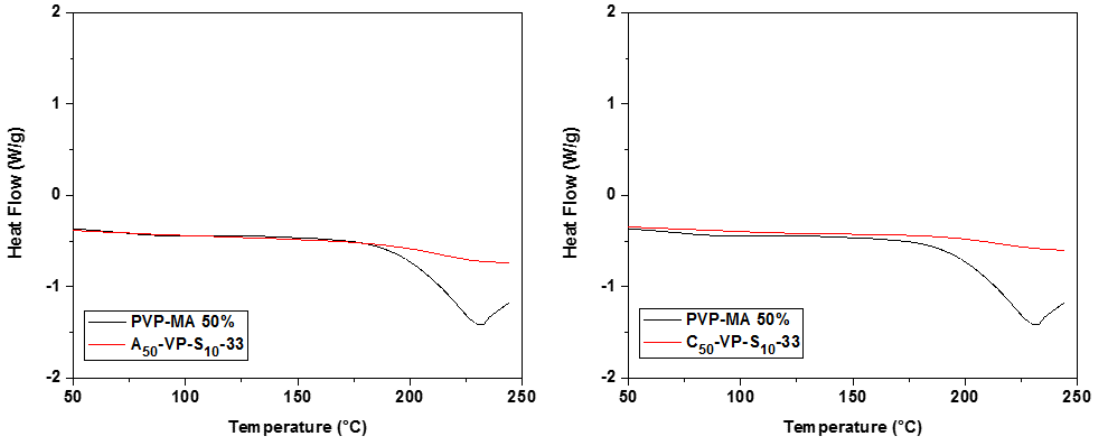

Figure A.21 Chapter 5 DSC thermograms (part 5)